SELECTIVE REGULATION OF BMP4 SIGNALING BY THE RECEPTOR TYROSINE KINASE MuSK

ATILGAN YILMAZ
B.S. MOLECULAR BIOLOGY AND GENETICS, BOĞAZİÇİ UNIVERSITY, 2005

A DISSERTATION SUBMITTED IN PARTIAL FULFILLMENT OF THE REQUIREMENTS FOR THE DEGREE OF DOCTOR OF PHILOSOPHY IN THE DIVISION OF BIOLOGY AND MEDICINE AT BROWN UNIVERSITY

PROVIDENCE, RHODE ISLAND
May 2013

This dissertation by Atılgan Yılmaz is accepted in its present form by the Division of Biology and Medicine, Department of Molecular Biology, Cell Biology and Biochemistry as satisfying the dissertation requirement for the degree of Doctor of Philosophy.

Date_____ _____
Dr. Justin R. Fallon, Advisor

Recommended to the Graduate Council

Date_____ _____
Dr. Kristi Wharton, Reader (Chairman)

Date_____ _____
Dr. Gilad Barnea, Reader

Date_____ _____
Dr. Mark Zervas, Reader

Date_____ _____
Dr. Steven Burden, Outside Reader

Approved by the Graduate Council

Date_____ _____
Dr. Peter Weber,
Dean of the Graduate School

ATILGAN YILMAZ

DOB: November 21, 1982
Mailing Address: Department of Neuroscience,
Brown University, Box G-LN
185 Meeting Street, Providence, RI 02912
Phone: 401 919 7262
E-mail: atilgan_yilmaz@brown.edu

EDUCATION

Ph.D. in Molecular Biology, Cellular Biology and Biochemistry (expected) Summer 2012
Brown University, Providence, RI
Thesis: "Selective regulation of BMP4 signaling by the receptor tyrosine kinase MuSK"

B.S. in Molecular Biology and Genetics June 2005
Bogazici University, Istanbul, Turkey, *with Honors*

RESEARCH EXPERIENCE

04/06 –
Graduate Student, Brown University, Providence, USA
Selective regulation of BMP4 signaling by the receptor tyrosine kinase MuSK
Advisor: **Prof. Justin Fallon,** Department of Neuroscience

06/04 – 09/04
Undergraduate Summer Research Trainee. UCLA, Los Angeles, USA
Mechanism of cofilin-mediated actin depolymerization.
Advisor: **Prof. Emil Reisler,** Department of Chemistry & Biochemistry

07/03 – 10/03
Undergraduate Summer Research Trainee, Georg August University, Göttingen, Germany
Molecular mechanisms of endocytosis and synaptic vesicle formation in neurons.
(Supported by the Science and Culture Ministry of Niedersachsen)
Advisor: **Prof. Volker Haucke,** Biochemistry Institute (relocated to Freie Universität Berlin)

11/01 – 06/05
Undergraduate Research Assistant. Bogazici University, **Istanbul, Turkey**
Role of FGF family in development and physiopathology in vertebrate retina.
Advisor: **Prof. Kuyas Bugra,** Department of Molecular Biology and Genetics

PUBLICATIONS

Amenta AR, Yilmaz A, Bogdanovich S, McKechnie BA, Abedi M, Khurana TS, Fallon JR. (2011) Biglycan recruits utrophin to the sarcolemma and counters dystrophic pathology in mdx mice. **PNAS** 108(2), 762-767

Bobkov AA, Muhlrad A, Pavlov DA, Kokabi K, Yilmaz A, Reisler E. (2006) Cooperative effects of cofilin (ADF) on actin structure suggest allosteric mechanism of cofilin function. **J Mol Biol.** 356(2), 325-334

Manuscripts in Progress:

Yilmaz A, Fallon JR. (in preparation) The receptor tyrosine kinase MuSK regulates BMP4 signaling.

Yilmaz A, Fallon JR. (in preparation) BMP4 induces acetylcholine receptor clustering in a MuSK-dependent manner.

PATENT APPLICATIONS

"Biglycan mutants and related therapeutics and methods of use"
Inventors: Amenta AR, McKechnie BA, Dechene M, Yilmaz A, Fallon JR.
U.S. Patent Application No.: 13/109,558

"Therapeutic and diagnostic methods involving biglycan and utrophin"
Inventors: Amenta AR, Yilmaz A, McKechnie BA, Fallon JR.
Provisional Application No.: 61/427,468

ABSTRACTS and INVITED LECTURES

Yilmaz A, Amenta A, McKechnie B, Fallon J. Biglycan recruits utrophin to the muscle membrane and is a potential therapeutic for Duchenne Muscular Dystrophy. **Poster**. EMBO Conference Series: Molecular and cellular basis of regeneration and tissue repair, Sesimbra, Portugal. September 26-30, **2010**.

A, Yilmaz. Mechanisms of action of biglycan, a potential therapeutic for Duchenne Muscular Dystrophy. **Invited Lecturer**. Department of Molecular Biology and Genetics, Boğaziçi University, Istanbul, Turkey. July, **2008**

TEACHING EXPERIENCE

Spring 2009 – Fall 2011 **Rotation student trainer**, 6 rotation students and 1 MD-PhD student

January 2011 **Graduate student assistant**, Suna Kıraç Workshop on Neurodegenerative Disease: From Genetic Models to Therapies, Boğaziçi University, Istanbul, Turkey

Spring 2011 **Guest Lecturer,** Analysis of Development, Axolotl Embryo Lab, Brown University

Spring 2010 **Guest Lecturer**, Analysis of Development, Axolotl Embryo Lab, Brown University

Spring 2007 **Teaching Assistant**, Analysis of Development, Brown University

AWARDS and HONORS

2011 Graduate International Colloquium Grant, approved by Brown University Office of International Affairs

LANGUAGES

Turkish, **English**, **German**, **French, Greek**

To my mother, father and sister...

Acknowledgements

I would like to first thank my advisor, Dr. Justin Fallon. Without his support and ideas this work would not have been possible. I am especially grateful to Dr. Fallon for trusting my ideas and for all our fruitful discussions which helped my training to become an independent scientist tremendously.

I also want to thank my thesis committee members, Dr. Kristi Wharton, Dr. Gilad Barnea and Dr. Mark Zervas for their valuable ideas that helped me bring together the work presented in this thesis. They were always available to discuss ideas and give me feedback. I would like to specifically thank Dr. Wharton with whom I had a phone interview before I came to Brown University. Thank you for giving me the chance to be here, Dr. Wharton!

I am also thankful to the past and present members of our laboratory: Beatrice Lechner for training me when I joined Dr. Fallon's laboratory, Anne Booker whom I will mention below, Michelle Dechene for her protein purifications that helped move my project greatly and also for advancing my baking skills, Julia Najera, Emily Stackpole and Hanna Berk Rauch for their discussions and friendship, Carolyn Schmiedel and Eamon Quick for helping me with cell cultures, Beth McKechnie and Sarah Mentzer for making sure that the laboratory is running efficiently, Michael Akins and Alison Amenta for their ideas, and all rotation students I worked with for their help in the experiments and for their interest in my thesis project.

I would also like to mention a few people who have great impacts on my life. Very special thanks go to two dear friends of mine: İlker Öztop, with whom I shared both laughter and tears very many times. I cannot imagine a life without such a great friend and I feel very lucky for knowing. İyi ki varsın! And Anne Booker, who not only was a great lab mate but is also a life-long friend. Without her, so many good memories would be missing from my life. I want to thank Konstantinos Kotakis for his constant support and life advices, Gökhan Demirkan and Ahmet Eken for their company throughout the graduate school and their friendship. I will always be grateful to all of you. I would like to thank Theocharis Vadivoulis for reviving me at one of the most hopeless times of my life and for reminding me that life is "plastic". I now hope for iluke-full of years. Ευχαριστώ πολύ!

All other friends whose names I could not mention here deserve many thanks.

Finally, I would like to thank three most special people to whom I dedicate my thesis: My mother and father , Fadime and Hüseyin Yılmaz, as well as my sister Nagihan Yılmaz. No matter how far we are, you have always been by my side. Sizi çok seviyorum....

Preface

Communication between the extracellular matrix and the intracellular environments of the cells is crucial for multiple processes such as survival, proliferation or maintenance of cellular states. Failure or mistakes in this communication leads to inability to form subcellular organizations or to give appropriate responses to the changes in the cellular environment or several disease states such as cancer. Therefore it is important to understand how cells employ different mechanisms to relay information from the extracellular matrix to their cytoplasm. One common way of such communication is established by the use of signaling molecules that are recognized by their receptors at the cell surface and the signaling cascades initiated by this receptor-ligand interaction. This mechanism is key to both the intercellular communication and the autocrine regulatory events. In this thesis I discuss two examples of interactions between signaling pathways, as well as mechanisms in which extracellular molecules regulate cytosolic proteins. The first project details the studies based on an incidental observation showing that the receptor tyrosine kinase MuSK and the signaling molecule BMP4 bind to each other. I also demonstrate how the muscle-specific receptor tyrosine kinase MuSK regulates BMP4 signaling in muscle cells (Chapter 2). The results of these studies show that MuSK binds to BMP4 and is required for the transcription of a subset of genes in response to BMP4. In Chapter 3, I demonstrate a role for BMP4 in the induction of AChR clusters in cultured muscle cells. My results suggest that this BMP4 effect requires MuSK and Wnt11 activities. In the last data chapter, I present

the work detailing biglycan's regulation of sarcolemmal utrophin expression, the therapeutic effect of this regulation for Duchenne Muscular Dystrophy (DMD) and the mechanisms thereof (Chapter 4). Finally, I discuss the importance of these findings and the future directions (Chapter 5).

Table of Contents

CHAPTER 2: The receptor tyrosine kinase MuSK binds BMPs and selectively regulates their signaling

CHAPTER 3: BMP4 induces acetylcholine receptor clustering in a MuSK- and Wnt11-dependent manner

CHAPTER 4: Biglycan recruits utrophin to the sarcolemma and counters dystrophic pathology in mdx mice

CHAPTER 5: DISCUSSION

List of Figures

List of Tables

CHAPTER 1

INTRODUCTION

1.1 BMP ligands

Bone Morphogenic Proteins (BMPs) are phylogenetically conserved growth factors that were first detected in bone extracts that have the ability to induce ectopic bone formation (Ferguson et al., 1992; Ray et al., 1991; Urist, 1965). Over 20 members of BMPs have been identified so far. This number makes them the largest subgroup of Transforming Growth Factor Beta (TGFβ) superfamily (Lavery et al., 2008; Kawabata et al., 1998). As opposed to the tissue restriction that is implied by their initial nomenclature, BMPs function during early development throughout the embryo in both invertebrates and vertebrates (Ferguson et al., 1992; Ray et al., 1991; Urist, 1965). Furthermore, this diverse group of growth factors functionally supports multiple processes such as organ morphogenesis and regeneration in a range of developing and adult tissues. Based on their functions and sequence similarity, BMPs are divided into at least four subgroups: BMP2/4, BMP5/6/7/8a/8b, BMP9/10 and BMP12/13/14 (Mazerbourg et al., 2006; von Bubnoff et al., 2001). BMP2, 4, 8b and 10 are involved at the earliest stages of the embryo. Hence their homozygous nulls are embryonic lethal (Zhang et al., 1996; Winnier et al., 1995; Zhao et al., 1996; Chen et al., 2004).

BMPs are synthesized as large precursors with an N-terminal signal peptide, a prodomain and a C-terminal mature peptide (Xiao et al., 2007; Sieber et al., 2009). Upon dimerization mature proteins are proteolytically cleaved from the prodomain

(Nelsen et al., 2009). BMPs can form biologically active heterodimers and homodimers.

BMP activity is regulated at several levels, which serves to regulate the ligand activity and increase the diversity of the signaling complexes. The expression of the ligand is the first step of regulation. Another type of regulation was shown recently for Glass bottom boat (Gbb), the Drosophila ortholog of vertebrate BMP 5, 6 and 7. In this study, Gbb was shown to have a second furin processing site in the prodomain, which generates a larger active ligand with greater signaling activity and a longer range (Akiyama et al., 2012). The bioavailability of the ligand in a particular tissue environment is also regulated by extracellular matrix and surface molecules. This class of regulation will be discussed in the following sections.

1.2 BMP pathway

Biologically active BMPs bind to two different classes of receptors on the cell surface; type-1 (Alk2, 4 or 6) and type-2 (BMPRII, ActRIIa) (ten Dijke et al., 1994, de Sousa Lopes et al., 2004, Nohno et al., 1995, Xia et al., 2007). For BMP ligands it has been shown that the binding to the type-1 receptor has a higher affinity than the binding to the type-2 receptor (Berasi et al., 2011). Upon binding of the ligand to the receptor complex, the constitutively active type-2 receptor phosphorylates the type-1 receptor (Wrana et al., 1994). This phosphorylation is required for the activation

of the type-1 receptor. The activated type-1 receptor phosphorylates the cytosolic member of the signaling pathway, SMAD1/5/8 (Kretzschmar et al., 1997). Phosphorylated SMAD1/5/8 forms a complex with SMAD4, translocates to and accumulates in the nucleus where it functions as part of a transcriptional activator or repressor complex for a range of genes at different stages of development or in the adult (Lagna et al., 1996, Liu et al., 1996, Hoodless et al., 1996) (Figure 1.1).

BMP binding to the type-1 receptor is regulated by multiple factors including ligand concentration and post-translational modifications. BMP binding to monomeric type-1 receptor requires high BMP concentrations (Heinecke et al., 2009). At low concentrations, BMPs bind to dimeric type-1 receptors since they have a higher affinity to the dimer than to the mononer. For the signaling to occur, a final assembly of a minimum of one type-1 and one type-2 receptor has to be formed in complex with the ligand. For TGFβ receptors, homodimerization of receptors leads to formation of a heterohexamerix complex that includes the dimeric ligand and homodimers of each receptor (Gilboa et al., 1998). However, for BMPs a final complex assembly has yet to be shown clearly. It is possible that heterodimerization of the ligand and of both receptor types and the formation of a heterohexameric complex of these heterodimers is used as a way to increase the complexity of the signaling.

The BMP pathway can also be regulated at the downstream steps, particularly at the level of SMAD1/5/8 phosphorylation. Fuentealba et al. have reported that

SMAD1/5/8 that is phosphorylated by type-1 receptors can be further phosphorylated by GSK3β and MAP kinases (Fuentealba et al., 2007). These phosphorylations are required for polyubiquitination of SMAD1/5/8.

1.3 Secreted extracellular regulators of BMPs

The bioavailability of the BMP ligands is regulated by various secreted extracellular matrix proteins. Among the best-characterized examples of such secreted antagonists are noggin, chordin and follistatin. These inhibitors bind to BMPs and prevent them from associating with their signaling receptors (Zimmerman et al., 1996, Piccolo et al., 1996, Fainsod et al., 1997). One of the most important functions of these antagonists was observed in early embryos. At the blastula stage of *Xenopus* embryos, chordin and noggin are secreted from Spemann's organizer at the dorsal half of the embryo where they prevent the signaling by BMP4 that is secreted from the ventral side (DeRobertis, 2009). Other antagonists such as Inhibin compete with BMPs for receptor binding (Rosen et al., 2006).

1.4 BMP regulators/co-receptors at the cell surface

Another regulatory mechanism of BMP signaling uses surface molecules that act as stimulatory or inhibitory co-receptors. Dragon family co-receptors are structurally

similar to type-1 receptors in their ectodomain and interact with BMPs to recruit type-2 receptors that would not ordinarily be used by a given BMP. These co-receptors intensify the BMP signaling by recruitment of type-2 receptors (Halbrooks et al., 2007). The transmembrane protein BAMBI inhibits BMP signaling by acting as a pseudo-type 1 receptor and occupying the available type-2 receptors (Onichtchouk et al., 1999). Neogenin, a receptor for netrins and proteins of the repulsive guidance molecule family, was recently shown to bind BMPs and inhibit Smad signal transduction through the activation of RhoA (Hagihara et al., 2011). Stem cell factor receptor (c-kit) was shown to interact with type-2 receptor BMPRII and positively regulate BMP signaling (Hassel et al., 2006).

1.5 BMP4

BMP4 is one of the most widely studied members of BMP family. It has crucial roles both in the embryo and in adult. Its fundamental function in the embryo is shown by the embryonic lethality of its homozygous null mutants (Winnier et al., 1995). BMP4 is highly expressed in extraembryonic ectoderm and the primitive streak before and during gastrulation (Winnier et al., 1995; Lawson et al., 1999; Ying et al., 2000; Ying et al., 2001). Mutations in decapentaplegic (dpp), the Drosophila ortholog of BMP2 and BMP4, cause dorsoventral patterning abnormalities at the blastoderm stage (Ray et al., 1991). BMP4 acts as a posterior-ventralizing factor in Xenopus embryos (Dale et al., 1992; Jones et al., 1992). BMP4 is also crucial factor for maintaining the

pluripotency of mouse ES cells by signaling through Alk3 to suppress p38 MAP kinase activity (Qi et al., 2004; Ying et al., 2003). BMP4 signaling is also required for normal induction of primordial germ cells (de Sousa et al., 2004; Lawson et al., 1999; Ying et al., 2001). Finally, BMP4 also functions in the mature organisms such as inhibiting melanin synthesis in epidermal melanocytes and regulating adult hippocampal neurogenesis (Singh et al., 2012, Tang et al., 2009).

Several BMP4 extracellular antagonists have been identified. These include Dan, PRDC, Gremlin, Cerberus, Coco, Tsg, Chordin, Noggin and Follistatin (Sudo et al., 2004; Khokha et al., 2003; Zuniga et al., 1999; Bell et al., 2003; Pearce et al., 1999; Nosaka et al., 2003; Oelgeschlager et al., 2000; Wardle et al., 1999; Zhang et al., 2002; Bachiller et al., 2000; Brunet et al., 1998; McMahon et al., 1998; Gazzerro et al., 1998; Lin et al., 2006). Notably, BMP4 activity is also modulated by transmembrane receptors such as neogenin (Hagihara et al., 2011) (Figure 1.2).

1.6 BMP4 in muscle

Several studies have shown functions for BMP4 in muscle tissue and myogenic cells. In myoblasts, Id1, one of the well-characterized downstream genes of BMP4, has been shown to inhibit differentiation by interfering with pro-differentiation bHLH transcription factor complexes (Kurabayashi et al., 1994). More recently, BMP4 and its antagonist Gremlin have been implicated in regulation of myogenic progenitor

proliferation in human fetal skeletal muscle (Frank et al., 2006). This study showed that BMP4 secreted by skeletal muscle side population cells, a stem-like cell type, inhibited differentiation of the main population mononuclear muscle-derived cells. In contrast to the previous studies, BMP2 and BMP4 have been shown to regulate a miRNA-mediated mechanism that enhances myocardial differentiation (Wang et al., 2010). Endogenous BMP4 in cultured C2C12 myoblasts has been also implicated in myotube formation (Umemoto et al., 2011). Finally, defective myogenesis in Duchenne Muscular Dystrophy patients has been correlated to increased BMP4 expression in these patients (Sterrenburg et al., 2006).

1.7 BMP4 target genes

BMP4 induces the expression of many genes in different tissues and at different developmental stages. Several BMP4 target genes in myogenic cells are studied in this thesis. Among those, Id1 and Id2 are well-characterized BMP targets. Ptgs2 has been previously shown to be expressed downstream of BMP2. On the other hand, several other genes studied here were previously not implicated downstream of BMP4. These include Ptger4, RGS4, Fabp7, Car3, Myh15 and Wnt11. These genes and their products will be discussed in the following sections.

1.7.1 Id1 and Id2

Id proteins are among most important targets of BMP signaling. Id1 promoter activity is specifically increased by BMPs and this effect requires Smad1 or Smad5 and Smad4 (Ogata et al., 1993; Hollnagel et al., 1999; Lopez-Rovira et al., 2002; Korchynskyi et al., 2002). Id proteins were identified as negative regulators of bHLH transcription factors and have been shown to interact with retinoblastoma (Rb) and Ets family members (Norton et al., 1998; Yokota et al., 2002). Id proteins are negative regulators of differentiation and positive regulators of proliferation. They inhibit cell differentiation by binding to the ubiquitous bHLH transcription factors and inhibiting their interaction with the tissue specific bHLH transcription factors. For example, in myoblasts Id1 interacts with E2A protein and inhibits the formation of the functional E2A-MyoD heterodimer, which leads to inhibition of differentiation and maintenance of undifferentiated phenotype of myoblasts (Kurabayashi et al., 1994). Id proteins also regulate cell cycle progression. Id2 binds to hypophosphorylated active form of Rb family proteins and inhibit their antiproliferative functions (Lasorella et al., 2000).

1.7.2 Ptgs2 and Ptger4

Ptgs2 is the gene encoding for the enzyme COX2. COX2 is one of the two isoforms of COX enzymes that catalyze the rate-limiting step in the synthesis of prostaglandins (PG). PGs are autocrine and paracrine signaling molecules that regulate

inflammation and are synthesized in response to growth factors, cytokines and cell injury (Funk, 2001). BMP2 induces COX2 expression through a noncanonical BMP pathway that requires the activity by p38 kinase (Susperregui et al., 2011). COX2 has been shown to regulate stretch-induced proliferation of skeletal muscle myoblasts, smooth muscle cells and retinal mesangial cells (Otis et al., 2005; Park et al., 1999; Akai et al., 1994). Myofiber growth during skeletal muscle regeneration is inhibited in COX2 null animals (Bondesen et al., 2004). The COX2 pathway has also been shown to regulate the growth of atrophied muscle by regulating myonuclear addition and satellite cell proliferation (Bondesen et al., 2006).

Ptger4 encodes for the receptor EP4, one of the four G-protein-coupled receptors for the prostaglandin PGE_2, which is in turn synthesized by COX2 pathway (Giuliano et al., 2002). EP4 expression is regulated by various stimuli including lipopolysaccharide in RAW 264.7 murine macrophage-like cell line (Arakawa et al., 1996). EP4 expression is upregulated by gonadotropin in ovarian granulosa and cumulus cells (Segi et al., 2003). In this thesis, Ptger4 is shown to be upregulated downstream of BMP4.

1.7.3 Regulator of G-protein signaling 4 (RGS4)

RGS4 is one of the 30 known regulators of G protein signaling (RGS) molecules identified to date (Willars, 2006). RGS molecules are GTPase activating proteins (GAP), a class of proteins that promote GTP hydrolysis by Gα proteins. This GAP

activity by RGS molecules is very crucial as the intrinsic GTPase activity of Gα proteins is weak and they rely on GAPs to sustain physiologically meaningful rates of GTP hydrolysis. Thus, RGS proteins are crucial modulators of G protein signaling. RGS4 expression is enriched in heart and central nervous system (Rogers et al., 2001; Erdely et al., 2004; Cifelli et al., 2008). It has been thought to counter-regulate $G_{\alpha}q$-induced signaling that is triggered by hypertrophic stimuli in the heart (Rogers et al., 2001; Tokudome et al., 2008). On the other hand, injection of RGS4 mRNA into *Xenopus* embryos resulted in decreased skeletal muscle (Wu et al., 2000).

1.7.4 Fatty acid binding protein 7 (Fabp7)

Fabp7 is a member of fatty acid binding protein (Fabp) family. Fabps are intracellular proteins involved in lipid trafficking and they have key roles in taking up fatty acids into cytoplasm and transporting them to appropriate cellular compartments (Chmurzynska et al., 2006; Furuhashi et al., 2008; Storch et al., 2009). Fabp7 is expressed in adult rodent brain (Owada et al., 1996; Owada et al., 2008). Fabp7 is also a well-established marker for neuronal stem cells and has been shown to be important for neurogenesis (Ming et al., 2011; Steiner et al., 2006; Duan et al., 2008). In this thesis Fabp7 expression in myogenic cells is shown to be induced by BMP4.

1.7.5 Carbonic Anhydrase 3 (Car3)

Carbonic anhydrase 3 (Car3) is a member of carbonic anhydrase family of enzymes that reversibly hydrate carbon dioxide and generate bicarbonate and hydrogen ions. This activity maintains a variety of physiological functions including acid-base balance, respiration, urinary acidification and bone resorption (Sly et al., 1995; Spicer et al., 1990; Stanton et al., 1991; Tashian et al., 1989). Car3 shows different characteristics than the other Car isoforms in especially its very low specific activity (Koester et al., 1981; Koester et al., 1977). It is very abundant in skeletal muscle and adipocytes and makes up to 8 and 25% of the soluble fraction in these tissues, respectively (Carter et al., 1991; Spicer et al., 1990). Car3 was originally purified in rabbit muscle where it was shown to constitute 1 to 2% of the total protein that was extracted (Blackburn et al., 1972). In humans and most large mammals, Car3 expression is enriched in slow skeletal muscle and is highly expressed in type 1, slow twitch fibers (Tashian, 1989; Wade et al., 1986; Wistrand et al., 1987; Brownson et al., 1988). Therefore, it was suggested to be a slow-twitch fiber marker. Car3 function in muscle tissue, however, is not known. In Car3 null animals, which develop normally and have normal life spans, fiber type composition of slow muscle Soleus is not affected. The main contractile properties of the muscles are also not changed in the absence of Car3 (Kim et al., 2004). Car3 was alternatively suggested to decrease oxidative stress (Raisanen et al., 1999).

1.7.6 Myosin Heavy Chain 15 (Myh15)

Myosin heavy chain 15 (Myh15) is a member of sarcomeric myosin heavy chain (MyHC) family proteins. MyHC isoforms in this family can assemble into highly ordered structures called sarcomeres, which are found in skeletal and cardiac muscles (Cripps, Suggs and Bernstain, 1999). The developmental regulation of the expression of these MyHC isoforms can change the contractile properties of individual striated muscle fibers (Barany, 1967; Schiaffino and Reggiani, 1996). Myh15 has been suggested as a slow-contracting MyHC isoform (Desjardins et al., 2002) with orthologs in *Xenopus* and chicken but not fish (McGuigan et al., 2004; Garriock et al., 2005; Ikeda et al., 2007). In a previous study, Myh15 was not deteceted in two skeletal muscles (slow-twitch Soleus and fast-twitch Tibialis Anterior) or in heart it was shown to be absent, whereas its expression was enriched in extraocular muscles (Rossi et al., 2010). In contrast to those reports, in this thesis Myh15 expression is shown to be present both in soleus and extensor digitorum longus (EDL) muscles and to be induced by BMP4 (Chapter 2).

1.7.7 Wnt11

Wnt11 is a member of the Wnt family growth factors. It belongs to Wnt5a subgroup of Wnt proteins along with Wnt 4 and 5a. Wnt11 is a 354 amino acid protein with a molecular weight of 45 kDa that is associated with the extracellular matrix

(Christiansen et al., 1996). Wnt11 is most similar in sequence to Wnt4, although their functions may differ in certain contexts (Kispert et al, 1998, Elizalde et al. 2010). In the embryo, Wnt11 is expressed in various tissues including somites, pre-cardiac mesoderm, mesenchyme of developing limb buds and the apical ectodermanl ridge (Christiansen et al, 1996, Kispert et al. 1996). In adults, it is expressed in heart, skeletal muscle, pancreas and liver (Kirikoshi et al., 2001). Wnt11 promotes cardiac differentiation and its overexpression leads to cardiac hyperthrophy (Eisenberg & Eisenberg, 1999; Abdul-Ghani et al., 2011). Several factors activate Wnt11 expression, including Ret/GDNF in developing kidney (Pepicelli et al., 1997) and Wnt3a in differentiating mES cells (Ueno et al., 2007). Recently, Wnt11 has been also shown to bind to MuSK and induce AChR clusters on cultured mouse myotubes (Zhang et al., 2012).

1.8 Acetylcholine Receptor (AChR) clustering and the neuromuscular junction (NMJ) formation

Acetylcholine released from motor neuron terminals in vertebrates binds to and opens AChRs in the postsynaptic domains of NMJs initiating the endplate potential that in turn is necessary to muscle contraction. Generation of a sufficiently large endplate potential requires a high density of AChRs at the NMJ. Thus AChR clustering is vital for the efficient neurotransmission, hence the communication between neurons and the muscle tissue.

AChR clustering occurs at two distinct stages during development. Prior to innervation of the muscle, AChRs are initially uniformly distributed throughout the muscle fiber. However, they eventually accumulate in the middle of the fiber where innervation will occur (Bevan et al., 1977; Braithwaite et al., 1979; Creazzo et al., 1983; Ziskind-Conhaim et al., 1982). This phenomenon is called pre-patterning and is nerve-independent (Yang et al., 2000). These so-called microclusters disappear after innervation and the bigger clusters form at the innervated sites (Lin et al., 2001; Vock et al., 2008, Yang et al., 2001). Importantly, both the aneural prepatterned and the neural clusters require Muscle Specific Kinase (MuSK) (Zhang et al., 2004). While agrin has been shown to be necessary for stabilizing neural clusters, Wnt11r has been suggested to be the inducer of aneural clusters in zebrafish (Jing et al., 2009). The subsequent Dishevelled (Dvl)-mediated signaling has also been implicated in guiding motor axons for NMJ formation in zebrafish (Jing et al., 2009).

1.9 Muscle Specific Kinase (MuSK)

MuSK is a receptor tyrosine kinase that is predominantly expressed at the NMJs in mature muscle cells (Valenzuela et al., 1995). However, it is also expressed at lower levels at the extrajunctional membrane of muscle cells (Bowen et al., 1998) and in other tissues such as brain (Garcia-Osta et al., 2006).

The extracellular domain of MuSK consists of 3 immunoglobulin-like (Ig) domains and a cysteine-rich domain (CRD). In its cytoplasmic domain it has a juxtamembrane domain (JM), which is followed by a catalytic tyrosine kinase (TK) domain (Figure 1.3). Several MuSK isoforms with the presence or absence of 3 short inserts (10, 15 and 8 amino acids) at the ectodomain of MuSK have been detected in neonatal and adult mice, as well as in cultured C2C12 myotubes (Kuehn et al., 2005). In addition, another MuSK isoform lacking the third Ig domain at the ectodomain has been identified (Hesser et al., 1999). It's been suggested that the alternative splicing of MuSK adds more complexity to the activities of MuSK.

MuSK also binds to LRP4, which is a receptor for agrin and forms a complex with MuSK. Binding of neural derived proteoglycan agrin (N-agrin) to LRP4 increases the association between LRP4 and MuSK and also activates MuSK (Kim et al., 2008). MuSK is activated by autophosphorylation and this activation leads to a cascade of events that is crucial for NMJ formation, maturation and stability. MuSK has a master regulatory role for these events (Herbst et al., 2000; Zhou et al. 1999; Zhu et al. 2008; Zong et al., 2012; Zang et al., 2011; DeChiara et al., 1996) (Figure 1.4). Mouse embryos lacking MuSK fail to form NMJs and the paralyzed embryos die before birth (DeChiara et al., 1996).

There are several interaction partners of MuSK, which are required for MuSK pathway to induce AChR clustering in response to N-agrin. One such interaction

partner is the adaptor protein downstream-of-tyrosine-kinase-7 (Dok7) that binds to tyrosine phosphorylated $NPXY_{553}$ motif in JM domain of MuSK (Bergamin et al. 2010; Okada et al., 2006). Another key molecule in this pathway is the tumorous imaginal disc protein (Tid1), which binds constitutively to the cytoplasmic domain of MuSK (Linnoila et al., 2008). Dvl binds to the JM and kinase domains of MuSK and couples MuSK to p21-activated kinase (Luo et al., 2002).

The signaling pathways in which MuSK acts as the master regulator for building the postsynaptic membrane at NMJs involve various other kinases and adaptor molecules. The assembly of AChRs into clusters requires the small GTPases Rac and Rho (Weston et al., 2003). MuSK activation by N-agrin leads to the activation of Rac I and the formation of AChR micro-aggregates (Luo et al., 2003). Rac activation is followed by the activation of Rho, which is thought to act through PAK I in order to enlarge AChR micro-aggregates into clusters bigger than 10 μm (Luo et al., 2002). Moreover, cytoplasmic tyrosine kinases Abl and Src are also activated by MuSK and they increase AChR clustering (Mittaud et al., 2004). Tyrosine phoshorylation of AchR β-subunit recruits the adaptor protein, rapsyn, after which the AChR clusters are stabilized (Borges et al., 2008).

Recently, Wnt11 has been also shown to bind to MuSK and induce AChR clusters on cultured mouse myotubes. Interestingly, Wnt11 clustering activity is not additive to agrin's, suggesting that agrin and Wnt11 may be using similar pathways to induce

clustering (Zhang et al., 2012). The significance of this interaction will be explored in the experiments described in Chapter 3.

1.10 Muscle fiber types and fiber-type switch

Mammalian skeletal muscles are heterogenous in their metabolic, electrical and contractile properties (Schiaffino and Reggiani, 1996; Bertchtold et al., 2000). This heterogeneity is the basis for the flexibility that allows muscles to be used for various activities ranging from low or high intensity contractions to repeated motions. Muscle fibers are divided into four main categories based on their expression of myosin heavy chains (MyHC) (Pette and Staron, 2000). The hindlimb muscles of adult rats express one slow myosin heavy chain isoform (MHC I (Myh7)) and three fast myosin heavy chain isoforms (MHC IIa (Myh2), IId (Myh1) and IIb (Myh14)) (Schiaffino and Reggiani, 1994; Weiss et al., 1999). The nomenclature for fiber types was also determined according to these myosin heavy chain isoforms: Type I, type IIa, type IId and type IIb. Although most fibers express only one myosin isoform, hence are referred to as pure fibers (Staron et al., 1993), some minor fraction of fibers expresses two myosin isoforms (Staron et al., 1993). The contractile properties of these hybrid fibers exhibit an intermediate level, which increases the number of fiber types and the complexity of fiber type composition of different muscle tissues (Pette and Staron, 2000).

Postural muscles are more enriched in slow fibers, which are highly vascularized and are dependent on oxidative phosphorylation for energy. On the other hand, muscles that are used for locomotion are more enriched in fast fibers, which are mostly dependent on glycolytic metabolism (Bassel-Duby and Olson, 2006). In C57BL6J mice, soleus muscle is enriched in type I slow fibers, whereas extensor digitorum longus (EDL) muscle is enriched in type IIb fast fibers (Augusto et al., 2004).

During embryogenesis and early postnatal life muscle fiber type is regulated by several factors such as the differences among progenitor cells, growth factors and neural activity (Wigmore and Evans, 2002) (Figure 1.5). The fibers that are innervated by the branches of the same motor neuron exhibit the same fiber phenotype (Burke et al., 1971, Burke et al., 1973). In the adult neural activity can reprogram muscle fibers towards different fiber types (Gauthier et al., 1983; Gorza et al., 1988; Ausoni et al., 1990). The roles of the nerve in reprogramming the fiber type was shown in cats and rats by reinnervating slow muscles with a fast nerve and reprogramming slow fibers to fast ones or vice versa (Buller et al., 1960; Hoh et al., 1975).

Several signaling pathways have been demonstrated to control muscle fiber type-specific gene programs. In mammals, Six factors, Six1-Six4, as well as the transcriptional repressor Sox6 were implicated in the control of the fast fiber induction program (Niro et al., 2010; Hagiwara et al., 2005; Hagiwara et al., 2007).

Calcineurin-dependent nuclear factor of activated T-cells (NFAT) transcription factors have been shown to increase MhHC-β/slow promoter activity in skeletal muscle, whereas the expression of this slow myosin was inhibited in response to thyroid hormone in mouse heart (McCullagh et al., 2004; Haddad et al., 2008). Moreover, peroxisome proliferator-activated receptors (PPARs) and peroxisome proliferator-activated receptor gamma coactivator-1α (PGC-1α) have been associated with slow fiber phenotype (Wang et al., 2004; Baar et al., 2002; Russell et al., 2003; Terada et al., 2002).

Conclusion

Signaling pathways often times do not function individually but rather are part of larger signaling networks in which multiple pathways crosstalk with each other. In this thesis, I explore the interactions between BMP4 and MuSK pathways. Chapter 2 and 3 comprise the main body of this work. In Chapter 2, I aimed to explore the regulation of BMP4 pathway in myogenic cells by MuSK. In Chapter 3, I explored BMP4 regulation of MuSK-dependent AChR clustering. Chapter 4 summarizes the work demonstrating therapeutic benefits of biglycan in a mouse model of Duchenne Muscular Dystrophy. In the final chapter (Chapter 5), the significance of these results and future directions are discussed.

REFERENCES

Abdul-Ghani, Mohammad, Daniel Dufort, Rebecca Stiles, Yves De Repentigny, Rashmi Kothary, and Lynn A Megeney. "Wnt11 Promotes Cardiomyocyte Development by Caspase-mediated Suppression of Canonical Wnt Signals." *Molecular and Cellular Biology* 31, no. 1 (January 2011): 163–178.

Augusto Valeria, Carlos Roberto Padovani and Gerson Eduardo Rocha Campos. "Skeletal Muscle Fiber Types in C57BL6J Mice." *Braz. J. morphol. Sci.* (2004) 21(2), 89-94.

Ausoni, S, L Gorza, S Schiaffino, K Gundersen, and T Lømo. "Expression of Myosin Heavy Chain Isoforms in Stimulated Fast and Slow Rat Muscles." *The Journal of Neuroscience: The Official Journal of the Society for Neuroscience* 10, no. 1 (January 1990): 153–160.

Akai, Y, T Homma, K D Burns, T Yasuda, K F Badr, and R C Harris. "Mechanical Stretch/relaxation of Cultured Rat Mesangial Cells Induces Protooncogenes and Cyclooxygenase." *The American Journal of Physiology* 267, no. 2 Pt 1 (August 1994): C482–490.

Akiyama, Takuya, Guillermo Marqués, and Kristi A Wharton. "A Large Bioactive BMP Ligand with Distinct Signaling Properties Is Produced by Alternative Proconvertase Processing." *Science Signaling* 5, no. 218 (April 3, 2012): ra28.

Arakawa, T, O Laneuville, C A Miller, K M Lakkides, B A Wingerd, D L DeWitt, and W L Smith. "Prostanoid Receptors of Murine NIH 3T3 and RAW 264.7 Cells. Structure and Expression of the Murine Prostaglandin EP4 Receptor Gene." *The Journal of Biological Chemistry* 271, no. 47 (November 22, 1996): 29569–29575.

Baar, Keith, Adam R Wende, Terry E Jones, Matthew Marison, Lorraine A Nolte, May Chen, Daniel P Kelly, and John O Holloszy. "Adaptations of Skeletal Muscle to Exercise: Rapid Increase in the Transcriptional Coactivator PGC-1." *FASEB Journal: Official Publication of the Federation of American Societies for Experimental Biology* 16, no. 14 (December 2002): 1879–1886.

Bachiller, D, J Klingensmith, C Kemp, J A Belo, R M Anderson, S R May, J A McMahon, et al. "The Organizer Factors Chordin and Noggin Are Required for Mouse Forebrain Development." *Nature* 403, no. 6770 (February 10, 2000): 658–661.

Bárány, M. "ATPase Activity of Myosin Correlated with Speed of Muscle Shortening." *The Journal of General Physiology* 50, no. 6 (July 1967): Suppl:197–218.

Bassel-Duby, Rhonda, and Eric N Olson. "Signaling Pathways in Skeletal Muscle Remodeling." *Annual Review of Biochemistry* 75 (2006): 19–37.

Bell, Esther, Ignacio Muñoz-Sanjuán, Curtis R Altmann, Alin Vonica, and Ali H Brivanlou. "Cell Fate Specification and Competence by Coco, a Maternal BMP, TGFbeta and Wnt Inhibitor." *Development (Cambridge, England)* 130, no. 7 (April 2003): 1381–1389.

Berasi, Stephen P, Usha Varadarajan, Joanne Archambault, Michael Cain, Tatyana A Souza, Abe Abouzeid, Jian Li, et al. "Divergent Activities of Osteogenic BMP2, and Tenogenic BMP12 and BMP13 Independent of Receptor Binding Affinities." *Growth Factors (Chur, Switzerland)* 29, no. 4 (August 2011): 128–139.

Berchtold, M W, H Brinkmeier, and M Müntener. "Calcium Ion in Skeletal Muscle: Its Crucial Role for Muscle Function, Plasticity, and Disease." *Physiological Reviews* 80, no. 3 (July 2000): 1215–1265.

Bergamin, Elisa, Peter T Hallock, Steven J Burden, and Stevan R Hubbard. "The Cytoplasmic Adaptor Protein Dok7 Activates the Receptor Tyrosine Kinase MuSK via Dimerization." *Molecular Cell* 39, no. 1 (July 9, 2010): 100–109.

Bevan, S, and J H Steinbach. "The Distribution of Alpha-bungarotoxin Binding Sites of Mammalian Skeletal Muscle Developing in Vivo." *The Journal of Physiology* 267, no. 1 (May 1977): 195–213.

Blackburn, M N, J M Chirgwin, G T James, T D Kempe, T Parsons, A M Register, K D Schnackerz, and E A Noltmann. "Pseudoisoenzymes of Rabbit Muscle Phosphoglucose Isomerase." *The Journal of Biological Chemistry* 247, no. 4 (February 25, 1972): 1170–1179.

Bondesen, Brenda A, Stephen T Mills, and Grace K Pavlath. "The COX-2 Pathway Regulates Growth of Atrophied Muscle via Multiple Mechanisms." *American Journal of Physiology. Cell Physiology* 290, no. 6 (June 2006): C1651–1659.

Borges, Lucia S, Sergey Yechikhov, Young I Lee, John B Rudell, Matthew B Friese, Steven J Burden, and Michael J Ferns. "Identification of a Motif in the Acetylcholine Receptor Beta Subunit Whose Phosphorylation Regulates Rapsyn Association and Postsynaptic Receptor Localization." *The Journal of Neuroscience: The Official Journal of the Society for Neuroscience* 28, no. 45 (November 5, 2008): 11468–11476.

Bowen, David C., John S. Park, Sue Bodine, Jennifer L. Stark, David M. Valenzuela, Trevor N. Stitt, George D. Yancopoulos, Ronald M. Lindsay, David J. Glass, and Peter S. DiStefano. "Localization and Regulation of MuSK at the Neuromuscular Junction." *Developmental Biology* 199, no. 2 (July 15, 1998): 309–319.

Braithwaite, A W, and A J Harris. "Neural Influence on Acetylcholine Receptor Clusters in Embryonic Development of Skeletal Muscles." *Nature* 279, no. 5713 (June 7, 1979): 549–551.

Brownson, C, H Isenberg, W Brown, S Salmons, and Y Edwards. "Changes in Skeletal Muscle Gene Transcription Induced by Chronic Stimulation." *Muscle & Nerve* 11, no. 11 (November 1988): 1183–1189.

Brunet, L J, J A McMahon, A P McMahon, and R M Harland. "Noggin, Cartilage Morphogenesis, and Joint Formation in the Mammalian Skeleton." *Science (New York, N.Y.)* 280, no. 5368 (May 29, 1998): 1455–1457.

BULLER, A J, J C ECCLES, and R M ECCLES. "Interactions Between Motoneurones and Muscles in Respect of the Characteristic Speeds of Their Responses." *The Journal of Physiology* 150 (February 1960): 417–439.

Burke, R E, D N Levine, and F E Zajac 3rd. "Mammalian Motor Units: Physiological-histochemical Correlation in Three Types in Cat Gastrocnemius." *Science (New York, N.Y.)* 174, no. 4010 (November 12, 1971): 709–712.

Burke, R E, D N Levine, P Tsairis, and F E Zajac 3rd. "Physiological Types and Histochemical Profiles in Motor Units of the Cat Gastrocnemius." *The Journal of Physiology* 234, no. 3 (November 1973): 723–748.

Carter, N. D. Hormonal and neuronal control of carbonic anhydrase III gene expression in skeletal muscle, (1991) p. 247–256. *In* S. J. Dodgson, R. E. Tashian, G. Gross, and N. D. Carter (ed.), The carbonic anhydrases: cellular physiology and molecular genetics. Plenum Publishing Corp., New York, N.Y.

Chen, Hanying, Shu Shi, Lourdes Acosta, Weiming Li, Jonathan Lu, Shideng Bao, Zhuang Chen, et al. "BMP10 Is Essential for Maintaining Cardiac Growth During Murine Cardiogenesis." *Development (Cambridge, England)* 131, no. 9 (May 2004): 2219–2231.

Chmurzyńska, Agata. "The Multigene Family of Fatty Acid-binding Proteins (FABPs): Function, Structure and Polymorphism." *Journal of Applied Genetics* 47, no. 1 (2006): 39–48.

Christiansen, J H, S J Monkley, and B J Wainwright. "Murine WNT11 Is a Secreted Glycoprotein That Morphologically Transforms Mammary Epithelial Cells." *Oncogene* 12, no. 12 (June 20, 1996): 2705–2711.

Cifelli, Carlo, Robert A Rose, Hangjun Zhang, Julia Voigtlaender-Bolz, Steffen-Sebastian Bolz, Peter H Backx, and Scott P Heximer. "RGS4 Regulates Parasympathetic Signaling and Heart Rate Control in the Sinoatrial Node." *Circulation Research* 103, no. 5 (August 29, 2008): 527–535.

Creazzo, T L, and G S Sohal. "Neural Control of Embryonic Acetylcholine Receptor and Skeletal Muscle." *Cell and Tissue Research* 228, no. 1 (1983): 1–12.

Cripps, R M, J A Suggs, and S I Bernstein. "Assembly of Thick Filaments and Myofibrils Occurs in the Absence of the Myosin Head." *The EMBO Journal* 18, no. 7 (April 1, 1999): 1793–1804.

Dale, L, G Howes, B M Price, and J C Smith. "Bone Morphogenetic Protein 4: a Ventralizing Factor in Early Xenopus Development." *Development (Cambridge, England)* 115, no. 2 (June 1992): 573–585.

DeChiara, T M, D C Bowen, D M Valenzuela, M V Simmons, W T Poueymirou, S Thomas, E Kinetz, et al. "The Receptor Tyrosine Kinase MuSK Is Required for Neuromuscular Junction Formation in Vivo." *Cell* 85, no. 4 (May 17, 1996): 501–512.
De Robertis, E M. "Spemann's Organizer and the Self-regulation of Embryonic Fields." *Mechanisms of Development* 126, no. 11–12 (December 2009): 925–941.

Desjardins, Philippe R., James M. Burkman, Joseph B. Shrager, Leonard A. Allmond, and Hansell H. Stedman. "Evolutionary Implications of Three Novel Members of the Human Sarcomeric Myosin Heavy Chain Gene Family." *Molecular Biology and Evolution* 19, no. 4 (April 1, 2002): 375–393.

de Sousa Lopes, Susana M Chuva, Bernard A J Roelen, Rui M Monteiro, Roul Emmens, Herbert Y Lin, En Li, Kirstie A Lawson, and Christine L Mummery. "BMP Signaling Mediated by ALK2 in the Visceral Endoderm Is Necessary for the Generation of Primordial Germ Cells in the Mouse Embryo." *Genes & Development* 18, no. 15 (August 1, 2004): 1838–1849.

Duan, Xin, Eunchai Kang, Cindy Y Liu, Guo-Li Ming, and Hongjun Song. "Development of Neural Stem Cell in the Adult Brain." *Current Opinion in Neurobiology* 18, no. 1 (February 2008): 108–115.

Elizalde, Carina, Victor M Campa, Mercedes Caro, Karin Schlangen, Ana María Aransay, Maria dm Vivanco, and Robert M Kypta. "Distinct Roles for Wnt-4 and Wnt-11 During Retinoic Acid-induced Neuronal Differentiation." *Stem Cells (Dayton, Ohio)* 29, no. 1 (January 2011): 141–153.

Erdely, Holly A, Robert A Lahti, Mary B Lopez, Carol S Myers, Rosalinda C Roberts, Carol A Tamminga, and Michael W Vogel. "Regional Expression of RGS4 mRNA in Human Brain." *The European Journal of Neuroscience* 19, no. 11 (June 2004): 3125–3128.

Fainsod, A, K Deissler, R Yelin, K Marom, M Epstein, G Pillemer, H Steinbeisser, and M Blum. "The Dorsalizing and Neural Inducing Gene Follistatin Is an Antagonist of BMP-4." *Mechanisms of Development* 63, no. 1 (April 1997): 39–50.

Ferguson, E L, and K V Anderson. "Localized Enhancement and Repression of the Activity of the TGF-beta Family Member, Decapentaplegic, Is Necessary for Dorsal-

ventral Pattern Formation in the Drosophila Embryo." *Development (Cambridge, England)* 114, no. 3 (March 1992): 583–597.

Frank, Natasha Y, Alvin T Kho, Tobias Schatton, George F Murphy, Michael J Molloy, Qian Zhan, Marco F Ramoni, Markus H Frank, Isaac S Kohane, and Emanuela Gussoni. "Regulation of Myogenic Progenitor Proliferation in Human Fetal Skeletal Muscle by BMP4 and Its Antagonist Gremlin." *The Journal of Cell Biology* 175, no. 1 (October 9, 2006): 99–110.

Fuentealba, Luis C., Edward Eivers, Atsushi Ikeda, Cecilia Hurtado, Hiroki Kuroda, Edgar M. Pera, and E. M. De Robertis. "Integrating Patterning Signals: Wnt/GSK3 Regulates the Duration of the BMP/Smad1 Signal." *Cell* 131, no. 5 (November 30, 2007): 980–993.

Funk, C D. "Prostaglandins and Leukotrienes: Advances in Eicosanoid Biology." *Science (New York, N.Y.)* 294, no. 5548 (November 30, 2001): 1871–1875.

Furuhashi, Masato, and Gökhan S Hotamisligil. "Fatty Acid-binding Proteins: Role in Metabolic Diseases and Potential as Drug Targets." *Nature Reviews. Drug Discovery* 7, no. 6 (June 2008): 489–503.

Garcia-Osta, Ana, Panayiotis Tsokas, Gabriella Pollonini, Emmanuel M Landau, Robert Blitzer, and Cristina M Alberini. "MuSK Expressed in the Brain Mediates Cholinergic Responses, Synaptic Plasticity, and Memory Formation." *The Journal of Neuroscience: The Official Journal of the Society for Neuroscience* 26, no. 30 (July 26, 2006): 7919–7932.

Garriock, Robert J, Stryder M Meadows, and Paul A Krieg. "Developmental Expression and Comparative Genomic Analysis of Xenopus Cardiac Myosin Heavy Chain Genes." *Developmental Dynamics: An Official Publication of the American Association of Anatomists* 233, no. 4 (August 2005): 1287–1293.

Gauthier, G F, R E Burke, S Lowey, and A W Hobbs. "Myosin Isozymes in Normal and Cross-reinnervated Cat Skeletal Muscle Fibers." *The Journal of Cell Biology* 97, no. 3 (September 1983): 756–771.

Gazzerro, E, V Gangji, and E Canalis. "Bone Morphogenetic Proteins Induce the Expression of Noggin, Which Limits Their Activity in Cultured Rat Osteoblasts." *The Journal of Clinical Investigation* 102, no. 12 (December 15, 1998): 2106–2114.

Gilboa, L, R G Wells, H F Lodish, and Y I Henis. "Oligomeric Structure of Type I and Type II Transforming Growth Factor Beta Receptors: Homodimers Form in the ER and Persist at the Plasma Membrane." *The Journal of Cell Biology* 140, no. 4 (February 23, 1998): 767–777.

Giuliano, Francesco, and Timothy D Warner. "Origins of Prostaglandin E2: Involvements of Cyclooxygenase (COX)-1 and COX-2 in Human and Rat Systems." *The Journal of Pharmacology and Experimental Therapeutics* 303, no. 3 (December 2002): 1001–1006.

Gorza, L, K Gundersen, T Lømo, S Schiaffino, and R H Westgaard. "Slow-to-fast Transformation of Denervated Soleus Muscles by Chronic High-frequency Stimulation in the Rat." *The Journal of Physiology* 402 (August 1988): 627–649.

Haddad, Fadia, Anqi X Qin, Paul W Bodell, Weihua Jiang, Julia M Giger, and Kenneth M Baldwin. "Intergenic Transcription and Developmental Regulation of Cardiac Myosin Heavy Chain Genes." *American Journal of Physiology. Heart and Circulatory Physiology* 294, no. 1 (January 2008): H29–40.

Hagihara, Meiko, Mitsuharu Endo, Katsuhiko Hata, Chikahisa Higuchi, Kunio Takaoka, Hideki Yoshikawa, and Toshihide Yamashita. "Neogenin, a Receptor for Bone Morphogenetic Proteins." *The Journal of Biological Chemistry* 286, no. 7 (February 18, 2011): 5157–5165.

Hagiwara, Nobuko, Betty Ma, and Alice Ly. "Slow and Fast Fiber Isoform Gene Expression Is Systematically Altered in Skeletal Muscle of the Sox6 Mutant, p100H." *Developmental Dynamics: An Official Publication of the American Association of Anatomists* 234, no. 2 (October 2005): 301–311.

Hagiwara, Nobuko, Michael Yeh, and Ann Liu. "Sox6 Is Required for Normal Fiber Type Differentiation of Fetal Skeletal Muscle in Mice." *Developmental Dynamics: An Official Publication of the American Association of Anatomists* 236, no. 8 (August 2007): 2062–2076.

Halbrooks, Peter J, Ru Ding, John M Wozney, and Gerard Bain. "Role of RGM Coreceptors in Bone Morphogenetic Protein Signaling." *Journal of Molecular Signaling* 2 (2007): 4.

Hassel, Sylke, Mariya Yakymovych, Ulf Hellman, Lars Rönnstrand, Petra Knaus, and Serhiy Souchelnytskyi. "Interaction and Functional Cooperation Between the Serine/threonine Kinase Bone Morphogenetic Protein Type II Receptor with the Tyrosine Kinase Stem Cell Factor Receptor." *Journal of Cellular Physiology* 206, no. 2 (February 2006): 457–467.

Heinecke, Kai, Axel Seher, Werner Schmitz, Thomas D Mueller, Walter Sebald, and Joachim Nickel. "Receptor Oligomerization and Beyond: a Case Study in Bone Morphogenetic Proteins." *BMC Biology* 7 (2009): 59.

Herbst, R, and S J Burden. "The Juxtamembrane Region of MuSK Has a Critical Role in Agrin-mediated Signaling." *The EMBO Journal* 19, no. 1 (January 4, 2000): 67–77.

Hesser, B A, A Sander, and V Witzemann. "Identification and Characterization of a Novel Splice Variant of MuSK." *FEBS Letters* 442, no. 2–3 (January 15, 1999): 133–137.

Hoh, J F. "Selective and Non-selective Reinnervation of Fast-twitch and Slow-twitch Rat Skeletal Muscle." *The Journal of Physiology* 251, no. 3 (October 1975): 791–801.

Hollnagel, A, V Oehlmann, J Heymer, U Rüther, and A Nordheim. "Id Genes Are Direct Targets of Bone Morphogenetic Protein Induction in Embryonic Stem Cells." *The Journal of Biological Chemistry* 274, no. 28 (July 9, 1999): 19838–19845.

Hoodless, P A, T Haerry, S Abdollah, M Stapleton, M B O'Connor, L Attisano, and J L Wrana. "MADR1, a MAD-related Protein That Functions in BMP2 Signaling Pathways." *Cell* 85, no. 4 (May 17, 1996): 489–500.

Ikeda, Daisuke, Yosuke Ono, Phil Snell, Yvonne J K Edwards, Greg Elgar, and Shugo Watabe. "Divergent Evolution of the Myosin Heavy Chain Gene Family in Fish and Tetrapods: Evidence from Comparative Genomic Analysis." *Physiological Genomics* 32, no. 1 (December 19, 2007): 1–15.

Jing, Lili, Julie L Lefebvre, Laura R Gordon, and Michael Granato. "Wnt Signals Organize Synaptic Prepattern and Axon Guidance Through the Zebrafish unplugged/MuSK Receptor." *Neuron* 61, no. 5 (March 12, 2009): 721–733.

Jones, C M, K M Lyons, P M Lapan, C V Wright, and B L Hogan. "DVR-4 (bone Morphogenetic Protein-4) as a Posterior-ventralizing Factor in Xenopus Mesoderm Induction." *Development (Cambridge, England)* 115, no. 2 (June 1992): 639–647.

Kawabata, M, T Imamura, and K Miyazono. "Signal Transduction by Bone Morphogenetic Proteins." *Cytokine & Growth Factor Reviews* 9, no. 1 (March 1998): 49–61.

Khokha, Mustafa K, David Hsu, Lisa J Brunet, Marc S Dionne, and Richard M Harland. "Gremlin Is the BMP Antagonist Required for Maintenance of Shh and Fgf Signals During Limb Patterning." *Nature Genetics* 34, no. 3 (July 2003): 303–307.

Kim, Geumsoo, Tae-Hoon Lee, Petra Wetzel, Cornelia Geers, Mary Ann Robinson, Timothy G Myers, Jennie W Owens, et al. "Carbonic Anhydrase III Is Not Required in the Mouse for Normal Growth, Development, and Life Span." *Molecular and Cellular Biology* 24, no. 22 (November 2004): 9942–9947.

Kim, Natalie, Amy L Stiegler, Thomas O Cameron, Peter T Hallock, Andrea M Gomez, Julie H Huang, Stevan R Hubbard, Michael L Dustin, and Steven J Burden. "Lrp4 Is a Receptor for Agrin and Forms a Complex with MuSK." *Cell* 135, no. 2 (October 17, 2008): 334–342.

Kirikoshi, H, H Sekihara, and M Katoh. "Molecular Cloning and Characterization of Human WNT11." *International Journal of Molecular Medicine* 8, no. 6 (December 2001): 651–656.

Kispert, A, S Vainio, L Shen, D H Rowitch, and A P McMahon. "Proteoglycans Are Required for Maintenance of Wnt-11 Expression in the Ureter Tips." *Development (Cambridge, England)* 122, no. 11 (November 1996): 3627–3637.

Korchynskyi, Olexander, and Peter ten Dijke. "Identification and Functional Characterization of Distinct Critically Important Bone Morphogenetic Protein-specific Response Elements in the Id1 Promoter." *The Journal of Biological Chemistry* 277, no. 7 (February 15, 2002): 4883–4891.

Koester, M K, A M Register, and E A Noltmann. "Basic Muscle Protein, a Third Genetic Locus Isoenzyme of Carbonic Anhydrase?" *Biochemical and Biophysical Research Communications* 76, no. 1 (May 9, 1977): 196–204.

Koester, M K, L M Pullan, and E A Noltmann. "The P-nitrophenyl Phosphatase Activity of Muscle Carbonic Anhydrase." *Archives of Biochemistry and Biophysics* 211, no. 2 (October 15, 1981): 632–642.

Kretzschmar, M, F Liu, A Hata, J Doody, and J Massagué. "The TGF-beta Family Mediator Smad1 Is Phosphorylated Directly and Activated Functionally by the BMP Receptor Kinase." *Genes & Development* 11, no. 8 (April 15, 1997): 984–995.

Kuehn, Rosemarie, Sallee A Eckler, and Medha Gautam. "Multiple Alternatively Spliced Transcripts of the Receptor Tyrosine Kinase MuSK Are Expressed in Muscle." *Gene* 360, no. 2 (November 7, 2005): 83–91.

Kurabayashi, M, R Jeyaseelan, and L Kedes. "Doxorubicin Represses the Function of the Myogenic Helix-loop-helix Transcription Factor MyoD. Involvement of Id Gene Induction." *The Journal of Biological Chemistry* 269, no. 8 (February 25, 1994): 6031–6039.

Lagna, G, A Hata, A Hemmati-Brivanlou, and J Massagué. "Partnership Between DPC4 and SMAD Proteins in TGF-beta Signalling Pathways." *Nature* 383, no. 6603 (October 31, 1996): 832–836.

Lasorella, A, M Noseda, M Beyna, Y Yokota, and A Iavarone. "Id2 Is a Retinoblastoma Protein Target and Mediates Signalling by Myc Oncoproteins." *Nature* 407, no. 6804 (October 5, 2000): 592–598.

Lavery, Karen, Pamela Swain, Dean Falb, and Moulay Hicham Alaoui-Ismaili. "BMP-2/4 and BMP-6/7 Differentially Utilize Cell Surface Receptors to Induce Osteoblastic Differentiation of Human Bone Marrow-derived Mesenchymal Stem Cells." *The Journal of Biological Chemistry* 283, no. 30 (July 25, 2008): 20948–20958.

Lawson, K A, N R Dunn, B A Roelen, L M Zeinstra, A M Davis, C V Wright, J P Korving, and B L Hogan. "Bmp4 Is Required for the Generation of Primordial Germ Cells in the Mouse Embryo." *Genes & Development* 13, no. 4 (February 15, 1999): 424–436.

Lin, W, R W Burgess, B Dominguez, S L Pfaff, J R Sanes, and K F Lee. "Distinct Roles of Nerve and Muscle in Postsynaptic Differentiation of the Neuromuscular Synapse." *Nature* 410, no. 6832 (April 26, 2001): 1057–1064.

Lin, S Jack, Thomas F Lerch, Robert W Cook, Theodore S Jardetzky, and Teresa K Woodruff. "The Structural Basis of TGF-beta, Bone Morphogenetic Protein, and Activin Ligand Binding." *Reproduction (Cambridge, England)* 132, no. 2 (August 2006): 179–190.

Linnoila, Jenny, Ying Wang, Yun Yao, and Zuo-Zhong Wang. "A Mammalian Homolog of Drosophila Tumorous Imaginal Discs, Tid1, Mediates Agrin Signaling at the Neuromuscular Junction." *Neuron* 60, no. 4 (November 26, 2008): 625–641.

Liu, F, A Hata, J C Baker, J Doody, J Cárcamo, R M Harland, and J Massagué. "A Human Mad Protein Acting as a BMP-regulated Transcriptional Activator." *Nature* 381, no. 6583 (June 13, 1996): 620–623.

López-Rovira, Teresa, Elisabet Chalaux, Joan Massagué, Jose Luis Rosa, and Francesc Ventura. "Direct Binding of Smad1 and Smad4 to Two Distinct Motifs Mediates Bone Morphogenetic Protein-specific Transcriptional Activation of Id1 Gene." *The Journal of Biological Chemistry* 277, no. 5 (February 1, 2002): 3176–3185.

Luo, Zhen G, Qiang Wang, Jian Z Zhou, Jianbo Wang, Zhijun Luo, Mingyao Liu, Xi He, et al. "Regulation of AChR Clustering by Dishevelled Interacting with MuSK and PAK1." *Neuron* 35, no. 3 (August 1, 2002): 489–505.

Mazerbourg, Sabine, and Aaron J W Hsueh. "Genomic Analyses Facilitate Identification of Receptors and Signalling Pathways for Growth Differentiation Factor 9 and Related Orphan Bone Morphogenetic Protein/growth Differentiation Factor Ligands." *Human Reproduction Update* 12, no. 4 (August 2006): 373–383.

McCullagh, Karl J A, Elisa Calabria, Giorgia Pallafacchina, Stefano Ciciliot, Antonio L Serrano, Carla Argentini, John M Kalhovde, Terje Lømo, and Stefano Schiaffino. "NFAT Is a Nerve Activity Sensor in Skeletal Muscle and Controls Activity-dependent Myosin Switching." *Proceedings of the National Academy of Sciences of the United States of America* 101, no. 29 (July 20, 2004): 10590–10595.

McGuigan, Katrina, Patrick C Phillips, and John H Postlethwait. "Evolution of Sarcomeric Myosin Heavy Chain Genes: Evidence from Fish." *Molecular Biology and Evolution* 21, no. 6 (June 2004): 1042–1056.

McMahon, J A, S Takada, L B Zimmerman, C M Fan, R M Harland, and A P McMahon. "Noggin-mediated Antagonism of BMP Signaling Is Required for Growth and Patterning of the Neural Tube and Somite." *Genes & Development* 12, no. 10 (May 15, 1998): 1438–1452.

Ming, Guo-Li, and Hongjun Song. "Adult Neurogenesis in the Mammalian Brain: Significant Answers and Significant Questions." *Neuron* 70, no. 4 (May 26, 2011): 687–702.

Mittaud, Peggy, Alain A Camilleri, Raffaella Willmann, Susanne Erb-Vögtli, Steven J Burden, and Christian Fuhrer. "A Single Pulse of Agrin Triggers a Pathway That Acts to Cluster Acetylcholine Receptors." *Molecular and Cellular Biology* 24, no. 18 (September 2004): 7841–7854.

Nelsen, Sylvia M, and Jan L Christian. "Site-specific Cleavage of BMP4 by Furin, PC6, and PC7." *The Journal of Biological Chemistry* 284, no. 40 (October 2, 2009): 27157–27166.

Niro, Claire, Josiane Demignon, Stéphane Vincent, Yubing Liu, Julien Giordani, Nicolas Sgarioto, Maryline Favier, Isabelle Guillet-Deniau, Alexandre Blais, and Pascal Maire. "Six1 and Six4 Gene Expression Is Necessary to Activate the Fast-type Muscle Gene Program in the Mouse Primary Myotome." *Developmental Biology* 338, no. 2 (February 15, 2010): 168–182.

Nohno, T, T Ishikawa, T Saito, K Hosokawa, S Noji, D H Wolsing, and J S Rosenbaum. "Identification of a Human Type II Receptor for Bone Morphogenetic Protein-4 That Forms Differential Heteromeric Complexes with Bone Morphogenetic Protein Type I Receptors." *The Journal of Biological Chemistry* 270, no. 38 (September 22, 1995): 22522–22526.

Norton, J D, R W Deed, G Craggs, and F Sablitzky. "Id Helix-loop-helix Proteins in Cell Growth and Differentiation." *Trends in Cell Biology* 8, no. 2 (February 1998): 58–65.

Nosaka, Tetsuya, Sumiyo Morita, Hidetomo Kitamura, Hideaki Nakajima, Fumi Shibata, Yoshihiro Morikawa, Yuki Kataoka, et al. "Mammalian Twisted Gastrulation Is Essential for Skeleto-lymphogenesis." *Molecular and Cellular Biology* 23, no. 8 (April 2003): 2969–2980.

Oelgeschläger, M, J Larraín, D Geissert, and E M De Robertis. "The Evolutionarily Conserved BMP-binding Protein Twisted Gastrulation Promotes BMP Signalling." *Nature* 405, no. 6788 (June 15, 2000): 757–763.

Ogata, T, J M Wozney, R Benezra, and M Noda. "Bone Morphogenetic Protein 2 Transiently Enhances Expression of a Gene, Id (inhibitor of Differentiation), Encoding a Helix-loop-helix Molecule in Osteoblast-like Cells." *Proceedings of the National*

Academy of Sciences of the United States of America 90, no. 19 (October 1, 1993): 9219–9222.

Qi, Xiaoxia, Teng-Guo Li, Jing Hao, Jie Hu, Jing Wang, Holly Simmons, Shigeto Miura, Yuji Mishina, and Guang-Quan Zhao. "BMP4 Supports Self-renewal of Embryonic Stem Cells by Inhibiting Mitogen-activated Protein Kinase Pathways." *Proceedings of the National Academy of Sciences of the United States of America* 101, no. 16 (April 20, 2004): 6027–6032.

Onichtchouk, D, Y G Chen, R Dosch, V Gawantka, H Delius, J Massagué, and C Niehrs. "Silencing of TGF-beta Signalling by the Pseudoreceptor BAMBI." *Nature* 401, no. 6752 (September 30, 1999): 480–485.

Okada, Kumiko, Akane Inoue, Momoko Okada, Yoji Murata, Shigeru Kakuta, Takafumi Jigami, Sachiko Kubo, et al. "The Muscle Protein Dok-7 Is Essential for Neuromuscular Synaptogenesis." *Science (New York, N.Y.)* 312, no. 5781 (June 23, 2006): 1802–1805.

Weiss, A, D McDonough, B Wertman, L Acakpo-Satchivi, K Montgomery, R Kucherlapati, L Leinwand, and K Krauter. "Organization of Human and Mouse Skeletal Myosin Heavy Chain Gene Clusters Is Highly Conserved." *Proceedings of the National Academy of Sciences of the United States of America* 96, no. 6 (March 16, 1999): 2958–2963.

Otis, Jeffrey S, Thomas J Burkholder, and Grace K Pavlath. "Stretch-induced Myoblast Proliferation Is Dependent on the COX2 Pathway." *Experimental Cell Research* 310, no. 2 (November 1, 2005): 417–425.

Owada, Y, T Yoshimoto, and H Kondo. "Spatio-temporally Differential Expression of Genes for Three Members of Fatty Acid Binding Proteins in Developing and Mature Rat Brains." *Journal of Chemical Neuroanatomy* 12, no. 2 (December 1996): 113–122.

Owada, Yuji. "Fatty Acid Binding Protein: Localization and Functional Significance in the Brain." *The Tohoku Journal of Experimental Medicine* 214, no. 3 (March 2008): 213–220.

Park, J M, T Yang, L J Arend, J B Schnermann, C A Peters, M R Freeman, and J P Briggs. "Obstruction Stimulates COX-2 Expression in Bladder Smooth Muscle Cells via Increased Mechanical Stretch." *The American Journal of Physiology* 276, no. 1 Pt 2 (January 1999): F129–136.

Pearce, J J, G Penny, and J Rossant. "A Mouse cerberus/Dan-related Gene Family." *Developmental Biology* 209, no. 1 (May 1, 1999): 98–110.

Pepicelli, C V, A Kispert, D H Rowitch, and A P McMahon. "GDNF Induces Branching and Increased Cell Proliferation in the Ureter of the Mouse." *Developmental Biology* 192, no. 1 (December 1, 1997): 193–198.

Pette, D, and R S Staron. "Myosin Isoforms, Muscle Fiber Types, and Transitions." *Microscopy Research and Technique* 50, no. 6 (September 15, 2000): 500–509.

Piccolo, S, Y Sasai, B Lu, and E M De Robertis. "Dorsoventral Patterning in Xenopus: Inhibition of Ventral Signals by Direct Binding of Chordin to BMP-4." *Cell* 86, no. 4 (August 23, 1996): 589–598.

Ray, R P, K Arora, C Nüsslein-Volhard, and W M Gelbart. "The Control of Cell Fate Along the Dorsal-ventral Axis of the Drosophila Embryo." *Development (Cambridge, England)* 113, no. 1 (September 1991): 35–54.

Räisänen, S R, P Lehenkari, M Tasanen, P Rahkila, P L Härkönen, and H K Väänänen. "Carbonic Anhydrase III Protects Cells from Hydrogen Peroxide-induced Apoptosis." *FASEB Journal: Official Publication of the Federation of American Societies for Experimental Biology* 13, no. 3 (March 1999): 513–522.

Rogers, J H, A Tsirka, A Kovacs, K J Blumer, G W Dorn 2nd, and A J Muslin. "RGS4 Reduces Contractile Dysfunction and Hypertrophic Gene Induction in Galpha q Overexpressing Mice." *Journal of Molecular and Cellular Cardiology* 33, no. 2 (February 2001): 209–218.

Rosen, Vicki. "BMP and BMP Inhibitors in Bone." *Annals of the New York Academy of Sciences* 1068 (April 2006): 19–25.

Rossi, Alberto C, Cristina Mammucari, Carla Argentini, Carlo Reggiani, and Stefano Schiaffino. "Two Novel/ancient Myosins in Mammalian Skeletal Muscles: MYH14/7b and MYH15 Are Expressed in Extraocular Muscles and Muscle Spindles." *The Journal of Physiology* 588, no. Pt 2 (January 15, 2010): 353–364.

Russell, Aaron P, Jonas Feilchenfeldt, Sylvia Schreiber, Manu Praz, Antoinette Crettenand, Charles Gobelet, Christoph A Meier, et al. "Endurance Training in Humans Leads to Fiber Type-specific Increases in Levels of Peroxisome Proliferator-activated Receptor-gamma Coactivator-1 and Peroxisome Proliferator-activated Receptor-alpha in Skeletal Muscle." *Diabetes* 52, no. 12 (December 2003): 2874–2881.

Schiaffino, S, and C Reggiani. "Myosin Isoforms in Mammalian Skeletal Muscle." *Journal of Applied Physiology (Bethesda, Md.: 1985)* 77, no. 2 (August 1994): 493–501.

Schiaffino, S, and C Reggiani. "Molecular Diversity of Myofibrillar Proteins: Gene Regulation and Functional Significance." *Physiological Reviews* 76, no. 2 (April 1996): 371–423.

Segi, Eri, Kayo Haraguchi, Yukihiko Sugimoto, Masayuki Tsuji, Hiroko Tsunekawa, Shigero Tamba, Kazuhito Tsuboi, Satoshi Tanaka, and Atsushi Ichikawa. "Expression of Messenger RNA for Prostaglandin E Receptor Subtypes EP4/EP2 and Cyclooxygenase Isozymes in Mouse Periovulatory Follicles and Oviducts During Superovulation." *Biology of Reproduction* 68, no. 3 (March 2003): 804–811.

Sieber, Christina, Jessica Kopf, Christian Hiepen, and Petra Knaus. "Recent Advances in BMP Receptor Signaling." *Cytokine & Growth Factor Reviews* 20, no. 5–6 (December 2009): 343–355.

Singh, Suman K, Waqas A Abbas, and Desmond J Tobin. "Bone Morphogenetic Proteins Differentially Regulate Pigmentation in Human Skin Cells." *Journal of Cell Science* (May 28, 2012). http://www.ncbi.nlm.nih.gov/pubmed/22641693.

Sly, W S, and P Y Hu. "Human Carbonic Anhydrases and Carbonic Anhydrase Deficiencies." *Annual Review of Biochemistry* 64 (1995): 375–401.

Spicer, S S, Z H Ge, R E Tashian, D J Hazen-Martin, and B A Schulte. "Comparative Distribution of Carbonic Anhydrase Isozymes III and II in Rodent Tissues." *The American Journal of Anatomy* 187, no. 1 (January 1990): 55–64.

Stanton, L W, P A Ponte, R T Coleman, and M A Snyder. "Expression of CA III in Rodent Models of Obesity." *Molecular Endocrinology (Baltimore, Md.)* 5, no. 6 (June 1991): 860–866.

Staron, R S, and D Pette. "The Continuum of Pure and Hybrid Myosin Heavy Chain-based Fibre Types in Rat Skeletal Muscle." *Histochemistry* 100, no. 2 (August 1993): 149–153.

Starke-Reed, P E, and C N Oliver. "Protein Oxidation and Proteolysis During Aging and Oxidative Stress." *Archives of Biochemistry and Biophysics* 275, no. 2 (December 1989): 559–567.

Steiner, Barbara, Friederike Klempin, Liping Wang, Monika Kott, Helmut Kettenmann, and Gerd Kempermann. "Type-2 Cells as Link Between Glial and Neuronal Lineage in Adult Hippocampal Neurogenesis." *Glia* 54, no. 8 (December 2006): 805–814.

Sterrenburg, Ellen, Caroline G C van der Wees, Stefan J White, Rolf Turk, Renée X de Menezes, Gert-Jan B van Ommen, Johan T den Dunnen, and Peter A C 't Hoen. "Gene Expression Profiling Highlights Defective Myogenesis in DMD Patients and a

Possible Role for Bone Morphogenetic Protein 4." *Neurobiology of Disease* 23, no. 1 (July 2006): 228–236.

Storch, Judith, and Lindsay McDermott. "Structural and Functional Analysis of Fatty Acid-binding Proteins." *Journal of Lipid Research* 50 Suppl (April 2009): S126–131.

Sudo, Satoko, Orna Avsian-Kretchmer, Lora Shuo Wang, and Aaron J W Hsueh. "Protein Related to DAN and Cerberus Is a Bone Morphogenetic Protein Antagonist That Participates in Ovarian Paracrine Regulation." *The Journal of Biological Chemistry* 279, no. 22 (May 28, 2004): 23134–23141.

Susperregui, Antonio R G, Cristina Gamell, Edgardo Rodríguez-Carballo, Maria José Ortuño, Ramon Bartrons, José Luis Rosa, and Francesc Ventura. "Noncanonical BMP Signaling Regulates Cyclooxygenase-2 Transcription." *Molecular Endocrinology (Baltimore, Md.)* 25, no. 6 (June 2011): 1006–1017.

Tang, Jun, Min Song, Yanyan Wang, Xiaotang Fan, Haiwei Xu, and Yun Bai. "Noggin and BMP4 Co-modulate Adult Hippocampal Neurogenesis in the APP(swe)/PS1(DeltaE9) Transgenic Mouse Model of Alzheimer's Disease." *Biochemical and Biophysical Research Communications* 385, no. 3 (July 31, 2009): 341–345.

Tashian, R E. "The Carbonic Anhydrases: Widening Perspectives on Their Evolution, Expression and Function." *BioEssays: News and Reviews in Molecular, Cellular and Developmental Biology* 10, no. 6 (June 1989): 186–192.

ten Dijke, P, H Yamashita, T K Sampath, A H Reddi, M Estevez, D L Riddle, H Ichijo, C H Heldin, and K Miyazono. "Identification of Type I Receptors for Osteogenic Protein-1 and Bone Morphogenetic Protein-4." *The Journal of Biological Chemistry* 269, no. 25 (June 24, 1994): 16985–16988.

Terada, Shin, Masahide Goto, Miyuki Kato, Kentaro Kawanaka, Teruhiko Shimokawa, and Izumi Tabata. "Effects of Low-intensity Prolonged Exercise on PGC-1 mRNA Expression in Rat Epitrochlearis Muscle." *Biochemical and Biophysical Research Communications* 296, no. 2 (August 16, 2002): 350–354.

Tokudome, Takeshi, Ichiro Kishimoto, Takeshi Horio, Yuji Arai, Daryl O Schwenke, Jun Hino, Ichiro Okano, et al. "Regulator of G-protein Signaling Subtype 4 Mediates Antihypertrophic Effect of Locally Secreted Natriuretic Peptides in the Heart." *Circulation* 117, no. 18 (May 6, 2008): 2329–2339.

Ueno, Shuichi, Gilbert Weidinger, Tomoaki Osugi, Aimee D Kohn, Jonathan L Golob, Lil Pabon, Hans Reinecke, Randall T Moon, and Charles E Murry. "Biphasic Role for Wnt/beta-catenin Signaling in Cardiac Specification in Zebrafish and Embryonic Stem Cells." *Proceedings of the National Academy of Sciences of the United States of America* 104, no. 23 (June 5, 2007): 9685–9690.

Umemoto, Takenao, Yuuma Furutani, Masaru Murakami, Tohru Matsui, and Masayuki Funaba. "Endogenous Bmp4 in Myoblasts Is Required for Myotube Formation in C2C12 Cells." *Biochimica Et Biophysica Acta* 1810, no. 12 (December 2011): 1127–1135.

Urist, M R. "Bone: Formation by Autoinduction." *Science (New York, N.Y.)* 150, no. 3698 (November 12, 1965): 893–899.

Valenzuela, D M, T N Stitt, P S DiStefano, E Rojas, K Mattsson, D L Compton, L Nuñez, J S Park, J L Stark, and D R Gies. "Receptor Tyrosine Kinase Specific for the Skeletal Muscle Lineage: Expression in Embryonic Muscle, at the Neuromuscular Junction, and After Injury." *Neuron* 15, no. 3 (September 1995): 573–584.

Vock, Vita M, Olga N Ponomareva, and Mendell Rimer. "Evidence for Muscle-dependent Neuromuscular Synaptic Site Determination in Mammals." *The Journal of Neuroscience: The Official Journal of the Society for Neuroscience* 28, no. 12 (March 19, 2008): 3123–3130.

von Bubnoff, A, and K W Cho. "Intracellular BMP Signaling Regulation in Vertebrates: Pathway or Network?" *Developmental Biology* 239, no. 1 (November 1, 2001): 1–14.

Wade, R, P Gunning, R Eddy, T Shows, and L Kedes. "Nucleotide Sequence, Tissue-specific Expression, and Chromosome Location of Human Carbonic Anhydrase III: The Human CAIII Gene Is Located on the Same Chromosome as the Closely Linked CAI and CAII Genes." *Proceedings of the National Academy of Sciences of the United States of America* 83, no. 24 (December 1986): 9571–9575.

Wang, Yong-Xu, Chun-Li Zhang, Ruth T Yu, Helen K Cho, Michael C Nelson, Corinne R Bayuga-Ocampo, Jungyeob Ham, Heonjoong Kang, and Ronald M Evans. "Regulation of Muscle Fiber Type and Running Endurance by PPARdelta." *PLoS Biology* 2, no. 10 (October 2004): e294.

Wang, Jun, Stephanie B Greene, Margarita Bonilla-Claudio, Ye Tao, Jue Zhang, Yan Bai, Zheng Huang, Brian L Black, Fen Wang, and James F Martin. "Bmp Signaling Regulates Myocardial Differentiation from Cardiac Progenitors Through a MicroRNA-mediated Mechanism." *Developmental Cell* 19, no. 6 (December 14, 2010): 903–912.

Wardle, F C, J V Welch, and L Dale. "Bone Morphogenetic Protein 1 Regulates Dorsal-ventral Patterning in Early Xenopus Embryos by Degrading Chordin, a BMP4 Antagonist." *Mechanisms of Development* 86, no. 1–2 (August 1999): 75–85.

Wigmore, Peter M, and Darrell J R Evans. "Molecular and Cellular Mechanisms Involved in the Generation of Fiber Diversity During Myogenesis." *International Review of Cytology* 216 (2002): 175–232.

Willars, Gary B. "Mammalian RGS Proteins: Multifunctional Regulators of Cellular Signalling." *Seminars in Cell & Developmental Biology* 17, no. 3 (June 2006): 363–376.

Winnier, G, M Blessing, P A Labosky, and B L Hogan. "Bone Morphogenetic Protein-4 Is Required for Mesoderm Formation and Patterning in the Mouse." *Genes & Development* 9, no. 17 (September 1, 1995): 2105–2116.

Wistrand, P J, N D Carter, and H Askmark. "Induction of Rat Muscle Carbonic Anhydrase by Denervation Demonstrated with Immunofluorescence." *Comparative Biochemistry and Physiology. A, Comparative Physiology* 86, no. 1 (1987): 177–184.

Wrana, J L, L Attisano, R Wieser, F Ventura, and J Massagué. "Mechanism of Activation of the TGF-beta Receptor." *Nature* 370, no. 6488 (August 4, 1994): 341–347.

Wu, C, Q Zeng, K J Blumer, and A J Muslin. "RGS Proteins Inhibit Xwnt-8 Signaling in Xenopus Embryonic Development." *Development (Cambridge, England)* 127, no. 13 (July 2000): 2773–2784.

Xia, Yin, Paul B Yu, Yisrael Sidis, Hideyuki Beppu, Kenneth D Bloch, Alan L Schneyer, and Herbert Y Lin. "Repulsive Guidance Molecule RGMa Alters Utilization of Bone Morphogenetic Protein (BMP) Type II Receptors by BMP2 and BMP4." *The Journal of Biological Chemistry* 282, no. 25 (June 22, 2007): 18129–18140.

Xiao, Yong-Tao, Li-Xin Xiang, and Jian-Zhong Shao. "Bone Morphogenetic Protein." *Biochemical and Biophysical Research Communications* 362, no. 3 (October 26, 2007): 550–553.

Yang, X, W Li, E D Prescott, S J Burden, and J C Wang. "DNA Topoisomerase IIbeta and Neural Development." *Science (New York, N.Y.)* 287, no. 5450 (January 7, 2000): 131–134.

Yang, X, S Arber, C William, L Li, Y Tanabe, T M Jessell, C Birchmeier, and S J Burden. "Patterning of Muscle Acetylcholine Receptor Gene Expression in the Absence of Motor Innervation." *Neuron* 30, no. 2 (May 2001): 399–410.

Ying, Y, X M Liu, A Marble, K A Lawson, and G Q Zhao. "Requirement of Bmp8b for the Generation of Primordial Germ Cells in the Mouse." *Molecular Endocrinology (Baltimore, Md.)* 14, no. 7 (July 2000): 1053–1063.

Ying, Y, and G Q Zhao. "Cooperation of Endoderm-derived BMP2 and Extraembryonic Ectoderm-derived BMP4 in Primordial Germ Cell Generation in the Mouse." *Developmental Biology* 232, no. 2 (April 15, 2001): 484–492.

Ying, Y, X Qi, and G Q Zhao. "Induction of Primordial Germ Cells from Murine Epiblasts by Synergistic Action of BMP4 and BMP8B Signaling Pathways."

Proceedings of the National Academy of Sciences of the United States of America 98, no. 14 (July 3, 2001): 7858–7862.

Ying, Qi Long, Jennifer Nichols, Ian Chambers, and Austin Smith. "BMP Induction of Id Proteins Suppresses Differentiation and Sustains Embryonic Stem Cell Self-renewal in Collaboration with STAT3." *Cell* 115, no. 3 (October 31, 2003): 281–292.

Zhang, H, and A Bradley. "Mice Deficient for BMP2 Are Nonviable and Have Defects in Amnion/chorion and Cardiac Development." *Development (Cambridge, England)* 122, no. 10 (October 1996): 2977–2986.

Zhang, Donghui, Cristin M Ferguson, Regis J O'Keefe, J Edward Puzas, Randy N Rosier, and Paul R Reynolds. "A Role for the BMP Antagonist Chordin in Endochondral Ossification." *Journal of Bone and Mineral Research: The Official Journal of the American Society for Bone and Mineral Research* 17, no. 2 (February 2002): 293–300.

Zhang, Jing, Julie L Lefebvre, Shuxia Zhao, and Michael Granato. "Zebrafish Unplugged Reveals a Role for Muscle-specific Kinase Homologs in Axonal Pathway Choice." *Nature Neuroscience* 7, no. 12 (December 2004): 1303–1309.

Zhang, Bin, Chuan Liang, Ryan Bates, Yiming Yin, Wen-Cheng Xiong, and Lin Mei. "Wnt Proteins Regulate Acetylcholine Receptor Clustering in Muscle Cells." *Molecular Brain* 5, no. 1 (February 6, 2012): 7.

Zhao, G Q, and B L Hogan. "Evidence That Mouse Bmp8a (Op2) and Bmp8b Are Duplicated Genes That Play a Role in Spermatogenesis and Placental Development." *Mechanisms of Development* 57, no. 2 (July 1996): 159–168.

Zhou, H, D J Glass, G D Yancopoulos, and J R Sanes. "Distinct Domains of MuSK Mediate Its Abilities to Induce and to Associate with Postsynaptic Specializations." *The Journal of Cell Biology* 146, no. 5 (September 6, 1999): 1133–1146.

Zhu, Dan, Zhihua Yang, Zhenge Luo, Shiwen Luo, Wen C Xiong, and Lin Mei. "Muscle-specific Receptor Tyrosine Kinase Endocytosis in Acetylcholine Receptor Clustering in Response to Agrin." *The Journal of Neuroscience: The Official Journal of the Society for Neuroscience* 28, no. 7 (February 13, 2008): 1688–1696.

Zimmerman, L B, J M De Jesús-Escobar, and R M Harland. "The Spemann Organizer Signal Noggin Binds and Inactivates Bone Morphogenetic Protein 4." *Cell* 86, no. 4 (August 23, 1996): 599–606.

Ziskind-Conhaim, L, and J I Bennett. "The Effects of Electrical Inactivity and Denervation on the Distribution of Acetylcholine Receptors in Developing Rat Muscle." *Developmental Biology* 90, no. 1 (March 1982): 185–197.

Zong, Yinong, Bin Zhang, Shenyan Gu, Kwangkook Lee, Jie Zhou, Guorui Yao, Dwight Figueiredo, Kay Perry, Lin Mei, and Rongsheng Jin. "Structural Basis of agrin-LRP4-MuSK Signaling." *Genes & Development* 26, no. 3 (February 1, 2012): 247–258.

Zúñiga, A, A P Haramis, A P McMahon, and R Zeller. "Signal Relay by BMP Antagonism Controls the SHH/FGF4 Feedback Loop in Vertebrate Limb Buds." *Nature* 401, no. 6753 (October 7, 1999): 598–602.

Figures

Figure 1.1

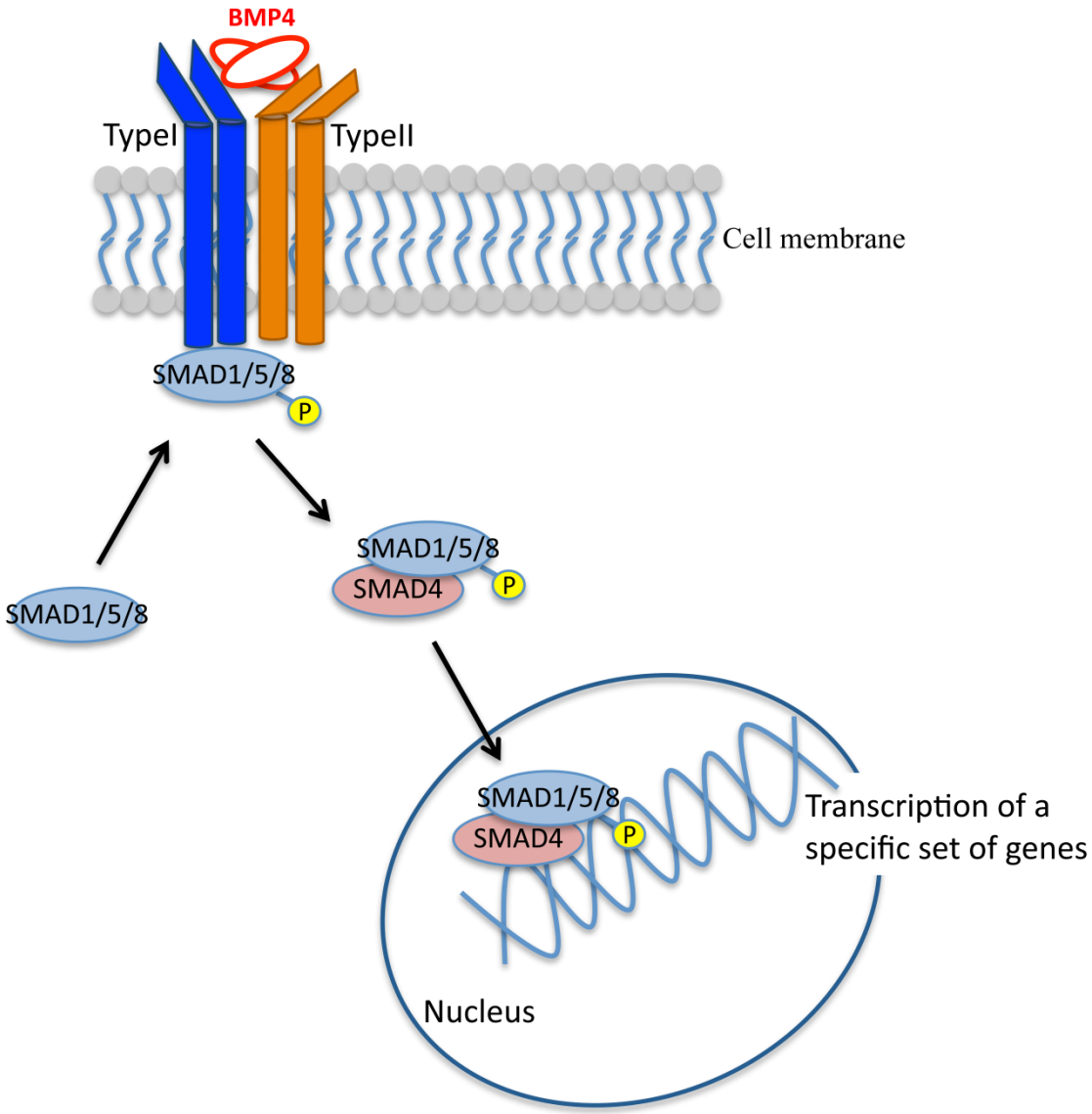

Figure 1.1

BMP pathway. Upon ligand binding and hexameric ligand-receptor formation, intracellular SMAD1/5/8 is phosphorylated by type-1 BMP receptors (Kretzschmar et al., 1997). Phosphorylated SMAD1/5/8 then associates with co-SMAD, SMAD4, and this complex translocates to and accumulates in the nucleus to serve as a transcriptional repressor or activator complex for a specific set of genes (Lagna et al., 1996, Liu et al., 1996, Hoodless et al., 1996).

Figure 1.2

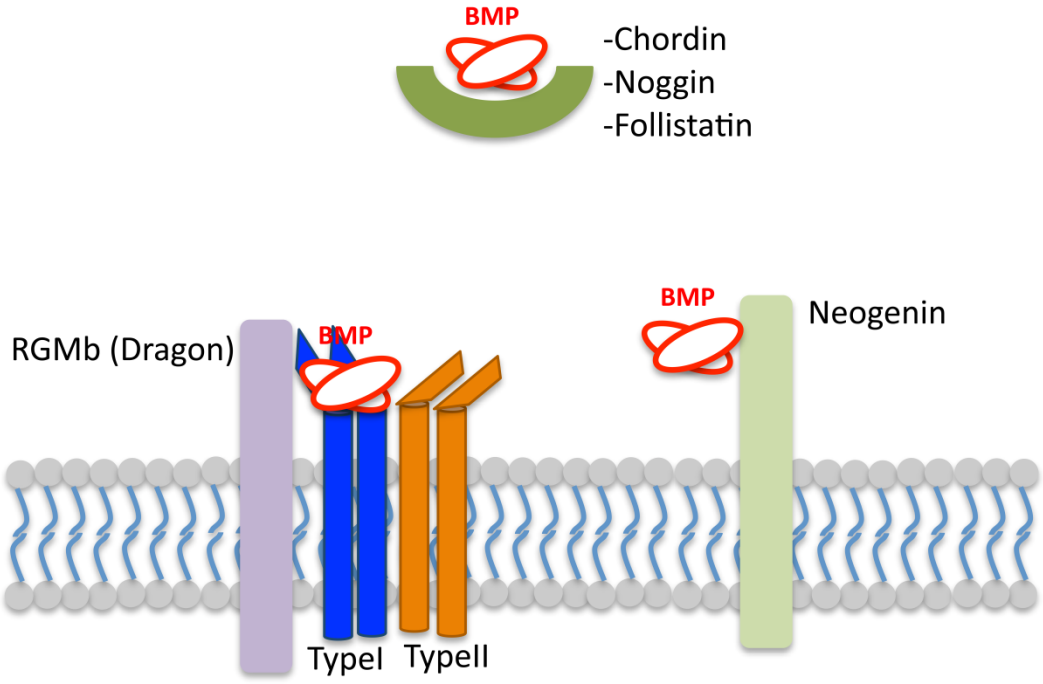
BMP
-Chordin
-Noggin
-Follistatin
BMP
Neogenin
RGMb (Dragon)
BMP
TypeI
TypeII

Figure 1.2

BMP4 inhibitors and co-receptors. Secreted antagonists of BMPs such as Chordin, Noggin and Follistatin bind to the ligand dimer and prevent it from binding to the receptor complex (Zimmerman et al., 1996, Piccolo et al., 1996, Fainsod et al., 1997). Dragon family co-receptors associate with type-1 BMP receptors and the BMPs and enhance the signaling initiated by the ligand (Halbrooks et al., 2007). Other surface molecules such as Neogenin act as inhibitory receptors for BMPs and their downstream signaling (Hagihara et al., 2011).

Figure 1.3

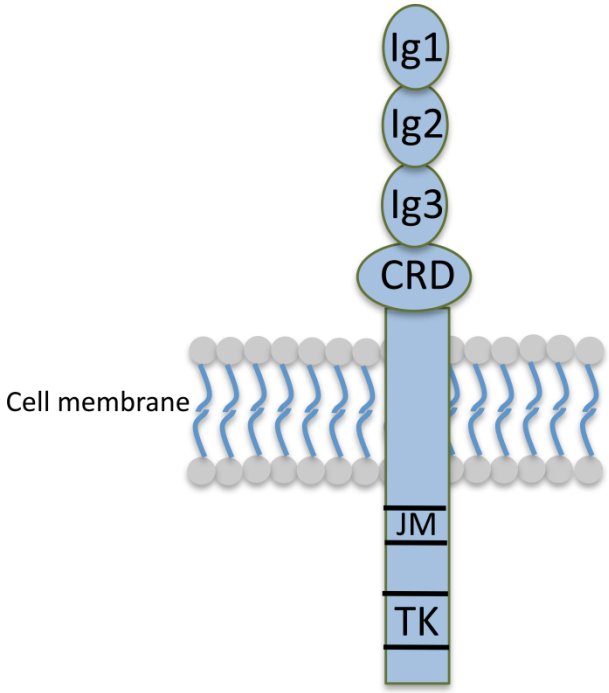

Figure 1.3

Schematic representation of MuSK. MuSK has three immunoglobulin-like (Ig) domains and a cycteine-rich domain (CRD) in its ectodomain. Its intracellular part comprises a juxtamembrane and a catalytic tyrosine kinase domain.

Figure 1.4

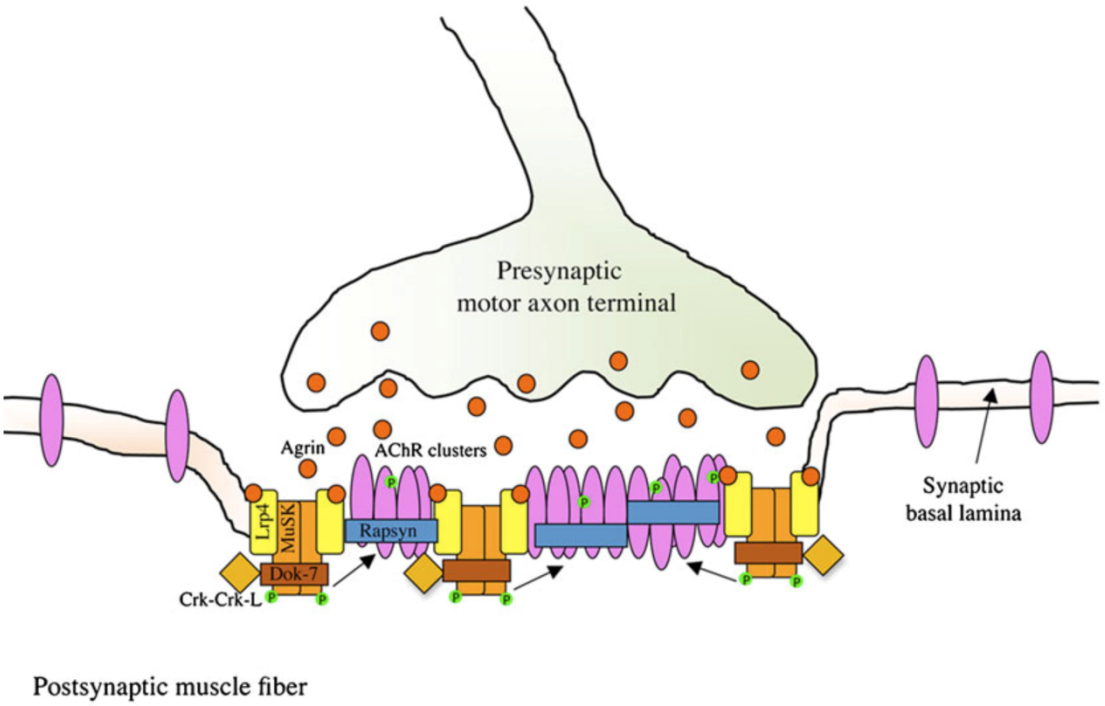
Presynaptic
motor axon terminal
Agrin
AChR clusters
Lrp4
MuSK
Rapsyn
Dok-7
Crk-Crk-L
Synaptic
basal lamina
Postsynaptic muscle fiber

Figure 1.4.

NMJ and AChR clusters (Adapted from Ferraro et al., 2012). Neural-derived agrin released from presynaptic terminal binds to Lrp4 and induces the phosphorylation and activation of MuSK (Herbst et al., 2000, Zhou et al. 1999, Zhu et al. 2008, Zong et al., 2012, Zang et al., 2011). Phosphorylated MuSK recruits Dok-7, which further fosters MuSK phosphorylation (Bergamin et al. 2010; Okada et al., 2006). This leads to the formation of AChR clusters and their stabilization. The adaptor protein rapsyn anchors AChRs and helps the stability of the clusters (Borges et al., 2008).

Figure 1.5

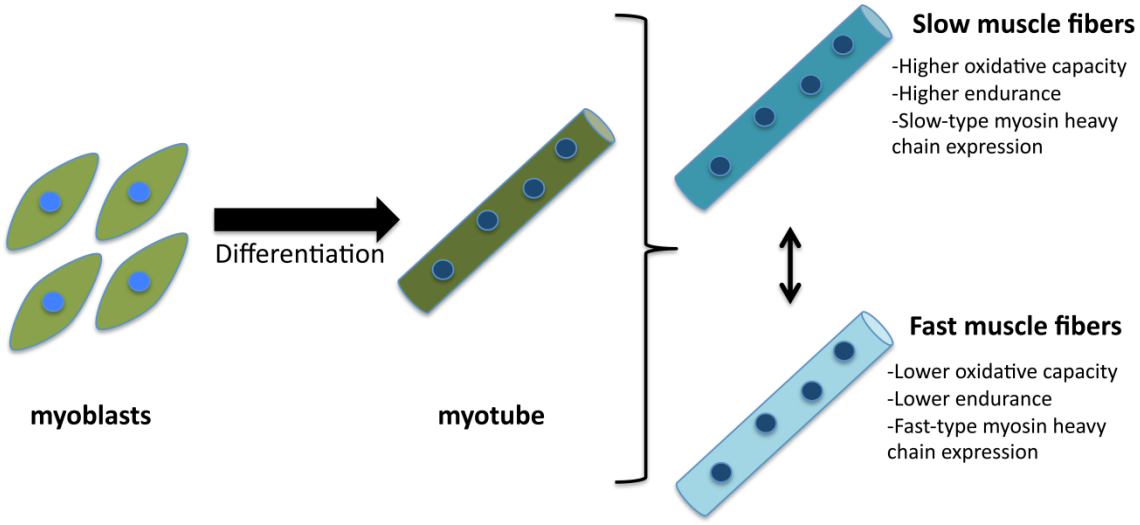
Differentiation
myoblasts
myotube
Slow muscle fibers
-Higher oxidative capacity
-Higher endurance
-Slow-type myosin heavy chain expression
Fast muscle fibers
-Lower oxidative capacity
-Lower endurance
-Fast-type myosin heavy chain expression

Figure 1.5

Skeletal muscle fiber types. Mononuclear myoblasts undergo fusion and differentiate into multi-nucleated myofibers, which can express different contractile properties. Two main categories of fibers and their properties are shown. Slow fibers have higher oxidative capacity and endurance compared to the fast fibers (Bassel-Duby and Olson, 2006). Slow myosin heavy chain isoforms are expressed in slow fibers, while fast myosin heavy chain isoforms are expressed in fast fibers. Differences among progenitor cells, growth factors and changes neural activity can trigger fiber type switch programs (Wigmore and Evans, 2002).

CHAPTER 2

The receptor tyrosine kinase MuSK binds BMPs and selectively regulates their signaling

Atilgan Yilmaz[1,3], Chandramohan Kattamuri[2], Christoph Schorl[3], Tom Thompson[2], Justin Fallon[1]

[1]Department of Neuroscience, Brown University, Providence, Rhode Island 02912, USA

[2] Department of Molecular Genetics, Biochemistry and Microbiology, University of Cincinnati Medical Sciences Building, Cincinnati, OH 45267, USA

[3] Department of Molecular Biology, Cell Biology and Biochemistry, Brown University, Providence, Rhode Island 02912, USA

SPR experiments in Figure 2 and Table 1 were conducted by Chandramohan Kattamuri.

Microarray experiments in Figures 5 and 6 were conducted by Christoph Schorl and me.

The rest of the experiments were conducted by me.

Abstract:

Bone morphogenic proteins (BMPs) induce signals in various tissues with unique outcomes. They are tightly regulated both during development and in adult. Various extracellular interactions between BMPs and their regulator proteins, both secreted and membrane-bound ones have been identified as means of regulation of BMP pathway. Here we propose a cell-type specific regulation of BMPs by Muscle Specific Kinase (MuSK), a receptor tyrosine kinase that is a master regulator in neuromuscular junction formation with high expression in myogenic cells. We show that MuSK directly binds to BMP4, BMP2 and BMP7 with low nM affinities. MuSK binding to BMP4 is partially mediated through the third immunoglobulin-like domain (Ig3) of MuSK that had been thought to be dispensable for MuSK's role at the neuromuscular junction. BMP4-induced pSMAD5 levels and ID1 transcript levels are reduced in the absence of MuSK in undifferentiated myoblasts. Furthermore, in these cells MuSK is required for BMP4-induced expression of a subset of genes, including RGS4. In cultured myotubes, MuSK positively regulates BMP4-induced expression of myosin heavy chain 15 (Myh15) and carbonic anhydrase 3 (Car3) both of which are expressed at higher levels in muscles with more slow-type fibers in mice. These results indicate a potential role for MuSK-BMP4 interaction in fiber type composition of muscle tissue. To our knowledge this is the first study that shows MuSK as a BMP regulator and attributes a non-synaptogenic role to it in myogenic cells. We hypothesize that our results point to a general mechanism for regulating BMP pathway with the use of tissue-specific proteins. They also

potentially give insights for the functions of MuSK in non-myogenic tissues (i.e. brain) where it is expressed at low levels.

Introduction

The interaction between the cells and their environment dictates various decisions that the cells have to make in terms of their survival, differentiation or death. Intercellular communication is one such interaction that has intricately evolved in multicellular organisms in order to tightly control the behavior of individual cells in complex tissue structures. One of the most commonly used communication systems involves a secreted polypeptide that is recognized by a cell surface receptor. The same polypeptide signal can act on different cell types with different outcomes, including differential transcriptional or post-transcriptional events. Maintaining this specificity is fundamental to distinguish cell fates or cellular responses in various tissues. Therefore, a very crucial question about signaling molecules is how the cell- or tissue-type specificity is achieved in their responses.

BMP4 belongs to the family of Bone Morphogenic Proteins (BMPs), which is a large group of phylogenetically conserved signaling molecules that are in turn a subfamily of the transforming growth factor-β (TGFβ) superfamily. Two different classes of receptors, type-1 (Alk2,4 or 6) and type-2 (BMPRII, ActRIIa), bind to BMP4 on the cell surface (ten Dijke et al., 1994, de Sousa Lopes et al., 2004, Nohno et al., 1995, Xia et al., 2007). The binding of the ligand to the type-1 receptor is followed by the phosphorylation of this receptor by the constitutively active type-2 receptor (Wrana

et al., 1994). This phosphorylation activates type 1 receptor that in turn phosphorylates the cytosolic intermediate of the pathway, SMAD1/5/8 (Kretzschmar et al., 1997). Phosphorylated SMAD1/5/8 forms a complex with SMAD4 and translocates to and accumulates in the nucleus where it functions as part of a transcriptional activator or repressor complex for a range of genes at different stages of development or in adult (Lagna et al., 1996, Liu et al., 1996, Hoodless et al., 1996). For example, although BMP4 is an inducer of differentiation in osteoblasts (Miyama et al., 1999), in muscle precursor cells it is shown to inhibit differentiation by inducing the transcription of Id1 gene, a well-characterized BMP target (Ono et al., 2011). Understanding how BMP4 is regulated is key to explain such major phenotypic changes seen in different cells as a response to the same BMP4 signal.

Having pivotal roles at different stages of development, in adult and in various tissues it is not unexpected that BMPs and the pathway they initiate are tightly regulated. One of the most common ways of regulation is to control the availability of the ligand extracellularly by either secreted molecules or surface receptors. Among the best-characterized examples of such secreted proteins are noggin, chordin and follistatin among others. These inhibitors bind to BMP4 and prevent it from associating with its signaling receptors (Zimmerman et al., 1996, Piccolo et al., 1996, Fainsod et al., 1997). Another regulatory mechanism involves surface molecules that may act as stimulatory or inhibitory co-receptors. For example, the GPI-anchored Dragon family of co-receptors was shown to positively regulate BMP

signaling (Halbrooks et al., 2007). On the other hand, the transmembrane protein, BAMBI, inhibits BMP signaling by acting as a pseudo-type1 receptor and occupying the available type-2 receptors (Onichtchouk et al., 1999). Recently, Neogenin, a receptor for netrins and proteins of the repulsive guidance molecule family, was shown to bind BMPs and inhibit Smad signal transduction through the activation of RhoA (Hagihara et al., 2011). Another interesting class of surface molecules regulating BMPs is the receptor tyrosine kinase family. Stem cell factor receptor (c-kit) has been shown to interact with type-2 receptor BMPRII and positively regulate BMP signaling (Hassel et al., 2006). Although it has not yet been shown for BMPs, the receptor tyrosine kinase Ror2 binds to the type-1 receptor Alk6 and modulates the signaling mediated by another TGF-β family member, GDF5, through inhibition of the Smad-dependent signaling and the activation of a Smad-independent pathway (Sammar et al., 2004, Sammar et al., 2009). These observations raise the question whether other tyrosine kinases may also regulate BMP pathway.

MuSK is a receptor tyrosine kinase that is predominantly expressed at the neuromuscular junctions (NMJ) in muscle cells (Valenzuela et al., 1995). It was shown to bind to LRP4 (Kim et al., 2008) and be activated by autophosphorylation upon binding of neural derived proteoglycan, agrin to LRP4 (Herbst et al., 2000, Zhou et al. 1999, Zhu et al. 2008, Zong et al., 2012). This activation leads to a cascade of events that is crucial for NMJ formation, maturation and stability and MuSK has a master regulatory role for these events (DeChiara et al., 1996). Studies on MuSK have been mainly focused on its roles at the NMJs. However, MuSK is also expressed

at lower levels at the extrajunctional membrane of muscle cells (Bowen et al., 1998) and in other tissues such as brain (Garcia-Osta et al., 2006). This expression profile indicates that MuSK may have other roles than what has been described so far.

Here we report that MuSK binds to BMP4 and modulates BMP4 signaling in myogenic cells. We show that in the absence of MuSK BMP4-induced SMAD5 phoshorylation and ID1 transcription are decreased. MuSK also selectively regulates BMP4-induced transcriptional response for a subset of genes. A transcriptome/microarray analysis revealed over 250 upregulated genes in myoblasts and over 150 up-regulated genes in myotubes only in the presence of MuSK. We confirmed that BMP4-induced transcription of RGS4, which is important for G-protein signaling, was dependent on the presence of MuSK. We also identified two BMP4-induced transcripts in myotubes, Carbonic Anhydrase 3 (Car3) and Myosin Heavy Chain 15 (Myh15) that were regulated by MuSK and were enriched in muscles enriched with slow-twitch muscle fibers in mice. Our results suggest that MuSK is a muscle-specific BMP4 regulator and it modulates BMP4-induced transcriptional response distinctively in undifferentiated and differentiated muscle cells, with potential downstream regulation on G-protein signaling and muscle fiber-type specification.

Results

MuSK binds to BMPs

To test for potential BMP regulators in myogenic cells we used the reporter cell line, C2C12BRA, which was generated by stably transfecting the immortalized myogenic C2C12 cells with a plasmid consisting of BMP-responsive elements from the Id1 promoter upstream of a luciferase reporter gene (Zilberberg et al., 2007). C2C12BRA cells were treated with BMP4 along with a purified recombinant MuSK ectodomain construct (Figure 2.1a). After 8 hours of treatment luciferase activity was measured for the indicated conditions. At a concentration between 50 and 100nM the soluble MuSK ectodomain inhibited BMP4 activity by 50%. The irrelevant his-tagged control protein used at 200nM did not show any significant inhibition of BMP4 activity. These experiments showed that the soluble MuSK ectodomain specifically inhibits BMP4 activity, as judged by the decreased luciferase activity (Figure 2.1b).

The ability of soluble MuSK ectodomain to inhibit BMP4 activity could reflect either a direct binding between these molecules or the presence of an indirect regulatory loop mediated by the MuSK ectodomain. In order to differentiate between those two possibilities, we performed a solution binding experiment. Soluble BMP4 was preincubated with MuSK ectodomain or the irrelevant His-tagged protein. MuSK ectodomain and the control protein were precipitated via their 6xHis-tag. Residual BMP4 activity in solution was then measured in the C2C12BRA reporter line (Figure

2.1c). When MuSK was pulled down, BMP4 activity decreased about 40%, indicating BMP4 co-precipitated with MuSK. There was not any significant inhibition in BMP4 activity when the irrelevant His-tagged control was pulled down. Specific pull-down of BMP4 by the MuSK ectodomain was confirmed by ELISA analysis of the pelleted ecto-MuSK-BMP4 complex (Figure 2.1d). Taken together, these results indicate that the MuSK ectodomain directly binds to BMP4.

To confirm and extend these results we assessed the kinetics and the affinity of the interaction between BMP4 and MuSK ectodomain using Surface Plasmon Resonance (SPR). BMP4 was immobilized as the ligand and MuSK ectodomain construct was used as the analyte. A kinetic analysis with the use of a heterogenous ligand model showed low nanomolar binding affinity for BMP4-MuSK interaction (Figure 2.2a and Table 2.1). BMP4 is closely related to BMP2 (von Bubnoff et al., 2001) and has been shown to form heterodimers with BMP7 (Suzuki et al, 1997). We investigated whether MuSK ectodomain could also bind to other closely related BMP family members. As shown in Fig. 2.2a and in Table 2.1, SPR analysis revealed that BMP2 and BMP7 bound to MuSK ectodomain with similar affinities to that of BMP4. Thus, the MuSK ectodomain binds to a closely related set of the BMPs that includes BMP2, 4 and 7.

MuSK Ig3 domain is required for BMP4 binding

We next asked if alternative splicing of MuSK might regulate its interaction with BMP4. One major splice isoform of MuSK lacks the Ig3 domain (Hesser et al., 1999). We designed Fc-fusion MuSK ectodomain constructs with ('full length') or without Ig3 domain (ΔIg3) (Figure 2.3a). Equivalent amounts of these constructs were immobilized on 96-well plates and were incubated with a range of BMP4 concentrations (Figure 2.3c). As shown in Figure 2.3b, BMP4 showed saturable, high affinity binding to FL-ecto-MuSK, while a lower and non-saturable binding was observed to the ΔIg3-ecto-MuSK. We also wanted to see if the deletion of Ig3 domain interfered with the overall MuSK structure, which could be one reason for its decreased binding to BMP4. For this, we tested the binding of each MuSK construct to biglycan, as we recently reported that biglycan binds to MuSK and potentiates its agrin-induced phosphorylation (Amenta et al., 2012). Biglycan was incubated with immobilized full-length and ΔIg3-MuSK ectodomain constructs and bound biglycan was detected. No difference was seen in the binding of biglycan to either construct, indicating the decrease in BMP4 binding was specific (Figure 2.3d). We conclude from these results that the Ig3 domain of MuSK is necessary for its BMP4 binding.

MuSK regulates canonical BMP4 signaling

We wanted to assess the possibility whether MuSK could have any regulatory effects on canonical BMP4 signaling, which is marked by SMAD1/5/8 phosphorylation upon ligand binding to the receptors and the pSMAD1/5/8 dependent transcription of downstream immediate gene targets (Kretzschmar et al., 1997, Liu et al., 1996,

Hoodless et al., 1996). To test this, we first compared the BMP4-induced pSMAD1/5/8 levels between wild type and MuSK null myoblasts by western blotting. In the absence of MuSK, a reduction was seen in the dose-response curve of BMP4-induced SMAD1/5/8 phosphorylation, indicating that MuSK positively regulates this early upstream event of BMP4 pathway (Figure 2.4a, 2.4b). We then wanted to test any potential transcriptional regulation by MuSK and analyzed BMP4-induced Id1 transcript levels, since Id1 is one of the best characterized BMP downstream gene targets and its BMP4-induced transcription depends on SMAD1/5/8 phosphorylation (Ogata et al., 1993; Hollnagel et al., 1999; Lopez-Rovira et al., 2002; Korchynskyi et al., 2002). We analyzed BMP4-induced Id1 transcripts in wild type and MuSK null myoblasts at an early time point at which the Id1 transcription peaks (data not shown). In the absence of MuSK BMP4-induced Id1 transcript levels were reduced compared to wild type levels (Figure 2.4c). This result was in accord with the decrease in BMP4-induced pSMAD1/5/8 in MuSK null myoblasts.

We also wanted to know if the reduction seen in the absence of MuSK could result from differences in the compartmentalization of pSMAD1/5/8 in the cell, aside from the reduction in its levels. To test this idea, we immunostained wild type and MuSK null myoblasts for pSMAD1/5/8. Although we did not observe any differential effect of BMP4 treatment in the distribution of pSMAD1/5/8 between wild type and MuSK null cultures (data not shown), there was a striking difference in pSMAD1/5/8 distribution under resting conditions between these cells. Wild type myoblasts

expressed distinct cytosolic pSMAD1/5/8 granules, which were reduced dramatically in MuSK null myoblasts (Figure 2.4d, 2.4e). This pattern of distribution did not change upon BMP4 treatment (data not shown).

MuSK selectively regulates distinct sets of BMP4-induced genes in myoblasts and myotubes

We investigated whether MuSK was required for the transcription of any downstream BMP4 target genes in myogenic cells. In order to test this possibility we performed a microarray analysis and compared BMP4-induced transcripts between wild type and MuSK null cells. To test whether cell context makes any difference for MuSK regulation we included both the undifferentiated myoblast and the differentiated myotube cultures in our analysis. Serum-deprived wild type and MuSK null cultures were treated with BMP4. RNA was harvested from the cultures and reverse transcribed into cDNA, which was then hybridized to Affymetrix array chips. Cultures were treated for 8 hours, a relatively long time for transcript analysis, in order to detect the transcription of potentially regulated late response genes, as well. In myoblasts, 269 upregulated genes were identified only in wild-type cells, indicating that these were MuSK-dependent BMP4 responses (Figure 2.5a and Supp. Table 1). 107 genes were upregulated both in wild type and MuSK null myoblasts and therefore were not qualitatively regulated by MuSK (Figure 2.5a and Supp. Table 2). 108 other genes were upregulated only in MuSK null myoblasts (Figure 2.5a and Supp. Table 3).

Using qRT-PCR we validated the responses for a group of genes focusing on some shared and MuSK-dependent responses. Id1 and Id2, two well-characterized canonical responses to BMPs, had a similar fold upregulation between wild type and MuSK null myoblasts (Figure 2.5b, 2.5c). We also identified a novel gene response downstream of BMP4, Fabp7, which was also not regulated by MuSK under these conditions (Figure 2.5d). The discrepancy in Id1 upregulation between the early (Figure 2.4c) and late time-points (Figure 2.5b) most likely stems from the fact that Id1 expression peaks earlier (data not shown) at which point MuSK regulation can be seen robustly and then it tapers to similar levels in both wild-type and MuSK null myoblasts. Next we validated a group of MuSK-dependent genes. BMP4-induced expression of Ptgs2, which encodes for Cox2, the key enzyme in prostaglandin pathway and of Ptger4, which encodes for a prostaglandin receptor was regulated by MuSK under these conditions (Figure 2.5e and Figure 2.5f). BMP4-induced expression of Rgs4, a regulator of G-protein signaling, was strictly dependent on the presence of MuSK (Figure 2.5g), as in MuSK null myoblasts BMP4 could not induce any Rgs4 expression, as opposed to slight increases in Ptgs2 and Ptger4. We also tested shorter treatment times for Rgs4 by which MuSK-regulation on BMP4-induced Id1 expression could be seen robustly. At 2 hours of BMP4 treatment, MuSK null myoblasts failed to induce any Rgs4 expression by BMP4, which was in accord with the results of the study with the longer treatment (Supplementary Figure 2.1).

In order to understand more about MuSK's regulation on Rgs4 expression, we wanted to see if BMP4-induced Rgs4 expression was dependent on the canonical BMP4 pathway. In wild-type myoblast cultures we used a selective inhibitor for type-1 BMP receptors, LDN193189 (Vogt et al., 2011) and indirectly inhibited SMAD dependent signaling. We then analyzed Rgs4 transcript levels. When LDN193189 was used with BMP4, Rgs4 expression was inhibited (Figure 2.5h), indicating that BMP4-induced Rgs4 expression requires canonical BMP4 pathway.

Like in myoblasts, BMP4-induced upregulation of 171 genes were dependent on the presence of MuSK in myotubes (Figure 2.6a, Supp. Table 4). While there are a few shared genes between MuSK-dependent BMP4 responses in myoblasts and myotubes, the majority of the upregulated genes were different between these two myogenic cell types. This result indicates that MuSK regulates BMP4 pathway in a cell-context dependent manner. Between wild type and MuSK null myotubes 117 gene responses were shared, whereas 325 genes were uniquely upregulated in MuSK null myotubes (Figure 2.6a, Supp. Table 5, Supp. Table 6).

Among the MuSK-regulated responses in myotubes, Carbonic Anhydrase 3 (Car3) and Myosin Heavy Chain 15 (Myh15) were two interesting novel transcript responses downstream of BMP4 since both of these proteins were previously suggested as slow-type fiber markers (Desjardins et al., 2002; Lyons et al., 1991). We validated the regulation of their mRNAs by MuSK with qRT-PCR in myotubes. On

the other hand, in myoblasts these two genes were not upregulated by BMP4, suggesting a cell-context specific expression (Figure 2.6b and Figure 2.6c).

Fiber type composition of muscle tissue varies in different muscles. Among the four major fiber types, type-1 slow muscle fibers are the most oxidative, fatigue resistant ones and are more suitable for prolonged low-intensity activities (Bassel-Duby and Olson, 2006). Soleus is one of the most highly enriched muscles for the slow fiber content (Augusto et al., 2004). We wanted to see if Myh15 and Car3 expression was higher in muscles that are enriched in slow fibers and therefore compared their expression between Soleus and Extensor digitorum longus (EDL) muscles of 5.5 weeks old adult mice. The expression of both of these genes was higher in Soleus as expected (Figure 2.6e and Figure 2.6f). Interestingly, MuSK expression was also shown to be higher in Soleus compared to EDL, recently (Punga et al., 2011). Our expression study was in agreement with this result (Figure 2. 6d).

MuSK kinase activity is not required for MuSK regulation of BMP4 signaling

MuSK is a receptor tyrosine kinase that can dimerize and undergo auto-phosphorylation (Bergamin et al., 2010). We wanted to know if BMP4 binding to MuSK induced receptor auto-phosphorylation. In order to test this, we used wild type myotubes in which neural-derived proteoglycan agrin is known to induce MuSK phosphorylation (Glass et al., 1996). Myotube cultures were treated with agrin for 1 hour, along with BMP4 for various time-points ranging from 10 minutes

to 3 hours. MuSK was immunoprecipitated, run in an SDS-PAGE and phospho-MuSK was detected in western blots. While agrin induced robust phosphorylation of MuSK at 1 hour, as expected, BMP4 failed to induce the phosphorylation of MuSK under these conditions (Figure 2.7a). It is important to note that MuSK regulation on BMP4 pathway was seen at the same ligand concentration and within the time window that were chosen in this experiment. Given this result, we conclude that BMP4 does not induce MuSK phosphorylation.

Finally, we wanted to further confirm that MuSK regulation on the transcripts downstream of BMP4 did not require MuSK's kinase activity. To address this question, we compared the BMP4-induced Rgs4 responses of rescue cell lines, which were generated by expressing wild type or mutant MuSK (kinase-dead MuSK and MuSK with a point mutation in the juxta-membrane Y553) (Mazhar et al., 2012). Serum-deprived cultures were treated with BMP4 and Rgs4 transcript levels were analyzed by qRT-PCR. As expected from the previous results, Rgs4 expression was not induced by BMP4 in MuSK null myoblasts, however wild type MuSK could rescue Rgs4 expression (Figure 2.7b and 2.7c). Interestingly, kinase-dead MuSK and MuSK with the point mutation in the juxta-membrane Y533 could also rescue Rgs4 expression (Figure 2.7d and 2.7e). Taken together, MuSK kinase activity is dispensable for its regulation on BMP4 pathway.

Discussion

Our data show that the MuSK ectodomain binds to BMP2, 4 and 7 with low nanomolar affinities. Furthermore, we demonstrate that MuSK regulates the magnitude of canonical BMP4 signaling, as judged by phospho-SMAD1/5/8 and induced Id1 levels and is required for the BMP4-induced expression of a group of genes. We propose that MuSK modulates the BMP pathway. There are several potential mechanisms by which MuSK could regulate BMP signaling. MuSK may associate with BMP receptors in a complex where BMP is bound both to MuSK and its canonical receptors (Figure 2.9a). MuSK in such a complex could serve as a chaperone for cell surface expression of BMP receptors and enhance the signaling by increasing cell surface expression of the receptors. MuSK could also regulate the assembly of BMP receptors and increase the signaling. In the same model, MuSK association with BMP receptors could also increase the avidity of BMPs for their receptor. Similarly, MuSK could act as a cell surface presenter of BMPs to their receptors (Figure 2.9b). MuSK intracellular domain interacts with various signaling and scaffolding molecules such as Dok7, Tid1, Dvl, Abl, Src kinase, ShcD (Wu et al., 2010). Therefore, association of MuSK with BMP receptors may bring such molecules in close proximity of cytosolic domains of BMP receptors and integrate different downstream signaling events to BMP signaling (Figure 2.9c). Alternatively, BMPs could bind to MuSK and BMP receptors separately and two distinct signaling events can converge downstream to regulate the transcriptional outcome as a response to BMP. While most of these scenarios are not mutually exclusive, they need to be tested directly to understand which ones could be working together.

MuSK binding to BMPs

A recent SPR study has shown that the binding affinity of BMP2 to Alk3 and Alk6 were 1.1 and 1.6nM, respectively. Low affinity type-2 receptor, BMPRII, showed a binding affinity of 26.7nM for BMP2 (Berasi et al., 2011). DRAGON, a positive regulatory BMP co-receptor, has been shown to have a binding affinity of 1.5nM for BMP2 (Samad et al., 2005). On the other hand, Neogenin, a negative regulatory co-receptor was predicted to bind to BMP2 with an affinity of 25nM (Hagihara et al., 2011). Our results show that BMP binding to MuSK ectodomain is in the range of high affinity type-1 receptor binding of BMPs and also has a similar affinity as the positive regulatory DRAGON co-receptor.

We also show that Ig3 domain of MuSK is required for its BMP4 binding. Previously, several extracellular domains of MuSK have been attributed different roles. The Ig1 domain is important for dimerization in agrin-induced receptor activation and AchR clustering and biglycan binding (Stiegler et al., 2006; Amenta et al., 2012). Ig2 domain is also critical for agrin-induced AchR clustering (Zhou et al., 1999). CRD domain was shown to be necessary for biglycan binding and has been implicated in Wnt binding (Amenta et al., 2012; Zhang et al., 2012). However, the function of the third Ig-like (Ig3) domain has yet to be shown. In addition, one of the several MuSK splice isoforms lacks the Ig3 domain (Hesser et al., 1999, Kuehn et al., 2005). To our knowledge this is the first study, which shows a function for the Ig3 domain. Furthermore, it opens up the possibility that MuSK regulation of BMP4 signaling can

be regulated by alternative splicing, given that there is an alternatively spliced ΔIg3-MuSK isoform. It is possible that in muscle tissue, at different stages of development and in adult alternative splicing of MuSK could change the outcomes of the BMP4 signaling. Targeted distribution of two isoforms in a muscle fiber can also modulate MuSK-dependent BMP4 signaling at different compartments of muscle fiber membrane. On the other hand, it brings up the question if lower levels of MuSK expression in other tissue types is regulated by alternative splicing, which would lead to differential regulation of BMP4 pathway in these tissues. Finally, the requirement of Ig3 domain for BMP4 binding of MuSK distinguishes this novel function from MuSK's well-known function in agrin pathway, as Ig3 domain was shown to be dispensable for agrin-MuSK pathway leading to the maturation of NMJs (Zhou et al., 1999).

The receptor tyrosine kinase Ror2 has a similar extracellular domain to MuSK ectodomain. It consists of a single Ig-like domain, followed by a frizzled-domain. Alk6 interaction with Ror2 was observed before (Sammar et al., 2004, Sammar et al., 2009). This interaction raises the question whether MuSK would also associate with Alk3 or Alk6 in myogenic cells and act as a BMP4 co-receptor. Future studies will reveal if the endogenous MuSK and type-1 receptors (Alk3 or Alk6) in myogenic cells are interacting.

MuSK regulation on canonical BMP4 pathway

We show that MuSK positively regulates canonical BMP4 pathway similar to DRAGON co-receptor. Future studies will determine if MuSK also serves as a BMP4 co-receptor and what the exact mechanism is for MuSK's regulation on the pSMAD1/5/8 levels. Furthermore, we observed cytosolic pSMAD1/5/8 granules being regulated by MuSK. In the absence of MuSK, their numbers diminish drastically. Interestingly, the receptor Lrp6 has been shown to induce cytosolic pSMAD1 puncta when overexpressed in Cos7 cells (Fuentealba et al., 2007). These puncta were predicted to be Lrp6 signalosomes, based on the observation that they colocalized with the endogenous GSK3 protein. Lrp4, which was shown to bind to MuSK (Kim et al., 2008), is implicated to have genetic interactions with BMP pathway during tooth morphogenesis or in the context of bone properties and fracture (Ohazama et al., 2008; Kumar et al., 2011). The cytosolic granules that we observed could well be Lrp4-signalosomes which function as a MuSK-dependent signaling unit in the cell and lead to MuSK-dependent transcriptional output of BMP4 pathway. In this regard, it would be interesting to see if Lrp4 associated with pSMAD1/5/8 cytosolic granules in myoblasts.

MuSK-dependence of a subset of BMP4 responses

Our results show that there are fundamental differences in transcriptional outputs of myoblasts and myotubes as a response to BMP4. MuSK regulates these cell-context dependent responses in both of these myogenic cell types. Even though we focused our analyses on the upregulated genes, there are several downregulated

genes shown in Appendix Tables 4-7 and MuSK seems to regulate some of these responses, as well. Further studies need to be done in order to understand the importance of the downregulated genes for the downstream events.

In our expression studies, we identified several novel transcripts downstream of BMP4 signal. One of these is Fabp7, which was suggested as a stem cell marker in neurons (Yun et al., 2012). In our microarray analysis, we compared Fabp7 expression between myoblasts and myotubes. Myoblasts had a few fold higher expression of Fabp7, which suggests that Fabp7 could be a stem-cell marker for myogenic cells, as well. This idea needs to be tested further. Strikingly, Fabp7 was the biggest hit in our microarray analyses for both BMP4-treated myoblasts and myotubes and it appeared to be a MuSK-independent BMP4 response.

In myoblasts we confirmed that Ptgs2, Ptger4 and Rgs4 were regulated by MuSK. Rgs4 expression by BMP4 is strictly dependent on the presence of MuSK whereas for Ptgs2 and Ptger4 the presence of MuSK significantly enhances the response. Ptgs2 and Ptger4 are components of the prostaglandin pathway. Ptgs2 encodes for Cox2 enzyme, which is a critical enzyme in the prostaglandin synthesis pathway. On the other hand, Ptger4 is a prostaglandin receptor. Cox2 pathway was shown to be important in myoblast proliferation, fusion and growth of muscle cells (Otis et al., 2005; Bondesen et al., 2006; Horsley et al., 2003). Further studies will determine if the Cox2 pathway is impaired in the absence of MuSK in myoblasts.

Rgs4 is a G-protein regulator, which was shown to inhibit cell growth and myofilament organization in neonatal cardiac myocytes (Tamirisa et al., 1999). It was also indicated to counteract the prostaglandin pathway, which uses G-protein coupled receptors (Song et al., 2009). Rgs4 expression downstream of BMP4 could be a negative feedback mechanism against the BMP4-induced expression of Ptgs2 and Ptger4. Since both of these prostaglandin pathway members are regulated by MuSK, regulation of BMP4-induced Rgs4 expression by MuSK would also be expected. The same signaling modules could be controlling the expression of these genes. We also showed that BMP4-induced Rgs4 expression requires the activity by type-1 BMP receptors. This result indicates that BMP4 induction of Rgs4 may be using the elements of canonical BMP4 pathway. However, the cytosolic pSMAD1/5/8 granules that are regulated by MuSK could be providing a specific intercellular signaling compartment, which then regulates the expression of MuSK-dependent transcripts like Rgs4.

One approach to understand more about the signaling leading to BMP4-induced MuSK-dependent Rgs4 expression would be to generate a myogenic reporter cell line using Rgs4 promoter elements. An RNAi screen in these cells could yield in identification of various signaling molecules involved downstream of cell surface interaction between MuSK and BMP4.

We identified Myh15 and Car3 as novel BMP4 responses. Both of these transcripts were expressed by BMP4 in a cell-context dependent manner only in myotubes and

this expression was regulated by MuSK. The importance of the cell-context may stem from additional regulatory factors of BMP4 pathway being expressed only in myotubes. The levels of MuSK in myotubes and myoblasts could also contribute to this observation, as MuSK levels are significantly increased in myotubes. (Valenzuela et al., 1995).

Myh15 was predicted to be a type-1 slow skeletal muscle myosin (Desjardins et al., 2002). Although Rossi et al. could not detect any Myh15 expression in skeletal muscles (Rossi et al., 2010), our expression studies showed that this myosin was expressed both in skeletal muscle tissue in animals and in the cultured myotubes. Similar to Myh15, Car3 was also shown to be enriched in slow muscle fibers (Lyons et al., 1991). In adult mice, we showed that both of these transcripts were present at much higher levels in Soleus muscle compared to EDL muscle. Interestingly, MuSK also shows the same expression pattern. Soleus muscle is enriched with slow muscle fibers. This correlation points the possibility that MuSK regulated and BMP4-induced expression of Myh15 and Car3 could be part of a fiber-type switch program. BMPs have not been indicated among several other factors shown to induce fiber-type switch in muscle to date. Further studies focusing on longer BMP4 treatments and the identification of downstream fiber-type specific transcripts will reveal if there is a global fiber-type reprogramming towards slow fibers that is induced and regulated by BMP4 and MuSK.

MuSK kinase activity and BMP4 pathway

Our experiments showed that tyrosine phosphorylation of MuSK is not induced by BMP4. This result indicates a novel MuSK pathway that is distinct from its role in organizing the postsynaptic apparatus (Herbst et al., 2000). Tyrosine 553 at the juxtamembrane domain and the tyrosine residues in the tyrosine kinase domain of MuSK are necessary residues for agrin-mediated signaling of MuSK (Figure 2.8b). However, these critical tyrosines are not required for MuSK regulation of BMP4 signaling (Figure 2.7b-e and Figure 2.8a). This difference separates the two functionalities of MuSK and assigns a novel role to MuSK. On the other hand, Lrp4 association of MuSK in the context of agrin-mediated signaling raises the question of whether Lrp4 also contributes to MuSK regulation of BMP4 signaling and if it is in complex with MuSK in that context.

Our results show that the receptor tyrosine kinase regulates BMP4 signaling in myogenic cells. The evidence we show here may point to a general mechanism in which other similar receptor tyrosine kinases or surface molecules regulate BMP signaling in other tissues. Further studies may also reveal if MuSK expressed at much lower levels in other tissues (i.e. brain, Garcia-Osta, 2006) could have a role in BMP signaling. Similarly, these results can potentially attribute a role to extra-synaptic MuSK that is expressed in muscle fibers, although this has to be tested more directly.

Materials and Methods

Antibodies and materials

Purified recombinant human BMP4, purified agrin, anti-BMP4 (1:250), normal goat IgG, biotinylated anti-BMP4 (1:500), anti-MuSK (1:20 for IPs and 1:500 for western blots), anti-Alk3 (1:20 for IPs and 1:500 for western blots), anti-Alk6 (1:20 for IPs and 1:500 for western blots) antibodies were obtained from R&D Systems (Minneapolis, MN, USA). Stretavidin-HRP antibody (1:2000) was obtained from Thermo. Anti-mouse HRP antibody (1:2000) was obtained from KPL. Anti-SMAD5 (1:1000) and anti-phosphoSMAD5 (1:1000 for western blots, 1:200 for immunocytochemistry) antibodies were obtained from Epitomics (Burlingame, CA, USA). Anti-phosphotyrosine (4G10) antibody was obtained from EMD Millipore Corporation (Billerica, MA, USA). Alexa-555-conjugated goat anti-rabbit IgG (1:1000) was obtained from Invitrogen. Expression vector containing His-tagged MuSK ectodomain was a gift from Dr. Markus Ruegg. His-tagged TEV protease was a gift from Dr. Rebecca Page. Full length and Ig3-lacking Fc-Fusion MuSK ectodomain constructs were obtained from GenScript (Piscataway, NJ, USA). LDN192189 was obtained from STEMGENT (Cambridge, MA, USA).

Mammalian cell culture and mice

Mouse C2C12 BRE cells (Zilberberg et al., 2007) were cultured in DMEM supplemented with 10% fetal bovine serum, 2% L-Glutamine and 1% Penicillin-

Streptomyocin and cultured at 37 ^{0}C in 8% CO2. Immortalized myoblast cultures of wild-type mouse H-2Kb-tsA58 (Morgan JE et al., 1994), MuSK-/- and MuSK rescue lines (wild type MuSK (B1), kinase-dead MuSK (KD) and MuSK Y553A) were cultured were cultured on gelatin-coated dishes in DMEM supplemented with 20% fetal bovine serum, 2% L-Glutamine, 1% Penicillin-Streptomyocin, 1% Chicken Embryo Extract, 1U interferon-γ and cultured under permissive temperature at 33 ^{0}C in 8% CO2. Myotubes were obtained by switching the confluent myoblast cultures to a medium with DMEM supplemented with 5% horse serum, 2% L-Glutamine and 1% Penicillin-Streptomyocin at 37 ^{0}C in 8% CO2.

Luciferase reporter assays

C2C12BRA cells were plated on 96-well culture dishes at 4-5 x 103 cells/well. The cells were allowed to attach overnight. The indicated recombinant proteins were premixed in DMEM containing 0.1%BSA for 20 minutes at 4 0Cand the medium was replaced with this solution. The cells were treated for 8 hours, washed twice with PBS and cell extracts were prepared with 50µl/well 1X cell lysis buffer (Roche). 40 µl of the lysate was transferred to an opaque white 96-well microplate and mixed with 100 µl of Luciferase substrate (Roche). The luciferase activity was read in a luminometer and reported as relative luciferase unit (RLU), which is the value of each condition after subtraction of mock-treatment (no-BMP4) value and normalization to BMP4-only condition. All assays were performed in 8 replicates and repeated at least two times with similar results.

For testing the remaining activity in the solution binding experiments, the indicated recombinant proteins were premixed in DMEM containing 0.1%BSA for 2 hours at 4 0C. After the addition of the magnetic Nickel-bound beads (Promega) into the solution, they were incubated in the same solution for another 2 hours at 4 0C. The same protocol detailed above was followed after this step to test the BMP4 activity.

Immunoprecipitation (IP) and co-immunoprecipitation (co-IP)

For MuSK phosphorylation IP, H-2Kb-tsA58 myotubes were lysed in extraction buffer (10mM Tris-HCl (pH 7.4), 1% Triton-X 100, 0.5% NP40, 150mM NaCl, 1mM EGTA, 1mM EDTA, 1mM sodium orthovanadate, 10mM sodium fluoride and 1X EDTA-free protease inhibitor cocktail (Roche Complete)) after treatments with indicated proteins. Lysates were pre-cleared with Protein-G bound magnetic beads (Invitrogen) and bicinchoninic acid (BCA) assay was used to quantify total protein levels in the lysates (Pierce). Equal amounts of lysates were mixed with equal amounts of the indicated IP/co-IP antibodies and tumbled overnight at 4 ^{0}C. After the addition of Protein-G bound magnetic beads lysates were tumbled for 4-6 hours at 4 ^{0}C. Beads were washed with extraction buffer for 3 times. 2X sample buffer was added for elution of the immunoprecipitated proteins from the beads. Proteins were eluted by boiling the samples at 98 ^{0}C for 5 minutes. Western blots were run for the samples as indicated below.

The extraction and bead washing buffer used for co-IPs was as follows: 10mM Tris-HCl (pH 7.4), 1% Triton-X 100, 150mM NaCl, 1mM EGTA, 1mM EDTA, 1mM sodium orthovanadate, 10mM sodium fluoride and 1X EDTA-free protease inhibitor cocktail (Roche Complete).

Western blots

For pSMAD1/5/8 westerns, cell lysates were prepared in extraction buffer containing 10mM Tris-HCl (pH 7.4), 1% Triton-X 100, 0.5% NP40, 150mM NaCl, 1mM EGTA, 1mM EDTA, 1mM sodium orthovanadate, 10mM sodium fluoride and 1X EDTA-free protease inhibitor cocktail (Roche Complete). Cells were serum-deprived in DMEM containing 0.1% BSA for 5-6 hours and then treated with indicated amounts of BMP4 for 15 minutes. Cells were washed in PBS three times, incubated in the extraction buffer for 30 minutes at 4 ^{0}C and the lysates were cleared by centrifugation at 13k rpm for 10 minutes ar 4 ^{0}C. Protein quantification of the samples was assessed by BCA (Pierce). Equal amounts of protein were run in 5%–15% gradient SDS-PAGE gels and immunoblotted with pSMAD1/5/8 antibody (Antiphosphotyrosine antibody for phospho-MuSK IPs; Alk3, Alk6, MuSK antibody or normal goat IgG for co-IPs). Membranes were then stripped and reprobed with SMAD1/5/8 antibody (MuSK antibody for phospho-MuSK IP).

ELISAs

For MuSK binding to BMP4, MuSK constructs were immobilized on 96-well plates at 2μg/ml overnight. Plates were blocked with 1% BSA in PBS. BMP4 (0-200nM) was incubated with immobilized MuSK. Bound BMP4 was detected with biotinylated anti-BMP4 antibody (R&D) followed by Streptavidin-conjugated HRP (Thermo). Color change in chromogenic substrate 3,3′,5,5′-Tetramethylbenzidine (TMB) as a result of HRP activity was measured with spectrophotometer at 450nm wavelength. Graphs are generated with absorbance values. Each data point represents the average of 4 replicate wells. For MuSK binding to biglycan, MuSK constructs were immobilized and His-tagged non-glycanated biglycan was incubated with immobilized MuSK. Bound biglycan was detected with anti-His antibody followed by HRP-conjugated anti-mouse secondary antibody.

Immunocytochemistry

12 hours after myoblast cultures were fed with their growth medium, cells were washed with PBS three times and fixed in 4% paraformaldehyde in PBS for 15 minutes at room temperature. Cells were then permeabilized with 0.2% Triton-X 100 in PBS containing 1% BSA for 10 minutes, blocked in PBS containing 1% BSA and 0.1% Triton-X 100 for 10 minutes, incubated with primary antibody (anti-pSMAD1/5/8) in PBS containing 1% BSA and 0.1% Triton-X 100 for 1 hour at room temperature. After 3 washes in PBS, cell were incubated with secondary antibody Alexa-555-conjugated goat anti-rabbit IgG for 1 hour at room temperature. After three PBS washes, cells were fixed again in cold methanol at -20 0C for 5 minutes.

Mounting medium with DAPI was used to visualize the nuclei. Protein localization was examined by laser-scanning confocal microscopy.

RNA extraction, reverse transcription and quantitative real time polymerase chain reaction (qRT-PCR)

Total RNA was isolated from cells with Trizol (Invitrogen). Total RNA was cleaned up and DNase-treated in Qiagen RNeasy columns. RNA was reverse transcribed into first strand cDNA (Invitrogen). qRT-PCR reaction consisted of initial incubation at 50 ^{0}C for 2 minutes and a denaturation at 95 ^{0}C for 5 minutes. The cycling parameters were as follows: 95 ^{0}C for 15 seconds, 60 ^{0}C for 30 seconds. After 40 cycles, the reactions underwent a final dissociation cycle as follows: 95 ^{0}C for 15 seconds, 60 ^{0}C for 1 minute, 95 ^{0}C 15 seconds and 60 ^{0}C for 15 seconds.
Based on the published sequences, the primer sequences used in qRT-PCR reactions were as follows: 5'- GGGATCTCTGGGAAAGACAC -3' and 5'- TCTCTGGAGGCTGAAAGGTG -3' for mouse Id1; 5'- GCCTTTTCACAAAGGTGGAG -3' and 5'- CAGCATTCAGTAGGCTCGTG -3' for mouse Id2; 5'- GTATTTCCATCGCTCCTTGG -3' and 5'- TGAGGCCTATAAAGCACATGG -3' for mouse Rgs4; 5'- TCTTCGGGCAAGAAACTCTG -3' and 5'- TTGCATGTGACTGCTTCTCC -3' for mouse Car3; 5'- CAGGCACACTTCTCCTTTCC-3' and 5'- CCTTCCTCATCATGGACCAG -3' for mouse Myh15; 5'- -3' and 5'- -3' for mouse MuSK; 5'- TCCTCTCTGTTGCGTGTGTC -3' and 5'- CGTTAAGCAACAGGACATGC -3' for mouse Ptger4; 5'- CGCTGATTGGGTTTTCGTAG-3' and 5'- CCTGAGCTGAGGTTTTCCTG-3' for mouse Ptgs2; 5'- CTTTGGGGATATCGTTGCTG -3' and 5'- GCTGGCTAACTCTGGACTC -3' for mouse Fabp7.

Microarrays and bioinformatics analysis

RNA was harvested from myoblast and myotube cultures of wild type and MuSK null cells after 8 hours of BMP4 treatment. 150-200 ng total RNA of good quality RNA (bioanalyzer RIN scores of >9) were used as input material for all arrays. Total RNA was converted to double-stranded cDNA and then in-vitro transcribed overnight using the WT expression kit from Invitrogen (cat # 4411981). After cleanup 10 μg IVT-cRNA was converted to dUTP labeled cDNA and 5.5 μg of the generated single stranded cDNA was enzymatically fragmented followed by TdT mediated biotin end labeling using Affymterix WT terminal labeling kit (cat # 900670). The fragmentation resulted in DNA fragments with a distribution peak at approximately 75 nucleotides and successful fragmentation was demonstrated on the bioanalyzer with RIN scores of 2.6. Approximately 2.5 μg of cDNA was hybridizied over night at 45 0C and 60 rpm to Affymterix Mouse 1.0 Gene ST(cat # 901168). The arrays were washed and stained following Affymetrix standard protocol using GeneChip® Hybridization Wash and Stain Kit (cat # 900720) and subsequently scanned on a Affymterix 3000 7G scanner.

Affymetrix Expression console was used to analyze the overall performance and quality of the arrays and Partek Genomics Suite was used to detect differentially expressed genes. To call genes differentially expressed between samples we used false discovery rate (FDR) as selection criteria or unadjusted p-values of 0.05.

Surface plasmon resonance experiments

The binding affinities and kinetic parameters between BMPs and MuSK were determined by SPR spectroscopy using the BIAcore3000 optical biosensor instrument (GE Healthcare Lifescience). The carboxymethylated surface of the sensor chip (CM5) was activated with N-hydroxysuccinimide (NHS) and 1-ethyl-3-(3-dimethylaminopropyl)carbodiimide hydrochloride (EDC). The CM5 chip contains four flow cells and among these four cells, three were used for the assay. Flow cell 1 was used as a control surface, whereas flow cells 2, 3 and 4 were used as test surfaces. Recombinant human BMP2 [2466 response units (RU)], BMP4 (2108 RU) and BMP7 (2050 RU) were covalently coupled in flow cells 2, 3 and 4 respectively. Unreacted active ester groups were blocked with 1M ethanolamine hydrochloride, pH8.5. The control flow cell 1 was treated in an identical manner but without coupling protein. The binding assays were carried out at 25 °C in 20 mM Hepes buffer (pH 7.5) 500 mM NaCl, 3.4 mM EDTA, and 0.005% surfactant P-20. Various concentrations of MuSK were applied over the biosensor chip at a flow rate of 20 µl/min for 360 s to measure the association phase followed by buffer only for 600 s to measure the dissociation phase. The sensor chip was regenerated with four short pulses of 2M guanidine hydrochloride at 100 µl/min. Data were evaluated using the software BIAevaluation 4.1.1 (BIAcore AB). SPR sensorgrams were globally analyzed using a distribution model for continuous affinity and rate constant analysis with the program EVILFIT (Svitel et al., 2003)

Statistical analysis

All statistical analyses used Student's t test unless otherwise noted.

Figures

Figure 2.1

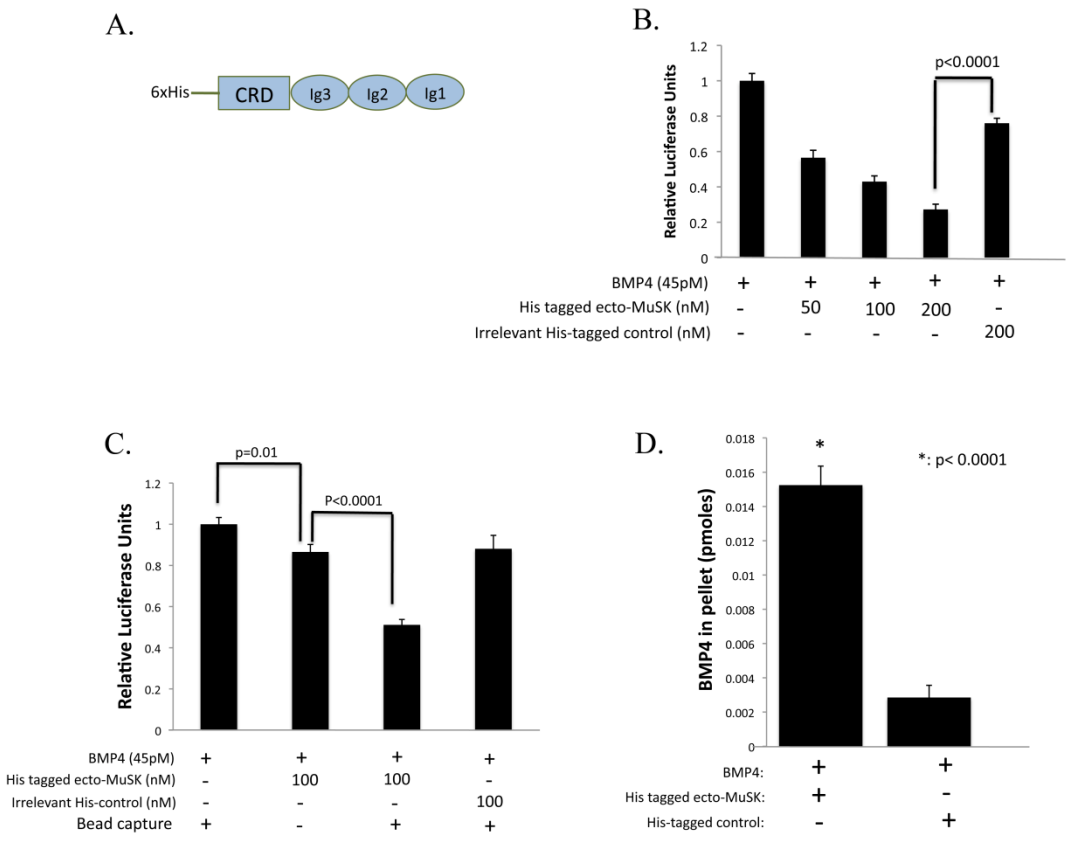

FIGURE 2.1

MuSK ectodomain binds to BMP4. A. Schematic representation of MuSK ectodomain construct used in the reporter and the solution-binding assays. The construct contains three Ig-like domains (Ig1, Ig2 and Ig3) and cycteine-rich domain (CRD) of ecto-MuSK, followed by a His-tag at the C-terminus. B. Soluble MuSK ectodomain inhibits BMP4 activity. BMP4 (45pM) was incubated with the indicated concentrations of MuSK ectodomain or an irrelevant his-tagged protein and then added to cultured C2C12BRA cells for 8 hours. Cells were then lysed and luciferase activity was determined. The average value of untreated cells was subtracted from each condition and everything was normalized to BMP4-only condition (100% activity). Each bar represents the average value from 8 replicate cultures. C. MuSK ectodomain depletes BMP4 from solution. Soluble BMP4 and MuSK ectodomain were mixed for 2 hours at 4 ^{0}C followed by addition of magnetic nickel-beads for 2 hours. After removal of the beads BMP4 activity in the supernatants was measured using the C2C12BRA reporter cell line. D. BMP4 co-precipitates with MuSK ectodomain. MuSK ectodomain and irrelevant his-tagged protein were eluted from the beads that were removed from the supernatant in C. Co-precipitated BMP4 in the elutes was detected with an ELISA. The graph shows the BMP4 amount (pmoles) pulled down with MuSK ectodomain or his-tagged control.

FIGURE 2.2

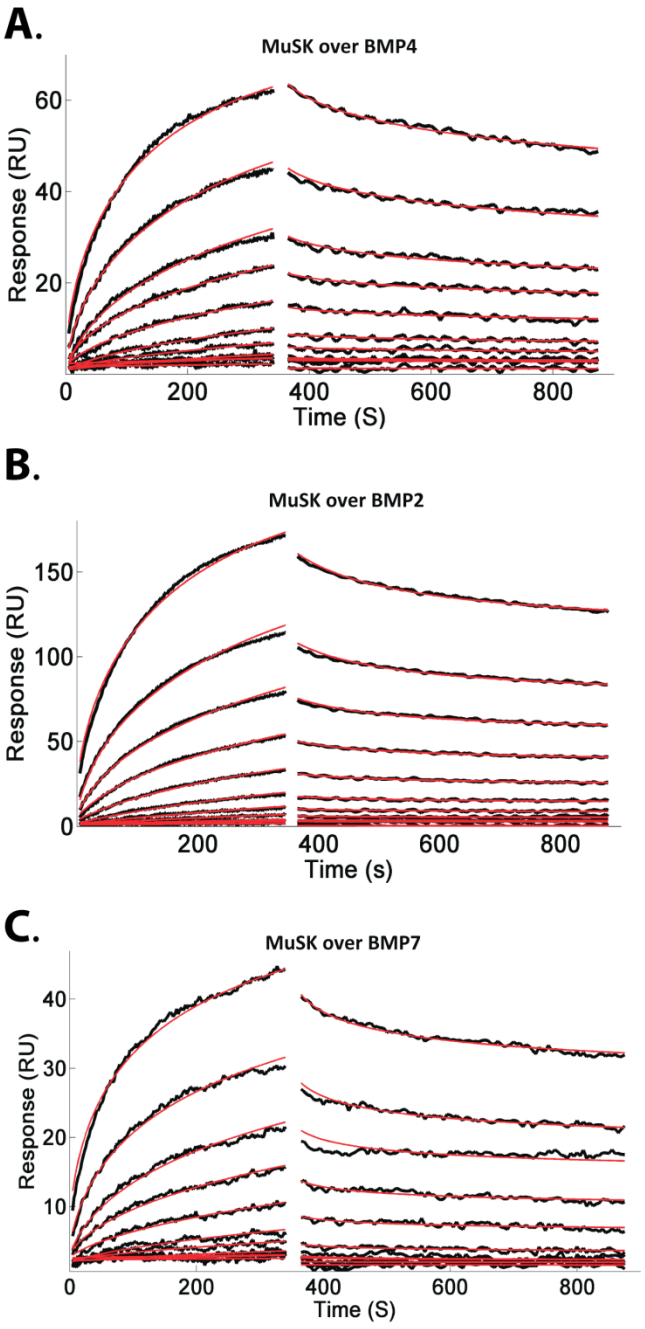
A.
MuSK over BMP4
Response (RU)
60
40
20
0
200
400
600
800
Time (S)
B.
MuSK over BMP2
Response (RU)
150
100
50
0
200
400
600
800
Time (s)
C.
MuSK over BMP7
Response (RU)
40
30
20
10
0
200
400
600
800
Time (S)

FIGURE 2.2

SPR binding analysis of MuSK with BMPs. A-C, MuSK binding to BMP2, BMP4 and BMP7 immobilized on a biosensor chip. Representative SPR profiles are shown for various concentrations of MuSK binding to BMP2 (A); BMP4 (B) and BMP7 (C). Sensograms were normalized for MuSK binding to a mock-coupled flow cell. The black lines show the experimental measurements of a two-fold serial dilution over the concentration range [2 mM-1.96 nM] of each sensorgram and the red lines correspond to global fits of the data to a 1:1 model using a heterogeneous surface model with the program EVILFIT.

FIGURE 2.3

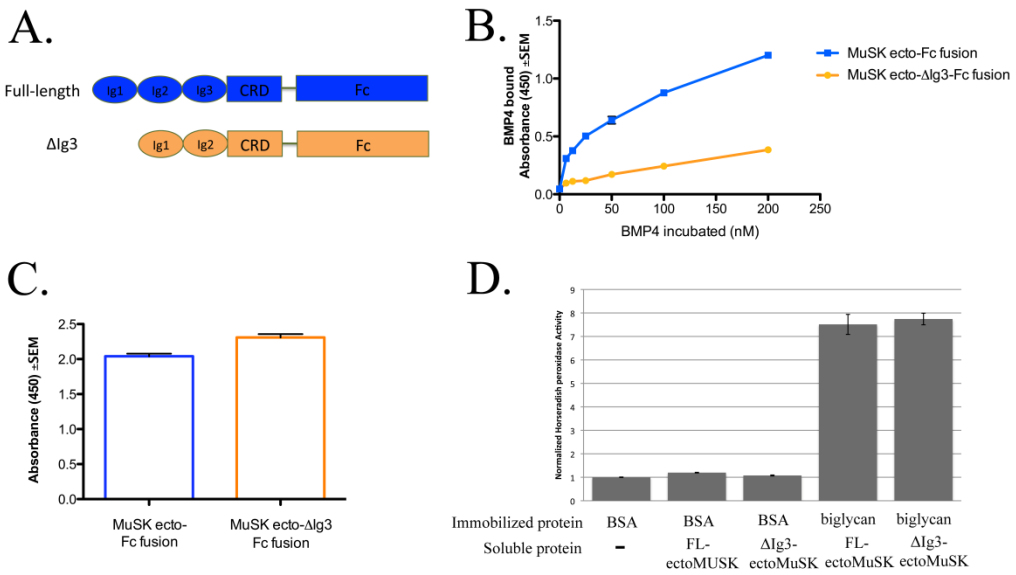
A.
Full-length
Ig1
Ig2
Ig3
CRD
Fc
ΔIg3
Ig1
Ig2
CRD
Fc
B.
BMP4 bound Absorbance (450) ±SEM
1.5
1.0
0.5
0.0
0
50
100
150
200
250
BMP4 incubated (nM)
MuSK ecto-Fc fusion
MuSK ecto-Δlg3-Fc fusion
C.
Absorbance (450) ±SEM
2.5
2.0
1.5
1.0
0.5
0.0
MuSK ecto-Fc fusion
MuSK ecto-Δlg3 Fc fusion
D.
Normalized Horseradish peroxidase Activity
Immobilized protein
Soluble protein
BSA
–
BSA
FL-ectoMUSK
BSA
ΔIg3-ectoMuSK
biglycan
FL-ectoMuSK
biglycan
ΔIg3-ectoMuSK

FIGURE 2.3

The MuSK Ig3 domain is required for BMP4 binding. A. Schematic of Fc-fusion full length (FL) and Ig3-lacking (ΔIg3) MuSK ectodomain constructs used in the binding ELISA. Both of the constructs have an Fc-domain at their C-termini. B. The MuSK Ig3 domain is required for BMP4 binding. FL and ΔIg3 MuSK ectodomain fusions were immobilized on 96-well plates and then incubated with BMP4 (0-200nM). Bound BMP4 was detected with biotinylated anti-BMP4 antibody and Streptavidin-conjugated HRP. Note the saturable binding observed with immobilized FL MuSK ectodomain, while only non-specific binding was observed with ΔIg3 MuSK. C. ELISA detection of the levels of immobilized FL and ΔIg3 MuSK ectodomain constructs. Control experiments showed that equivalent amounts of FL and ΔIg3 MuSK ectodomain fusions were immobilized on the plastic. D. MuSK binding to biglycan was not affected by the deletion of Ig3 domain of MuSK. FL and ΔIg3 MuSK ectodomain fusions were immobilized on 96-well plates and then incubated with biglycan. Bound His-tagged biglycan was detected with anti-His and HRP-conjugated anti-mouse secondary antibodies. FL and ΔIg3 MuSK ectodomain fusions bind to biglycan at comparable levels.

FIGURE 2.4

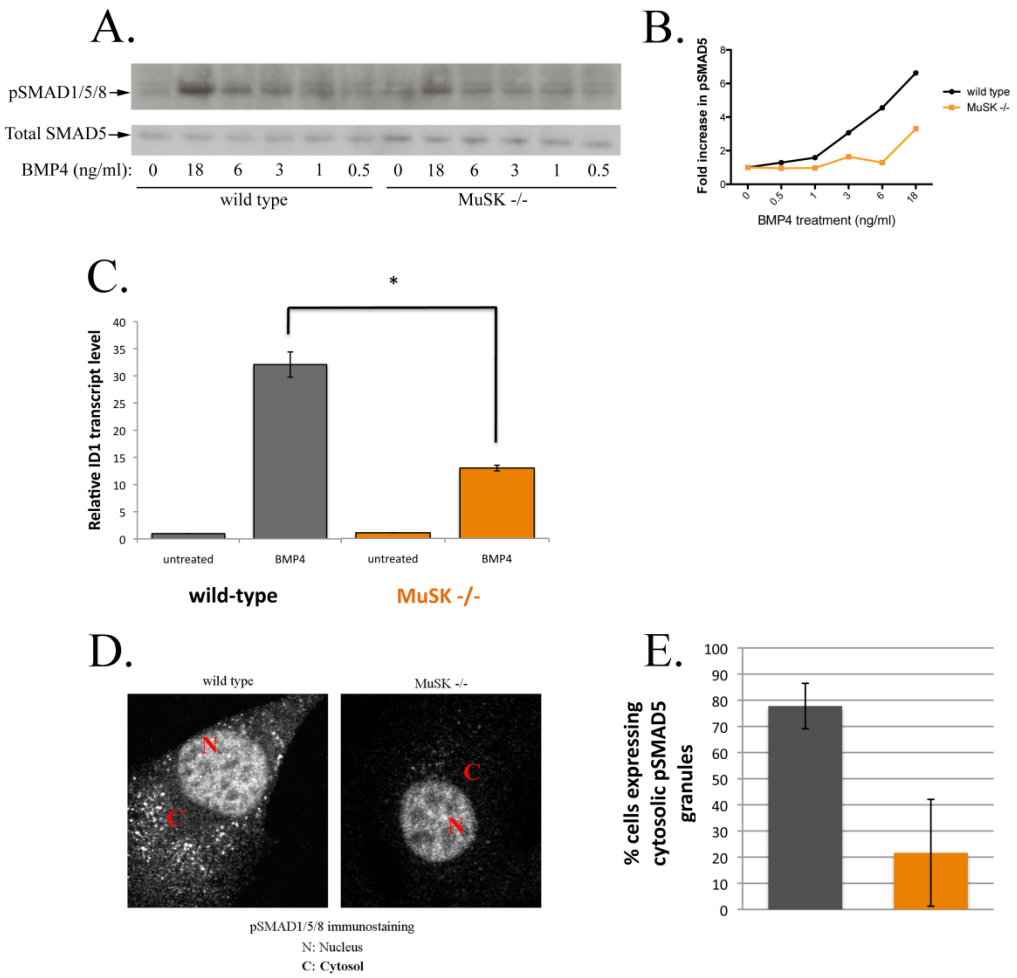
A.
pSMAD1/5/8
Total SMAD5
BMP4 (ng/ml): 0 18 6 3 1 0.5 0 18 6 3 1 0.5
wild type
MuSK -/-
B.
Fold increase in pSMAD5
BMP4 treatment (ng/ml)
wild type
MuSK -/-
C.
*
Relative ID1 transcript level
untreated
BMP4
untreated
BMP4
wild-type
MuSK -/-
D.
wild type
MuSK -/-
N
C
C
N
pSMAD1/5/8 immunostaining
N: Nucleus
C: Cytosol
E.
% cells expressing cytosolic pSMAD5 granules

FIGURE 2.4

MuSK regulates the canonical BMP4 pathway. A. Phospho-SMAD1/5/8 (pSMAD1/5/8) induction is reduced in the absence of MuSK. Wild type H-2Kb-tsA58 and MuSK null myoblasts were serum deprived for 5-6 hours and treated with BMP4 at the indicated concentrations for 15 minutes. Cells were lysed and pSMAD1/5/8 levels were detected by Western blotting. B. Quantification of pSMAD1/5/8 induction in wild type and MuSK null myoblasts. Fold increase for each BMP4 concentration is shown on line graphs. C. BMP4-induced Id1 expression decreases in the absence of MuSK. Wild type H-2Kb-tsA58 and MuSK null myoblasts were serum-deprived for 5-6 hours and treated with 3.25ng/ml BMP4 for 2 hours. Id1 transcript levels were measured by qRT-PCR. Each bar represents at least n=3. Student's t-test was used for assessing the statistical significance. ($p < 0.001$) D. Cytosolic pSMAD1/5/8 granules are reduced in the absence of MuSK. E. Quantification of the percentage of wild type H-2Kb-tsA58 and MuSK null myoblasts expressing cytosolic pSMAD1/5/8 granules at detectable levels. ($n=3$, $p < 0.05$)

FIGURE 2.5

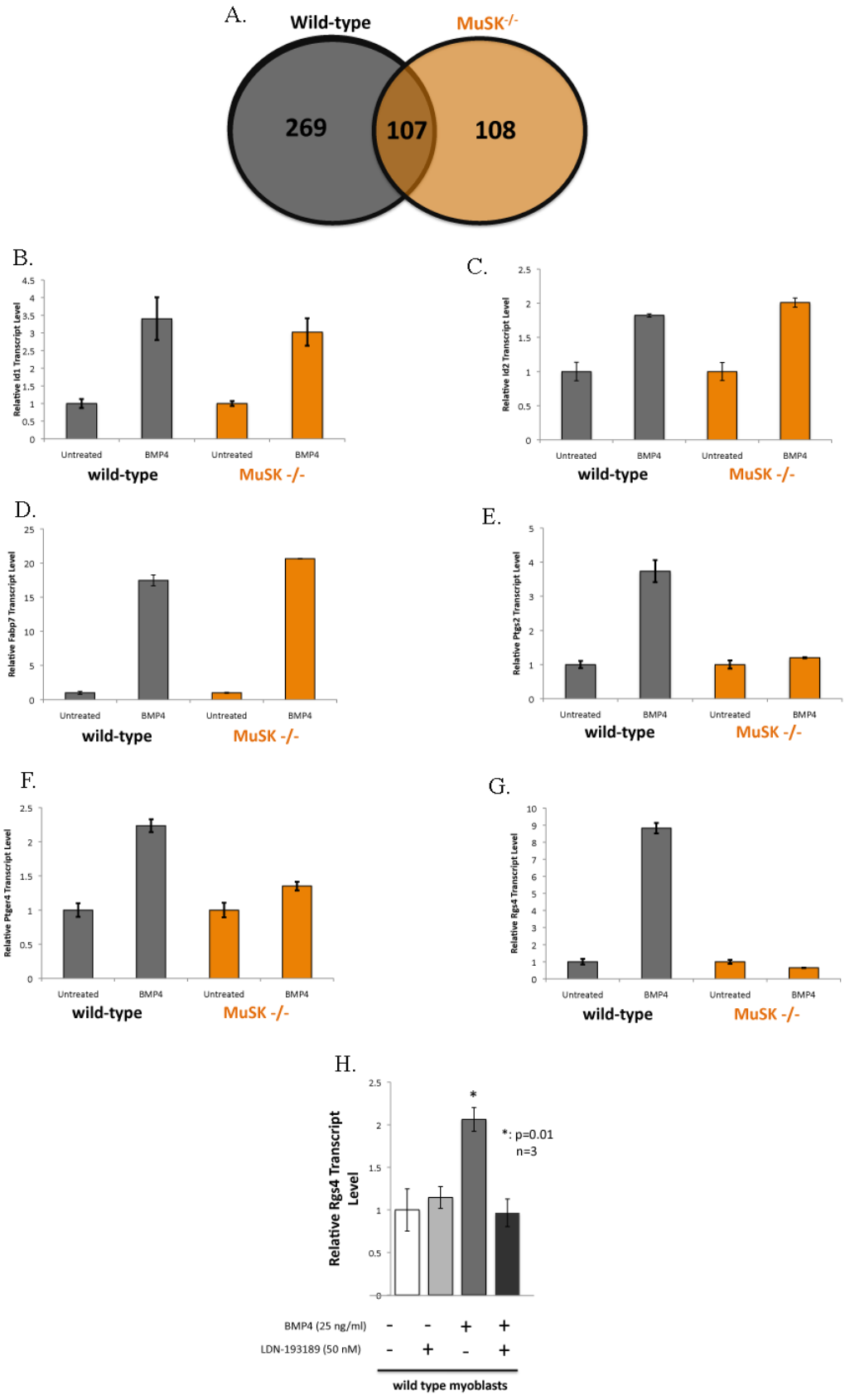
A.
Wild-type
MuSK-/-
269
107
108
B.
Relative Id1 Transcript Level
Untreated
BMP4
Untreated
BMP4
wild-type
MuSK -/-
C.
Relative Id2 Transcript Level
Untreated
BMP4
Untreated
BMP4
wild-type
MuSK -/-
D.
Relative Fabp7 Transcript Level
Untreated
BMP4
Untreated
BMP4
wild-type
MuSK -/-
E.
Relative Ptgs2 Transcript Level
Untreated
BMP4
Untreated
BMP4
wild-type
MuSK -/-
F.
Relative Ptger4 Transcript Level
Untreated
BMP4
Untreated
BMP4
wild-type
MuSK -/-
G.
Relative Rgs4 Transcript Level
Untreated
BMP4
Untreated
BMP4
wild-type
MuSK -/-
H.
Relative Rgs4 Transcript Level
*
*: p=0.01
n=3
BMP4 (25 ng/ml) - - + +
LDN-193189 (50 nM) - + - +
wild type myoblasts

FIGURE 2.5

MuSK selectively regulates BMP4-induced expression of a subset of genes in myoblasts. A. MuSK modulates transcriptional output of BMP4 in myobasts. Wild type H-2Kb-tsA58 and MuSK null myoblasts were serum deprived for 4 hours and treated with 25ng/ml BMP4 for 8 hours. RNA was isolated, reverse-transcribed into double stranded cDNA. cRNAs were synthesized from cDNA templates and hybridized to Affymetrix chips after fragmentation. Analysis of the array data was done with Partek Genomics Suite software with an FDR filter. BMP4 responses for upregulated genes in wild type and MuSK null myoblasts are grouped into a Venn diagram as wild type only, shared and MuSK null only responses. (n=3) B-E. Validation of microarray results for a group of genes. A separate experiment under the same conditions of microarray samples was performed. RNA was harvested and reverse transcribed into cDNA. Transcript levels for the shared responses of (B) Id1, (C) Id2 and (D) Fabp7 and wild type only responses of (E) Ptgs2, (F) Ptger4 and (G) Rgs4 were measured by qRT-PCR. (n=3) H. Inhibition of BMP type-1 receptors also inhibits the BMP4-induced Rgs4 expression. Wild type H-2Kb-tsA58 myoblasts were serum deprived for 5-6 hours and treated with 25ng/ml BMP4 for 2 hours. For the conditions with LDN193189, cells were treated with the drug (50nM) for 30 minutes prior to BMP4 treatment and the drug was kept in cultures during the course of the treatment. RNA was isolated, reverse-transcribed into double stranded cDNA. Rgs4 transcript levels were measured by qRT-PCR. (n=3)

FIGURE 2.6

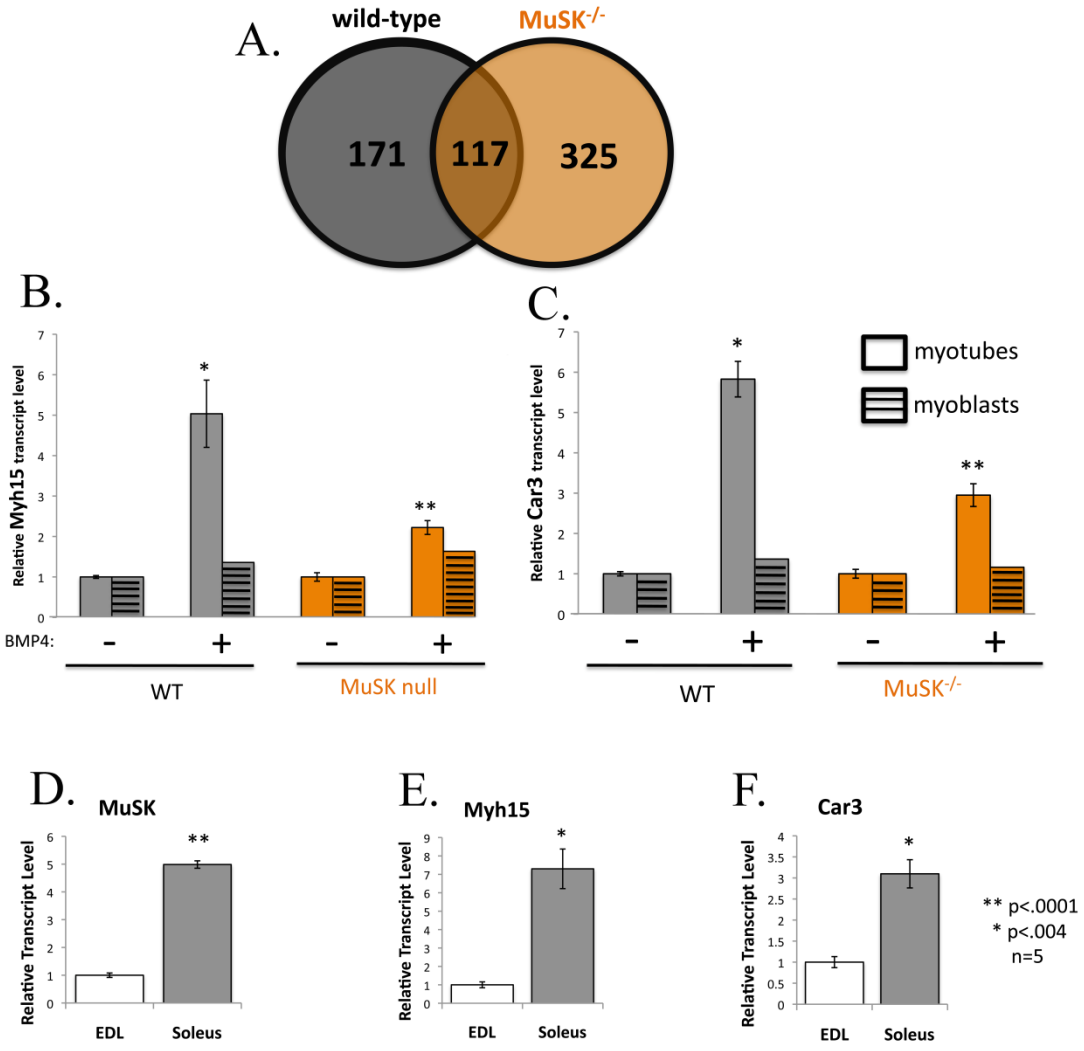
A.
wild-type
MuSK-/-
171
117
325
B.
Relative Myh15 transcript level
BMP4:
WT
MuSK null
C.
Relative Car3 transcript level
myotubes
myoblasts
WT
MuSK-/-
D.
MuSK
Relative Transcript Level
EDL
Soleus
E.
Myh15
Relative Transcript Level
EDL
Soleus
F.
Car3
Relative Transcript Level
EDL
Soleus
** p<.0001
* p<.004
n=5

FIGURE 2.6

MuSK selectively regulates BMP4-induced expression of a subset of genes in myotubes. A. MuSK modulates transcriptional response of BMP4 in myotubes. Wild type H-2Kb-tsA58 and MuSK null myoblasts were grown into confluence and differentiated into myotubes for 3 days. Myotube cultures were treated with 25ng/ml BMP4 for 8 hours. RNA was isolated, reverse-transcribed into double stranded cDNA. cRNAs were synthesized from cDNA templates and hybridized to Affymetrix chips after fragmentation. Analysis of the array data was done with Partek Genomics Suite software with an FDR filter. BMP4 responses for upregulated genes in wild type and MuSK null myotubes are grouped into a Venn diagram as wild type only, shared and MuSK null only responses. (n=3) B-C. Validation of microarray results. A separate experiment under the same conditions of microarray samples was performed. RNA was harvested and reverse transcribed into cDNA. Transcript levels of (B) Myh15 and (C) Car3 were analyzed in myoblasts and myotubes by qRT-PCR. (n=3) D-F. MuSK, Myh15 and Car3 expression is higher in Soleus muscles compared to EDL muscles. Soleus and EDL muscles were harvested from 5.5 month old C57Bl6 mice. RNA was isolated, reverse transcribed into cDNA. Transcript levels of (D) MuSK, (E) Myh15 and (F) Car3 were analyzed by qRT-PCR. (n=5)

FIGURE 2.7

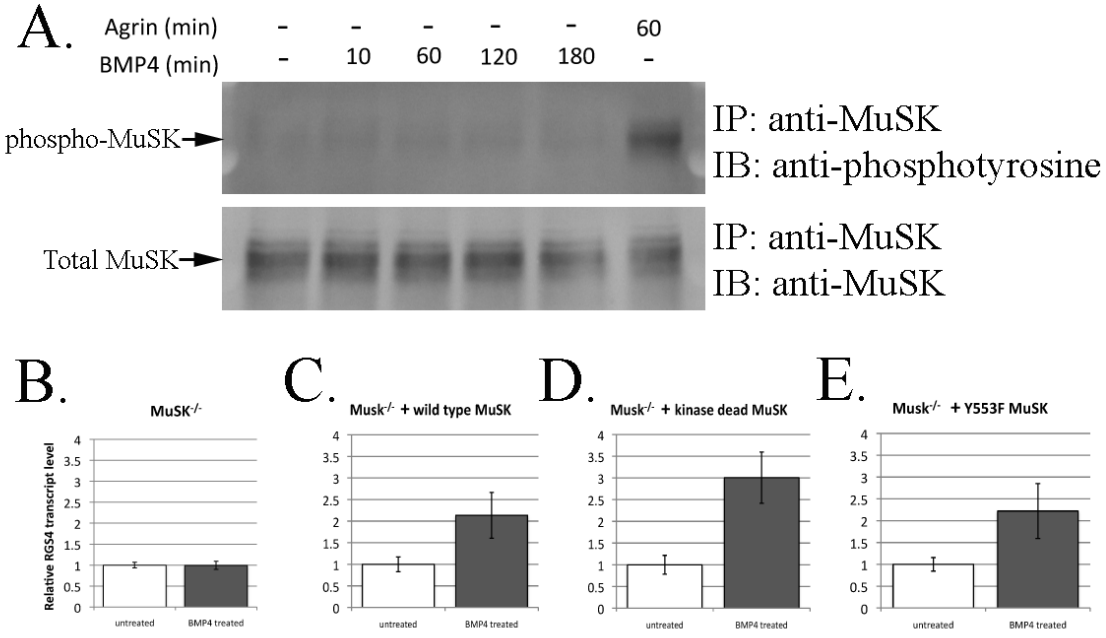
A.
Agrin (min) - - - - - 60
BMP4 (min) - 10 60 120 180 -
phospho-MuSK
IP: anti-MuSK
IB: anti-phosphotyrosine
Total MuSK
IP: anti-MuSK
IB: anti-MuSK
B.
MuSK-/-
Relative RG54 transcript level
untreated
BMP4 treated
C.
Musk-/- + wild type MuSK
D.
Musk-/- + kinase dead MuSK
E.
Musk-/- + Y553F MuSK

FIGURE 2.7

BMP4 does not induce MuSK phosphorylation. A. Wild type H-2Kb-tsA58 myoblasts were grown into confluence and differentiated into myotubes for 3 days. Myotube cultures were treated with 1ng/ml agrin for 1 hour or with 25ng/ml BMP4 for 10 minutes, 1 hour, 2 or 3 hours. The myotubes were lysed and MuSK was immunoprecipitated. Elutes were run in an SDS-PAGE and immunoblotted with an anti-phosphotyrosine antibody (upper panel). The blots were stripped and reprobed with anti-MuSK antibody to assess the total levels of MuSK in each condition (lower panel). B-E. BMP4-induced Rgs4 expression is rescued by wild type, kinase dead and tyrosine 553 mutant MuSK. A) MuSK null, B) wild type MuSK expressing, C) kinase dead MuSK expressing, D) tyrosine 553 mutant (Y553F) MuSK expressing MuSK null myoblasts were serum-deprived for 5-6 hours and treated with 3.25ng/ml BMP4 for 2.5 hours. Rgs4 transcript levels were measured by qRT-PCR. Each bar represents at least n=3.

FIGURE 2.8

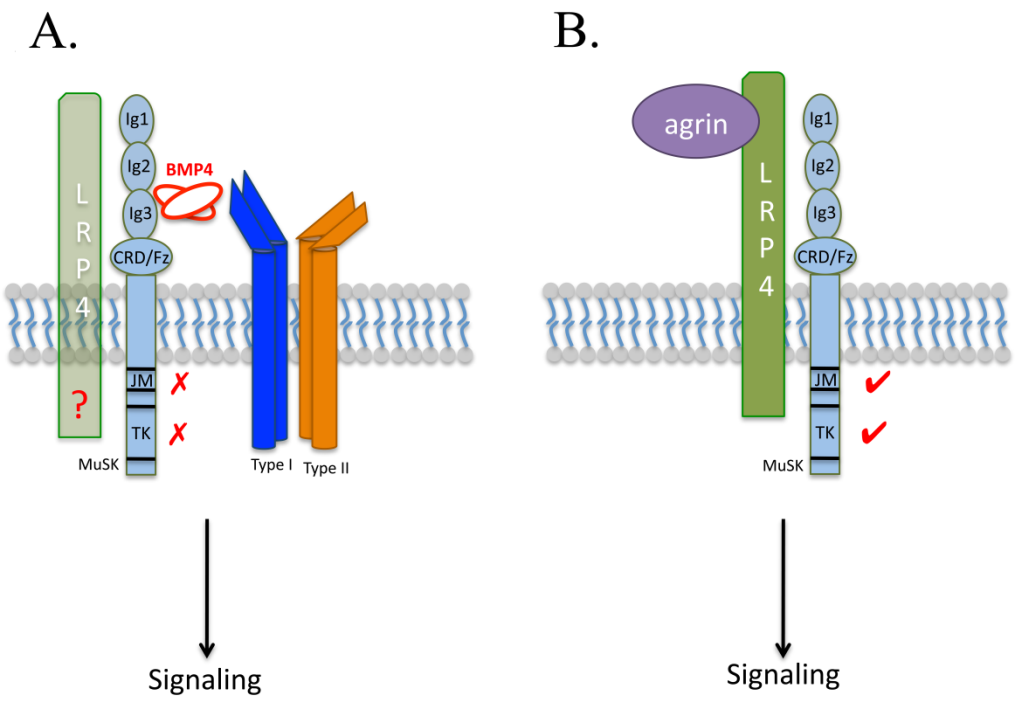

FIGURE 2.8. Differences between BMP4- and agrin-mediated signaling of MuSK.

FIGURE 2.9

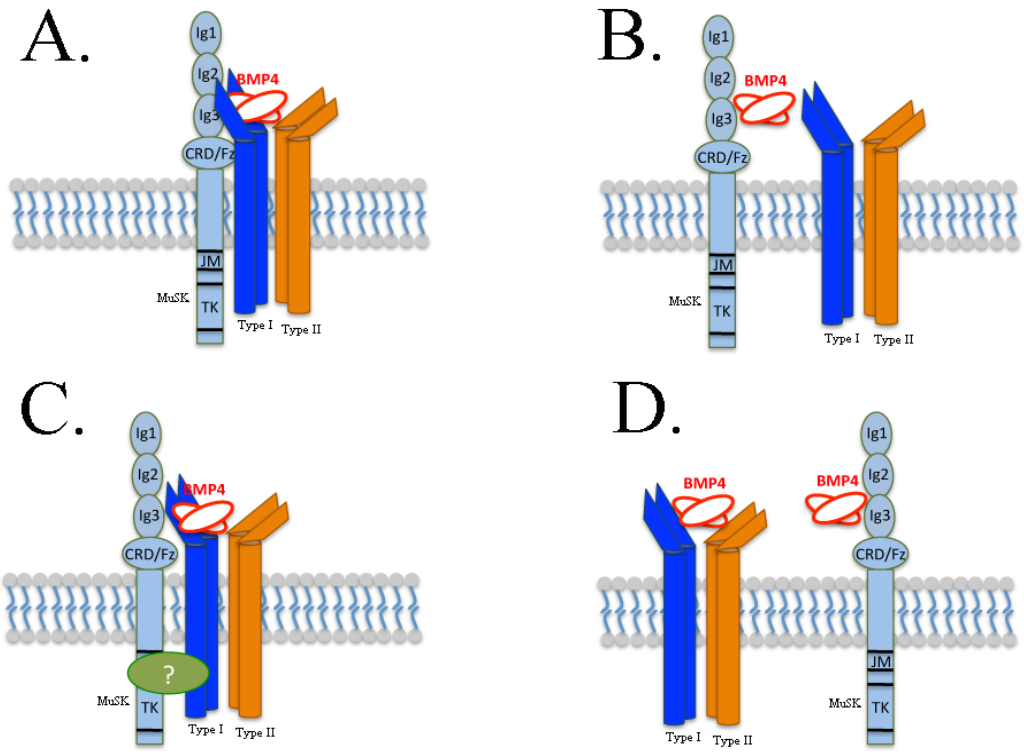

FIGURE 2.9. Putative models for MuSK regulation of BMP4 signaling.

TABLE 2.1

Immobilized Ligand	Analyte MuSK		
	K_{on} ($M^{-1}S^{-1}$)	K_{off} (S^{-1})	K_D (M)
BMP2	$1.7x10^{3}$	$9.6x10^{-6}$	$5.6x10^{-9}$
BMP4	$2.6x10^{3}$	$1.6x10^{-5}$	$6.1x10^{-9}$
BMP7	$1.1x10^{3}$	$1.3x10^{-5}$	$11.8x10^{-9}$

TABLE 2.1

K_D values for the interaction of the MuSK with BMP2, 4 & 7 as determined using SPR.

References

Amenta, Alison R, Hilliary E Creely, Mary Lynn T Mercado, Hiroki Hagiwara, Beth A McKechnie, Beatrice E Lechner, Susana G Rossi, et al. "Biglycan Is an Extracellular MuSK Binding Protein Important for Synapse Stability." The Journal of Neuroscience: The Official Journal of the Society for Neuroscience 32, no. 7 (February 15, 2012): 2324–2334.

Augusto Valeria, Carlos Roberto Padovani and Gerson Eduardo Rocha Campos. "Skeletal Muscle Fiber Types in C57BL6J Mice." *Braz. J. morphol. Sci*. (2004) 21(2), 89-94.

Bassel-Duby, Rhonda, and Eric N Olson. "Signaling Pathways in Skeletal Muscle Remodeling." *Annual Review of Biochemistry* 75 (2006): 19–37.

Berasi, Stephen P, Usha Varadarajan, Joanne Archambault, Michael Cain, Tatyana A Souza, Abe Abouzeid, Jian Li, et al. "Divergent Activities of Osteogenic BMP2, and Tenogenic BMP12 and BMP13 Independent of Receptor Binding Affinities." Growth Factors (Chur, Switzerland) 29, no. 4 (August 2011): 128–139.

Bondesen, Brenda A, Stephen T Mills, and Grace K Pavlath. "The COX-2 Pathway Regulates Growth of Atrophied Muscle via Multiple Mechanisms." American Journal of Physiology. Cell Physiology 290, no. 6 (June 2006): C1651–1659.

Bowen, David C., John S. Park, Sue Bodine, Jennifer L. Stark, David M. Valenzuela, Trevor N. Stitt, George D. Yancopoulos, Ronald M. Lindsay, David J. Glass, and Peter S. DiStefano. "Localization and Regulation of MuSK at the Neuromuscular Junction." Developmental Biology 199, no. 2 (July 15, 1998): 309–319.

DeChiara, T M, D C Bowen, D M Valenzuela, M V Simmons, W T Poueymirou, S Thomas, E Kinetz, et al. "The Receptor Tyrosine Kinase MuSK Is Required for Neuromuscular Junction Formation in Vivo." Cell 85, no. 4 (May 17, 1996): 501–512.

Desjardins, Philippe R., James M. Burkman, Joseph B. Shrager, Leonard A. Allmond, and Hansell H. Stedman. "Evolutionary Implications of Three Novel Members of the Human Sarcomeric Myosin Heavy Chain Gene Family." Molecular Biology and Evolution 19, no. 4 (April 1, 2002): 375–393.

de Sousa Lopes, Susana M Chuva, Bernard A J Roelen, Rui M Monteiro, Roul Emmens, Herbert Y Lin, En Li, Kirstie A Lawson, and Christine L Mummery. "BMP Signaling Mediated by ALK2 in the Visceral Endoderm Is Necessary for the Generation of Primordial Germ Cells in the Mouse Embryo." Genes & Development 18, no. 15 (August 1, 2004): 1838–1849.

Fainsod, A, K Deissler, R Yelin, K Marom, M Epstein, G Pillemer, H Steinbeisser, and M Blum. “The Dorsalizing and Neural Inducing Gene Follistatin Is an Antagonist of BMP-4.” Mechanisms of Development 63, no. 1 (April 1997): 39–50.

Fuentealba, Luis C., Edward Eivers, Atsushi Ikeda, Cecilia Hurtado, Hiroki Kuroda, Edgar M. Pera, and E. M. De Robertis. “Integrating Patterning Signals: Wnt/GSK3 Regulates the Duration of the BMP/Smad1 Signal.” Cell 131, no. 5 (November 30, 2007): 980–993.

Glass, David J, David C Bowen, Trevor N Stitt, Czeslaw Radziejewski, JoAnne Bruno, Terence E Ryan, David R Gies, et al. “Agrin Acts via a MuSK Receptor Complex.” *Cell* 85, no. 4 (May 17, 1996): 513–523.

Garcia-Osta, Ana, Panayiotis Tsokas, Gabriella Pollonini, Emmanuel M Landau, Robert Blitzer, and Cristina M Alberini. “MuSK Expressed in the Brain Mediates Cholinergic Responses, Synaptic Plasticity, and Memory Formation.” The Journal of Neuroscience: The Official Journal of the Society for Neuroscience 26, no. 30 (July 26, 2006): 7919–7932.

Gordon, Laura R, Katherine D Gribble, Camille M Syrett, and Michael Granato. “Initiation of Synapse Formation by Wnt-induced MuSK Endocytosis.” Development (Cambridge, England) 139, no. 5 (March 2012): 1023–1033.

Hagihara, Meiko, Mitsuharu Endo, Katsuhiko Hata, Chikahisa Higuchi, Kunio Takaoka, Hideki Yoshikawa, and Toshihide Yamashita. “Neogenin, a Receptor for Bone Morphogenetic Proteins.” *The Journal of Biological Chemistry* 286, no. 7 (February 18, 2011): 5157–5165.

Halbrooks, Peter J, Ru Ding, John M Wozney, and Gerard Bain. “Role of RGM Coreceptors in Bone Morphogenetic Protein Signaling.” Journal of Molecular Signaling 2 (2007): 4.

Hartung, Anke, Keren Bitton-Worms, Maya Mouler Rechtman, Valeska Wenzel, Jan H. Boergermann, Sylke Hassel, Yoav I. Henis, and Petra Knaus. “Different Routes of Bone Morphogenic Protein (BMP) Receptor Endocytosis Influence BMP Signaling.” Molecular and Cellular Biology 26, no. 20 (October 15, 2006): 7791–7805.

Hassel, Sylke, Mariya Yakymovych, Ulf Hellman, Lars Rönnstrand, Petra Knaus, and Serhiy Souchelnytskyi. “Interaction and Functional Cooperation Between the Serine/threonine Kinase Bone Morphogenetic Protein Type II Receptor with the Tyrosine Kinase Stem Cell Factor Receptor.” Journal of Cellular Physiology 206, no. 2 (February 2006): 457–467.

Herbst, R, and S J Burden. “The Juxtamembrane Region of MuSK Has a Critical Role in Agrin-mediated Signaling.” *The EMBO Journal* 19, no. 1 (January 4, 2000): 67–77.

Hesser, B A, A Sander, and V Witzemann. “Identification and Characterization of a Novel Splice Variant of MuSK.” FEBS Letters 442, no. 2–3 (January 15, 1999): 133–137.

Hollnagel, A, V Oehlmann, J Heymer, U Rüther, and A Nordheim. “Id Genes Are Direct Targets of Bone Morphogenetic Protein Induction in Embryonic Stem Cells.” *The Journal of Biological Chemistry* 274, no. 28 (July 9, 1999): 19838–19845.

Hoodless, P A, T Haerry, S Abdollah, M Stapleton, M B O’Connor, L Attisano, and J L Wrana. “MADR1, a MAD-related Protein That Functions in BMP2 Signaling Pathways.” Cell 85, no. 4 (May 17, 1996): 489–500.

Horsley, Valerie, and Grace K Pavlath. “Prostaglandin F2(alpha) Stimulates Growth of Skeletal Muscle Cells via an NFATC2-dependent Pathway.” The Journal of Cell Biology 161, no. 1 (April 14, 2003): 111–118.

Kim, Natalie, Amy L Stiegler, Thomas O Cameron, Peter T Hallock, Andrea M Gomez, Julie H Huang, Stevan R Hubbard, Michael L Dustin, and Steven J Burden. “Lrp4 Is a Receptor for Agrin and Forms a Complex with MuSK.” Cell 135, no. 2 (October 17, 2008): 334–342.

Korchynskyi, Olexander, and Peter ten Dijke. “Identification and Functional Characterization of Distinct Critically Important Bone Morphogenetic Protein-specific Response Elements in the Id1 Promoter.” *The Journal of Biological Chemistry* 277, no. 7 (February 15, 2002): 4883–4891.

Kretzschmar, M, F Liu, A Hata, J Doody, and J Massagué. “The TGF-beta Family Mediator Smad1 Is Phosphorylated Directly and Activated Functionally by the BMP Receptor Kinase.” Genes & Development 11, no. 8 (April 15, 1997): 984–995.

Kuehn, Rosemarie, Sallee A Eckler, and Medha Gautam. “Multiple Alternatively Spliced Transcripts of the Receptor Tyrosine Kinase MuSK Are Expressed in Muscle.” Gene 360, no. 2 (November 7, 2005): 83–91.

Kumar, Jitender, Maria Swanberg, Fiona McGuigan, Mattias Callreus, Paul Gerdhem, and Kristina Akesson. “LRP4 Association to Bone Properties and Fracture and Interaction with Genes in the Wnt- and BMP Signaling Pathways.” Bone 49, no. 3 (September 2011): 343–348.

Lagna, G, A Hata, A Hemmati-Brivanlou, and J Massagué. “Partnership Between DPC4 and SMAD Proteins in TGF-beta Signalling Pathways.” Nature 383, no. 6603 (October 31, 1996): 832–836.

Liu, F, A Hata, J C Baker, J Doody, J Cárcamo, R M Harland, and J Massagué. "A Human Mad Protein Acting as a BMP-regulated Transcriptional Activator." Nature 381, no. 6583 (June 13, 1996): 620–623.

López-Rovira, Teresa, Elisabet Chalaux, Joan Massagué, Jose Luis Rosa, and Francesc Ventura. "Direct Binding of Smad1 and Smad4 to Two Distinct Motifs Mediates Bone Morphogenetic Protein-specific Transcriptional Activation of Id1 Gene." *The Journal of Biological Chemistry* 277, no. 5 (February 1, 2002): 3176–3185.

Lyons, G E, M E Buckingham, S Tweedie, and Y H Edwards. "Carbonic Anhydrase III, an Early Mesodermal Marker, Is Expressed in Embryonic Mouse Skeletal Muscle and Notochord." Development (Cambridge, England) 111, no. 1 (January 1991): 233–244.

Mazhar, Sania, and Ruth Herbst. "The Formation of Complex Acetylcholine Receptor Clusters Requires MuSK Kinase Activity and Structural Information from the MuSK Extracellular Domain." *Molecular and Cellular Neuroscience* 49, no. 4 (April 2012): 475–486.

Miyama, K, G Yamada, T S Yamamoto, C Takagi, K Miyado, M Sakai, N Ueno, and H Shibuya. "A BMP-inducible Gene, Dlx5, Regulates Osteoblast Differentiation and Mesoderm Induction." Developmental Biology 208, no. 1 (April 1, 1999): 123–133.

Morgan, J E, J R Beauchamp, C N Pagel, M Peckham, P Ataliotis, P S Jat, M D Noble, K Farmer, and T A Partridge. "Myogenic Cell Lines Derived from Transgenic Mice Carrying a Thermolabile T Antigen: a Model System for the Derivation of Tissue-specific and Mutation-specific Cell Lines." *Developmental Biology* 162, no. 2 (April 1994): 486–498.

Nohno, T, T Ishikawa, T Saito, K Hosokawa, S Noji, D H Wolsing, and J S Rosenbaum. "Identification of a Human Type II Receptor for Bone Morphogenetic Protein-4 That Forms Differential Heteromeric Complexes with Bone Morphogenetic Protein Type I Receptors." The Journal of Biological Chemistry 270, no. 38 (September 22, 1995): 22522–22526.

Ogata, T, J M Wozney, R Benezra, and M Noda. "Bone Morphogenetic Protein 2 Transiently Enhances Expression of a Gene, Id (inhibitor of Differentiation), Encoding a Helix-loop-helix Molecule in Osteoblast-like Cells." *Proceedings of the National Academy of Sciences of the United States of America* 90, no. 19 (October 1, 1993): 9219–9222.

Ohazama, Atsushi, Eric B Johnson, Masato S Ota, Hong Y Choi, Hong J Choi, Thantrira Porntaveetus, Shelly Oommen, et al. "Lrp4 Modulates Extracellular Integration of Cell Signaling Pathways in Development." PloS One 3, no. 12 (2008): e4092.

Onichtchouk, D, Y G Chen, R Dosch, V Gawantka, H Delius, J Massagué, and C Niehrs. "Silencing of TGF-beta Signalling by the Pseudoreceptor BAMBI." Nature 401, no. 6752 (September 30, 1999): 480–485.

Ono, Y, F Calhabeu, J E Morgan, T Katagiri, H Amthor, and P S Zammit. "BMP Signalling Permits Population Expansion by Preventing Premature Myogenic Differentiation in Muscle Satellite Cells." Cell Death and Differentiation 18, no. 2 (February 2011): 222–234.

Otis, Jeffrey S, Thomas J Burkholder, and Grace K Pavlath. "Stretch-induced Myoblast Proliferation Is Dependent on the COX2 Pathway." Experimental Cell Research 310, no. 2 (November 1, 2005): 417–425.

Pandey, Kailash N. "Functional Roles of Short Sequence Motifs in the Endocytosis of Membrane Receptors." Frontiers in Bioscience : a Journal and Virtual Library 14 (June 1, 2009): 5339–5360.

Piccolo, S, Y Sasai, B Lu, and E M De Robertis. "Dorsoventral Patterning in Xenopus: Inhibition of Ventral Signals by Direct Binding of Chordin to BMP-4." Cell 86, no. 4 (August 23, 1996): 589–598.

Punga, Anna R, Marcin Maj, Shuo Lin, Sarina Meinen, and Markus A Rüegg. "MuSK Levels Differ Between Adult Skeletal Muscles and Influence Postsynaptic Plasticity." The European Journal of Neuroscience 33, no. 5 (March 2011): 890–898.

Rossi, Alberto C, Cristina Mammucari, Carla Argentini, Carlo Reggiani, and Stefano Schiaffino. "Two Novel/ancient Myosins in Mammalian Skeletal Muscles: MYH14/7b and MYH15 Are Expressed in Extraocular Muscles and Muscle Spindles." *The Journal of Physiology* 588, no. Pt 2 (January 15, 2010): 353–364.

Samad, Tarek A., Anuradha Rebbapragada, Esther Bell, Ying Zhang, Yisrael Sidis, Sung-Jin Jeong, Jason A. Campagna, et al. "DRAGON, a Bone Morphogenetic Protein Co-receptor." Journal of Biological Chemistry 280, no. 14 (April 8, 2005): 14122–14129.

Sammar, Marei, Christina Sieber, and Petra Knaus. "Biochemical and Functional Characterization of the Ror2/BRIb Receptor Complex." *Biochemical and Biophysical Research Communications* 381, no. 1 (March 27, 2009): 1–6.

Sammar, Marei, Sigmar Stricker, Georg C Schwabe, Christina Sieber, Anke Hartung, Michael Hanke, Isao Oishi, et al. "Modulation of GDF5/BRI-b Signalling Through Interaction with the Tyrosine Kinase Receptor Ror2." *Genes to Cells: Devoted to Molecular & Cellular Mechanisms* 9, no. 12 (December 2004): 1227–1238.

Song, Kyoung Seob, Yeon Ho Choi, Jong-Mu Kim, Hyunjae Lee, Tae-Jin Lee, and Joo-Heon Yoon. "Suppression of Prostaglandin E2-induced MUC5AC Overproduction by RGS4 in the Airway." American Journal of Physiology. Lung Cellular and Molecular Physiology 296, no. 4 (April 2009): L684–692.

Stiegler, Amy L., Steven J. Burden, and Stevan R. Hubbard. "Crystal Structure of the Agrin-responsive Immunoglobulin-like Domains 1 and 2 of the Receptor Tyrosine Kinase MuSK." Journal of Molecular Biology 364, no. 3 (December 2006): 424–433.

Suzuki, A, E Kaneko, J Maeda, and N Ueno. "Mesoderm Induction by BMP-4 and -7 Heterodimers." Biochemical and Biophysical Research Communications 232, no. 1 (March 6, 1997): 153–156.

Svitel, Juraj, Andrea Balbo, Roy A Mariuzza, Noreen R Gonzales, and Peter Schuck. "Combined Affinity and Rate Constant Distributions of Ligand Populations from Experimental Surface Binding Kinetics and Equilibria." Biophysical Journal 84, no. 6 (June 2003): 4062–4077.

Tamirisa, P, K J Blumer, and A J Muslin. "RGS4 Inhibits G-protein Signaling in Cardiomyocytes." Circulation 99, no. 3 (January 26, 1999): 441–447.

ten Dijke, P, H Yamashita, T K Sampath, A H Reddi, M Estevez, D L Riddle, H Ichijo, C H Heldin, and K Miyazono. "Identification of Type I Receptors for Osteogenic Protein-1 and Bone Morphogenetic Protein-4." The Journal of Biological Chemistry 269, no. 25 (June 24, 1994): 16985–16988.

Valenzuela, D M, T N Stitt, P S DiStefano, E Rojas, K Mattsson, D L Compton, L Nuñez, J S Park, J L Stark, and D R Gies. "Receptor Tyrosine Kinase Specific for the Skeletal Muscle Lineage: Expression in Embryonic Muscle, at the Neuromuscular Junction, and After Injury." *Neuron* 15, no. 3 (September 1995): 573–584.

Vogt, Janis, Ryan Traynor, and Gopal P Sapkota. "The Specificities of Small Molecule Inhibitors of the TGFß and BMP Pathways." *Cellular Signalling* 23, no. 11 (November 2011): 1831–1842.

von Bubnoff, A, and K W Cho. "Intracellular BMP Signaling Regulation in Vertebrates: Pathway or Network?" Developmental Biology 239, no. 1 (November 1, 2001): 1–14.

Wrana, J L, L Attisano, R Wieser, F Ventura, and J Massagué. "Mechanism of Activation of the TGF-beta Receptor." Nature 370, no. 6488 (August 4, 1994): 341–347.

Xia, Yin, Paul B Yu, Yisrael Sidis, Hideyuki Beppu, Kenneth D Bloch, Alan L Schneyer, and Herbert Y Lin. "Repulsive Guidance Molecule RGMa Alters Utilization of Bone

Morphogenetic Protein (BMP) Type II Receptors by BMP2 and BMP4." The Journal of Biological Chemistry 282, no. 25 (June 22, 2007): 18129–18140.

Yun, Seong-Wook, Cheryl Leong, Duanting Zhai, Yee Ling Tan, Linda Lim, Xuezhi Bi, Jae-Jung Lee, et al. "Neural Stem Cell Specific Fluorescent Chemical Probe Binding to FABP7." Proceedings of the National Academy of Sciences of the United States of America 109, no. 26 (June 26, 2012): 10214–10217.

Zhang, Wei, Anne-Sophie Coldefy, Stevan R Hubbard, and Steven J Burden. "Agrin Binds to the N-terminal Region of Lrp4 Protein and Stimulates Association Between Lrp4 and the First Immunoglobulin-like Domain in Muscle-specific Kinase (MuSK)." The Journal of Biological Chemistry 286, no. 47 (November 25, 2011): 40624–40630.

Zhang, Bin, Chuan Liang, Ryan Bates, Yiming Yin, Wen-Cheng Xiong, and Lin Mei. "Wnt Proteins Regulate Acetylcholine Receptor Clustering in Muscle Cells." *Molecular Brain* 5 (2012): 7.

Zhu, Dan, Zhihua Yang, Zhenge Luo, Shiwen Luo, Wen C Xiong, and Lin Mei. "Muscle-Specific Receptor Tyrosine Kinase Endocytosis in Acetylcholine Receptor Clustering in Response to Agrin." *The Journal of Neuroscience* 28, no. 7 (February 13, 2008): 1688–1696.

Zhou, H, D J Glass, G D Yancopoulos, and J R Sanes. "Distinct Domains of MuSK Mediate Its Abilities to Induce and to Associate with Postsynaptic Specializations." The Journal of Cell Biology 146, no. 5 (September 6, 1999): 1133–1146.

Zilberberg, Lior, Peter ten Dijke, Lynn Y Sakai, and Daniel B Rifkin. "A Rapid and Sensitive Bioassay to Measure Bone Morphogenetic Protein Activity." *BMC Cell Biology* 8 (2007): 41.

Zimmerman, L B, J M De Jesús-Escobar, and R M Harland. "The Spemann Organizer Signal Noggin Binds and Inactivates Bone Morphogenetic Protein 4." Cell 86, no. 4 (August 23, 1996): 599–606.

Zong, Yinong, Bin Zhang, Shenyan Gu, Kwangkook Lee, Jie Zhou, Guorui Yao, Dwight Figueiredo, Kay Perry, Lin Mei, and Rongsheng Jin. "Structural Basis of agrin-LRP4-MuSK Signaling." Genes & Development 26, no. 3 (February 1, 2012): 247–258.

Supplemental Material

Supplementary Figure 2.1

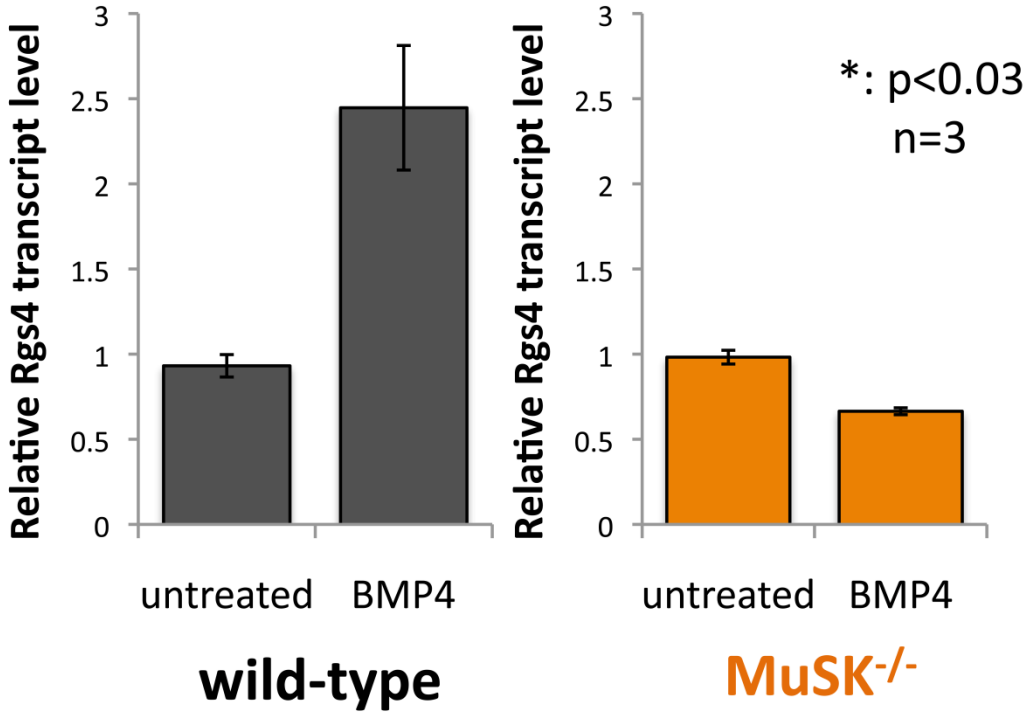

Supplementary Figure 2.1. BMP4 induced Rgs4 expression at an earlier time-point. Wild type H-2Kb-tsA58 and MuSK null myoblasts were serum deprived for 5-6 hours and treated with 3.25ng/ml BMP4 for 2 hours. RNA was isolated, reverse-transcribed into double stranded cDNA. Rgs4 transcript levels were measured by qRT-PCR. (n=3)

Supplementary Table 2.1

Gene Symbol	Fold-Change	p-value
Rgs4	5.70	0.0000143
Msx2	4.13	0.0000505
Avpr1a	4.01	0.0001288
2310002L13Rik	3.78	0.0005764
Kazald1	3.42	0.0000567
Foxc2	2.92	0.0000421

Sema6d	2.88	0.0000498
Lgr4	2.66	0.0000446
Ptx3	2.62	0.0000194
Serpinb2	2.62	0.0001340
Ptger4	2.56	0.0000180
Timp3	2.51	0.0007816
Nog	2.51	0.0000139
Pcp4l1	2.44	0.0002664
Orai2	2.43	0.0002012
Slc5a7	2.40	0.0003592
Orai2	2.38	0.0009485
Gprin3	2.38	0.0001323
Plcb1	2.33	0.0000312
Slc25a13	2.32	0.0001249
Snai2	2.24	0.0000299
Inhba	2.23	0.0000116
Prr9	2.22	0.0008294
Lef1	2.21	0.0006123
Insc	2.17	0.0000814
Hoxc13	2.11	0.0008357
Asphd2	2.09	0.0004314
Tiam2	2.08	0.0002241

Rasl11a	2.07	0.0002635
Ptch1	2.05	0.0004419
Itgb1bp3	2.02	0.0002875
Dio2	2.02	0.0001115
Tmem56	2.01	0.0000034
Erc1	2.00	0.0000768
Dlx3	2.00	0.0000510
Trps1	1.98	0.0002073
Hoxc11	1.98	0.0000027
Prr5l	1.96	0.0004528
Kcnf1	1.96	0.0002341
Myf5	1.96	0.0007566
Pappa	1.94	0.0010591
Skil	1.93	0.0000764
Cpne4	1.93	0.0000746
A630033H20Rik	1.89	0.0004233
Thsd7a	1.89	0.0000377
Pdk4	1.89	0.0001955
Vasn	1.89	0.0004233
Lpl	1.88	0.0004933
Rarres1	1.87	0.0001771
Ttc39b	1.87	0.0000794

Ier3	1.87	0.0001215
Tm4sf1	1.86	0.0000067
Hoxa11	1.86	0.0001793
Fzd1	1.84	0.0001878
Has2	1.84	0.0000313
Car8	1.83	0.0010320
Htr1b	1.82	0.0001701
Erc1	1.82	0.0001232
Pcdh7	1.82	0.0000127
Pcolce2	1.82	0.0004945
Ptpru	1.82	0.0007651
Mab21l1	1.82	0.0001930
Smoc1	1.80	0.0000532
Fzd7	1.80	0.0004557
Papss2	1.78	0.0005405
Col10a1	1.78	0.0004565
Tmeff1	1.76	0.0000932
Ssfa2	1.75	0.0006513
Junb	1.74	0.0000945
Gcnt4	1.74	0.0000814
Prss35	1.73	0.0000027
Itgb8	1.73	0.0000536

2900062L11Rik	1.73	0.0010198
Klf10	1.72	0.0004308
Rpgrip1l	1.71	0.0003224
9330159F19Rik	1.71	0.0010531
Ccdc34	1.70	0.0001323
Smpdl3a	1.70	0.0000142
Flrt2	1.67	0.0000579
Jak2	1.67	0.0000748
Pi15	1.66	0.0010803
Cpm	1.65	0.0010810
Il17ra	1.64	0.0000204
Cldn1	1.63	0.0008935
Mpp2	1.62	0.0004449
Ppap2b	1.61	0.0003542
Alpk1	1.61	0.0001941
	1.61	0.0007314
Grb14	1.60	0.0002481
	1.60	0.0007166
Tmeff2	1.60	0.0000023
Clcf1	1.60	0.0000406
Epha7	1.60	0.0005076
	1.60	0.0010815

Lrrc8c	1.59	0.0000875
Podnl1	1.59	0.0002083
Rusc2	1.59	0.0010403
Rhou	1.59	0.0005517
Jhdm1d	1.58	0.0001653
Cxcr4	1.58	0.0002609
Irx5	1.57	0.0003214
Mtmr11	1.56	0.0004627
Ephb2	1.56	0.0005772
Fmn2	1.56	0.0004682
Sh3bp4	1.56	0.0009683
Egr2	1.56	0.0004437
Asap1	1.56	0.0000804
Kremen1	1.55	0.0000011
Fam135a	1.55	0.0000553
Twist2	1.55	0.0002147
Syn1	1.55	0.0003857
Dok4	1.54	0.0004804
Mapkapk3	1.54	0.0002218
Zfp462	1.54	0.0001355
Angptl2	1.53	0.0002387
Tsc22d1	1.53	0.0000225

Cenpp	1.53	0.0010767
Sstr2	1.53	0.0004486
Col12a1	1.52	0.0008099
Rai14	1.52	0.0004927
Stmn2	1.52	0.0005157
Stra6	1.51	0.0003715
Pdgfra	1.51	0.0009207
Zbtb2	1.50	0.0007063
Tmem45a	1.49	0.0003357
Tnfrsf12a	1.48	0.0010481
Timp1	1.48	0.0001630
Musk	1.47	0.0003490
Retsat	1.47	0.0002800
Prickle1	1.47	0.0006212
	1.47	0.0000158
Pgm2l1	1.47	0.0009379
	1.47	0.0006998
Isl1	1.46	0.0008981
	1.46	0.0007626
Itpripl2	1.45	0.0009280
Stbd1	1.45	0.0009528
Glis1	1.45	0.0004584

Wnt5a	1.44	0.0000137
Mmp28	1.44	0.0005021
Pax3	1.44	0.0000540
Rgnef	1.44	0.0001481
Msx1	1.43	0.0007694
Abcc4	1.43	0.0006269
Ephb6	1.43	0.0002071
Phldb2	1.42	0.0000237
Rnf125	1.42	0.0001259
Rab3a	1.42	0.0006564
Btg3	1.42	0.0004979
Aaas	1.41	0.0007230
Ikzf2	1.41	0.0003251
3110006E14Rik	1.41	0.0007078
2810030E01Rik	1.40	0.0010775
Kalrn	1.40	0.0003756
Tmem119	1.40	0.0000023
Rgl1	1.40	0.0003680
Rufy3	1.40	0.0007387
B3gnt2	1.39	0.0005389
Btg3	1.39	0.0006596
Fam161a	1.39	0.0009682

Srxn1	1.39	0.0004043
Rab39b	1.39	0.0007812
Zfp365	1.38	0.0006040
Prrx1	1.38	0.0009289
Rab27b	1.38	0.0004361
Cc2d2a	1.38	0.0007264
Slc39a14	1.38	0.0000693
Phtf2	1.38	0.0001752
Ell2	1.37	0.0007072
Arl10	1.37	0.0006908
Dnajb14	1.37	0.0006226
	1.36	0.0003009
Golim4	1.36	0.0008862
Manea	1.36	0.0009809
Lrrk2	1.36	0.0000905
	1.35	0.0004983
Kif21b	1.35	0.0008825
Rnf41	1.35	0.0006670
Slc44a2	1.35	0.0003451
Dusp8	1.34	0.0001000
Sertad1	1.34	0.0009626
Mupcdh	1.34	0.0007916

E2f5	1.34	0.0002054
Prkaa1	1.34	0.0001647
Nr1d1	1.33	0.0000138
Pqlc3	1.33	0.0007139
Epb4.1l3	1.33	0.0001960
Slc1a4	1.33	0.0001838
Slc9a2	1.33	0.0008544
	1.32	0.0000151
Wwc2	1.32	0.0009414
Zeb2	1.32	0.0006631
Elk3	1.30	0.0000771
Slc7a1	1.29	0.0001372
Tmem104	1.29	0.0001430
Derl3	1.29	0.0010716
Akap2	1.29	0.0001063
Carf	1.28	0.0005280
Rnf138	1.28	0.0005703
Adamts12	1.28	0.0002444
Eml3	1.28	0.0009465
Sash1	1.27	0.0006048
Cdc2l6	1.27	0.0003786
Ddr1	1.27	0.0002264

Bag3	1.27	0.0000268
	1.26	0.0008388
Bcor	1.26	0.0010313
Ppt2	1.26	0.0002808
Tmem54	1.26	0.0009634
Fdxr	1.25	0.0006297
9030425E11Rik	1.25	0.0000867
Slc10a7	1.25	0.0000017
Dbc1	1.24	0.0000049
Rnf149	1.24	0.0006702
Chpf2	1.24	0.0004279
Purg	1.24	0.0009966
Svep1	1.23	0.0003406
	1.23	0.0010206
0610007P08Rik	1.23	0.0003946
Synj1	1.23	0.0004797
Mras	1.23	0.0005532
Rdx	1.23	0.0010236
4930402H24Rik	1.22	0.0003672
Tmem173	1.22	0.0003495
Mknk2	1.21	0.0006977
Hdac5	1.20	0.0000641

Metrnl	1.20	0.0008875
Pcnx	1.20	0.0001538
Blzf1	1.20	0.0000531
Phlda3	1.20	0.0007703
Shroom4	1.20	0.0010561
9430015G10Rik	1.20	0.0002910

Supplementary Table 2.1. Transcripts upregulated by BMP4 only in wild type myoblasts. Fold-changes indicate the upregulation of the listed transcript by BMP4. Fold changes greater than 1.2 are shown in the table.

Supplementary Table 2.2

Gene Symbol	Fold-Change	p-value
Sp7	10.58	0.0000161
Fabp7	9.08	0.0000059
Grem2	8.22	0.0000176
Id1	5.42	0.0000003
Dlx2	5.38	0.0000138
Ptgs2	5.21	0.0000067

Id3	5.08	0.0000081
Smad6	4.88	0.0000018
Alpl	4.39	0.0001661
Foxq1	3.77	0.0000168
Unc5b	3.65	0.0005125
Smad7	3.63	0.0000009
Serpinb8	3.38	0.0000107
Bambi	3.16	0.0000401
Lgr6	3.16	0.0000976
Fgfr2	3.09	0.0002492
Atoh8	3.02	0.0000126
Id2	2.99	0.0000118
Smad9	2.91	0.0000144
Lxn	2.90	0.0002553
Adamts9	2.83	0.0000691
Nkd2	2.80	0.0005255
Gcnt2	2.73	0.0000001
1300014I06Rik	2.70	0.0000098
Dlx1	2.69	0.0000282
Rspo3	2.68	0.0003037
Smoc2	2.67	0.0000152
Enc1	2.63	0.0000118

Pgf	2.63	0.0000596
Lfng	2.58	0.0000033
Baalc	2.51	0.0000981
Ctgf	2.46	0.0000830
Adamts9	2.44	0.0000339
Foxl1	2.36	0.0000183
Serpine1	2.20	0.0001436
Gnb4	2.19	0.0000485
Wnt2	2.17	0.0003486
Kif26b	2.12	0.0001033
Kctd12	2.11	0.0000301
Myo1d	2.10	0.0000039
Pde8a	2.05	0.0000085
Fam84a	2.01	0.0002542
Ahcyl2	2.01	0.0000317
Adamts9	2.00	0.0005875
Csrp2	1.99	0.0000552
Wnt4	1.97	0.0009629
Optn	1.95	0.0000805
Fam19a5	1.95	0.0002117
Cspg4	1.94	0.0000833
Gas6	1.89	0.0003323

Nfkbia	1.86	0.0005386
Hoxa10	1.85	0.0000558
Prrx2	1.83	0.0000337
Slc7a11	1.82	0.0000160
Cxcl14	1.82	0.0000347
Dock5	1.80	0.0000034
Ank	1.80	0.0000172
Samhd1	1.76	0.0003039
Npr3	1.76	0.0004214
Mmp11	1.76	0.0010683
Chmp2b	1.75	0.0001108
Dpysl3	1.70	0.0000034
Pcdh18	1.69	0.0006087
Jag1	1.69	0.0003387
Cux1	1.63	0.0000370
1110032E23Rik	1.62	0.0004655
Relt	1.60	0.0002817
Adamtsl3	1.57	0.0001643
Tpbg	1.56	0.0000216
Fam38b2	1.55	0.0009779
Sox9	1.55	0.0003365
Epha2	1.53	0.0008823

Tnfrsf21	1.53	0.0000233
Ptprm	1.52	0.0001927
Crim1	1.52	0.0002062
Atp10d	1.50	0.0002664
Man1a	1.50	0.0006539
Lyst	1.50	0.0000019
Kif26b	1.50	0.0001586
Fzd6	1.44	0.0000429
Ass1	1.43	0.0005171
Ass1	1.43	0.0005998
Tmem2	1.42	0.0001204
Gclc	1.42	0.0001196
Slc44a1	1.42	0.0001084
Slc5a3	1.39	0.0003938
Palld	1.39	0.0004808
Atp2c1	1.39	0.0002947
Slc7a2	1.38	0.0001401
Kirrel	1.38	0.0002013
Capn5	1.37	0.0003373
6330416G13Rik	1.36	0.0004968
Chst11	1.36	0.0000544
Peli2	1.35	0.0009524

Ahr	1.35	0.0003480
Lrp6	1.33	0.0000117
Ednra	1.32	0.0000278
Tln2	1.32	0.0008167
Acvr1	1.31	0.0003443
Galnt2	1.27	0.0004890
Dlst	1.26	0.0004482
Fam65a	1.24	0.0001126
Csnk1g3	1.23	0.0007569

Supplementary Table 2.2. Transcripts upregulated by BMP4 both in wild-type and MuSK null myoblasts. Fold-changes indicate the upregulation of the listed transcript by BMP4. Fold changes greater than 1.2 are shown in the table. (For simplicity, only the fold-changes from wild-type cultures are shown in the table)

Supplementary Table 2.3

Gene Symbol	Fold-Change	p-value
Lin7a	4.94	0.0003900
Gm12824	4.22	0.0004426

Hey1	3.89	0.0002575
Selp	3.46	0.0000023
Tbx1	2.72	0.0001291
Stc2	2.68	0.0001532
Slc1a3	2.53	0.0000955
Irf5	2.53	0.0002718
Emb	2.44	0.0005802
Klhl29	2.26	0.0004717
Kcnh5	2.24	0.0000496
Gjb3	2.19	0.0000546
Il15	2.18	0.0001363
Adam12	2.16	0.0000011
Fam55c	2.15	0.0000145
Fst	2.06	0.0000663
Ppp1r3c	2.05	0.0000727
Slc2a13	1.97	0.0003914
Tbx20	1.96	0.0000647
Ankrd44	1.94	0.0000566
Depdc6	1.90	0.0001964
Hmgcll1	1.86	0.0002828
Krt19	1.85	0.0003951
Adcy8	1.82	0.0004721

Adamtsl1	1.76	0.0000295
Bmp2k	1.75	0.0001046
Grem1	1.75	0.0001096
Pparg	1.74	0.0001149
Fzd4	1.71	0.0000923
Pdgfrl	1.70	0.0000023
	1.69	0.0003142
Acss3	1.69	0.0005332
Osbpl6	1.64	0.0001490
Adamtsl1	1.62	0.0004975
A930038C07Rik	1.62	0.0000051
Rims2	1.61	0.0000332
Iqgap2	1.61	0.0000418
Vegfc	1.59	0.0005939
Asb4	1.58	0.0002124
Efna3	1.56	0.0004736
4931406P16Rik	1.56	0.0005929
Prrg1	1.55	0.0007051
	1.54	0.0003099
Grhl1	1.53	0.0005838
Esyt3	1.52	0.0004370
Hoxb2	1.48	0.0002266

Sostdc1	1.45	0.0002509
Acsl1	1.45	0.0000729
Zbtb25	1.44	0.0004446
Cish	1.44	0.0003414
Cd47	1.44	0.0001359
	1.42	0.0004539
Pgam2	1.42	0.0001249
Il13ra1	1.41	0.0005407
Hoxa9	1.40	0.0001565
Chsy3	1.39	0.0004188
Nrp2	1.39	0.0000050
Trib2	1.38	0.0000093
Gramd2	1.38	0.0000013
Glis3	1.37	0.0004675
Freq	1.37	0.0006113
	1.35	0.0002059
Pdlim5	1.32	0.0003320
Calhm2	1.32	0.0001093
Mtag2	1.32	0.0005917
Pmepa1	1.32	0.0003797
Mrps6	1.32	0.0002322
	1.31	0.0005392

Adam10	1.30	0.0000215
Ceacam9	1.30	0.0002529
Thrb	1.30	0.0005348
Npnt	1.30	0.0004299
	1.30	0.0002977
Ppme1	1.29	0.0000400
Mdga1	1.27	0.0004805
Magi1	1.27	0.0003866
Xdh	1.26	0.0003931
Cdc14b	1.25	0.0007062
N4bp2l1	1.25	0.0005779
Alms1	1.25	0.0005051
Hspa1a	1.24	0.0003844
Pkp2	1.22	0.0002850
Ficd	1.22	0.0001747
Olfr177	1.21	0.0004665
Tmem50b	1.20	0.0001369
Tlcd1	1.20	0.0001759
Cbx8	1.20	0.0006164

Supplementary Table 2.3. Transcripts upregulated by BMP4 only in MuSK null myoblasts. Fold-changes indicate the upregulation of the listed transcript by BMP4. Fold changes greater than 1.2 are shown in the table.

Supplementary Table 2.4

Gene Symbol	Fold-Change	p-value
Sp7	8.69	0.0000045
Dhrs3	3.04	0.0001081
Rgs4	3.01	0.0000770
Adamts9	2.99	0.0001131
Lfng	2.89	0.0000963
Myh15	2.88	0.0004291
Slc10a4	2.72	0.0003353
Pgf	2.60	0.0000181
Adamts9	2.50	0.0000494
Selp	2.36	0.0001861
Hpgd	2.34	0.0001262
Grin3a	2.21	0.0007673
Arc	2.19	0.0001589
Ccdc74a	2.18	0.0004563
Ptgs2	2.18	0.0000096
Fgf2	2.18	0.0001711

Alpl	2.16	0.0000146
Kctd12	2.14	0.0000521
Kif26b	2.13	0.0000401
Nebl	2.11	0.0000497
Ptger4	2.10	0.0000079
Etl4	2.10	0.0000101
Wnt11	2.02	0.0007674
1300014I06Rik	2.02	0.0000951
Tbx1	2.00	0.0005592
Serpine1	1.96	0.0001781
Fam19a5	1.94	0.0004988
Slc24a4	1.93	0.0000356
Junb	1.90	0.0000435
Insc	1.86	0.0000349
St3gal6	1.84	0.0005664
Sdc3	1.84	0.0000133
--	1.84	0.0006638
Epha7	1.84	0.0000574
Kcnc4	1.82	0.0002959
Adcy1	1.81	0.0000157
Fzd5	1.81	0.0000247
Hoxc11	1.81	0.0003600

Cspg4	1.80	0.0005948
--	1.78	0.0006569
Orai2	1.77	0.0004315
Adamts9	1.77	0.0000795
Areg	1.76	0.0005841
Ptx3	1.75	0.0002167
Avpr1a	1.72	0.0002434
Orai2	1.71	0.0002898
Dpysl3	1.71	0.0000126
P4ha3	1.70	0.0000480
Shroom1	1.69	0.0005762
Nfkbia	1.67	0.0007483
Stbd1	1.67	0.0004681
Kremen1	1.66	0.0000332
Fam84a	1.64	0.0004296
Mex3b	1.62	0.0004509
Thsd7a	1.61	0.0000033
Wnt2	1.60	0.0001420
Chst11	1.60	0.0005794
Tnfrsf13c	1.60	0.0006128
Pank1	1.59	0.0000273
Ctgf	1.59	0.0004759

Podn	1.57	0.0005206
Kif26b	1.57	0.0004820
Dok7	1.56	0.0006384
Efna2	1.56	0.0001189
Jag1	1.55	0.0000886
Rps6ka5	1.54	0.0001718
Nr4a2	1.54	0.0002394
Hes6	1.53	0.0005466
Plxnd1	1.53	0.0003838
Slitrk4	1.53	0.0005484
Cyr61	1.52	0.0001222
9030425E11Rik	1.52	0.0005533
Cachd1	1.52	0.0005673
Plekha2	1.51	0.0004628
Rgs12	1.51	0.0001235
Pde5a	1.50	0.0000909
Itga1	1.50	0.0005239
9330159F19Rik	1.50	0.0006368
Fgfr2	1.49	0.0004556
Slc7a2	1.49	0.0000048
Mmp11	1.49	0.0004240
Timp3	1.48	0.0006282

Tgm2	1.47	0.0003525
E030011O05Rik	1.47	0.0001135
Inhba	1.47	0.0001435
Lgals3	1.47	0.0002452
Ier3	1.46	0.0001405
Fam135a	1.45	0.0005020
Ext1	1.44	0.0003667
Vdr	1.43	0.0007582
Fam46c	1.41	0.0007399
Myf6	1.41	0.0002346
--	1.41	0.0000537
Gas6	1.41	0.0004738
Rab3b	1.39	0.0005589
Bdnf	1.38	0.0000905
Tle1	1.38	0.0007446
Suv39h1	1.37	0.0003284
Rarres1	1.36	0.0003906
Pde7b	1.36	0.0007270
Ern1	1.35	0.0000349
Ncf1	1.35	0.0005654
Tln2	1.35	0.0003608
--	1.35	0.0001115

Slc43a2	1.34	0.0000659
--	1.32	0.0007619
Kif1a	1.32	0.0005083
Serpinf1	1.32	0.0006135
Dync1i1	1.31	0.0005698
BY080835	1.30	0.0003441
Vasn	1.30	0.0001598
Kif21b	1.30	0.0006049
Klf10	1.29	0.0000891
Parp8	1.29	0.0000783
Chmp2b	1.29	0.0000763
Chst2	1.28	0.0006049
Rarg	1.28	0.0007196
Fstl1	1.28	0.0000142
Olfr415	1.28	0.0003046
Capn1	1.28	0.0004650
Mbnl1	1.27	0.0001958
Ntan1	1.27	0.0000545
Zeb2	1.27	0.0000344
Zcchc14	1.27	0.0006383
A630091E08Rik	1.26	0.0004318
Elk3	1.26	0.0004549

Nbl1	1.26	0.0002941
Bmp2k	1.26	0.0002739
Rdx	1.24	0.0003980
Fkbp10	1.24	0.0003927
Arntl	1.24	0.0002645
Slc29a4	1.23	0.0001504
Gpr157	1.23	0.0002073
Jarid2	1.22	0.0001485
Maz	1.22	0.0000079
Snx15	1.22	0.0004358
Itfg3	1.21	0.0003037
Htra3	1.20	0.0000322
Mtus1	1.20	0.0004251
Lrp6	1.20	0.0003000

Supplementary table 2.4. Transcripts upregulated by BMP4 only in wild-type myotubes. Fold-changes indicate the upregulation of the listed transcript by BMP4. Fold changes greater than 1.2 are shown in the table.

Supplementary table 2.5

Gene Symbol	Fold-	p-value

	Change	
Fabp7	19.98	0.0000005
Cxcr4	4.35	0.0000090
Id1	4.14	0.0000046
Id3	3.68	0.0001405
Smad6	3.44	0.0000010
Atoh8	3.38	0.0000022
2310002L13Rik	3.15	0.0000115
Smad7	2.97	0.0000491
Prrx2	2.92	0.0000011
Dlx2	2.88	0.0000523
Gnb4	2.88	0.0000005
Greb1	2.74	0.0000804
Baalc	2.73	0.0002523
Grhl1	2.70	0.0002370
Hey1	2.67	0.0000070
St3gal1	2.60	0.0000172
Smad9	2.49	0.0000067
Palmd	2.36	0.0000462
Spry2	2.34	0.0000465
Kcnf1	2.29	0.0001802
Esr1	2.25	0.0000226

Gm12824	2.25	0.0000683
Smoc2	2.18	0.0001098
Tmeff1	2.17	0.0000287
Sema6d	2.16	0.0000715
Rasl11a	2.16	0.0000208
Hbegf	2.08	0.0000916
Serpinb8	2.05	0.0001995
Optn	2.03	0.0000065
Inha	2.03	0.0001186
Tiam2	2.00	0.0000049
Angptl2	1.99	0.0000190
Bambi	1.98	0.0002266
Csrp2	1.97	0.0000023
Unc5b	1.97	0.0000165
9130213B05Rik	1.95	0.0000049
Cthrc1	1.93	0.0001716
Hoxc13	1.93	0.0002313
Dlx1	1.91	0.0001567
Car13	1.89	0.0001202
Lxn	1.89	0.0005318
Tle3	1.86	0.0000084
Prg4	1.86	0.0007615

Id2	1.84	0.0001083
Runx2	1.82	0.0001272
Tmeff2	1.80	0.0000042
Enc1	1.80	0.0001272
Snai2	1.79	0.0001333
Ddr1	1.77	0.0000060
Foxc2	1.76	0.0000225
Gcnt2	1.75	0.0002086
Net1	1.73	0.0000298
Gse1	1.71	0.0001256
Tgfb1	1.71	0.0000291
S ept5	1.70	0.0000301
Gm12824	1.69	0.0005883
Sh3bp4	1.69	0.0000496
Tmem119	1.68	0.0000646
Pde8a	1.67	0.0001179
Ilkap	1.66	0.0002247
Dusp1	1.63	0.0002534
Myf5	1.61	0.0000898
Il17ra	1.60	0.0001803
Pdgfc	1.59	0.0000244
Cux1	1.57	0.0000448

Grem1	1.57	0.0001576
Lgr6	1.57	0.0007254
Jun	1.56	0.0000517
Tmem47	1.55	0.0004474
Unc5c	1.55	0.0002032
Ptprm	1.54	0.0001361
Golim4	1.51	0.0002435
Slc25a32	1.50	0.0000003
Eya4	1.50	0.0000048
Ankrd28	1.49	0.0003675
Plcd3	1.49	0.0007339
6330442E10Rik	1.47	0.0000921
Creb3l1	1.44	0.0005052
Skil	1.44	0.0006181
Tmem64	1.43	0.0001431
Flrt2	1.43	0.0002298
Fzd1	1.43	0.0000388
Aebp1	1.42	0.0002442
Col12a1	1.41	0.0000003
Ass1	1.41	0.0002622
Prrx1	1.41	0.0000528
Socs2	1.40	0.0001829

Ass1	1.40	0.0003002
6330416G13Rik	1.40	0.0003925
Snai1	1.40	0.0007220
Nav3	1.39	0.0001079
Snx25	1.36	0.0001355
3425401B19Rik	1.36	0.0005191
Dock5	1.35	0.0003001
Zbtb38	1.35	0.0005623
Raph1	1.34	0.0000467
Slc44a2	1.34	0.0000742
Myo10	1.32	0.0006481
Meis2	1.31	0.0000803
Asb5	1.31	0.0000008
Rai14	1.31	0.0001686
Prr16	1.31	0.0005664
Ugdh	1.29	0.0002734
Atp6v1g1	1.29	0.0000195
Ids	1.28	0.0001785
Epb4.1l1	1.27	0.0001063
Atp6v1g1	1.26	0.0000453
Cdon	1.26	0.0006243
Lysmd3	1.25	0.0007054

Osbpl3	1.24	0.0001454
Slc6a8	1.24	0.0005387
Lpin3	1.23	0.0005065
Xirp1	1.23	0.0007062
Car3	1.22	0.0004624

Supplementary table 2.5. Transcripts upregulated by BMP4 both in wild-type and MuSK null myotubes. Fold-changes indicate the upregulation of the listed transcript by BMP4. Fold changes greater than 1.2 are shown in the table. (For simplicity, only the fold-changes from wild-type cultures are shown in the table)

Supplementary table 2.6

Gene Symbol	Fold-Change	p-value
Prr9	6.80	0.0000111
Pcolce2	4.18	0.0000352
A530098C11Rik	4.11	0.0000177
4930412O13Rik	3.66	0.0000523
Olr1	3.52	0.0001038

Samd7	3.52	0.0002913
Itgb1bp3	3.27	0.0003820
Alpk2	2.98	0.0000111
Slc7a11	2.89	0.0000278
Tpbg	2.89	0.0000879
Fam55c	2.67	0.0003726
Slc9a2	2.58	0.0000714
Sfrp2	2.52	0.0000026
Gpr37	2.50	0.0004724
Ak3l1	2.46	0.0000657
---	2.46	0.0001367
Gata3	2.45	0.0000952
Lin7a	2.42	0.0000257
4930412O13Rik	2.41	0.0002443
2310045A20Rik	2.39	0.0000527
Rrm2	2.37	0.0002429
Hgf	2.37	0.0003182
Grem2	2.29	0.0002533
BC023105	2.28	0.0012488
Slc2a3	2.28	0.0001941
Prkg2	2.24	0.0000147
Ankrd37	2.20	0.0002882

Rorb	2.19	0.0004124
Sfrp4	2.18	0.0005419
Slco2a1	2.17	0.0000705
Dhrs9	2.13	0.0001824
Adm	2.04	0.0003952
Ppp1r3c	2.03	0.0006259
Nxf7	2.03	0.0001944
Atp10d	2.02	0.0012311
Tec	1.99	0.0000423
Timp1	1.98	0.0002008
Kcnq4	1.98	0.0001019
Adcy8	1.97	0.0000116
Tbx20	1.97	0.0008294
Opn3	1.96	0.0000020
---	1.94	0.0007543
Has2	1.93	0.0006286
Fosl1	1.93	0.0001022
Ereg	1.91	0.0011558
Itgb3	1.90	0.0003136
---	1.88	0.0000037
Ptpn3	1.88	0.0010442
Aldh1a3	1.88	0.0005623

Syn1	1.86	0.0002084
Tmem117	1.86	0.0002393
Ano5	1.86	0.0003671
Alcam	1.85	0.0001332
Ptpn3	1.85	0.0002888
Ptpn3	1.85	0.0001371
Uhrf1bp1l	1.85	0.0002515
Rufy3	1.84	0.0003425
Ifi202b	1.84	0.0002364
Ankrd1	1.84	0.0000325
Jak2	1.84	0.0002009
Nog	1.84	0.0006659
Pdk4	1.84	0.0000367
Fam110a	1.83	0.0004013
Rims2	1.83	0.0007488
2010002N04Rik	1.81	0.0002615
Gja5	1.81	0.0000447
Hcn1	1.81	0.0000544
Mylk2	1.80	0.0007058
Ces2	1.80	0.0009719
Csrp3	1.80	0.0001515
Stap1	1.79	0.0011733

Tmsb15a	1.78	0.0003148
Pappa2	1.78	0.0006261
Sdf2l1	1.77	0.0001956
Atp1b1	1.76	0.0000575
Crlf1	1.76	0.0007661
Serpinb1a	1.76	0.0000093
Btg3	1.75	0.0003358
Pappa2	1.75	0.0001141
Btg3	1.74	0.0003832
Tgfb2	1.74	0.0001445
Pfkfb3	1.73	0.0001441
Olfm1	1.72	0.0000829
Gm1078	1.72	0.0001417
Sema3a	1.71	0.0004086
Tmem56	1.71	0.0002192
Nol4	1.71	0.0011101
Kremen2	1.71	0.0004522
Fam178a	1.71	0.0005730
Hspa1l	1.69	0.0009244
Frrs1	1.68	0.0002168
Tspan18	1.68	0.0009213
Herc3	1.68	0.0002117

Irf6	1.68	0.0010943
Dnajb4	1.67	0.0011273
Rrad	1.66	0.0010142
Dapk2	1.66	0.0001043
Ptpn3	1.65	0.0000242
Erc1	1.65	0.0005432
Bnip3	1.65	0.0002628
Fhdc1	1.64	0.0005928
Hspb6	1.63	0.0000432
Tnfrsf12a	1.63	0.0008864
Dnajb9	1.63	0.0000073
Btg2	1.61	0.0007912
Ptpn3	1.61	0.0007389
Auts2	1.61	0.0000241
Gcnt4	1.61	0.0010965
---	1.61	0.0001520
Slc16a1	1.60	0.0000166
Egln3	1.60	0.0000363
Cnnm2	1.60	0.0002476
Pdk1	1.60	0.0006768
Slc2a1	1.60	0.0002767
Calml3	1.59	0.0006882

Csf1	1.58	0.0000031
Fst	1.58	0.0003351
Uaca	1.58	0.0000487
Nlrc3	1.58	0.0000295
Slc16a3	1.57	0.0002283
Lpin2	1.57	0.0008676
Lnx2	1.57	0.0000448
Gclc	1.56	0.0001883
Bmper	1.56	0.0007731
Rhou	1.56	0.0001063
Slc5a3	1.56	0.0005752
Fam38b	1.56	0.0005059
Ndst3	1.55	0.0006954
Porcn	1.55	0.0008788
Tmem45a	1.55	0.0006069
Rnf138	1.55	0.0001778
Paqr4	1.55	0.0005520
Ehd3	1.54	0.0001322
Acss2	1.54	0.0007382
Nox4	1.54	0.0000771
Krt80	1.54	0.0011012
Jhdm1d	1.53	0.0007790

Adra1b	1.53	0.0001887
Ube2cbp	1.52	0.0007181
Obsl1	1.52	0.0001203
Hspb7	1.52	0.0000132
1700008I05Rik	1.52	0.0003705
Fzd6	1.51	0.0004153
Dlk1	1.51	0.0006232
Cox19	1.51	0.0012160
C1qtnf3	1.51	0.0002855
Leprel1	1.50	0.0005599
Slc1a3	1.50	0.0010638
Parvb	1.50	0.0010983
Ccng2	1.50	0.0006620
Slc44a1	1.49	0.0001075
Pdlim3	1.49	0.0002185
Erc1	1.48	0.0008846
---	1.48	0.0001325
Acvr1	1.48	0.0004291
Ccnd1	1.47	0.0009187
Tiparp	1.47	0.0005305
Wbscr27	1.47	0.0001901
Ak5	1.47	0.0000163

---	1.47	0.0011302
Manf	1.46	0.0002446
Hmga2	1.46	0.0011419
---	1.46	0.0001911
Snx18	1.45	0.0007219
Spcs3	1.45	0.0010616
Nrap	1.45	0.0000537
Myo1d	1.44	0.0010639
Hspa1a	1.44	0.0001049
Cilp2	1.44	0.0010480
Prrg4	1.44	0.0012115
Ssfa2	1.43	0.0000731
Inpp4b	1.43	0.0009030
Plcxd2	1.43	0.0001205
Slc5a7	1.43	0.0003299
Ebf1	1.43	0.0009412
Zmynd17	1.42	0.0000140
Frs2	1.42	0.0001723
Nuak1	1.41	0.0001013
Gm129	1.41	0.0008077
Pknox1	1.41	0.0010963
Relt	1.41	0.0006280

Arfgap3	1.41	0.0009624
Sp6	1.41	0.0000379
Myh7b	1.41	0.0007000
Mylk4	1.40	0.0000096
Prkar1b	1.40	0.0007132
Arrb1	1.40	0.0000538
Gm9861	1.39	0.0011039
Loxl3	1.39	0.0006197
Ang2	1.39	0.0002183
---	1.39	0.0006508
Slc35f5	1.39	0.0006986
Fibin	1.39	0.0003849
Adam17	1.39	0.0006154
Tjap1	1.39	0.0009743
Cast	1.39	0.0004449
Adamtsl3	1.39	0.0009885
Fxyd5	1.39	0.0000197
Ibtk	1.38	0.0001982
Whrn	1.38	0.0001877
---	1.37	0.0005115
Spsb2	1.36	0.0012493
Rabgef1	1.36	0.0007778

Fance	1.35	0.0005121
Fhl1	1.35	0.0002216
Hk2	1.35	0.0003439
Erf	1.35	0.0005380
Klhl21	1.34	0.0007800
Sertad1	1.34	0.0006213
Abcg2	1.34	0.0010350
Foxp1	1.34	0.0005838
Clic4	1.34	0.0003693
Rel	1.34	0.0002851
Ints9	1.34	0.0000383
Hoxc9	1.34	0.0005140
Creld2	1.33	0.0002281
Plekhh2	1.33	0.0008819
Fat1	1.33	0.0004384
Pgam1	1.33	0.0008862
Pgam1	1.33	0.0008862
Hspa1a	1.33	0.0003968
Etv4	1.33	0.0001280
Mycl1	1.32	0.0008536
Fam72a	1.32	0.0005329
Fam134b	1.31	0.0004316

Slc30a4	1.31	0.0007531
Lox	1.31	0.0000602
Zfp451	1.31	0.0010512
Hspa5	1.31	0.0003681
4930503L19Rik	1.31	0.0011781
Myot	1.31	0.0008148
Gpc6	1.31	0.0006981
---	1.31	0.0000089
Ltbp2	1.31	0.0003162
Acvr1b	1.30	0.0008132
Fam57a	1.30	0.0003703
Samd8	1.30	0.0008466
Npat	1.30	0.0002675
M arch8	1.30	0.0008292
Yap1	1.30	0.0001202
Bag2	1.29	0.0004260
Pgam1	1.29	0.0008670
H47	1.29	0.0002790
---	1.29	0.0009139
Sorbs1	1.29	0.0002711
Me1	1.29	0.0011375
---	1.28	0.0005734

Iqgap1	1.28	0.0008691
Wwc2	1.28	0.0003887
Prepl	1.28	0.0006085
Zhx3	1.28	0.0002617
Tacc1	1.28	0.0002677
Ank	1.27	0.0012465
Dnaja4	1.27	0.0004575
Fam65a	1.27	0.0006524
E2f3	1.27	0.0008708
Dlg5	1.27	0.0011113
Myd116	1.27	0.0000237
Ldb3	1.27	0.0006414
Itgb6	1.26	0.0011358
Hipk2	1.26	0.0000079
Ccdc58	1.26	0.0004561
Tmem50b	1.26	0.0000931
Zfp568	1.25	0.0004845
---	1.25	0.0004449
Mdfic	1.25	0.0000982
Sec23b	1.24	0.0006352
Fabp3	1.24	0.0010290
Anxa7	1.24	0.0007889

Smyd1	1.24	0.0006076
Pfn2	1.24	0.0004366
Il13ra1	1.24	0.0012106
Slc6a6	1.24	0.0002429
Zc3h10	1.24	0.0011189
Atxn1	1.23	0.0000300
---	1.23	0.0003211
---	1.23	0.0002072
LOC100044416	1.22	0.0007953
Tmem39a	1.22	0.0007496
Dync1li1	1.21	0.0000406
Dnajb14	1.21	0.0005548
Zkscan5	1.21	0.0006842
Tagln2	1.20	0.0001127
Gm249	1.20	0.0000389
Rhoj	1.20	0.0000696

Supplementary table 2.6. Transcripts upregulated by BMP4 only in MuSK null myotubes. Fold-changes indicate the upregulation of the listed transcript by BMP4. Fold changes greater than 1.2 are shown in the table.

CHAPTER 3

BMP4 induces acetylcholine receptor clustering in a MuSK- and Wnt11-dependent manner

Atilgan Yilmaz[1,2], Carolyn Schmiedel[1], Justin Fallon[1]

[1]Department of Neuroscience, Brown University, Providence, Rhode Island 02912, USA

[2] Department of Molecular Biology, Cell Biology and Biochemistry, Brown University, Providence, Rhode Island 02912, USA

All experiments were conducted by me.

Carolyn Schmiedel performed the AChR cluster counting analysis in Figure 2 and 4.

Abstract:

Acetylcholine receptor (AChR) clustering on the muscle membrane is a defining step for neuromuscular junction formation. In vertebrate muscle, both the neural-drived extracellular matrix protein agrin as well as Wnt11 have been shown to induce AChR clusters via a mechanism requiring Muscle Specific Kinase (MuSK). Bone morphogenic proteins (BMPs) have been suggested to have roles in retrograde signaling in neuromuscular junctions of invertebrates. However, their roles at the postsynaptic muscle membrane have not been described. Here we show that BMP4 induces AChR clustering on cultured myotubes. This clustering requires MuSK but is agrin-independent. BMP4-induced AChR clusters are morphologically different than the agrin-induced clusters and form only after overnight treatment of cultured myotubes. BMP4 induces Wnt11 expression and Wnt11 activity is required for the clustering activity. Our study suggests that BMP4 acts upstream of Wnt11 to induce MuSK-dependent AChR clustering.

Introduction

Acetylcholine released from motor neuron terminals in vertebrates binds to and opens AChRs in the postsynaptic domains of NMJs initiating the endplate potential that in turn is necessary to muscle contraction. Generation of a sufficiently large endplate potential requires a high density of AChRs at the NMJ. Thus AChR clustering is vital for the efficient neurotransmission, hence the communication between neurons and the muscle tissue.

Muscle Specific Kinase (MuSK) is a receptor tyrosine kinase that was originally purified from the synapse-rich electric organ of Torpedo californica (Jennings et al., 1993). MuSK co-localizes with AChRs and NMJs (Valenzuela et al., 1995). It is essential for the stability of the AChR clusters and is concentrated within those (DeChiara et al., 1996; Kummer et al., 2006). MuSK-/- mice die prenatally due to the failure to form NMJs and the MuSK-/- muscle fibers lack AChR clusters (DeChiara et al., 1996; Lin et al., 2001; Yang et al., 2001). Furthermore, ectopic MuSK expression triggers NMJ formation (Kim and Burden, 2008). These observations led to the conclusion that MuSK has a master regulatory role in NMJ formation, a process that involves AChR clustering.

Neural-derived proteoglycan agrin is the best-characterized inducer of AChR clustering in muscle fibers. After being secreted from the motor nerve terminal, agrin can induce MuSK autophosphorylation and hence activate the receptor (Mittaud et al., 2004). MuSK is endocytosed upon its activation and this

internalization is required for AChR clustering (Zhu et al., 2008). MuSK activation eventually leads to diverse downstream signaling events including reorganization of the actin cytoskeleton and recruitment of AChR-binding scaffolding proteins, both of which are crucial for AChR clustering (Bloch et al., 1986; Dai et al., 2000; Okada et al., 2006; Linnoila et al., 2008).

Prior to innervation in developing muscle, aneural, 'pre-patterned' AChR clusters are present. Upon innervation and the secretion of neural agrin these clusters mature, grow in size and become stable. Agrin is necessary for these later stages in synapse differentiation - agrin-/- mice fail to form AChR clusters after innervation and lack NMJs (Gautam et al., 1996). However, the pre-patterned aneural AChR clusters can still form in agrin-/- mice, indicating that there might be additional signals regulating the formation of these early clusters (Lin et al., 2001; Yang et al., 2001). Indeed, Wnt11r, mouse Wnt11 ortholog in zebrafish, has been shown to induce aneural clusters and guide motor axons for NMJ formation in zebrafish (Jing et al., 2009). Notably, MuSK and its co-receptor LRP4 are required for the formation of both aneural and neural AChR clusters (Zhang et al., 2004; Wu et al., 2012).

Wnt11 belongs to the Wnt family of secreted glycoproteins that have crucial roles in development (van Amerongen et al., 2009). Recently, Wnt11 has also been shown to induce AChR clusters on cultured mouse myotubes (Zhang et al., 2012). This study showed that Wnt11 binds to MuSK and Wnt11 clustering activity is not additive to

that of agrin, suggesting that agrin and Wnt11 may be using similar pathways to induce clustering.

The TGFβ superfamily of signaling molecules includes TGFβ, BMPs and activins. They are recognized by two different types of cell surface receptors - type-1 and type-2 (ten Dijke et al., 1994, de Sousa Lopes et al., 2004, Nohno et al., 1995, Xia et al., 2007). Activation of the receptors leads to Smad-dependent or Smad-independent downstream signaling, including transcription of a variety of genes (Kretzschmar et al., 1997; Lagna et al., 1996; Liu et al., 1996; Hoodless et al., 1996). In Drosophila, muscle-derived BMP ortholog Gbb was shown to be involved in retrograde signaling to coordinate neuromuscular synapse development and growth (McCabe et al., 2003). In mice, on the other hand, it is unknown if TGFβ has any function on NMJ development. Here we show that BMP4 induces distinct AChR clusters in a MuSK-dependent manner by upregulating Wnt11 expression.

Results

BMP4 induces AChR clusters in a MuSK-dependent fashion

Our recent work showed that MuSK binds BMP4 and regulates the transcriptional output of the BMP4 signaling pathway (Chapter 2, Yilmaz et al.). Here we asked whether BMP4 plays a role in the canonical function of MuSK – AchR clustering. In order to test BMP4's potential involvement with AChR clustering, we used a well-

established system that is based on labeling AChR clusters formed in cultured mouse myotubes. H-2Kb-tsA58 wild type mouse myotubes were treated with agrin or BMP4 overnight. As expected, agrin-treated myotubes formed elongated large clusters after overnight treatment. Interestingly, BMP4 treatment also induced AChR clustering. (Figure 3.1a, upper panels). As a negative control, we treated the wild type myotubes with Wnt5a, which was not implicated in the induction of AChR clustering. As expected, Wnt5a did not form any clusters above baseline levels.

We then wondered if MuSK was required for BMP4-induced clusters. To test this idea, MuSK null myotubes were treated with agrin or BMP4. Consistent with previous results, agrin failed to induce AChR clusters in the absence of MuSK (Glass et al., 1996). Notably, BMP4 induction of AChR clustering was also defective in the absence of MuSK. In both cases AChRs remained uniformly distributed throughout the myotube membrane (Figure 3.1a, lower panels). Quantification of clusters per myotube segment showed BMP4 induced a significant increase in the number of AChR clusters on wild type myotubes (Figure 3.1b).

We then analyzed the time-course of BMP4-induced AChR clustering (0-16 hours). BMP4-induced clusters were only detected after 8 hours of incubation (Figure 3.2). This time course is distinct from that of agrin-induced clusters, which are readily detected within 2 hours of treatment (Wallace et al., 1988; Nastuk et al., 1991)

BMP4 induces Wnt11 expression

The long time course of BMP4-induced AChR clustering, together with the observation that BMP4 does not induce MuSK phosphorylation (Chapter 2, Yilmaz et al.) suggested that there may be an intermediate signal required for BMP4-mediated AChR clustering. One candidate for such a BMP-dependent signal is Wnt11. To test whether BMP4 induces Wnt11 expression, we treated wild type myotubes with BMP4 and analyzed Wnt11 gene expression by qRT-PCR. BMP4 induced the expression of Wnt11 by 2-fold after 8 hours of treatment. Interestingly, MuSK was not necessary for BMP4-induced Wnt11 upregulation (Figure 3.3).

Wnt11 activity is necessary for the formation of BMP4-induced AchR clusters

We next tested whether BMP4-induced AChR clustering requires Wnt11. We used neutralizing antibodies to inhibit Wnt11 activity. BMP4 failed to induce AChR clusters in the presence of anti-Wnt11 antibody, while there was no significant reduction in the presence of control IgG (Figure 3.4a, b). Neutralization of Wnt11 worked best when the antibody was added 3-4 hours after BMP4 addition.

Discussion

The Drosophila BMP ortholog Gbb was shown to regulate synaptic growth at the Drosophila NMJs via a retrograde signaling (McCabe et al., 2003). In its absence, decreased neurotransmitter release, reduced NMJ synapse size and aberrant

presynaptic ultrastructure have been observed. However, no function at the postsynaptic muscle membrane organization has been attributed to BMPs. In this report we show the evidence that mammalian BMP4 has AChR clustering activity in cultured mouse muscle cells.

AChR clustering occurs at two different stages during development. Prior to innervation of the muscle, a phenomenon called prepatterning occurs in which Wnt11r was suggested to be the inducer of aneural clusters and guide motor axons for NMJ formation in zebrafish (Jing et al., 2009; Nitkin et al., 1987). On the other hand, after innervation neural-derived agrin induces larger neural clusters (Burden, 2011). Importantly, both aneural and neural clusters require MuSK (Zhang et al., 2004). Our results suggest that BMP4 induces morphologically different clusters compared to agrin induced ones. BMP4-induced clusters are smaller and rounder in shape and less in numbers. It would be interesting to test the idea if BMP4 has any role in prepatterning. BMP4 signal from the neighboring tissue notochord or autocrine BMP signaling in early muscle fibers in the embryo could regulate prepatterning.

We also show that BMP4 upregulates the expression of Wnt11 message. To our knowledge this is the first study indicating Wnt11 downstream of BMP4 signal. Given the suggested role for Wnt11 in prepatterning, BMP4 regulation of Wnt11 expression could be a muscle-specific mechanism to orchestrate surface distribution of AChRs and provide guidance for NMJ formation.

Wnt9a and Wnt11 were shown to bind to MuSK, activate it and induce AChR clustering in cultured mouse C2C12 myotubes (Zhang et al., 2012). Our results show that Wnt11 activity is required for BMP4-induced AChR clustering, as blocking Wnt11 with neutralizing antibodies specifically inhibited BMP4-induced clusters. The requirement of MuSK and Wnt11 is in accord with the previous studies and attributes a regulatory role for BMP4 in this process.

In this report we demonstrate a role for BMP4 in the induction of AChR clusters in cultured muscle cells. Our results indicate the possibilities that BMPs are a novel class of regulators of prepatterning or postsynaptic muscle membrane organization at NMJs. Further in vivo and in vitro studies will determine the exact stages that BMP4-induced AChR clustering takes place in muscle.

Future Directions

Some of the future studies that will help explain the mechanism of BMP4 induction of AChR clustering should focus on the requirement of MuSK activities. The previous finding by Zhang et al. about Wnt11's binding and activation of MuSK would lead to prediction that MuSK kinase activity would be needed for BMP4-induced clustering. Even though BMP4 itself does not induce phosphorylation of MuSK up until 3 hours of treatment (Chapter 2, Yilmaz et al.), MuSK could be phosphorylated by Wnt11 at a

later point after Wnt11 is expressed and secreted from cells. The requirement of MuSK kinase activity can be tested by treating myotubes that express kinase-dead MuSK with BMP4.

Materials and Methods

Antibodies and materials

Purified recombinant human BMP4, purified recombinant rat agrin, purified recombinant human/mouse Wnt5a, normal goat IgG, anti-Wnt11 antibody were obtained from R&D Systems (Minneapolis, MN, USA). Rhodamine-α-bungarotoxin was obtained from Invitrogen and was used to label acetylcholine receptors.

Mammalian cell culture

Wild-type mouse H-2Kb-tsA58 (Morgan JE et al., 1994) and MuSK-/- immortalized myoblasts were cultured on gelatin-coated dishes in DMEM supplemented with 20% fetal bovine serum, 2% L-Glutamine, 1% Penicillin-Streptomyocin, 1% Chicken Embryo Extract, 1U interferon-γ and cultured under permissive temperature at 33 ^{o}C in 8% CO_2. Myotubes were obtained by switching the confluent myoblast cultures to a medium with DMEM supplemented with 5% horse serum, 2% L-Glutamine and 1% Penicillin-

Streptomyocin.

Acetylcholine receptor clustering assay

Wild-type and MuSK null myoblasts were grown to confluence on Permanox chamber slides (Nunc and Nalgene, Thermo Fisher Scientific) and differentiated to myotubes for 2-4 days as described. Myotubes were incubated for 16 hours with 25ng/ml BMP4, 1ng/ml agrin, 400ng/ml Wnt5a or the indicated amounts of Wnt11 antibody. AChRs were labeled with rh-α-bungarotoxin for 15 minutes at 33°C. Myotubes were washed with PBS three times and fixed with methanol for 5 minutes at −20°C. AChR clusters were counted on a Nikon Eclipse 800 microscope.

RNA extraction, reverse transcription and quantitative real time polymerase chain reaction (qRT-PCR)

Total RNA was isolated from cells with Trizol (Invitrogen). Total RNA was cleaned up and DNase-treated in Qiagen RNeasy columns. RNA was reverse transcribed into first strand cDNA (Invitrogen). qRT-PCR reaction consisted of initial incubation at 50 ^{0}C for 2 minutes and a denaturation at 95 ^{0}C for 5 minutes. The cycling parameters were as follows: 95 ^{0}C for 15 seconds, 60 ^{0}C for 30 seconds. After 40 cycles, the reactions underwent a final dissociation cycle as follows: 95 ^{0}C for 15 seconds, 60 ^{0}C for 1 minute, 95 ^{0}C 15 seconds and 60 ^{0}C for 15 seconds.

Based on the published sequences, Wnt11 primer sequences used in qRT-PCR

reactions were as follows: 5'- GCCCATACTATTGCCCTGTC -3' and 5'- GCACATCAGTAGCCACAAGC -3'

Statistical analysis

All statistical analyses used Student's t test unless otherwise noted. Quantifications for Acetylcholine clustering assays were performed by observers blinded to experimental conditions.

FIGURES

FIGURE 3.1

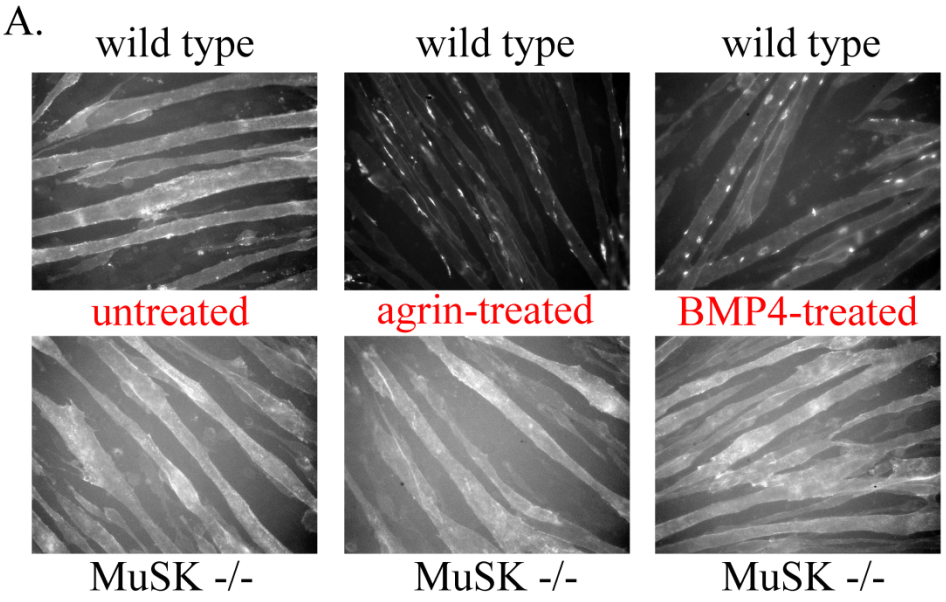

FIGURE 3.1. BMP4 induces AChR clustering and this activity requires MuSK.

A. Agrin and BMP4-induced clusters in wild type and MuSK-/- myotubes. Myotubes of indicated genotype were differentiated from immortalized myoblast lines and treated with 1ng/ml agrin or 25 ng/ml BMP4 for 16 hours. Elongated large clusters formed after agrin treatment, whereas BMP4 treatment led to formation of smaller and rounder clusters in wild type myotubes. Both agrin and BMP4 failed to induced clusters in MuSK-/- myotubes. B. Quantification of AChR clusters. The number of AChR clusters (>4 μm in length and <1 × 103 μm2) per myotube segment on cultures treated with agrin, BMP4 or Wnt5a was scored (n=74 segments/condition). The results were repeated with at least 3 independent experiments. Error bars represent SEM. Wnt5a treatment showed no significant change, all the other conditions were significantly different than each other (One was ANOVA, p< <0.0001)

FIGURE 3.2

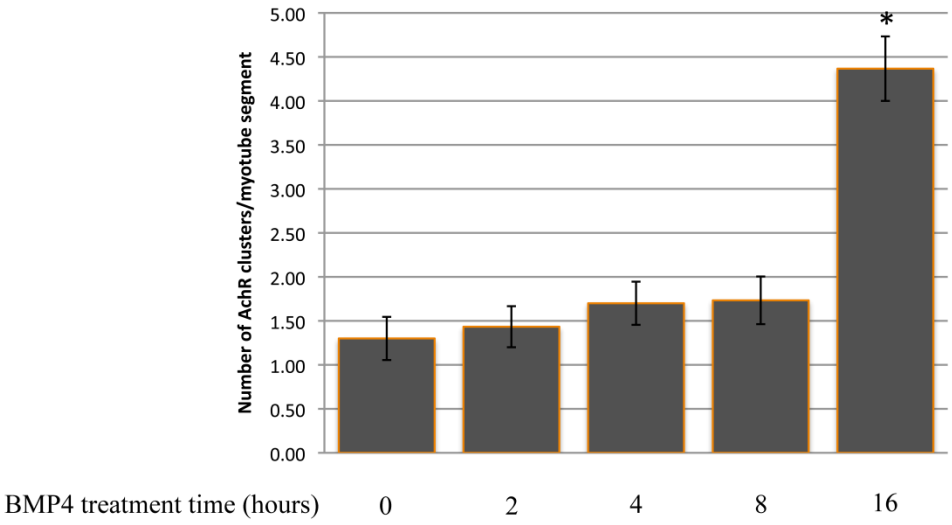
Number of AchR clusters/myotube segment
5.00
4.50
4.00
3.50
3.00
2.50
2.00
1.50
1.00
0.50
0.00
*
BMP4 treatment time (hours)
0
2
4
8
16

FIGURE 3.2. BMP4-induced AChR clusters form between 8 and 16 hours after treatment.

Time-course of BMP4 induced AChR clustering in wild-type myotubes. Wild type myotubes were treated with 25ng/ml BMP4 for 2, 4, 8 and 16 hours. Short duration BMP4 treatments (2, 4, 8 hours) did not cause any significant changes in the number of AChR clusters. Overnight BMP4 treatment induced AChR clustering. Error bars represent SEM (n=30 segments/condition).

FIGURE 3.3

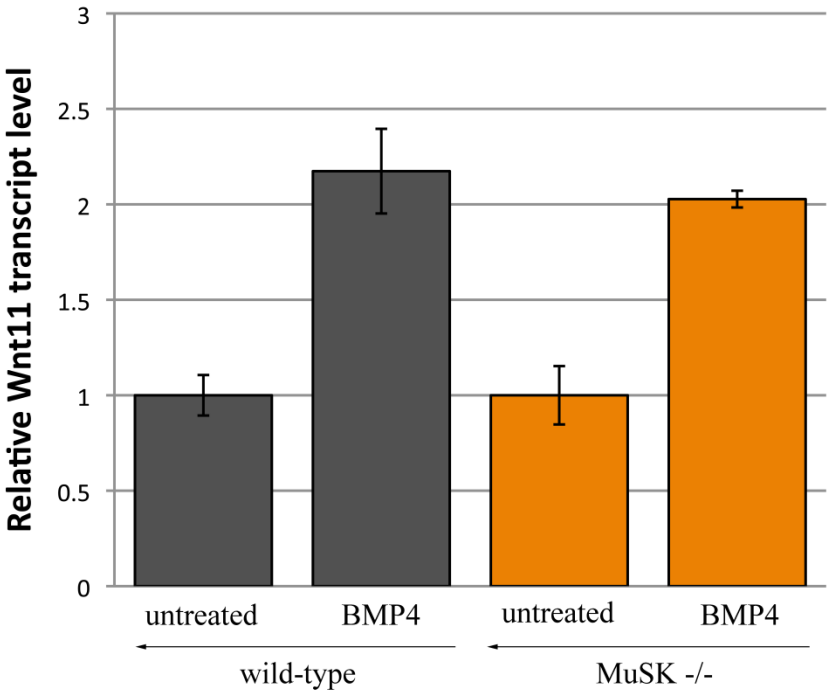
Relative Wnt11 transcript level
3
2.5
2
1.5
1
0.5
0
untreated
BMP4
untreated
BMP4
wild-type
MuSK -/-

FIGURE 3.3. BMP4 induces Wnt11 expression in a MuSK-independent manner.

Analysis of mRNA levels of Wnt11 by qRT-PCR after 8 hours of BMP4 treatment. Wild type H-2Kb-tsA58 and MuSK null myoblasts were grown into confluence and differentiated into myotubes for 3 days. Myotube cultures were treated with 25ng/ml BMP4 for 8 hours. RNA was isolated, reverse-transcribed into double stranded cDNA. Relative transcript level of Wnt11 was analyzed by qRT-PCR. (n=3) BMP4 induced Wnt11 expression both in wild type and MuSK-/- myotubes by ~2 fold.

FIGURE 3.4.

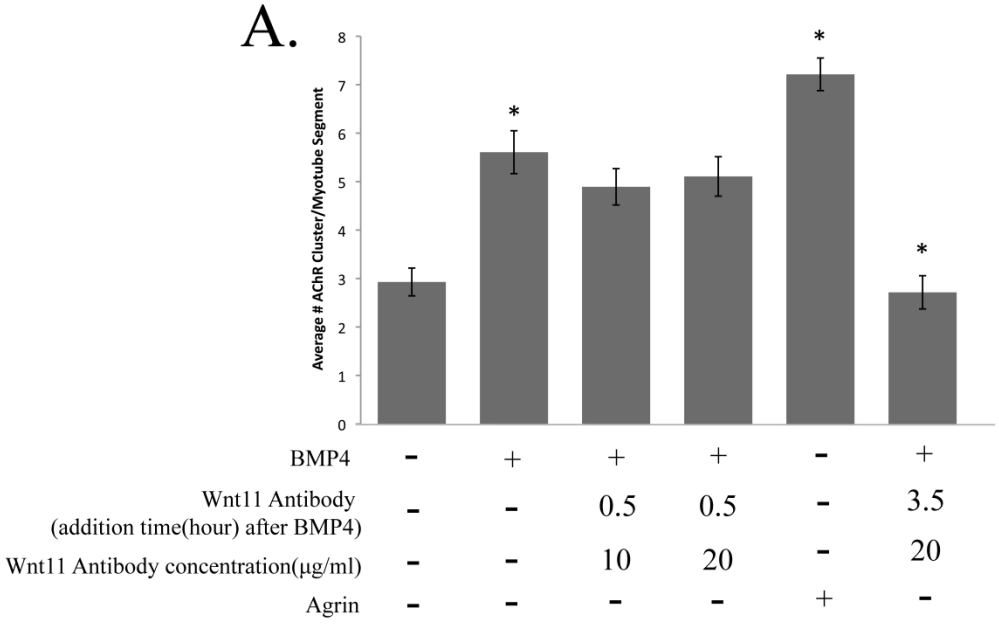
A.
Average # AChR Cluster/Myotube Segment
0
1
2
3
4
5
6
7
8
*
*
*
BMP4 - + + + - +
Wnt11 Antibody (addition time(hour) after BMP4) - - 0.5 0.5 - 3.5
Wnt11 Antibody concentration(μg/ml) - - 10 20 - 20
Agrin - - - - + -

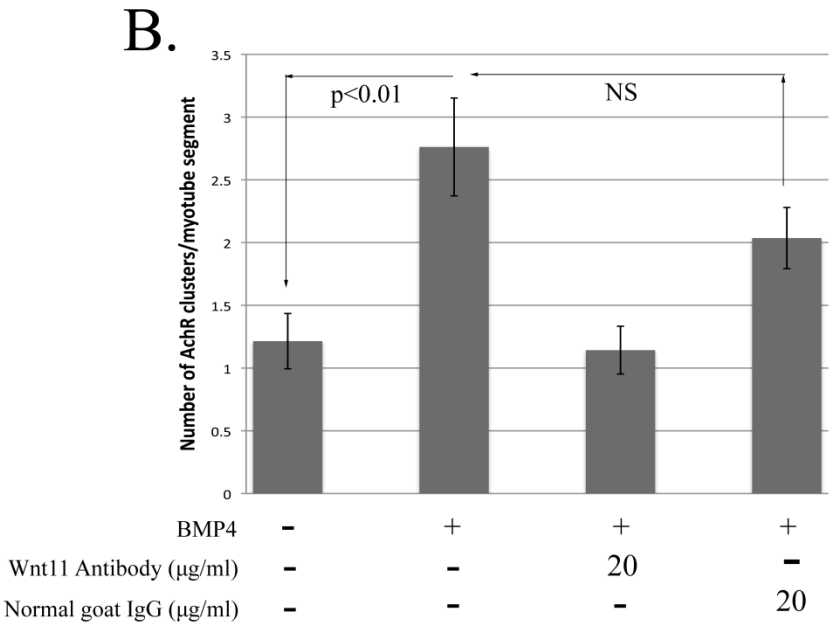
B.
Number of AchR clusters/myotube segment
0
0.5
1
1.5
2
2.5
3
3.5
p<0.01
NS
BMP4 - + + +
Wnt11 Antibody (μg/ml) - - 20 -
Normal goat IgG (μg/ml) - - - 20

FIGURE 3.4. Wnt11 activity is required for BMP4-induced AchR clusters.

A. Quantification of AChR clusters under indicated conditions. Wild type H-2Kb-tsA58 myotubes were treated with 1ng/ml agrin or 25ng/ml BMP4 for 16 hours. BMP4 induced AChR clusters ($p<0.0001$, Student's t-test). Wnt11 neutralization antibody was added 0.5 and 3.5 hours after BMP4 treatment. When added 3.5 hours after BMP4 treatment, AChR clustering activity of BMP4 was inhibited ($p<0.0001$, Student's t-test). (n=28 segments/condition) B. Quantification of AChR clusters under indicated conditions. Wild type H-2Kb-tsA58 myotubes were treated with 25ng/ml BMP4 along with Wnt11 antibody or normal goat IgG for 16 hours. Wnt11 antibody inhibited AChR clustering activity of BMP4 significantly ($p< 0.002$, Student's t-test), whereas normal goat IgG did not (non-significant, Student's t-test). (n=21-28 segments/condition)

References

Bloch, R J. "Actin at Receptor-rich Domains of Isolated Acetylcholine Receptor Clusters." *The Journal of Cell Biology* 102, no. 4 (April 1986): 1447–1458.

Burden, Steven J. "SnapShot: Neuromuscular Junction." *Cell* 144, no. 5 (March 4, 2011): 826–826.e1.

Dai, Z, X Luo, H Xie, and H B Peng. "The Actin-driven Movement and Formation of Acetylcholine Receptor Clusters." *The Journal of Cell Biology* 150, no. 6 (September 18, 2000): 1321–1334.

DeChiara, T M, D C Bowen, D M Valenzuela, M V Simmons, W T Poueymirou, S Thomas, E Kinetz, et al. "The Receptor Tyrosine Kinase MuSK Is Required for Neuromuscular Junction Formation in Vivo." *Cell* 85, no. 4 (May 17, 1996): 501–512.

de Sousa Lopes, Susana M Chuva, Bernard A J Roelen, Rui M Monteiro, Roul Emmens, Herbert Y Lin, En Li, Kirstie A Lawson, and Christine L Mummery. "BMP Signaling Mediated by ALK2 in the Visceral Endoderm Is Necessary for the Generation of Primordial Germ Cells in the Mouse Embryo." *Genes & Development* 18, no. 15 (August 1, 2004): 1838–1849.

Gautam, M, T M DeChiara, D J Glass, G D Yancopoulos, and J R Sanes. "Distinct Phenotypes of Mutant Mice Lacking Agrin, MuSK, or Rapsyn." *Brain Research. Developmental Brain Research* 114, no. 2 (May 14, 1999): 171–178.

Glass, David J, David C Bowen, Trevor N Stitt, Czeslaw Radziejewski, JoAnne Bruno, Terence E Ryan, David R Gies, et al. "Agrin Acts via a MuSK Receptor Complex." *Cell* 85, no. 4 (May 17, 1996): 513–523.

Gordon, Laura R, Katherine D Gribble, Camille M Syrett, and Michael Granato. "Initiation of Synapse Formation by Wnt-Induced MuSK Endocytosis." *Development* 139, no. 5 (March 1, 2012): 1023–1033.

Hoodless, P A, T Haerry, S Abdollah, M Stapleton, M B O'Connor, L Attisano, and J L Wrana. "MADR1, a MAD-related Protein That Functions in BMP2 Signaling Pathways." *Cell* 85, no. 4 (May 17, 1996): 489–500.

Jennings, C G, S M Dyer, and S J Burden. "Muscle-specific Trk-related Receptor with a Kringle Domain Defines a Distinct Class of Receptor Tyrosine Kinases." *Proceedings of the National Academy of Sciences of the United States of America* 90, no. 7 (April 1, 1993): 2895–2899.

Jing, Lili, Julie L Lefebvre, Laura R Gordon, and Michael Granato. "Wnt Signals Organize Synaptic Prepattern and Axon Guidance Through the Zebrafish unplugged/MuSK Receptor." *Neuron* 61, no. 5 (March 12, 2009): 721–733.

Kim, Natalie, and Steven J Burden. "MuSK Controls Where Motor Axons Grow and Form Synapses." *Nature Neuroscience* 11, no. 1 (January 2008): 19–27.

Kretzschmar, M, F Liu, A Hata, J Doody, and J Massagué. "The TGF-beta Family Mediator Smad1 Is Phosphorylated Directly and Activated Functionally by the BMP Receptor Kinase." *Genes & Development* 11, no. 8 (April 15, 1997): 984–995.

Kummer, Terrance T, Thomas Misgeld, and Joshua R Sanes. "Assembly of the Postsynaptic Membrane at the Neuromuscular Junction: Paradigm Lost." *Current Opinion in Neurobiology* 16, no. 1 (February 2006): 74–82.

Lagna, G, A Hata, A Hemmati-Brivanlou, and J Massagué. "Partnership Between DPC4 and SMAD Proteins in TGF-beta Signalling Pathways." *Nature* 383, no. 6603 (October 31, 1996): 832–836.

Lin, W, R W Burgess, B Dominguez, S L Pfaff, J R Sanes, and K F Lee. "Distinct Roles of Nerve and Muscle in Postsynaptic Differentiation of the Neuromuscular Synapse." *Nature* 410, no. 6832 (April 26, 2001): 1057–1064.

Linnoila, Jenny, Ying Wang, Yun Yao, and Zuo-Zhong Wang. "A Mammalian Homolog of Drosophila Tumorous Imaginal Discs, Tid1, Mediates Agrin Signaling at the Neuromuscular Junction." *Neuron* 60, no. 4 (November 26, 2008): 625–641.

Liu, F, A Hata, J C Baker, J Doody, J Cárcamo, R M Harland, and J Massagué. "A Human Mad Protein Acting as a BMP-regulated Transcriptional Activator." *Nature* 381, no. 6583 (June 13, 1996): 620–623.

McCabe, Brian D, Guillermo Marqués, A Pejmun Haghighi, Richard D Fetter, M Lisa Crotty, Theodore E Haerry, Corey S Goodman, and Michael B O'Connor. "The BMP Homolog Gbb Provides a Retrograde Signal That Regulates Synaptic Growth at the Drosophila Neuromuscular Junction." *Neuron* 39, no. 2 (July 17, 2003): 241–254.

Mittaud, P, P A Marangi, S Erb-Vögtli, and C Fuhrer. "Agrin-induced Activation of Acetylcholine Receptor-bound Src Family Kinases Requires Rapsyn and Correlates with Acetylcholine Receptor Clustering." *The Journal of Biological Chemistry* 276, no. 17 (April 27, 2001): 14505–14513.

Morgan, J E, J R Beauchamp, C N Pagel, M Peckham, P Ataliotis, P S Jat, M D Noble, K Farmer, and T A Partridge. "Myogenic Cell Lines Derived from Transgenic Mice Carrying a Thermolabile T Antigen: a Model System for the Derivation of Tissue-specific and Mutation-specific Cell Lines." *Developmental Biology* 162, no. 2 (April 1994): 486–498.

Nastuk, M A, E Lieth, J Y Ma, C A Cardasis, E B Moynihan, B A McKechnie, and J R Fallon. “The Putative Agrin Receptor Binds Ligand in a Calcium-dependent Manner and Aggregates During Agrin-induced Acetylcholine Receptor Clustering.” *Neuron* 7, no. 5 (November 1991): 807–818.

Nitkin, R M, M A Smith, C Magill, J R Fallon, Y M Yao, B G Wallace, and U J McMahan. “Identification of Agrin, a Synaptic Organizing Protein from Torpedo Electric Organ.” *The Journal of Cell Biology* 105, no. 6 Pt 1 (December 1987): 2471–2478.

Nohno, T, T Ishikawa, T Saito, K Hosokawa, S Noji, D H Wolsing, and J S Rosenbaum. “Identification of a Human Type II Receptor for Bone Morphogenetic Protein-4 That Forms Differential Heteromeric Complexes with Bone Morphogenetic Protein Type I Receptors.” *The Journal of Biological Chemistry* 270, no. 38 (September 22, 1995): 22522–22526.

Okada, Kumiko, Akane Inoue, Momoko Okada, Yoji Murata, Shigeru Kakuta, Takafumi Jigami, Sachiko Kubo, et al. “The Muscle Protein Dok-7 Is Essential for Neuromuscular Synaptogenesis.” *Science (New York, N.Y.)* 312, no. 5781 (June 23, 2006): 1802–1805.

Sugiyama, J. E, D. J Glass, G. D Yancopoulos, and Z. W Hall. “Laminin-Induced Acetylcholine Receptor Clustering: An Alternative Pathway.” *The Journal of Cell Biology* 139, no. 1 (October 6, 1997): 181–191.

ten Dijke, P, H Yamashita, T K Sampath, A H Reddi, M Estevez, D L Riddle, H Ichijo, C H Heldin, and K Miyazono. “Identification of Type I Receptors for Osteogenic Protein-1 and Bone Morphogenetic Protein-4.” *The Journal of Biological Chemistry* 269, no. 25 (June 24, 1994): 16985–16988.

Valenzuela, D M, T N Stitt, P S DiStefano, E Rojas, K Mattsson, D L Compton, L Nuñez, J S Park, J L Stark, and D R Gies. “Receptor Tyrosine Kinase Specific for the Skeletal Muscle Lineage: Expression in Embryonic Muscle, at the Neuromuscular Junction, and After Injury.” *Neuron* 15, no. 3 (September 1995): 573–584.

van Amerongen, Renée, and Roel Nusse. “Towards an Integrated View of Wnt Signaling in Development.” *Development (Cambridge, England)* 136, no. 19 (October 2009): 3205–3214.

Wallace, B G. “Regulation of Agrin-induced Acetylcholine Receptor Aggregation by Ca++ and Phorbol Ester.” *The Journal of Cell Biology* 107, no. 1 (July 1988): 267–278.

Wu, Haitao, Yisheng Lu, Chengyong Shen, Neil Patel, Lin Gan, Wen C Xiong, and Lin Mei. “Distinct Roles of Muscle and Motoneuron LRP4 in Neuromuscular Junction Formation.” *Neuron* 75, no. 1 (July 12, 2012): 94–107.

Xia, Yin, Paul B Yu, Yisrael Sidis, Hideyuki Beppu, Kenneth D Bloch, Alan L Schneyer, and Herbert Y Lin. "Repulsive Guidance Molecule RGMa Alters Utilization of Bone Morphogenetic Protein (BMP) Type II Receptors by BMP2 and BMP4." *The Journal of Biological Chemistry* 282, no. 25 (June 22, 2007): 18129–18140.

Yang, X, S Arber, C William, L Li, Y Tanabe, T M Jessell, C Birchmeier, and S J Burden. "Patterning of Muscle Acetylcholine Receptor Gene Expression in the Absence of Motor Innervation." *Neuron* 30, no. 2 (May 2001): 399–410.

Zhang, Jing, Julie L Lefebvre, Shuxia Zhao, and Michael Granato. "Zebrafish Unplugged Reveals a Role for Muscle-specific Kinase Homologs in Axonal Pathway Choice." *Nature Neuroscience* 7, no. 12 (December 2004): 1303–1309.

Zhang, Bin, Chuan Liang, Ryan Bates, Yiming Yin, Wen-Cheng Xiong, and Lin Mei. "Wnt Proteins Regulate Acetylcholine Receptor Clustering in Muscle Cells." *Molecular Brain* 5 (2012): 7.

Zhu, Dan, Zhihua Yang, Zhenge Luo, Shiwen Luo, Wen C Xiong, and Lin Mei. "Muscle-specific Receptor Tyrosine Kinase Endocytosis in Acetylcholine Receptor Clustering in Response to Agrin." *The Journal of Neuroscience: The Official Journal of the Society for Neuroscience* 28, no. 7 (February 13, 2008): 1688–1696.

CHAPTER 4

Biglycan recruits utrophin to the sarcolemma and counters dystrophic pathology in mdx mice

Alison R. Amenta[a], Atilgan Yilmaz[b], Sasha Bogdanovich[c], Beth A. McKechnie[a], Mehrdad Abedi[d], Tejvir S. Khurana[c], and Justin R. Fallon[a]

[a]Department of Neuroscience and [b]Department of Molecular Biology, Cell Biology and Biochemistry, Brown University, Providence, RI 02912; [c]Department of Physiology and Pennsylvania Muscle Institute, University of Pennsylvania School of Medicine, Philadelphia, PA 19104; and [d]Division of Hematology and Oncology, University of California–Davis Medical Center, Sacramento, CA 95817

Edited by Louis M. Kunkel, Children's Hospital Boston, Boston, MA, and approved November 22, 2010 (received for review September 2, 2010)

Contributed by

Author contributions: A.R.A., A.Y., S.B., B.A.M., T.S.K., and J.R.F. designed research; A.R.A., A.Y., S.B., and B.A.M. performed research; M.A. contributed new reagents/analytic tools; A.R.A., A.Y., S.B., B.A.M., T.S.K., and J.R.F. analyzed data; and A.R.A. and J.R.F. wrote the paper.

This work has been adapted from the original article to fit this thesis format.

This chapter has been published as: Amenta, Alison R, Atilgan Yilmaz, Sasha Bogdanovich, Beth A McKechnie, Mehrdad Abedi, Tejvir S Khurana, and Justin R Fallon. "Biglycan Recruits Utrophin to the Sarcolemma and Counters Dystrophic Pathology in Mdx Mice." *Proceedings of the National Academy of Sciences of the United States of America* 108, no. 2 (January 11, 2011): 762–767.

I performed the qRT-PCR analysis in Figures 4.2C and 4.3C the protein analysis in Figures 4.2A and 4.2B

ABSTRACT

Duchenne muscular dystrophy (DMD) is caused by mutations in dystrophin and the subsequent disruption of the dystrophin-associated protein complex (DAPC). Utrophin is a dystrophin homolog expressed at high levels in developing muscle that is an attractive target for DMD therapy. Here we show that the extracellular matrix protein biglycan regulates utrophin expression in immature muscle and that recombinant human biglycan (rhBGN) increases utrophin expression in cultured myotubes. Systemically delivered rhBGN up-regulates utrophin at the sarcolemma and reduces muscle pathology in the mdx mouse model of DMD. RhBGN treatment also improves muscle function as judged by reduced susceptibility to eccentric contraction-induced injury. Utrophin is required for the rhBGN therapeutic effect. Several lines of evidence indicate that biglycan acts by recruiting utrophin protein to the muscle membrane. RhBGN is well tolerated in animals dosed for as long as 3 months. We propose that rhBGN could be a therapy for DMD.

INTRODUCTION

Duchenne muscular dystrophy (DMD) is a hereditary disease that affects ~1:3,500 boys, the majority of whom will die by their midtwenties (Emery et al., 1993). DMD is caused by mutations in dystrophin that result in the faulty assembly and function of an ensemble of structural and signaling molecules at the muscle cell surface termed the dystrophin-associated protein complex (DAPC) (Koenig et al., 1987; Blake et al., 2002; Muntoni et al., 2003). There are currently no treatments that target the primary pathology of DMD.

One attractive therapeutic approach for DMD is the stabilization of the muscle cell membrane through up-regulation of utrophin, a dystrophin homolog. Transgenic overexpression of utrophin rescues dystrophic pathology and restores function in the dystrophin-deficient mdx mouse (Tinsley et al., 1998; Khurana et al., 2003; Miura et al., 2006). In mature muscle, utrophin expression is restricted to the neuromuscular and myotendinous junctions. However, utrophin is expressed over the entire myofiber in developing and regenerating muscle (Khurana et al., 1991; Clerk et al., 1993; Pons et al., 1993). These observations raise the possibility that marshalling pathways that normally regulate utrophin expression in developing muscle could be a productive approach for developing DMD treatments.

The extracellular matrix protein biglycan plays an important role in developing muscle. In both humans and mice, biglycan is most highly expressed in immature and regenerating muscle (Casar et al., 2004, Lechner et al., 2006). Biglycan is a

component of the DAPC, where it binds to α-dystroglycan (Bowe et al., 2000) and α- and γ-sarcoglycan (Rafii et al., 2006). Biglycan regulates the expression of the sarcoglycans as well as dystrobrevins, syntrophins, and nNOS, particularly in immature muscle. Finally, biglycan is important for timely muscle regeneration (Casar et al., 2004).

Locally delivered recombinant human biglycan (rhBGN) incorporates into the extracellular matrix of $bgn^{-/o}$ muscle where it persists for at least 2 wk and rescues the expression of several DAPC components (Mercado et al., 2006). These results raise the possibility that rhBGN might enhance function in muscle that lacks dystrophin. Here we show that utrophin is down-regulated in immature biglycan null ($bgn^{-/o}$) mice and that rhBGN up-regulates membrane-associated utrophin in cultured myotubes. Importantly, rhBGN can be delivered systemically to dystrophin-deficient mdx mice, where it up-regulates utrophin and other DAPC components at the sarcolemma, ameliorates muscle pathology, and improves function. Several lines of evidence indicate that biglycan acts by recruiting utrophin to the plasma membrane. We propose rhBGN as a candidate therapeutic for DMD.

RESULTS

Endogenous Biglycan Regulates Utrophin Expression in Immature Muscle.

At postnatal day 14 (P14), utrophin is highly expressed in the perisynaptic sarcolemma (Figure 4.1A) (Clerk et al., 1993). To compare utrophin expression

levels in the presence and absence of biglycan, we immunostained sections of muscle from bgn$^{-/o}$ mice and age-matched congenic controls. In all cases, the mutant and WT sections were mounted on the same slides, stained together and imaged concurrently (Materials and Methods). Figure 4.1A shows that utrophin expression is decreased at the perisynaptic sarcolemma in bgn$^{-/o}$ muscle, whereas sarcolemmal dystrophin expression was unchanged. Quantification of 50 sarcolemmal segments from each of three animals from each genotype showed that utrophin levels were reduced by ~28% (Figure 4.1B; Bgn−/o: 0.72 ± 0.03, WT: 1.0 ± 0.04, unpaired Student t test, $P < 0.0001$). In contrast, there was no significant difference in the expression of dystrophin in the sarcolemma (Figure 4.1C; Bgn−/o: 1.01 ± 0.03, WT: 1.00 ± 0.03, unpaired Student t test, $P = 0.76$). Notably, the amount of utrophin transcript was indistinguishable in WT as compared with bgn$^{-/o}$ P14 muscle (text below and Figure 4.1D). These results indicate that utrophin protein expression at the sarcolemma is selectively decreased in the absence of biglycan.

RhBGN Treatment Up-Regulates Membrane-Associated Utrophin in Cultured Muscle Cells.

We next turned to a cell culture system to more precisely delineate the role of biglycan in regulating utrophin association with the sarcolemma. We stimulated bgn$^{-/o}$ myotubes with 1 nM rhBGN and assessed the levels of utrophin and γ-sarcoglycan in membrane fractions by Western blotting. As shown in Figure 4.2A, rhBGN treatment up-regulates utrophin and γ-sarcoglycan protein in these

membrane fractions. On the other hand, there was a reduction in utrophin transcript levels following rhBGN treatment (untreated: 1 ± 0.10; rhBGN treated: 0.7 ± 0.06; unpaired Student t test, P = 0.02; n = 6 separate experiments with three replicate flasks in each). Thus, the up-regulation of utrophin protein expression at the membrane is not associated with increases in the level of its transcript.

The results described above suggest that biglycan could regulate utrophin protein by mechanisms involving elevated translation, increased stability, and/or targeting of utrophin to the membrane. To distinguish among these possibilities, we assessed the level of total utrophin protein in control and biglycan-treated cultures. As shown in Figure 4.2, total utrophin protein levels are indistinguishable in treated and untreated myotubes. The failure to detect changes in total cellular utrophin protein under conditions in which the membrane-bound fraction is increased indicates that biglycan regulates the association of utrophin with the membrane.

Systemic Delivery of rhBGN.

The role for biglycan in recruiting utrophin to the membrane, taken together with previous results, showing that both endogenous biglycan and intramuscularly delivered rhBGN can regulate DAPC proteins in vivo (Mercado et al., 2006), raising the possibility that rhBGN could be a therapeutic agent for DMD. As a first step toward developing such a therapy, we asked whether rhBGN could be delivered systemically. A capture ELISA showed that rhBGN was readily detected in the

circulation 30 and 60 min after i.p. delivery (Supp. Figure 4.1A). To detect the recombinant protein in tissue, where endogenous biglycan is expressed (Bowe et al., 2000), we injected animals i.p. with rhBGN conjugated to Alexa-555. As shown in Supp. Figure 4.1B, this rhBGN is readily detected in the muscle extracellular matrix 48 h following injection. These observations indicate that the circulating recombinant protein partitions to muscle where it becomes stably associated with the ECM. This result is in agreement with our earlier findings that intramuscularly delivered rhBGN is stable in muscle for at least 2 wk following a single intramuscular injection in $bgn^{-/o}$ mice (Mercado et al., 2006). This finding is also consistent with the efficacy of rhBGN observed 2 wk after a single injection in mdx mice (discussed below). Taken together, these findings indicate that rhBGN can be delivered systemically and can become localized to muscle for prolonged periods.

RhBGN Up-Regulates Utrophin and Other DAPC Components in mdx Mice.

We next asked whether rhBGN can up-regulate utrophin in mdx mice. A single i.p. dose of rhBGN was delivered to ~P18 mdx mice, and utrophin levels at the sarcolemma were assessed 2 wk later. Because utrophin expression increases transiently in regenerating myofibers (Helliwell et al., 1992) and is known to be enriched at synaptic and perisynaptic regions (Khurana et al., 1991; Nguyen et al., 1995), we restricted our analysis to extrasynaptic areas of nonregenerated (peripherally nucleated) myofibers. As shown in Figure 4.3 A and B, rhBGN treatment increased utrophin expression at the sarcolemma >2.5-fold in quadriceps

muscle mdx mice (vehicle: 1.0 ± 0.05, rhBGN: 2.5 ± 0.08, unpaired Student t test, $P < 0.0001$, n = 200 sarcolemmal segments from two animals from each group). Utrophin levels at the sarcolemma were also significantly increased in the tibialis anterior muscle (Supp. Figure 4.2, vehicle: 1.0 ± 0.1, rhBGN: 1.7 ± 0.1, unpaired Student t test; n = 300 sarcolemmal segments from three animals from each group).

The levels of γ-sarcoglycan, β2-syntrophin, and nNOS are also increased at the sarcolemma following a single dose of rhBGN (Figure 4.4). We observed no change in α-syntrophin levels. The elevation in γ-sarcoglycan and nNOS is in agreement with our observations in cell culture, in which rhBGN treatment increased the levels of these proteins at the membrane (Figure 4.2) (Mercado et al., 2006). Furthermore, these proteins as well as β2 syntrophin are dysregulated in $bgn^{-/o}$ mice (Rafii et al., 2006; Mercado et al., 2006). Western blotting of membrane fractions provided further evidence that rhBGN treatment increased the levels of both utrophin and γ-sarcoglycan mdx mice (Figure 4.3 C and D). Taken together, these results indicate that rhBGN treatment restores the expression of utrophin and DAPC proteins to the sarcolemma.

Utrophin transcript levels were unchanged in rhBGN-treated mdx (Figure 4.3C). This finding is in agreement with our in vivo and cell culture results with $bgn^{-/o}$ muscle (Figure 4.1 and 4.2), and indicates than rhBGN regulates utrophin in mdx mice at a posttranscriptional level. Finally, these results show that rhBGN effects can be observed after multiple doses spanning 6–13 wk of treatment (Figure 4.3D and

E). Taken together, these immunohistochemical and biochemical results show that systemically delivered rhBGN can up-regulate utrophin and other DAPC protein in the membranes of dystrophic mice.

RhBGN Reduces Dystrophic Pathology in mdx Mice.

To determine whether rhBGN counters dystrophic pathology in mdx mice, we first administered a single i.p. dose of rhBGN or vehicle alone to ~P18 mdx mice and assessed muscle histologically 2 or 3 wk later. Figure 4.5A (Upper Panel) shows a section of diaphragm from vehicle-injected mice displaying characteristic dystrophic pathology including a high proportion of centrally nucleated fibers (CNFs) and foci of necrosis/regeneration and areas of mononuclear cell infiltration (Coulton et al., 1988). Strikingly, rhBGN treatment resulted in a ~50% reduction in the proportion of CNFs observed in muscle from rhBGN treated mice (17.7% ± 2.8 and 9.6% ± 1.7 for vehicle- and rhBGN-injected animals, respectively; unpaired Student t test, P = 0.028, n = 13 vehicle- and 11 rhBGN-injected animals; Figure 4.5B). We also assessed serum creatine kinase (CK) levels, a marker of muscle damage, in mice that had been given 1, 2, or 10 mg/kg rhBGN. As reported by others (Coulton et al., 1988), there was considerable variation in the baseline levels of CK among experiments. Although we observed a trend toward decreased CK levels in these animals, the data did not reach statistical significance (Supp. Figure 4.3). Taken together, these findings indicate that rhBGN treatment reduces dystrophic pathology in mdx mice.

RhBGN Efficacy Is Utrophin Dependent.

We next asked whether the ability of rhBGN to counter dystrophic pathology in mdx mice is dependent upon utrophin. If utrophin is necessary for rhBGN action in mdx mice, the pathology of mice mutant for both utrophin and dystrophin would be unaffected by rhBGN administration. Supp. Figure 4.4 shows that the histology and number of regenerated muscle fibers in mdx:utrn$^{-/-}$ mice were indistinguishable after a single injection of rhBGN or vehicle. Thus, utrophin is necessary for the therapeutic action of rhBGN.

RhBGN Treatment Improves Muscle Function in mdx Mice.

An effective treatment for DMD must improve muscle function. One of the primary causes of myofiber pathology, dysfunction, and death in DMD is increased susceptibility to contraction-induced damage. Such muscle damage can be assessed ex vivo by measuring the force produced after each of several successive eccentric (lengthening) contractions (ECCs) (Moens et al., 1993; Gillis et al., 1999). In these ex vivo mdx muscles, susceptibility to injury is evidenced by an increase in force drop after a series of ECCs. We injected mdx mice at 3-wk intervals (starting at P14) with either rhBGN or vehicle until 15 wk of age, and measured muscle physiology as previously described (Bogdanovich et al., 2002; Bogdanovich et al., 2005). RhBGN treatment improved performance on muscle function measurements, as shown by a

reduced amount of force drop following each consecutive ECC (Figure 4.6 C and D). This improvement was robust and statistically significant from the second ECC onward (Figure 4.6C.). We observed no change in other parameters of muscle function including the amount of specific force generated (Supplementary Table 4.1). Such a profile of physiological improvement—increased resistance to damage with no change in specific force—is similar to that observed with adeno-associated virus delivery of microdystrophin (R4–R23) (Liu et al., 2005) or heregulin treatment (Krag et al., 2004). Thus rhBGN treatment improves muscle function in mdx mice.

RhBGN Is Well Tolerated in mdx Mice.

We have not observed deleterious effects of rhBGN administration in mdx mice, even after 3 mo of treatment. Organ weight is a long-standing and widely accepted measure of pharmacological toxicity (Michael et al., 2007; Peters et al., 1966). As shown in Supp. Figure 4.5A, there were no significant differences in the weights of the liver, kidney, lung, or spleen. There was an 8% decrease in the weight of the heart. Whole-animal weights were equivalent in vehicle- and rhBGN-dosed animals. Muscle weights were also unchanged with the exception of the soleus, which was 17% larger in rhBGN-treated animals. Furthermore, no indication of kidney or liver dysfunction was observed: there were no significant changes in the levels of serum creatinine, blood urea nitrogen (BUN), aspartate transaminase (AST), or bilirubin at single doses ranging from 1 to 10 mg/kg (Supp. Figure 4.5B).

DISCUSSION

In this report, we introduce a unique therapeutic approach for DMD based upon the systemic delivery rhBGN, a recombinant form of the extracellular matrix protein biglycan. Several characteristics of rhBGN suggest that it could be an effective therapy for DMD. (i) RhBGN counters dystrophic pathology and improves muscle function. (ii) Systemically delivered rhBGN localizes to muscle and a single dose is effective for up to 3 wk. Multiple doses at 3-wk intervals can sustain the response for at least 3 mo. (iii) RhBGN acts at least in part through utrophin, a pathway that has been extensively validated in animal studies (Tinsley et al., 1998, Ebihara et al., 2000; Cerletti et al., 2003). (iv) RhBGN restores the expression of DAPC components that are important for muscle integrity and function. (v) RhBGN could selectively target the tissues affected in DMD, as it binds to α- and γ-sarcoglycan (Rafii et al., 2006), which are components of the dystrophin/utrophin protein complex and are expressed selectively in heart and skeletal muscle (Hack et al., 2000; Barresi et al., 2000; Wheeler et al., 2003; Anastasi et al., 2007). (vi) RhBGN is well tolerated in mdx mice. (vii) Endogenous biglycan is expressed in normal and DMD muscle (Haslett et al., 2002; Zanotti et al., 2005) and is a highly conserved protein. RhBGN could thus be expected to elicit a minimal immune response. (viii) RhBGN is nonglycanated (i.e., lacking glycosaminoglycan side chains). This relatively uncomplicated structure simplifies its manufacture in a homogeneous form.

Several lines of evidence suggest that rhBGN counters pathology and improves

muscle function through the up-regulation of utrophin and other DAPC components at the sarcolemma. First, rhBGN treatment up-regulates sarcolemmal utrophin in both acute (single dose) and prolonged, multidose paradigms (Figure 4.3). Utrophin is necessary for rhBGN action, as we observed no improvement in muscle pathology in mdx:utrophin double null mice (Supp. Figure 4.3). Importantly, up-regulation of utrophin by increasing gene expression (Tinsley et al., 1998) or rhBGN treatment, which recruits utrophin protein to the sarcolemma, both result in assembly of DAPC components and improvement in muscle function as measured by resistance to ECC. Furthermore, as discussed below, the recruitment of utrophin and other DAPC components to the sarcolemma, rather than the global up-regulation of utrophin mRNA or protein, is likely to be the therapeutically salient feature of rhBGN action.

Our results show that a single systemic injection of rhBGN is active for a strikingly long period (Figure 4.3 and 4.5). This prolonged action of rhBGN is consistent with our previous studies in $bgn^{-/o}$ mice showing that intramuscularly delivered rhBGN is stable and biologically active for 3 wk (Mercado et al., 2006). This protracted action seems likely to result from the binding of rhBGN to the ECM. Circulating levels of rhBGN fall rapidly and are undetectable by 24 h after i.p. injection (Supp. Figure 4.1A). However, rhBGN is readily detected in the muscle ECM 2 d after i.p. injection. This stable association could be due in part to binding to collagen VI in the ECM (Wilberg et al., 2001) and to sarcoglycans at the sarcolemma (Rafii et al., 2006). The long-acting properties of systemically delivered rhBGN in mice suggest that this therapeutic strategy could be practical for use in humans, where treatment will

likely be required for years.

The results presented here indicate that rhBGN acts by recruiting utrophin protein to the sarcolemma. In cell culture, rhBGN rapidly up-regulates utrophin content in membrane fractions, but there is no increase in total utrophin protein levels (Figure 4.2). In vivo, utrophin levels at the sarcolemma of immature biglycan$^{-/o}$ mice are decreased, whereas transcript levels are unchanged (Figure 4.1). Furthermore, treatment of mdx mice with rhBGN results in up-regulation of utrophin at the sarcolemma with no increase in transcript levels (Figure 4.3). The posttranscriptional action of rhBGN is further supported by its ability to increase the levels of membrane-associated utrophin in cultured myotubes after 8 h of treatment; this interval is far less than the 16 h required to synthesize a mature utrophin transcript (Tennyson et al., 1995). The data in cultured myotubes (Figure 4.2) are consistent with a model in which increased levels of membrane (but not total) utrophin provide negative feedback for utrophin transcript levels. Taken together, our observation support the proposal that the recruitment of utrophin and other DAPC components to the membrane is the mechanism by which rhBGN counters dystrophic pathology in mdx mice. It is of particular note that total utrophin protein levels are up-regulated in DMD muscle (Love et al., 1991; Khurana et al., 1990; Gramolini et al., 1999). Therefore rhBGN can be expected to be effective in DMD patients.

Systemically delivered rhBGN increases nNOS at the sarcolemma (Figure 4.4). We have previously reported that biglycan increases nNOS at the membrane in cultured

myotubes (Mercado et al., 2006). These data are in agreement with studies by Sonnemann et al. (Sonnemann et al., 2009), in which delivery of TAT-μutr protein restores sarcolemmal nNOS in mdx mice. These observations are of particular interest, as up-regulation of nNOS could counter fatigue in dystrophic muscle (Kobayashi et al., 2008). However, studies using viral delivery of utrophin failed to detect rescue of nNOS expression at the membrane (Li et al., 2010). The basis for this discrepancy is unknown. One possibility is that are multiple mechanisms of utrophin-mediated DAPC restoration. For example, rhBGN binds DAPC components at the cell surface, a property that could promote the assembly of a more complete utrophin-associated complex, including nNOS.

The biglycan-mediated recruitment of utrophin to the sarcolemma represents a novel pathway for DMD treatment. Previous work has shown that utrophin expression is also regulated at transcriptional and translational levels, and efforts are underway to develop therapies that target these mechanisms (Khurana et al., 2003, Gramolini et al., 1998; Gramolini et al., 2001; Miura et al., 2008). In addition to having therapeutic efficacy on its own, the unique action of biglycan in recruiting utrophin to the sarcolemma could synergize with these other utrophin-directed strategies. Finally, rhBGN could be used in combination with therapies aimed at increasing muscle mass (Bogdanovich et al., 2002; Bogdanovich et al., 2005), reducing inflammation (Merlini et al., 2003, Biggar et al., 2004), or restoring dystrophin by antisense oligonucleotide-mediated exon skipping (Mann et al., 2001; van Deutekom et al., 2007).

Numerous protein-based therapies for a range of human disorders are currently in the clinic, and many more are in development. The methods for the manufacture and delivery of protein therapeutics are well understood. Furthermore, as a class, protein therapies have proved to be remarkably safe. Therefore, the path from these laboratory studies to clinical trials of rhBGN-based DMD therapies is clear.

MATERIALS AND METHODS

Biglycan. Recombinant, nonglycanated human biglycan (rhBGN) was produced in mammalian cells and purified as previously described (Mercado et al., 2006). This form lacks GAG side chains. The Alexa 555 protein labeling kit (Invitrogen Corporation) was used to conjugate this fluor to rhBGN.

Animals and Injections. All protocols were conducted under accordance and with the approval of Brown University's Institutional Animal Care and Use Committee. For single injections, P16-19 mice received an i.p. injection of 100 μg rhBGN in 25 μL 20 mM Tris, 0.5M NaCl, 0.2% CHAPS, or vehicle (20 mM Tris, 0.5 M NaCl, 0.2% CHAPS). Multiply injected mice received additional i.p. injections of 100 μg rhBGN or vehicle at 3-wk intervals. Mice were harvested 13–25 d after the final injection. For tracing studies, adult mdx mice received an i.p. injection of Alexa 555-labeled rhBGN, and diaphragms were harvested 48 h later.

Histology and Immunohistochemistry. Frozen sections were prepared and

stained as previously described (Mercado et al., 2006). For bgn$^{-/o}$ analysis, P14 congenic bgn$^{-/o}$ and WT sections were mounted on the same slide, immunostained simultaneously, and imaged with a cooled CCD camera in the same session using identical exposures. All comparisons of sections from injected mice (vehicle and rhBGN) were also mounted, stained and imaged together. Sections were observed using a Nikon (Melville, NY) Eclipse E800 microscope and images acquired with Scanalytics IP Lab Spectrum software or NIS Elements (Nikon). Utrophin and dystrophin immunoreactivity intensity was quantified using Metamorph image analysis software (Universal Imaging) or ImageJ software (National Institutes of Health). We also observed structures in the interstitial space, which may be blood vessels, that showed increased utrophin in some experiments (Fig. 3). These structures were not included in our measurements. The average pixel intensities of sarcolemmal segments were measured, and the mean background (determined by measuring nonsarcolemmal regions from each condition) was subtracted from them. The average background levels were indistinguishable between conditions. Analysis in mdx mice was performed on quadriceps from two mice of each condition and on TAs from three mice of each condition. Sources and conditions for antibodies are given in SI Materials and Methods. For scoring the percentage of CNFs, all cross-sectioned myofibers outside of necrosis/regenerative foci in H&E-stained sections were counted under a 20× objective (270–1,913 fibers/muscle section).

Quantitative RT-PCR and Western Blot Analysis. Utrophin transcript levels were measured using SYBR-Green (Invitrogen) as described in SI Materials and Methods.

Culture methods, preparation of lysates, and membrane fractions and analysis by Western blot were by standard procedures detailed in SI Materials and Methods.

Muscle Physiology. Mdx mice were injected i.p. with rhBGN (25 μg/animal) or vehicle every 3 wk starting at P14 and the physiological properties of the extensor digitorum longus (EDL) muscles were analyzed ex vivo at 3.5 mo of age as described previously (Bogdanovich et al., 2002; Bogdanovich et al., 2005). Muscle length was adjusted to achieve maximal twitch response and this length (Lo) was measured. Eccentric contraction force decrease was calculated for each tetanus of a standard ECC protocol of supramaximal stimulus 700 ms, total lengthening Lo/10; lengthening velocity 0.5 Lo/s. EDL sections were obtained and images were acquired as above. Cross-sectional area was measured using ImageJ software (National Institutes of Health).

FIGURES

Figure 4.1

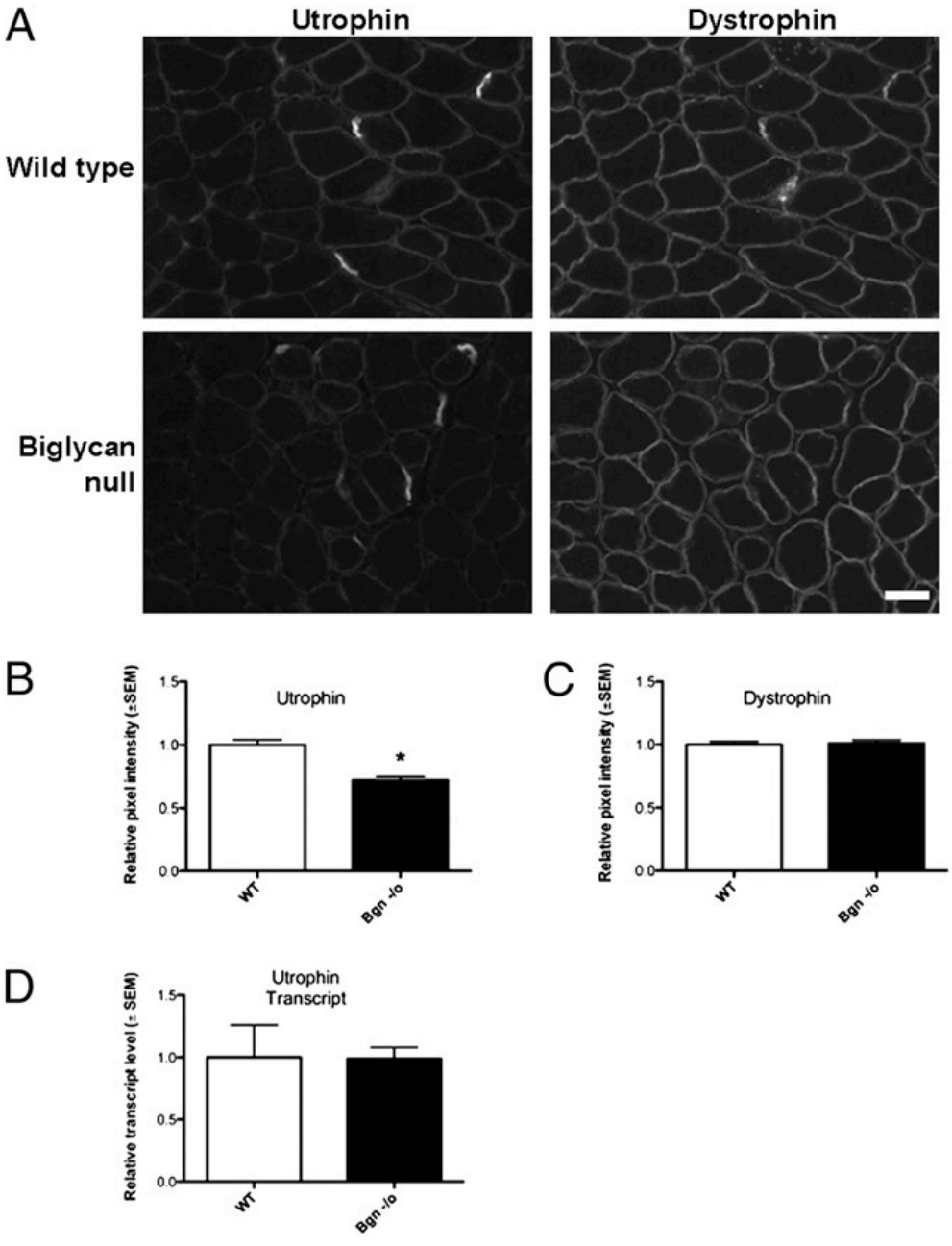

Figure 4.1. Utrophin is reduced at the sarcolemma of immature bgn−/o mice.

(A) Quadriceps muscles from congenic P14 WT (Upper Panels) DJS and bgn−/o (Lower Panels) mice were harvested, sectioned, mounted on the same slides, and immunostained for dystrophin and utrophin. Utrophin expression is decreased in these developing biglycan null mice compared with WT mice, whereas dystrophin expression is not detectably altered. (Scale bar = 25 μm.) (B) Quantification of sarcolemmal utrophin expression. Images of utrophin-stained muscle sections as prepared in A were acquired and the levels of utrophin immunostaining at the perijunctional sarcolemma were measured as described in Materials and Methods. A total of 50 sarcolemmal segments from each of three animals from each genotype were analyzed. Utrophin immunoreactivity was decreased 28% in sections from bgn−/o muscle compared with WT (Bgn−/o: 0.72 ± 0.03, WT: 1.0 ± 0.04, unpaired Student t test, $P < 0.0001$; n = 150 sarcolemmal segments from three mice of each genotype). (C) Quantification of perijunctional sarcolemmal dystrophin. Dystrophin-stained sections were imaged and measured as in B. Dystrophin immunoreactivity was equivalent in P14 WT and bgn−/o sections (Bgn−/o: 1.01 ± 0.03, WT: 1.00 ± 0.03, unpaired Student t test, $P = 0.76$). (D) Quantitative real-time PCR analysis of utrophin transcripts in P14 WT and bgn−/o mice. Total RNA was extracted from quadriceps muscles from WT and bgn−/o mice and used for cDNA synthesis. Expression of utrophin mRNA was indistinguishable in WT and Bgn−/o muscles (WT: 1.0 ± 0.26, Bgn−/o: 0.99 ± 0.09, n = 3 animals from each genotype).

Figure 4.2.

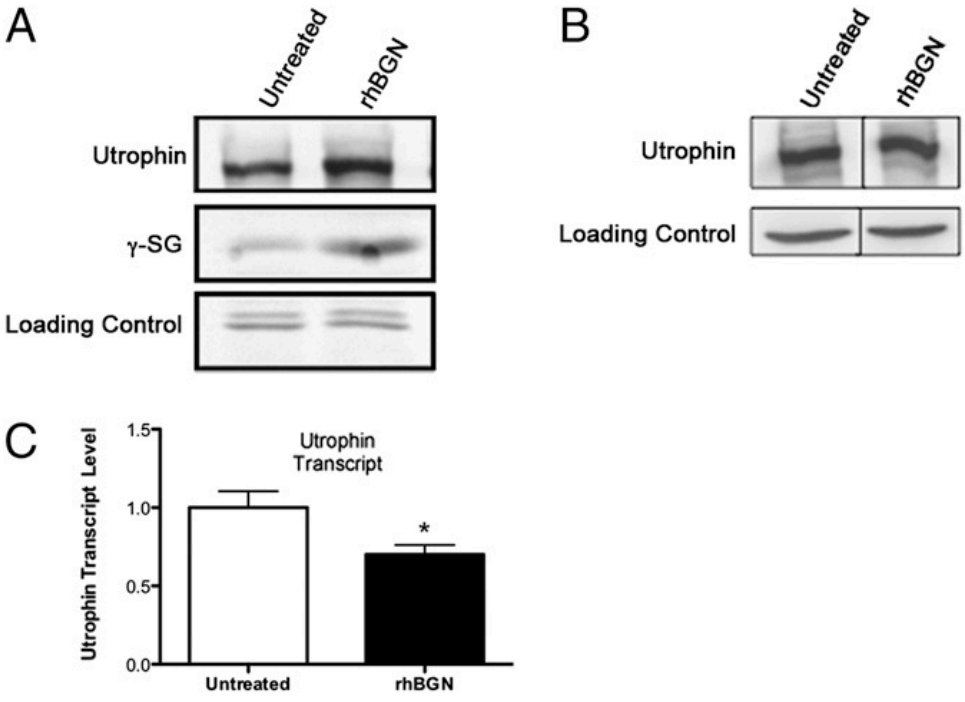
A
Untreated
rhBGN
Utrophin
γ-SG
Loading Control
B
Untreated
rhBGN
Utrophin
Loading Control
C
Utrophin Transcript
Utrophin Transcript Level
1.5
1.0
0.5
0.0
*
Untreated
rhBGN

Figure 4.2. RhBGN treatment increases membrane-associated utrophin and γ-sarcoglycan protein in cultured myotubes.

(A) Cultured bgn−/o myotubes were incubated for 8 h with either 1 nM rhBGN or vehicle as indicated. Shown are Western blots of membrane fractions probed for utrophin and γ-sarcoglycan (γ-SG). Note the increased expression of both utrophin and γ-sarcoglycan following rhBGN treatment. (B) Bgn−/o myotubes were treated as in A and whole-cell extracts were prepared. Proteins were separated by SDS/PAGE and immunoblotted for utrophin and actin (loading control). Total utrophin protein levels were similar in untreated and rhBGN treated cultures. (C) Quantitative RT-PCR analysis of untreated and rhBGN treated cultured bgn−/o myotubes. RhBGN treatment decreased utrophin transcript levels by ∼30% (untreated: 1 ± 0.10; rhBGN treated: 0.7 ± 0.06; unpaired Student t test, P = 0.02; n = 6 separate experiments with three replicate flasks in each).

Figure 4.3.

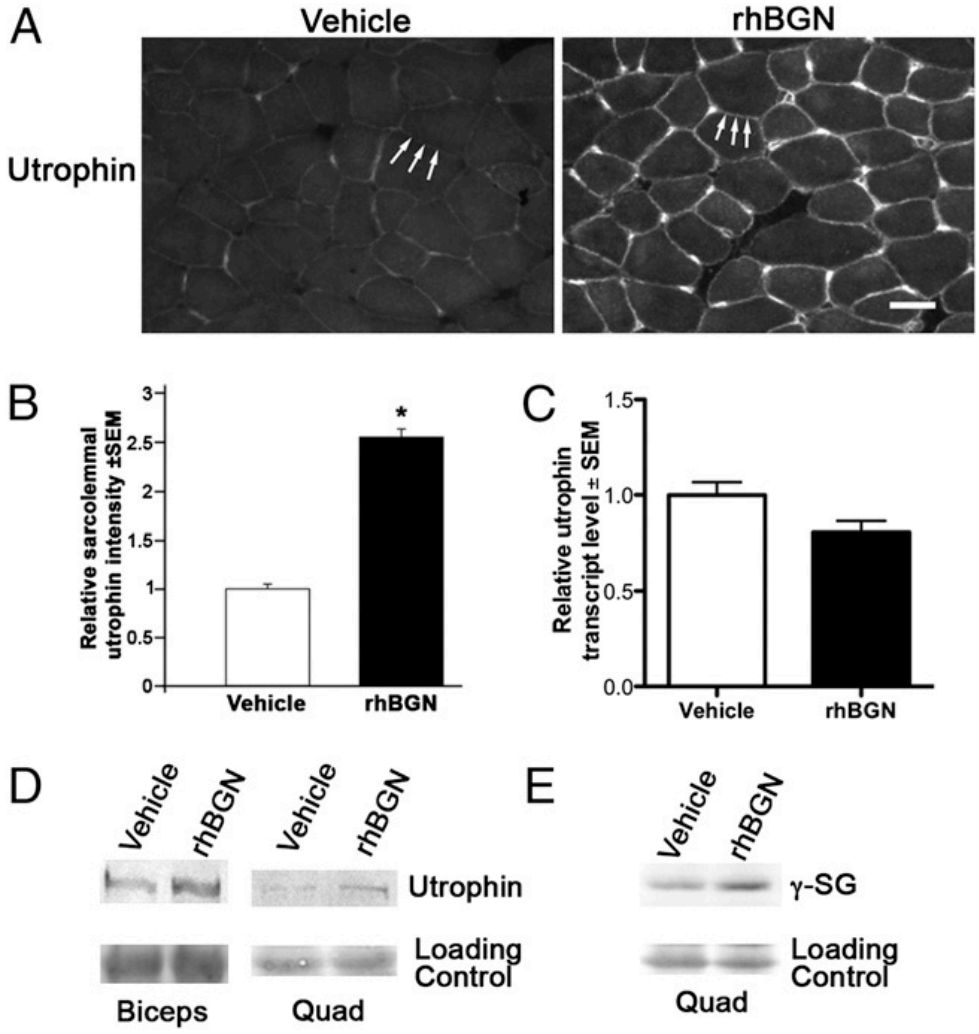
A
Vehicle
rhBGN
Utrophin
B
Relative sarcolemmal utrophin intensity ±SEM
3
2.5
2
1.5
1
0.5
0
*
Vehicle
rhBGN
C
Relative utrophin transcript level ± SEM
1.5
1.0
0.5
0.0
Vehicle
rhBGN
D
Vehicle
rhBGN
Vehicle
rhBGN
Utrophin
Loading Control
Biceps
Quad
E
Vehicle
rhBGN
γ-SG
Loading Control
Quad

Figure 4.3. RhBGN treatment up-regulates utrophin at the sarcolemma of mdx mice.

(A) Utrophin immunostaining of quadriceps muscles from P33 mdx littermate mice that received a single i.p. injection of either rhBGN or vehicle at P19. (Scale bar = 25 μm.) (B) Levels of immunostaining at the sarcolemma (e.g., arrows in A) of peripherally nucleated fibers. A total of 100 sarcolemmal segments from each of four animals were analyzed (two littermate pairs, one rhBGN- and one vehicle-injected animal per pair). Sarcolemmal utrophin immunoreactivity was >2.5-fold higher in sections from rhBGN- as compared with vehicle-injected animals (unpaired Student t test, $P < 0.0001$). (C) qRT PCR analysis of utrophin transcripts in from vehicle- or rhBGN-injected mdx mice. There was no significant difference in utrophin transcript levels in rhBGN treated mice compared with vehicle-injected controls (unpaired Student t test, $P = 0.057$; n = 8 vehicle- and 6 rhBGN-treated mice). (D) RhBGN treatment increases utrophin expression in muscle membrane fractions. Mdx mice from a single litter were injected at P16 and P38 (Left Pair) or P16, P38, and P63 (Right Pair) with rhBGN or vehicle. Muscles were harvested 3 wk after the last injection. (E) RhBGN treatment increases γ-sarcoglycan expression. Mdx mice were injected at 3-wk intervals starting at P14 with rhBGN or vehicle alone. Muscles were harvested at 15 wk of age and immunoblotted for γ-sarcoglycan. γ-Sarcoglycan is increased in the membrane fractions from rhBGN treated mdx mice compared with vehicle-treated animals.

Figure 4.4.

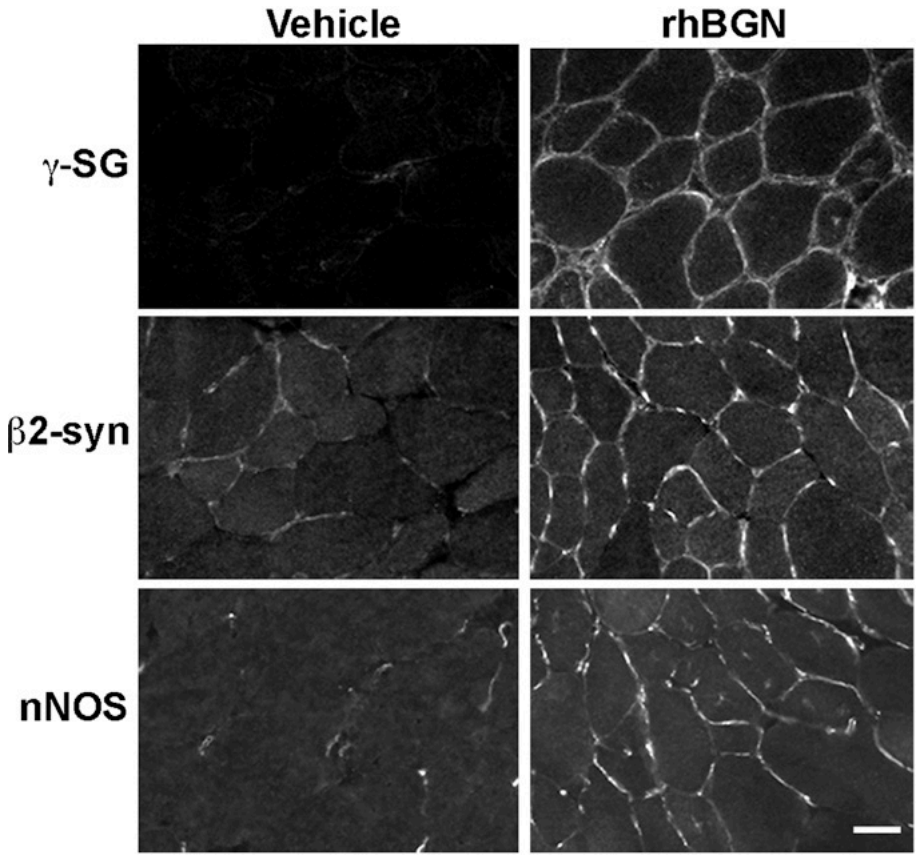

Figure 4.4. RhBGN up-regulates DAPC components at the sarcolemma of mdx mice.

Mdx mice were injected with rhBGN or vehicle at P18 and muscles were harvested at 32P. Sections of TA from vehicle- or rhBGN-treated animals were immunostained with antibodies to the indicated DAPC components as described in Materials and Methods. RhBGN treatment increased the expression of sarcolemmal γ-sarcoglycan, β2-syntrophin, and nNOS in mdx mice.

Figure 4.5.

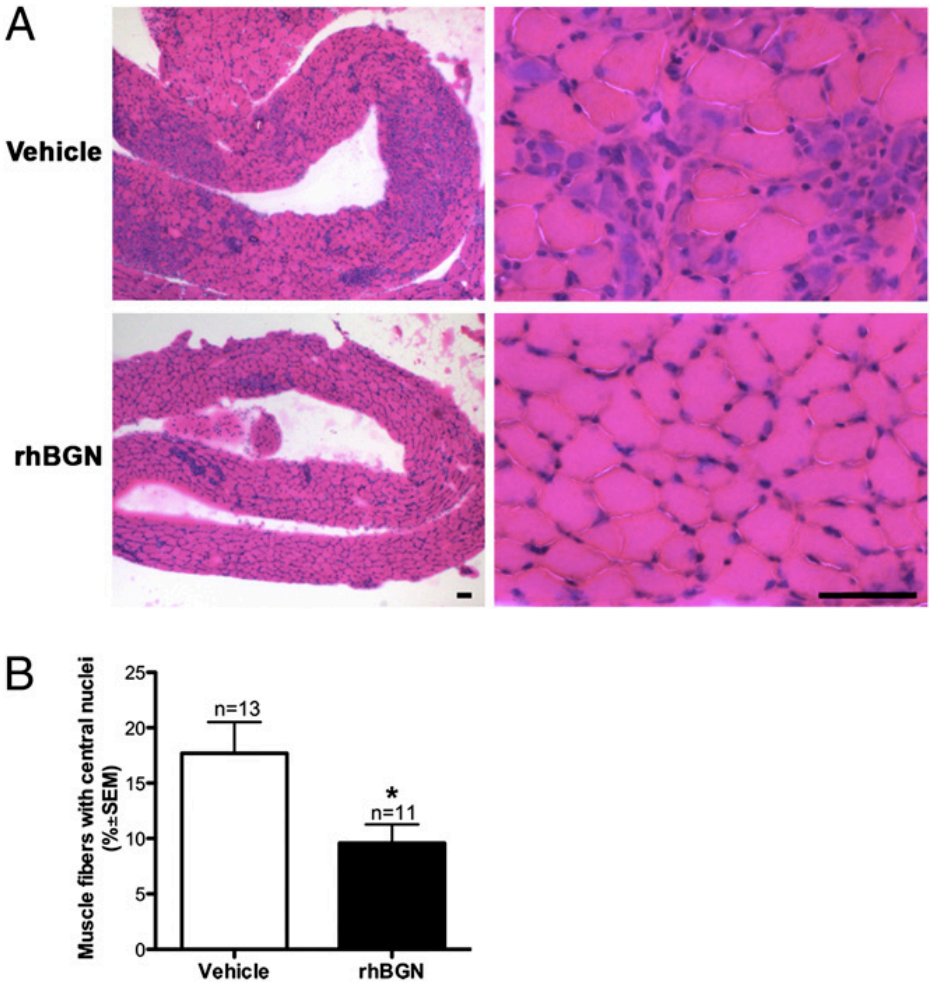
A
Vehicle
rhBGN
B
Muscle fibers with central nuclei (%±SEM)
25
20
15
10
5
0
n=13
*
n=11
Vehicle
rhBGN

Figure 4.5. Systemically administered rhBGN counters dystrophic pathology in mdx mice.

(A) H&E-stained sections of diaphragm from littermate mdx mice that were injected i.p. with vehicle (Upper Panels) or 100 μg rhBGN (Lower Panels) at P18 and harvested at P38. (Right Panels) Magnified view. Note the extensive areas of necrosis/regeneration and mononuclear cell infiltration in muscle from vehicle-injected as compared with rhBGN-injected mice. (Scale bars = 50 μm.) (B) RhBGN administration decreases proportion of CNFs in mdx muscle compared with vehicle-injected littermates (single injection; Materials and Methods). Percentages of CNFs were determined from H&E-stained diaphragm sections. RhBGN-treated mdx mice had ∼50% fewer centrally nucleated myofibers as compared with vehicle-injected mdx mice (17.7% ± 2.8 and 9.6% ± 1.7 for vehicle- and rhBGN-injected animals, respectively; n = 13 vehicle-injected and 11 rhBGN-injected animals; unpaired Student t test, P = 0.028).

Figure 4.6

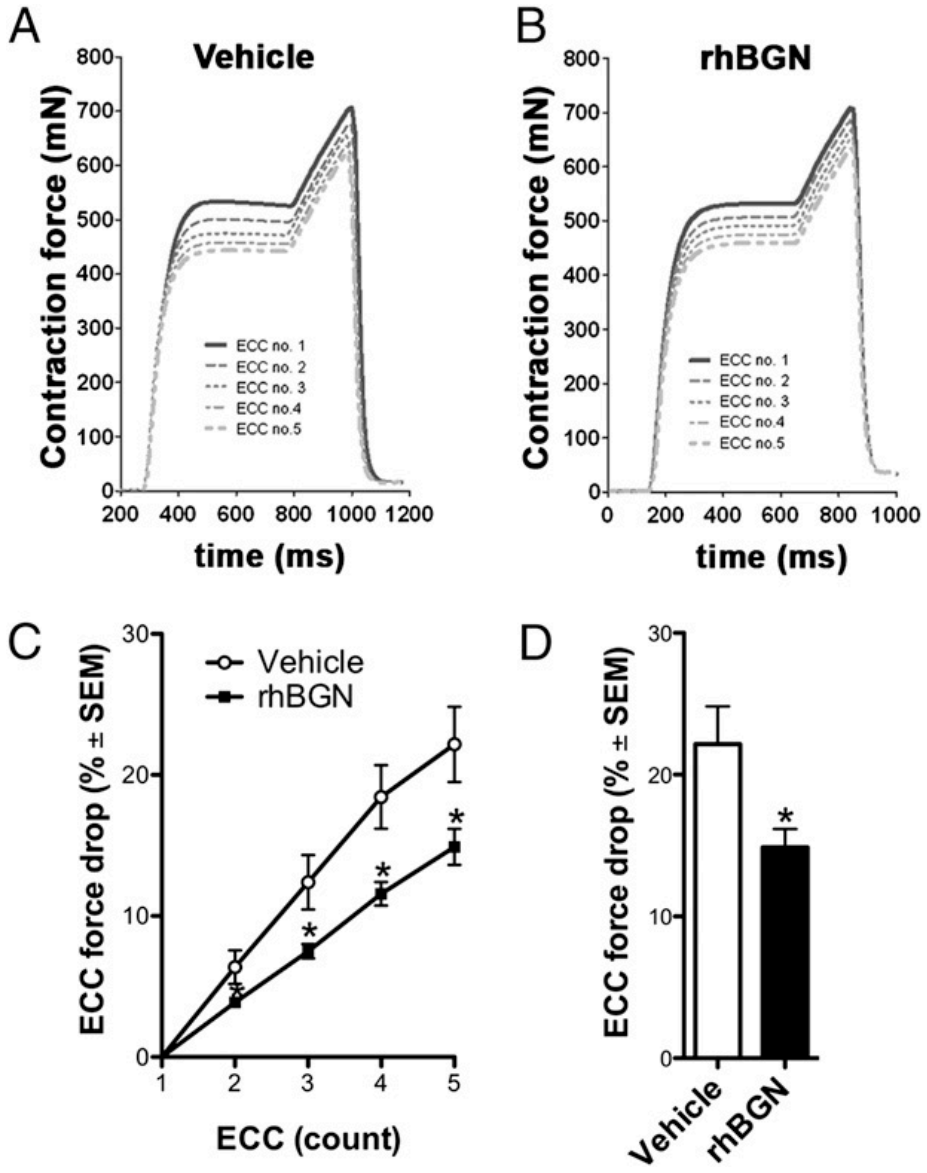
A
Vehicle
Contraction force (mN)
time (ms)
ECC no. 1
ECC no. 2
ECC no. 3
ECC no.4
ECC no.5
B
rhBGN
Contraction force (mN)
time (ms)
ECC no. 1
ECC no. 2
ECC no. 3
ECC no.4
ECC no.5
C
Vehicle
rhBGN
ECC force drop (% ± SEM)
ECC (count)
D
ECC force drop (% ± SEM)
Vehicle
rhBGN

Figure 4.6. Physiological improvement of muscle in rhBGN-treated mdx mice.

Mdx mice were injected at 3-wk intervals starting at P14 with either rhBGN (25 μg/injection; i.p.) or vehicle and tissue was harvested at 15 wk of age. Representative first to fifth ECCs of extensor digitorum longus (EDL) muscles from mdx mice injected with (A) vehicle, or (B) rhBGN. (C) Comparisons of ECC force drop between the first and the second, third, fourth, and fifth ECC of vehicle-treated (6.4 ± 1.2%; 12.4 ± 1.9%; 18.4 ± 2.3%; 22.2 ± 7%; n = 16) and rhBGN-treated (3.9 ± 0.3%; 7.5 ± 0.5%; 11.6 ± 0.8%; 14.9 ± 1.2%; n = 16) mdx mice, respectively. There is significant difference in the force drop between ECCs of vehicle-treated and rhBGN-treated mdx mice on the second, third, fourth, and fifth contractions (P = 0.05, 0.02, 0.01, 0.02, respectively; unpaired Student t test). (D) Average force drop between first and fifth ECC in vehicle-treated and rhBGN-treated mdx mice (22.2 ± 2.7% vs.14.9 ± 1.2%, respectively; P = 0.02; n = 16 muscles in each group; unpaired Student t test).

REFERENCES

Anastasi G, et al. (2007) Sarcoglycan subcomplex expression in normal human smooth muscle. J Histochem Cytochem 55:831–843.

Barresi R, Moore SA, Stolle CA, Mendell JR, Campbell KP (2000) Expression of gammasarcoglycan in smooth muscle and its interaction with the smooth muscle sarcoglycansarcospan complex. J Biol Chem 275:38554–38560.

Biggar WD, et al. (2004) Deflazacort in Duchenne muscular dystrophy: A comparison of two different protocols. Neuromuscul Disord 14:476–482.

Blake DJ, Weir A, Newey SE, Davies KE (2002) Function and genetics of dystrophin and dystrophin-related proteins in muscle. Physiol Rev 82:291–329.

Bogdanovich S, et al. (2002) Functional improvement of dystrophic muscle by myostatin blockade. Nature 420:418–421.

Bogdanovich S, Perkins KJ, Krag TO, Whittemore LA, Khurana TS (2005) Myostatin propeptide-mediated amelioration of dystrophic pathophysiology. FASEB J 19:543–549.

Bowe MA, Mendis DB, Fallon JR (2000) The small leucine-rich repeat proteoglycan biglycan binds to alpha-dystroglycan and is upregulated in dystrophic muscle. J Cell Biol 148:801–810.

Casar JC, McKechnie BA, Fallon JR, Young MF, Brandan E (2004) Transient upregulation of biglycan during skeletal muscle regeneration: Delayed fiber growth along with decorin increase in biglycan-deficient mice. Dev Biol 268:358–371.

Cerletti M, et al. (2003) Dystrophic phenotype of canine X-linked muscular dystrophy is mitigated by adenovirus-mediated utrophin gene transfer. Gene Ther 10:750–757.

Clerk A, Morris GE, Dubowitz V, Davies KE, Sewry CA (1993) Dystrophin-related protein, utrophin, in normal and dystrophic human fetal skeletal muscle. Histochem J 25:554–561.

Coulton GR, Morgan JE, Partridge TA, Sloper JC (1988) The mdx mouse skeletal muscle myopathy: I. A histological, morphometric and biochemical investigation. Neuropathol Appl Neurobiol 14:53–70.

Ebihara S, et al. (2000) Differential effects of dystrophin and utrophin gene transfer in immunocompetent muscular dystrophy (mdx) mice. Physiol Genomics 3:133–144.

Emery AEH (1993) Duchenne Muscular Dystrophy (Oxford University Press, Oxford)
2nd Ed.

Gramolini AO, et al. (1998) Muscle and neural isoforms of agrin increase utrophin expression in cultured myotubes via a transcriptional regulatory mechanism. J Biol Chem 273:736–743.

Gramolini AO, Karpati G, Jasmin BJ (1999) Discordant expression of utrophin and its transcript in human and mouse skeletal muscles. J Neuropathol Exp Neurol 58:235–244.

Gramolini AO, Bélanger G, Jasmin BJ (2001) Distinct regions in the 3′ untranslated region are responsible for targeting and stabilizing utrophin transcripts in skeletal muscle cells. J Cell Biol 154:1173–1183.

Gillis JM (1999) Understanding dystrophinopathies: An inventory of the structural and functional consequences of the absence of dystrophin in muscles of the mdx mouse. J Muscle Res Cell Motil 20:605–625.

Hack AA, Groh ME, McNally EM (2000) Sarcoglycans in muscular dystrophy. MicroscRes Tech 48:167–180.

Haslett JN, Kunkel LM (2002) Microarray analysis of normal and dystrophic skeletal muscle. Int J Dev Neurosci 20:359–365.

Helliwell TR, Man NT, Morris GE, Davies KE (1992) The dystrophin-related protein, utrophin, is expressed on the sarcolemma of regenerating human skeletal muscle fibres in dystrophies and inflammatory myopathies. Neuromuscul Disord 2:177–184.

Khurana TS, Hoffman EP, Kunkel LM (1990) Identification of a chromosome 6-encoded dystrophin-related protein. J Biol Chem 265:16717–16720.

Khurana TS, et al. (1991) Immunolocalization and developmental expression of dystrophin related protein in skeletal muscle. Neuromuscul Disord 1:185–194.

Khurana TS, Davies KE (2003) Pharmacological strategies for muscular dystrophy. Nat Rev Drug Discov 2:379–390.

Kobayashi YM, et al. (2008) Sarcolemma-localized nNOS is required to maintain activity after mild exercise. Nature 456:511–515.

Koenig M, et al. (1987) Complete cloning of the Duchenne muscular dystrophy (DMD) cDNA and preliminary genomic organization of the DMD gene in normal and

affected individuals. Cell 50:509–517.

Krag TO, et al. (2004) Heregulin ameliorates the dystrophic phenotype in mdx mice. Proc Natl Acad Sci USA 101:13856–13860.

Lechner BE, Lim JH, Mercado ML, Fallon JR (2006) Developmental regulation of biglycan expression in muscle and tendon. Muscle Nerve 34:347–355.

Li D, et al. (2010) Sarcolemmal nNOS anchoring reveals a qualitative difference between dystrophin and utrophin. J Cell Sci 123:2008–2013.

Liu M, et al. (2005) Adeno-associated virus-mediated microdystrophin expression protects young mdx muscle from contraction-induced injury. Mol Ther 11:245–256.

Love DR, et al. (1991) Tissue distribution of the dystrophin-related gene product and expression in the mdx and dy mouse. Proc Natl Acad Sci USA 88:3243–3247.

Mann CJ, et al. (2001) Antisense-induced exon skipping and synthesis of dystrophin in the mdx mouse. Proc Natl Acad Sci USA 98:42–47.

Mercado ML, et al. (2006) Biglycan regulates the expression and sarcolemmal localization of dystrobrevin, syntrophin, and nNOS. FASEB J 20:1724–1726.

Merlini L, et al. (2003) Early prednisone treatment in Duchenne muscular dystrophy. Muscle Nerve 27:222–227.

Michael B, et al. (2007) Evaluation of organ weights for rodent and non-rodent toxicity studies: A review of regulatory guidelines and a survey of current practices.Toxicol Pathol 35:742–750.

Miura P, Jasmin BJ (2006) Utrophin upregulation for treating Duchenne or Becker muscular dystrophy: How close are we? Trends Mol Med 12:122–129.
Moens P, Baatsen PH, Maréchal G (1993) Increased susceptibility of EDL muscles from mdx mice to damage induced by contractions with stretch. J Muscle Res Cell Motil 14:446–451.

Miura P, Andrews M, Holcik M, Jasmin BJ (2008) IRES-mediated translation of utrophin A is enhanced by glucocorticoid treatment in skeletal muscle cells. PLoS ONE 3:e2309.

Muntoni F, Torelli S, Ferlini A (2003) Dystrophin and mutations: One gene, several proteins, multiple phenotypes. Lancet Neurol 2:731–740.

Nguyen TM, et al. (1995) Full-length and short forms of utrophin, the dystrophinrelated protein. FEBS Lett 358:262–266.

Peters JM, Boyd EM (1966) Organ weights and water levels of the rat following reduced food intake. J Nutr 90:354–360.

Rafii MS, et al. (2006) Biglycan binds to alpha- and gamma-sarcoglycan and regulates their expression during development. J Cell Physiol 209:439–447.

Sonnemann KJ, et al. (2009) Functional substitution by TAT-utrophin in dystrophindeficient mice. PLoS Med 6:e1000083.

Tennyson CN, Klamut HJ, Worton RG (1995) The human dystrophin gene requires 16 hours to be transcribed and is cotranscriptionally spliced. Nat Genet 9:184–190.

Tinsley J, et al. (1998) Expression of full-length utrophin prevents muscular dystrophy in mdx mice. Nat Med 4:1441–1444.

van Deutekom JC, et al. (2007) Local dystrophin restoration with antisense oligonucleotide PRO051. N Engl J Med 357:2677–2686.

Wheeler MT, McNally EM (2003) Sarcoglycans in vascular smooth and striated muscle.Trends Cardiovasc Med 13:238–243.

Wiberg C, et al. (2001) Biglycan and decorin bind close to the n-terminal region of the collagen VI triple helix. J Biol Chem 276:18947–18952.

Zanotti S, et al. (2005) Decorin and biglycan expression is differentially altered in several muscular dystrophies. Brain 128:2546–2555.

SUPPLEMENTARY INFORMATION

SI Materials and Methods

Western Blot Analysis. For cell membrane preparations, biglycan null myotubes were washed in PBS, scraped from tissue culture flasks and homogenized in dissection buffer (0.3 M sucrose, 35 mM Tris, pH 7.4, 10 mM EDTA, 10 mM EGTA ,and protease inhibitor mixture; Roche Applied Science). Samples were centrifuged at 7,000 × g at 4 °C for 5 min. Membranes were then collected by centrifugation of the supernatants at 38,000 × g for 60 min at 4 °C. Protein concentrations were determined by the bicinchoninic acid protein concentration assay (Pierce). For total protein extraction from biglycan null myotubes, cells were washed in PBS and sol- ubilized in RIPA lysis buffer (Santa Cruz Biotechnology) for 25 min, lysates were centrifuged at 10,000 × g, and supernatants were collected. Membrane fractions from quadriceps and biceps femoris were prepared as previously described (Emery, 1993).

Cell or muscle fractions were separated by SDS/PAGE and proteins were transferred to nitrocellulose membranes. Total protein staining (SYPRO Ruby; Invitrogen) was visualized on a Storm Imager (Amersham Bioscience). Blots were incubated with primary antibody followed by goat anti-mouse IgG conju- gated to HRP (Amersham). Signal was detected with ECL plus (Amersham) using a Storm Imager.

Quantitative RT-PCR. RNA extraction from the biglycan null immortalized muscle

cell line and quadriceps femoris muscles from injected mdx animals was performed using the TRIzol method (Invitrogen). Purified RNA was converted to cDNA using the SuperScript III First-Strand Synthesis System Kit (Invitrogen). qPCR reactions were performed using the SYBR-Green method (Invitrogen) on the ABI PRISM 7300 real-time thermocycler. Primers were designed using DS Gene primer design software (Accelrys). ATP synthase was used for normalization. Data analysis was performed using the standard curve method (Koenig et al., 1987).

The primers used were as follows: ATPSase forward: 5′-TGG GAA AAT CGG ACT CTT TG-3′; ATPSase reverse: 5′-AGT AAC CAC CAT GGG CTT TG; Utrophin forward: 5′-TCC CAA GAC CCA TTC AAC CC; Utrophin reverse: TGG ATA GTC AGT GTT TGG TTC C (gi110431377; 3′ UTR between bases 10383–12382).

Animals. Congenic biglycan null mice on a C3H background were generated as described previously (1) and were compared with WT C3H from the Jackson Laboratory. C57BL/10ScSn-mdx/J mice were obtained from Jackson Laboratory; mdx:utrn−/− mice were bred as described (Blake et al., 2002).

Antibodies. The following primary antibodies were used: mono- clonal anti-utrophin (Vector Labs), rabbit anti-utrophin (a gen- erous gift of S. Froehner, University of Washington, Seattle, WA), rabbit anti-dystrophin (Abcam), monoclonal anti–γ-sarcoglycan (Vector), rabbit anti-laminin (Sigma), rabbit anti–β2-syntrophin (Muntoni et al., 2003), and rabbit anti-nNOS (Invitrogen). The specificity of the

monoclonal anti-biglycan (2A5) (Emery, 1993) and rabbit anti-biglycan (Tinsley et al., 1998) was established by Western blot (Emery, 1993; Tinsley et al., 1998; Khurana et al., 2003) and ELISA (Results); no reactivity was observed when these reagents were tested on bi- glycan null samples. The following secondary antibodies were used: Alexa 488 goat anti-mouse IgG and Alexa 555 goat anti- rabbit IgG (Invitrogen), HRP goat anti-mouse IgG, and HRP goat anti-rabbit IgG.

Cell Culture. Immortalized biglycan null cells were grown as previously described (Emery, 1993). Cells were differentiated for 4–5 d and then treated with 1 nm rhBGN in differentiation medium for 8 h.

Serum Chemistries. Blood was collected by cardiac puncture from rhBGN and vehicle injected mice and spun at 3,300 RPM for 10 min to separate serum. Serum creatine kinase, BUN, creati- nine, AST, and total bilirubin analyses were performed by the University of Californai–Davis Comparative Pathology Laboratory.
Detection of rhBGN in Serum. Adult C57/B6 mice were injected i.p. with 10 mg/kg rhBGN, and blood was collected by cardiac puncture 30 min, 1 h, and 24 h postinjection (n = 3–4 mice/ condition). Control experiments showed that comparable levels of rhBGN were present in plasma (0.12 μg/mL at 1 h post-injection, n = 2). For two-site ELISAs, plates were coated with mouse anti-biglycan antibody, blocked, and incubated with se- rum samples or standard biglycan dilutions followed by rabbit anti-biglycan and goat anti-rabbit HRP. Sensitivity of the assays was ~5 ng/mL.

References:

Biggar WD, et al. (2004) Deflazacort in Duchenne muscular dystrophy: A comparison of two different protocols. Neuromuscul Disord 14:476–482.

Bowe MA, Mendis DB, Fallon JR (2000) The small leucine-rich repeat proteoglycan biglycan binds to alpha-dystroglycan and is upregulated in dystrophic muscle. J Cell Biol 148:801–810.

Bowe MA, Mendis DB, Fallon JR (2000) The small leucine-rich repeat proteoglycan biglycan binds to alpha-dystroglycan and is upregulated in dystrophic muscle. J Cell Biol 148:801–810.

Mann CJ, et al. (2001) Antisense-induced exon skipping and synthesis of dystrophin in the mdx mouse. Proc Natl Acad Sci USA 98:42–47.

Mercado ML, et al. (2006) Biglycan regulates the expression and sarcolemmal localization of dystrobrevin, syntrophin, and nNOS. FASEB J 20:1724–1726.

Rafii MS, et al. (2006) Biglycan binds to alpha- and gamma-sarcoglycan and regulates their expression during development. J Cell Physiol 209:439–447.

van Deutekom JC, et al. (2007) Local dystrophin restoration with antisense oligonucleotide PRO051. N Engl J Med 357:2677–2686.

Supplementary Figures

Supplementary Figure 4.1

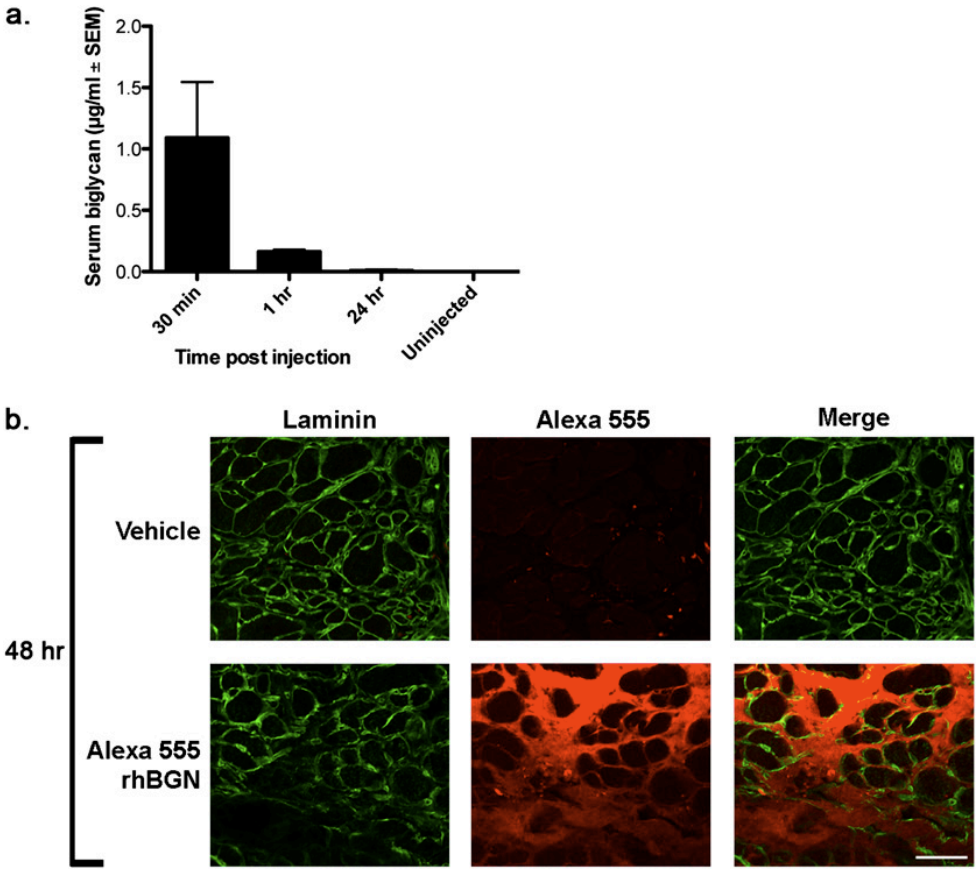

Supplementary Figure 4.1. Systemically delivered rhBGN can be detected in the circulation and becomes localized to muscle. (A) Detection of rhBGN in serum following i.p. delivery. Mice were injected i.p. with 10 mg/kg rhBGN, and serum was collected 30 min, 1, and 24 h postinjection (n = 3–4 animals/group). Two-site ELISAs were performed as described in Materials and Methods. Biglycan (endogenous) was not detected in serum from uninjected mice. However, rhBGN was readily detected in serum following a systemic injection of the recombinant protein. (Scale bar = 50 μm.) (B) Systemically delivered rhBGN becomes stably localized to muscle. Alexa 555-rhBGN (Materials and Methods) was injected i.p. into adult mdx mice, and diaphragms were harvested 48 h later. Endogenous laminin was detected by indirect immunofluoresence. Systemically delivered Alexa 555-rhBGN is localized in the extracellular matrix surrounding the myofibers.

Supplementary Figure 4.2.

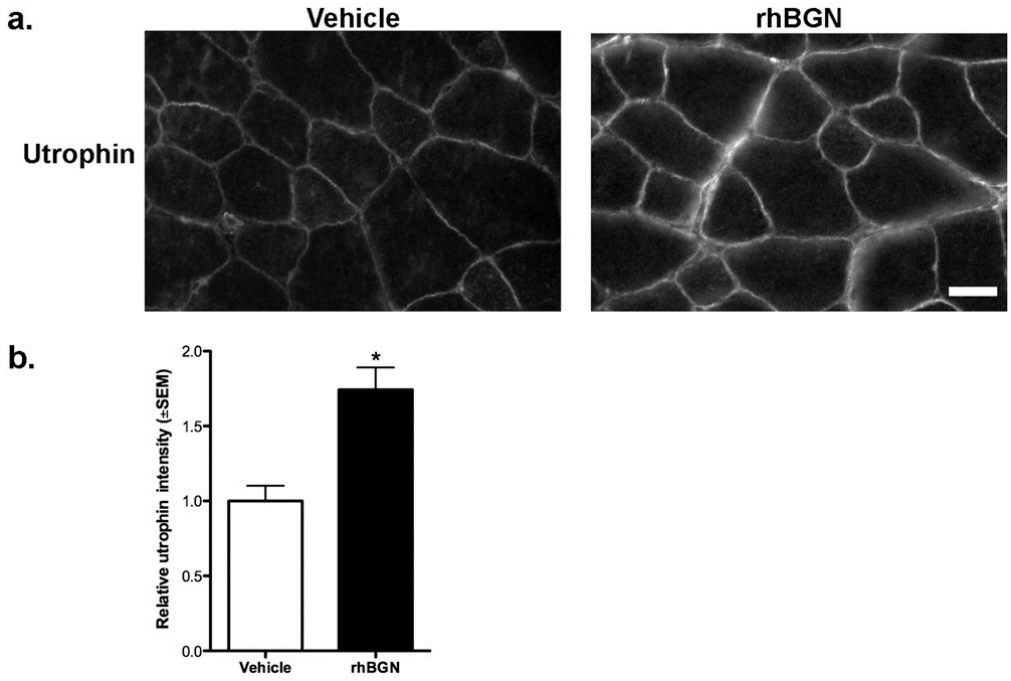

Supplementary Figure 4.2. RhBGN treatment increases sarcolemmal utrophin expression in the tibialis anterior of mdx mice.

(A) Utrophin immunostaining of TA muscles from mdx mice that received one i.p. injection of rhBGN or vehicle. Systemically delivered rhBGN increased utrophin expression in TAs of mdx mice compared with vehicle-injected mice. (B) Quantification of increased utrophin expression in TA muscle from rhBGN treated mice (1.74-fold increase, *P < 0.001, Student unpaired t test; n = 300 sarcolemmal segments from three muscles for each group). (Scale bar = 25 μM.)

Supplementary Figure 4.3

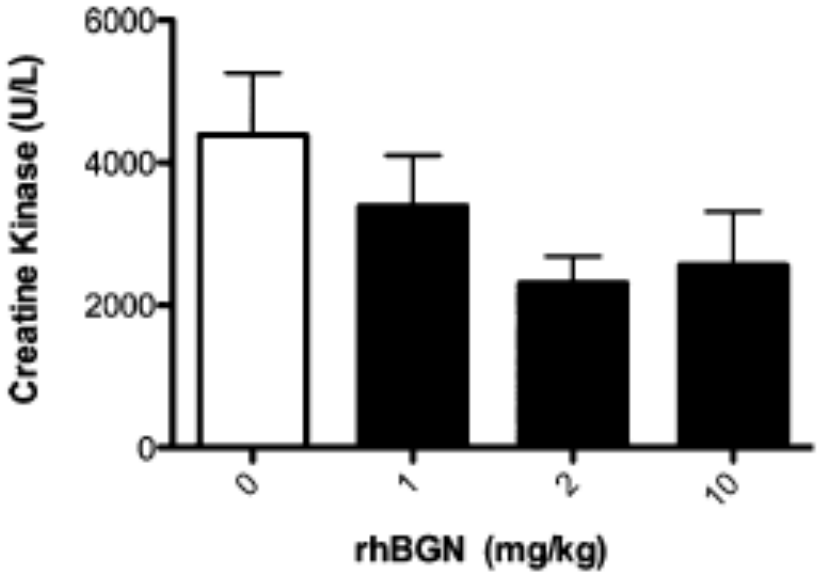

Supplementary Figure 4.3. Creatine kinase levels in rhBGN-treated mdx mice.

Creatine kinase levels in 32P mdx mice that received a single injection of 1 mg/kg (n = 23), 2 mg/kg (n = 12), or 10 mg/kg (n = 11) rhBGN or vehicle alone (n = 24) at P18. RhBGN-treated mice showed trends of decreased CK levels, but the results did not reach statistical significance (one-way ANOVA, $P > 0.05$).

Supplementary Figure 4.4

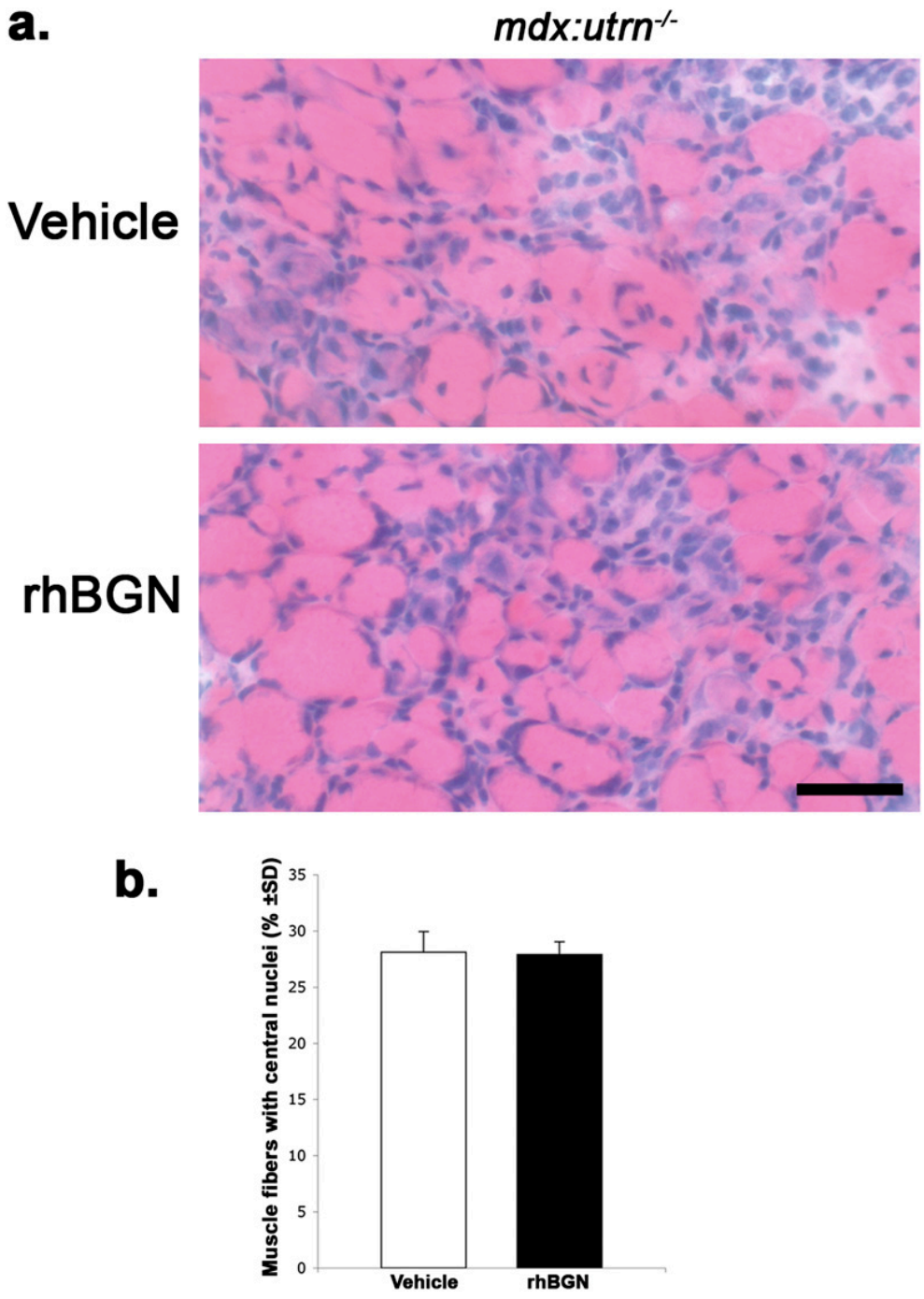

Supplementary Figure 4.4. RhBGN fails to counter dystrophic pathology in mdx:utrn−/− double KO animals.

(A) Mutant mice lacking both dystrophin and utrophin (mdx:utrn−/−) were injected at P19 with recombinant rhBGN or vehicle. Diaphragms were isolated 3 wk later, sectioned, and stained with H&E. Characteristic extensive muscle pathology of these double KO animals—areas of mononuclear cell infiltration and foci of necrosis/regeneration and centrally nucleated myofibers— was comparable in rhBGN- and vehicle- injected animals. (Scale bar = 50 μm.) (B) RhBGN administration does not decrease CNFs in mdx:utrn−/− mice. Per- centages of centrally nucleated muscle fibers were determined from the H&E-stained diaphragm sections from rhBGN and vehicle injected mdx:utrn−/− (n = 2 vehicle-injected and 3 rhBGN-injected mice; unpaired Student t test, P = 0.45).

Supplementary Figure 4.5.

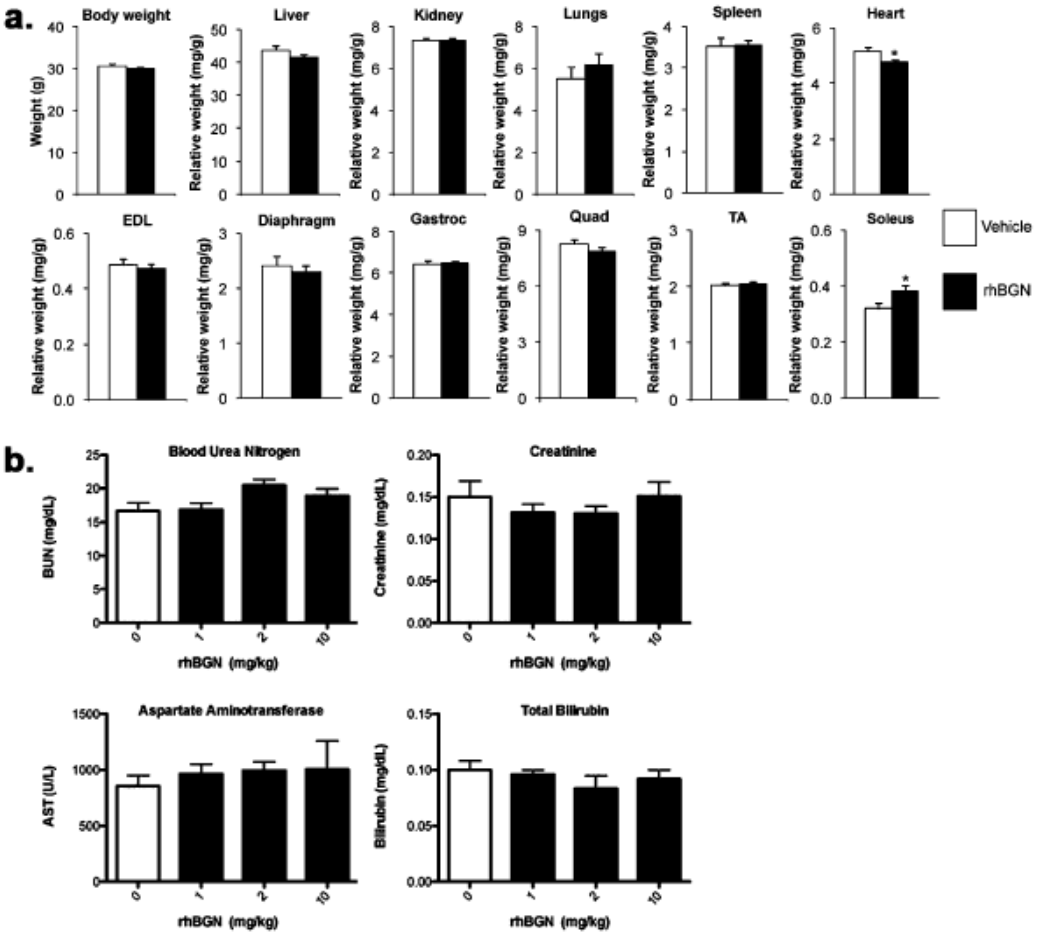

Supplementary Figure 4.5. RhBGN is well tolerated in mdx mice.

(A) P14 mdx mice were injected at 3-wk intervals for 3 mo with either rhBGN or vehicle. Tissues were harvested at 15 wk and weighed. All organ and muscle weights are plotted relative to total body weight in mg/g (n = 8 animals/group; *P < 0.05; unpaired Student t test). (B) Liver and kidney function in rhBGN treated mice. Serum was collected from 32P mdx mice that received an i.p. injection of 1, 2, or 10 mg/kg rhBGN or vehicle only. There were no significant changes in serum levels of BUN, creatinine, AST, or total bilirubin.

Supplementary Table 4.1

Table S1. Contractile properties of extensor digitorum longus (EDL) muscles

Parameter	Control mdx (n = 16 muscles)	Treated mdx (n = 16 muscles)
ECC force drop 1–5 (%)	22.2 ± 2.7	14.9 ± 1.2*
Twitch		
Absolute force (mN)	108.9 ± 5.1	107.3 ± 6.2
Specific force (mN/mm^2)	54.0 ± 3.2	56.6 ± 4.0
Tetanus		
Absolute force (mN)	577.5 ± 27.6	559.4 ± 30.5
Specific force (mN/mm^2)	287.0 ± 18.3	295.0 ± 19.7
EDL weight (mg)	14.7 ± 0.7	14.2 ± 0.4
EDL Lo (mm)	12.4 ± 0.2	12.5 ± 0.1
CSA (mm^2)	2.07 ± 0.07	2.00 ± 0.08

Mdx mice were injected at 3-wk intervals starting at P14 with either rhBGN (25 μg/injection, i.p.) or vehicle, and tissue was harvested at 15 wk of age. Data were collected and analyzed as described in *Materials and Methods* and are from the same set of muscles as presented in Fig. 8. CSA, cross sectional area; ECC, eccentric contraction; Lo, muscle length.

*P = 0.02, unpaired Student t test.

CHAPTER 5

DISCUSSION

BMPs comprise one of the largest growth factor families and function during early development throughout the embryo (Ferguson et al., 1992; Ray et al., 1991; Urist, 1965). Furthermore, this diverse group of growth factors functionally supports multiple processes such as organ morphogenesis and regeneration in a range of developing and adult tissues. Given their critical roles, it is not surprising that tightly controlled regulatory mechanisms evolved for restricting or enhancing the signaling that BMPs employ. In Chapter 2, I present data demonstrating MuSK as a novel regulator of BMP signaling in myogenic cells. There are several conclusions to draw from these results. First, the high affinity of the binding between MuSK ectodomain and BMPs is similar to what was reported previously for type-1 receptor binding to BMPs using SPR (Berasi et al., 2011). This puts MuSK into a high-affinity receptor category along with BMPs' canonical type-1 receptors, as well as certain co-receptors such as DRAGON (Samad et al., 2005). It is therefore expected that MuSK will interact with BMPs and its downstream pathway in the mature muscle fibers where it is expressed the most. Moreover, my results demonstrate that MuSK regulates BMP pathway also in undifferentiated myoblast cultures, where MuSK is expressed at lower levels. This observation raises the question whether MuSK acts as a BMP regulator in other tissues where it is expressed at very low levels. The kinetics of the binding suggests that MuSK may well be interacting with BMP4 pathway in other tissues, as well. Though this binding would not necessarily mean that the outcomes of this interaction would be the same as in myogenic cells. Indeed,

some of the transcripts regulated by MuSK include genes such as Car3 and Myh15 that are selectively enriched in muscle.

The findings about the requirement of Ig3 domain of MuSK for its BMP4 binding add another level of complexity to this regulation. The presence of a naturally occurring isoform of MuSK lacking Ig3 domain suggests that MuSK binding to BMP4 can be regulated through alternative splicing of MuSK. This regulation could occur at multiple stages of development, as well as under different stimuli in adult. This result also attributes a function to Ig3 domain, which has yet to be shown as a requirement for other known functions of MuSK in the context of NMJ.

In the absence of MuSK, SMAD-mediated BMP signaling is downregulated. This effect is shown by decreased levels of BMP4-induced SMAD1/5/8 phosphorylation, as well as Id1 transcription. This result suggests that MuSK could be acting as a stimulatory co-receptor to BMP4. The molecular mechanisms of this regulation need to be studied further. Future studies will reveal whether MuSK is indeed a co-receptor and binds to BMP4 receptors in myogenic cells. It is also noteworthy that MuSK regulates the presence of cytosolic pSMAD1/5/8 granules in myoblasts. We hypothesize that these granules may be a specific signaling compartment in which MuSK modulates BMP4 pathway. The interaction between MuSK and Lrp4 and the previously reported cytosolic Lrp signalosomes in other cellular contexts further support this idea and raise the questions whether Lrp4 is also present in these

granules or if the granules are reduced in the absence of Lrp4. These questions will be addressed in future studies.

Another key finding in this study is the modulation of the transcriptional output of BMP4 signaling by MuSK. This study identified a group of BMP4 target transcripts that require MuSK in order to be expressed in response to BMP4. This result points to a mechanism in which different surface interactions can potentially lead to specific transcriptional outputs of BMP signaling. It is very tempting to speculate that the cytosolic granules expressed at high levels in the presence of MuSK are signaling compartments regulated by MuSK and are necessary for the transcription of a subset of genes downstream of BMP4. Future studies focusing on the roles and contents of these granules will help us understand if they are such specific signalosomes.

BMP4 induces the expression of distinct gene sets in undifferentiated myoblasts as compared to differentiated myotubes. This result may not be surprising given that upon differentiation the gene expression profile, and hence the cellular context changes drastically. However, it is interesting to see that both in myoblasts and in myotubes there are different sets of transcripts whose BMP4 responsiveness is regulated by MuSK. This could be due to differences in several additional factors modulating BMP4 pathway or simply because of the difference in MuSK concentration between these two cell types.

In this thesis, I identified Car3 and Myh15 as novel downstream targets of BMP4 in myotubes. Both Car3 and Myh15 had been suggested as slow muscle markers. Interestingly, their expression was higher in slow fiber enriched soleus muscle compared to fast fiber enriched EDL. This correlation indicates that BMP4 may be a novel regulatory signal for fiber-type determination and/or switching. Furthermore, MuSK regulates the transcriptional response of Car3 and Myh15 to BMP4. The potential involvement of MuSK and BMP4 in fiber type determination or reprogramming needs to be tested more directly.

In vivo studies will be very useful to test the functional outcomes of the MuSK-BMP4 interaction. Since MuSK Ig3 domain is dispensable for the roles of MuSK at the NMJ, however is necessary for MuSK-BMP4 interaction, the generation of knock-in mice expressing MuSK that lacks Ig3 domain would allow to have viable animals with intact NMJs and to study the specific outcomes of BMP4-MuSK interaction. The involvement of MuSK-BMP4 interaction in muscle fiber type determination can be tested in these mice by analyzing the distribution of fiber types. The role of MuSK-BMP4 interaction in fiber type switching can also be addressed in these mice by using re-innervation models with either slow or fast type neurons where fiber type switch can be induced.

Cell-type specific effects of BMP4 can vary tremendously. This raises the question how the same signal can have such diverse outcomes. The data that is presented in Chapter 2 supports the idea that the cellular context and the cell type specific

expression of BMP4 regulators can modulate the signaling downstream of BMP4 and lead to cell type specific outcomes.

In Chapter 3, I demonstrate a role for BMP4 in the induction of AChR clusters in cultured muscle cells. High densities of AChRs expressed at the postsynaptic muscle membrane of the vertebrate NMJ are crucial for communication between neurons and muscle. Several factors such as laminin, Wnt11 and agrin have been previously shown to induce AChR clustering. However, BMPs have not been implicated in this process. The study presented in Chapter 3 shows that BMP4 increases the expression of Wnt11, which is required for BMP4's clustering activity. Wnt11 binds to MuSK and induces AChR clusters through activation of MuSK (Zhang et al., 2012). Therefore our results suggest that BMP4 is an upstream regulator of Wnt11 expression and indirectly regulates clustering, as well.

To our knowledge, this is the first study showing Wnt11 downstream of BMP4. As discussed above, Wnt11 could be a muscle specific BMP4 response. Since Wnt11 has been suggested as an inducer of prepatterning before innervation of the muscle, BMP4 could regulate this process upstream of Wnt11. In the embryo, BMP4 released from neighboring embryonic tissues before NMJ formation could upregulate Wnt11 expression in early myofibers and regulate the prepatterning. Further in vivo and in vitro studies are needed to determine the potential role of BMPs in synapse formation in muscle.

In Chapter 4, I collaborated with Dr. Alison Amenta to examine biglycan's regulation of sarcolemmal utrophin expression, the therapeutic effect of this regulation for Duchenne Muscular Dystrophy (DMD) and the mechanisms thereof. We showed that the non-glycanated form of biglycan increases membrane association of utrophin in the absence of dystrophin and this increase counters the dystrophic pathology in *mdx* mice, the mouse model of DMD. My contribution was to show that in cultured biglycan null myotubes, non-glycanated biglycan increases utrophin levels in membrane fractions, however it does not increase total protein or transcript levels of utrophin. This result points to a post-transcriptional mechanism in which biglycan may regulate membrane targeting of utrophin. This effect could either be mediated by a structural stabilization of utrophin at the membrane or through a signaling mechanism. Another alternative mechanism for biglycan regulation of sarcolemmal utrophin expression could involve microRNAs. In Appendix Table 3, I show the list of microRNAs up- and downregulated in response to non-glycanated form of biglycan in biglycan null myotubes.

In Appendix Figure 1, I show that the injection of the non-glycanated form of biglycan into *mdx* mice increases the transcription of two muscle proteins, Car3 and γ-sarcoglycan. At two different injection doses, there is also a trend for downregulation of utrophin transcript. This is in accord with the published results in Chapter 4. This downregulation could be due to a negative feedback mechanism triggered by the stabilization of utrophin protein at the membrane.

γ-Sarcoglycan binds to biglycan and its protein levels were shown to be reduced in developing biglycan null animals (Rafii et al., 2006). In Chapter 4, we also show that biglycan injection into *mdx* mice increases protein levels of γ-sarcoglycan at the membrane fractions of muscle. The result in Appendix Figure 1, showing increased transcript levels of γ-sarcoglycan in biglycan treated *mdx* mice is in accord with these previous studies and further supports the idea that γ-sarcoglycan expression is regulated by biglycan.

The increase in Car3 transcript levels by non-glycanated biglycan is very intriguing as BMP4 also increases Car3 levels (Chapter 2). Biglycan was also shown to bind to BMP4 (Moreno et al., 2005). In Appendix Figure 2, I demonstrate differential binding of non-glycanated and proteoglycan forms of biglycan to BMP4. Moreover, in Appendix Table 1 and 2, differences in transcriptional response of biglycan null myotubes in response to both of these forms of biglycan are shown. Two forms of biglycan not only bind to BMP4 with different affinities, but they also seem to regulate expression of different group of genes. Further studies will determine whether non-glycanated biglycan increases Car3 transcript levels through BMP4 and if Car3 response is specific to non-glycanated form of biglycan.

Understanding the mechanism of action of biglycan in regulation of sarcolemmal utrophin expression is crucial for biglycan's future use as a therapeutic for DMD. It would be interesting to see if the mechanism involves BMP4 and it's signaling.

References:

Berasi, Stephen P, Usha Varadarajan, Joanne Archambault, Michael Cain, Tatyana A Souza, Abe Abouzeid, Jian Li, et al. "Divergent Activities of Osteogenic BMP2, and Tenogenic BMP12 and BMP13 Independent of Receptor Binding Affinities." *Growth Factors (Chur, Switzerland)* 29, no. 4 (August 2011): 128–139.

Ferguson, E L, and K V Anderson. "Localized Enhancement and Repression of the Activity of the TGF-beta Family Member, Decapentaplegic, Is Necessary for Dorsal-ventral Pattern Formation in the Drosophila Embryo." *Development (Cambridge, England)* 114, no. 3 (March 1992): 583–597.

Moreno, Mauricio, Rosana Muñoz, Francisco Aroca, Mariana Labarca, Enrique Brandan, and Juan Larraín. "Biglycan Is a New Extracellular Component of the Chordin-BMP4 Signaling Pathway." *The EMBO Journal* 24, no. 7 (April 6, 2005): 1397–1405.

Rafii, Michael S, Hiroki Hagiwara, Mary Lynn Mercado, Neung S Seo, Tianshun Xu, Tracey Dugan, Rick T Owens, et al. "Biglycan Binds to Alpha- and Gamma-sarcoglycan and Regulates Their Expression During Development." *Journal of Cellular Physiology* 209, no. 2 (November 2006): 439–447.

Ray, R P, K Arora, C Nüsslein-Volhard, and W M Gelbart. "The Control of Cell Fate Along the Dorsal-ventral Axis of the Drosophila Embryo." *Development (Cambridge, England)* 113, no. 1 (September 1991): 35–54.

Samad, Tarek A., Anuradha Rebbapragada, Esther Bell, Ying Zhang, Yisrael Sidis, Sung-Jin Jeong, Jason A. Campagna, et al. "DRAGON, a Bone Morphogenetic Protein Co-receptor." *Journal of Biological Chemistry* 280, no. 14 (April 8, 2005): 14122–14129.

Urist, M R. "Bone: Formation by Autoinduction." *Science (New York, N.Y.)* 150, no. 3698 (November 12, 1965): 893–899.

Zhang, Bin, Chuan Liang, Ryan Bates, Yiming Yin, Wen-Cheng Xiong, and Lin Mei. "Wnt Proteins Regulate Acetylcholine Receptor Clustering in Muscle Cells." *Molecular Brain* 5 (2012): 7.

APPENDIX

Appendix Figure 1

A.

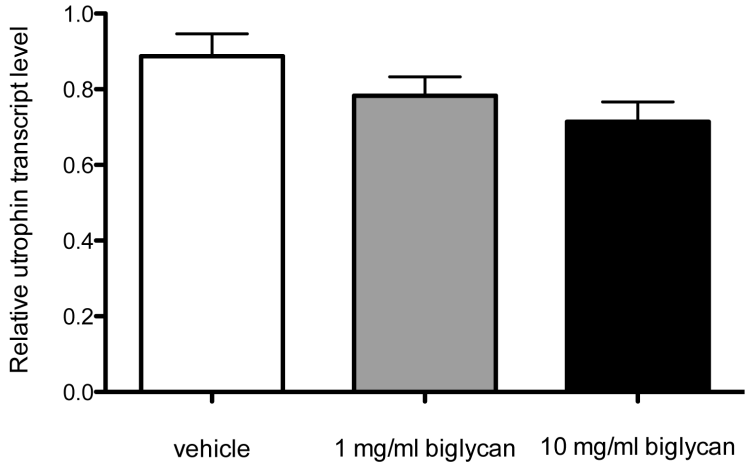
Relative utrophin transcript level
1.0
0.8
0.6
0.4
0.2
0.0
vehicle
1 mg/ml biglycan
10 mg/ml biglycan

B.

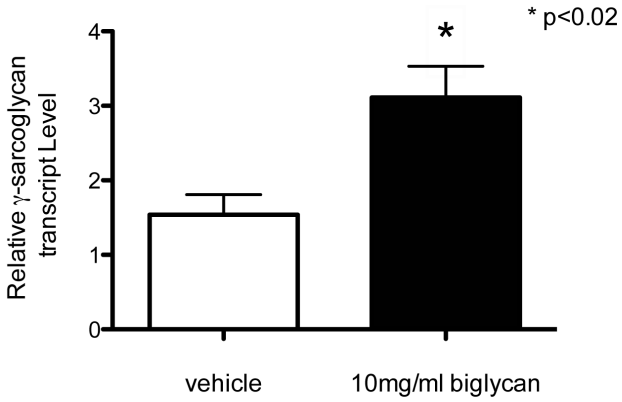
Relative γ-sarcoglycan transcript Level
4
3
2
1
0
*
* p<0.02
vehicle
10mg/ml biglycan

C.

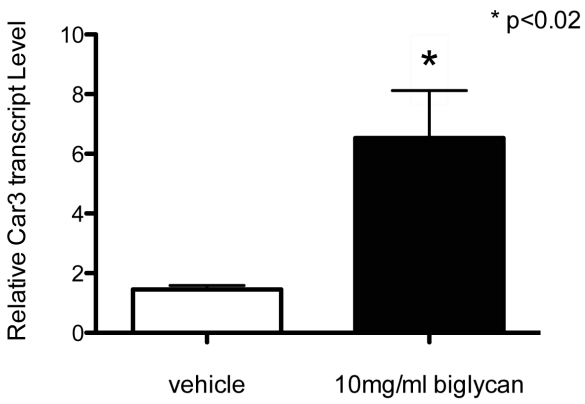
Relative Car3 transcript Level
10
8
6
4
2
0
*
* p<0.02
vehicle
10mg/ml biglycan

Appendix Figure 1. Car3 and γ-sarcoglycan messages are upregulated by rhBiglycan in *mdx* mice.

P18 *mdx* mice were intraperitoneally injected with vehicle and two concentrations of non-glycanated rhBiglycan (1 and 10mg/kg). At P32 quadriceps femoris muscles were harvested from injected mice. RNA was harvested and reverse transcribed into cDNA. Transcript levels of (A) utrophin, (B) γ-sarcoglycan and (C) Car3 were analyzed by qRT-PCR. In accord with the results presented in Chapter 4, utrophin transcripts were not increased by non-glycanated biglycan injection. However, there was a significant increase at the transcript levels of Car3 and γ-sarcoglycan upon non-glycanated biglycan injection. (n=6)

Appendix Figure 2

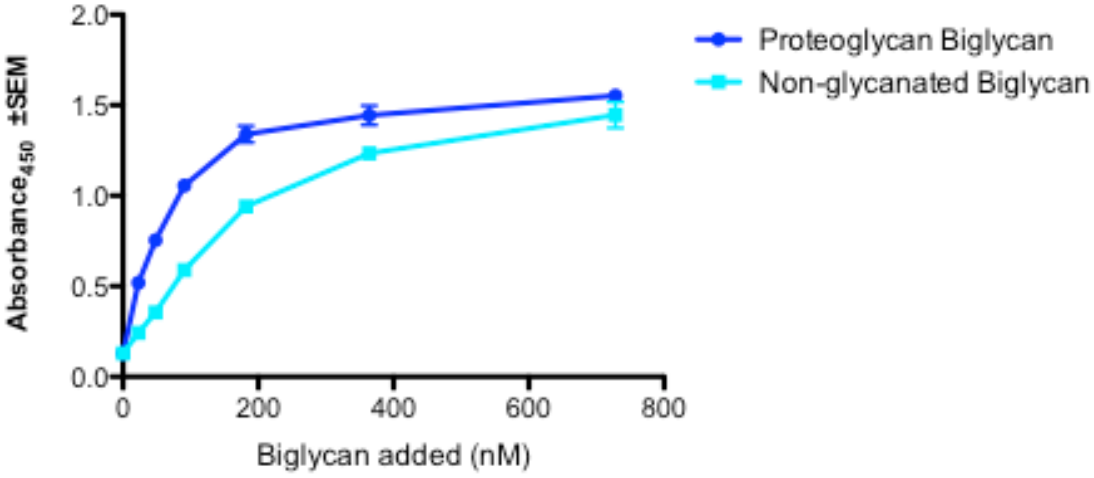

Appendix Figure 2. Non-glycanated biglycan exhibits less binding to BMP4 than proteoglycan form of biglycan.

BMP4 was immobilized on 96-well plates and then incubated with His-tagged proteoglycan and non-glycanated forms of biglycan (0-728nM). Bound biglycan was detected with anti-His antibody and HRP-conjugated anti-mouse secondary antibody. The graph represents the absorbance values read for the enzymatic activity of HRP. Each point represents the average of four replicates. As indicated in the shift in binding curves, proteoglycan form of biglycan binds to BMP4 better than the non-glycanated form.

Appendix Figure 3

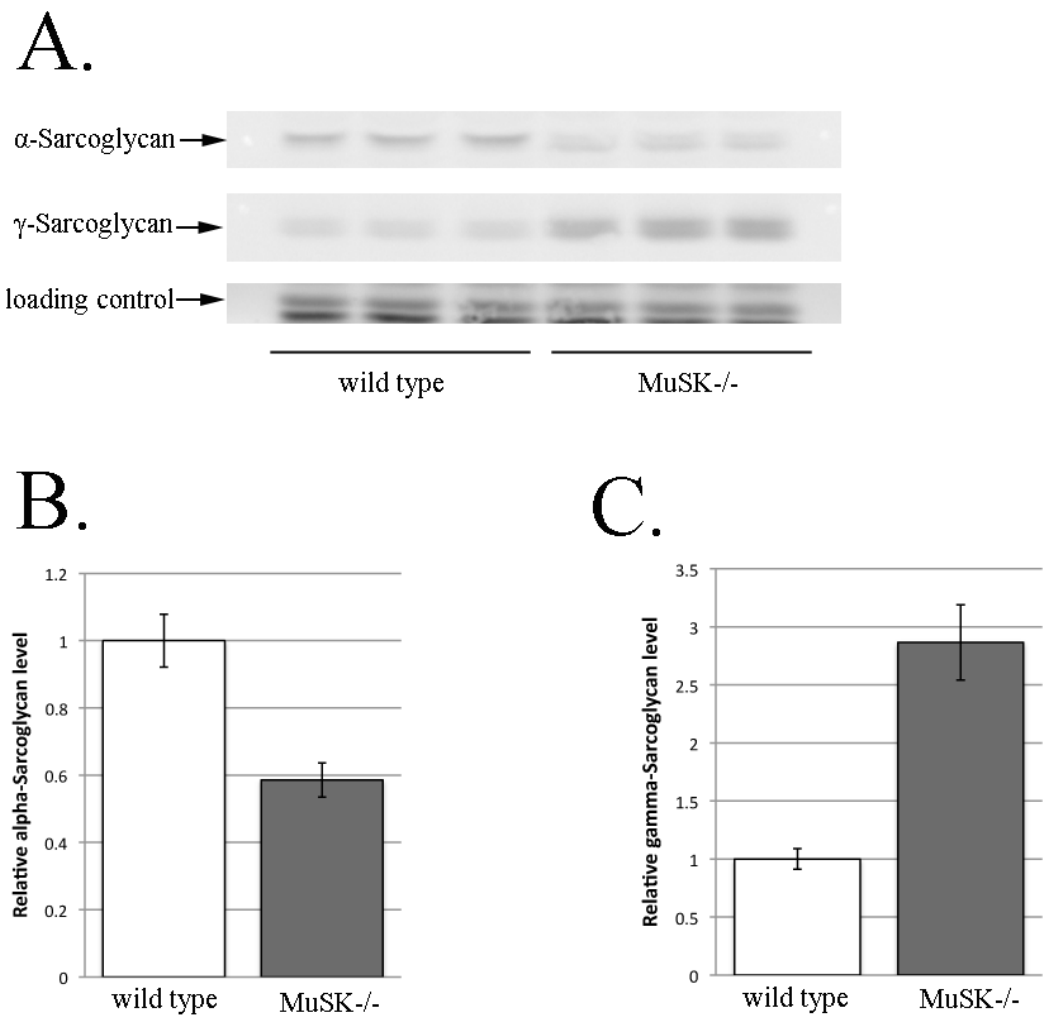

Appendix Figure 3. DAPC regulation by MuSK.

Wild type and MuSK null myoblasts were grown into confluence and differentiated for 3-4 days. Membrane fractions were isolated from myotube cultures as described in Chapter 4 Supporting Information Materials and Methods. (A) α- and γ-sarcoglycan protein levels in membrane fractions were detected by Western blots. Total protein staining was used as loading control. B-C. Quantifications of (B) α- and (C) γ-sarcoglycan levels. In the absence of MuSK, α-sarcoglycan levels were decreased in myotubes. Furthermore, the migration pattern of α-sarcoglycan band was also changed in the absence of MuSK. An additional band with a slightly less molecular weight appears when MuSK is absent, indicating that MuSK could also be regulating a posttranslational modification of α-sarcoglycan. γ-sarcoglycan levels, on the other hand, were increased in the absence of MuSK, suggesting a negative regulation of γ-sarcoglycan by MuSK.

Appendix Table 1

Transcript ID	Gene Symbol	p-value	Fold-Change
10339808		0.02271	5.25
10343609		0.04192	2.02
10341524		0.00296	2.00
10340228		0.01317	1.98
10338084		0.00590	1.86
10342420		0.02064	1.86
10339273		0.01940	1.80
10340928		0.01707	1.78
10341475		0.03816	1.75
10341200		0.01250	1.70
10343265		0.04457	1.68
10343619		0.02265	1.68
10341953		0.01522	1.64
10343220		0.02409	1.58
10339420		0.00624	1.56
10341887		0.00563	1.55
10340251		0.00891	1.55
10342672		0.04112	1.53
10338131		0.01660	1.53
10339977		0.01585	1.52
10551282	LOC100047728	0.02176	1.52
10339151		0.00556	1.51
10339549		0.01469	1.48
10339060		0.01943	1.46
10466298	Olfr1436	0.00274	1.46
10339724		0.04868	1.45
10341564		0.04673	1.44
10596958		0.02426	1.43
10344298		0.00554	1.43
10342029		0.02100	1.42
10414258		0.00826	1.42
10340815		0.02075	1.42
10338902		0.01725	1.41
10343872		0.00481	1.41
10338100		0.00818	1.39
10339087		0.03898	1.39
10341172		0.03565	1.38
10338533		0.02911	1.37
10339716		0.01309	1.37

10340713		0.02260	1.36
10343109		0.03454	1.36
10341584		0.00609	1.36
10340166		0.01041	1.36
10338552		0.00589	1.36
10342342		0.03505	1.35
10559728		0.04882	1.35
10342667		0.04047	1.35
10339946		0.03813	1.34
10344387		0.03732	1.34
10340541		0.04840	1.33
10341139		0.00404	1.33
10599213		0.02632	1.32
10344464		0.02943	1.32
10341386		0.03274	1.32
10340766		0.01097	1.32
10342692		0.02925	1.32
10412646		0.02000	1.31
10339965		0.04016	1.31
10361680	BC013529	0.00048	1.31
10552613	Klk1b4	0.01333	1.31
10342528		0.02707	-1.30
10343888		0.01441	-1.31
10344460		0.03351	-1.31
10340813		0.01756	-1.32
10343930		0.03481	-1.32
10349634		0.03188	-1.32
10342853		0.01926	-1.32
10339179		0.04931	-1.33
10344603		0.03716	-1.33
10484590	Olfr1056	0.02234	-1.33
10591853	Tbx20	0.04557	-1.33
10344088		0.04025	-1.34
10339869		0.00149	-1.34
10339964		0.00010	-1.34
10358785		0.00560	-1.35
10401834	Gm5039	0.01444	-1.36
10545210	Gm1524	0.01009	-1.36
10344401		0.03504	-1.36
10340719		0.01273	-1.36
10341733		0.00218	-1.36
10338584		0.02887	-1.36
10340738		0.01710	-1.37
10344595		0.01353	-1.38

10341186		0.04672	-1.38
10490923	Car2	0.02166	-1.39
10340673		0.02694	-1.39
10338470		0.04445	-1.39
10342652		0.02086	-1.39
10340703		0.03562	-1.41
10338539		0.02167	-1.41
10341945		0.04548	-1.41
10343819		0.01720	-1.41
10338692		0.03773	-1.42
10340205		0.01545	-1.42
10341801		0.04163	-1.42
10341559		0.00009	-1.42
10341928		0.01495	-1.43
10343004		0.03890	-1.43
10342840		0.00771	-1.43
10339519		0.02775	-1.43
10338980		0.03170	-1.44
10343700		0.04341	-1.44
10338702		0.00455	-1.45
10341234		0.03702	-1.45
10344257		0.03617	-1.45
10339650		0.02222	-1.46
10341616		0.00680	-1.46
10341886		0.02025	-1.47
10342424		0.01435	-1.47
10342982		0.01087	-1.47
10343755		0.02099	-1.48
10341435		0.04701	-1.49
10344372		0.04955	-1.49
10342061		0.02593	-1.49
10340037		0.00422	-1.49
10344259		0.02984	-1.50
10341074		0.01048	-1.51
10340683		0.03180	-1.51
10343336		0.00197	-1.51
10344551		0.01625	-1.52
10342729		0.02573	-1.52
10339483		0.00187	-1.52
10343392		0.02980	-1.52
10344207		0.00403	-1.53
10341383		0.02160	-1.54
10338846		0.00430	-1.55
10339256		0.03514	-1.55

10341148		0.00881	-1.56
10342796		0.00377	-1.56
10342948		0.04466	-1.57
10342469		0.00711	-1.58
10343321		0.00398	-1.60
10547793	Rnu7	0.01068	-1.61
10525914		0.01560	-1.61
10342217		0.01701	-1.62
10340762		0.02333	-1.63
10338350		0.01370	-1.63
10342258		0.03060	-1.64
10343694		0.00498	-1.66
10342648		0.04731	-1.66
10341753		0.04383	-1.67
10339684		0.03328	-1.68
10339838		0.01068	-1.69
10341819		0.02677	-1.70
10344013		0.01706	-1.70
10339268		0.03647	-1.71
10339380		0.00631	-1.71
10338807		0.03441	-1.73
10344267		0.03950	-1.73
10338420		0.04750	-1.74
10341090		0.00371	-1.75
10344021		0.04551	-1.75
10342299		0.01005	-1.76
10338287		0.03949	-1.77
10342874		0.01467	-1.77
10341044		0.03349	-1.78
10339594		0.04275	-1.78
10339278		0.04879	-1.79
10344009		0.03885	-1.79
10339364		0.03825	-1.80
10340222		0.04186	-1.83
10342868		0.00409	-1.84
10342403		0.00232	-1.87
10343326		0.01427	-1.87
10341231		0.04160	-1.89
10341236		0.04004	-1.91
10341177		0.00105	-1.96
10343822		0.00583	-2.00
10341214		0.01906	-2.02
10341229		0.00213	-2.14
10342481		0.01474	-2.18

10339113		0.04737	-2.26
10338230		0.04952	-2.27
10344131		0.00721	-2.38
10340970		0.01531	-2.57

Appendix Table 1. Genome-wide gene expression analysis of non-glycanated biglycan-treated biglycan null myotubes.

Biglycan null myoblasts were grown into confluence and differentiated for four days. The myotubes were treated with non-glycanated biglycan for 8 hours. RNA was harvested from the cultures and reverse transcribed into cDNA, which was then hybridized to Affymetrix array chips. The results of the microarray analysis are summarized in Table 1. Fold changes greater than 1.3 are shown in the table. The positive values indicate the fold change in upregulation of the listed transcript by non-glycanated biglycan whereas the negative values indicate the fold change in downregulation of the listed transcript. The majority of the transcript hits are control probe sets. Thus, overall there was not a strong transcriptional response to non-glycanated biglycan treatment in biglycan null myotubes.

Appendix Table 2

Transcript ID	Gene Symbol	p-value	Fold-Change
10341131		0.04173	2.71
10338194		0.00034	2.64
10340698		0.03910	2.11
10344256		0.04527	2.10
10339420		0.00049	2.08
10341475		0.01629	2.01
10343669		0.03547	1.98
10413012	Fut11	0.01557	1.93

10417068		0.03501	1.91
10340066		0.01631	1.91
10339208		0.00248	1.90
10341484		0.01094	1.89
10338778		0.01937	1.87
10343307		0.00382	1.85
10341448		0.02990	1.84
10340228		0.02052	1.84
10339273		0.01855	1.81
10339121		0.00252	1.81
10338426		0.03860	1.81
10342672		0.01417	1.75
10339254		0.03913	1.74
10342590		0.00359	1.73
10339309		0.02556	1.72
10338756		0.00070	1.71
10344045		0.00112	1.71
10476590	Macrod2	0.00073	1.70
10344366		0.02092	1.70
10341367		0.02315	1.68
10339724		0.01462	1.66
10343084		0.00190	1.66
10596958		0.00592	1.65
10338533		0.00406	1.64
10339418		0.00461	1.63
10566205	Dub2a	0.00322	1.63
10339151		0.00257	1.63
10340482		0.04297	1.62
10343860		0.03282	1.61
10342554		0.02463	1.61
10453688		0.00309	1.61
10343368		0.01933	1.61
10342089		0.02161	1.61
10339240		0.01128	1.59
10338637		0.04188	1.59
10340619		0.02299	1.57
10339894		0.00252	1.56
10343263		0.00356	1.55
10424555		0.04061	1.54
10476393		0.00045	1.54
10339977		0.01414	1.54
10340674		0.04346	1.54
10341868		0.00680	1.54
10344387		0.00870	1.52

10524394		0.01029	1.51
10532903		0.01029	1.51
10340199		0.02967	1.51
10341524		0.02931	1.51
10341953		0.03321	1.50
10338092		0.02410	1.50
10338932		0.02614	1.50
10339294		0.03293	1.49
10344298		0.00338	1.49
10339136		0.02799	1.49
10341194		0.00788	1.48
10338309		0.01026	1.48
10458764	LOC100046618	0.03538	1.48
10341456		0.00752	1.47
10343220		0.04489	1.47
10340295		0.03201	1.47
10340713		0.00933	1.47
10341926		0.02174	1.47
10560385	Psg23	0.01917	1.46
10403031	V165-D-J-C	0.01907	1.46
10341172		0.01993	1.46
10339461		0.00005	1.45
10342025		0.02486	1.44
10492165		0.00426	1.44
10338787		0.02749	1.44
10340523		0.00135	1.44
10411506	Gm2524	0.03311	1.43
10491913		0.00018	1.43
10343982		0.02030	1.43
10341068		0.04787	1.42
10340281		0.04639	1.42
10338887		0.01002	1.42
10338553		0.02635	1.41
10340230		0.00354	1.41
10581643		0.01272	1.41
10484720	Olfr1166	0.02012	1.41
10343036		0.00618	1.41
10341633		0.01363	1.41
10340244		0.00122	1.40
10412657		0.02694	1.40
10491474	Gm5708	0.00290	1.40
10340234		0.02044	1.39
10460194		0.01927	1.39
10560164	Obox6	0.00662	1.39

10338100		0.00843	1.39
10416897		0.03751	1.39
10339010		0.02633	1.39
10344238		0.03590	1.39
10343904		0.02660	1.39
10340466		0.04657	1.39
10415011		0.01141	1.38
10340946		0.02290	1.38
10344019		0.04762	1.38
10339731		0.01763	1.38
10340749		0.02899	1.38
10339965		0.02160	1.38
10353413		0.04043	1.37
10412663	Gm8429	0.00974	1.37
10536147	Gm16367	0.04767	1.37
10604954		0.00217	1.37
10338441		0.02218	1.36
10360538	Pppde1	0.01726	1.36
10342197		0.00002	1.36
10341058		0.02022	1.36
10341642		0.00218	1.36
10343491		0.03472	1.35
10433197	Olfr161	0.01164	1.35
10362113	Gm10824	0.01347	1.35
10338983		0.00168	1.35
10343872		0.00867	1.35
10421873	Gm10845	0.02435	1.35
10338401		0.00536	1.34
10340251		0.04204	1.34
10600741	Gm5941	0.02938	1.34
10444995	EG547347	0.00111	1.34
10602825		0.01136	1.34
10397538		0.01711	1.34
10550167		0.01132	1.33
10564041		0.03041	1.33
10600720	Gm6027	0.00022	1.33
10461055		0.02779	1.33
10342029		0.04621	1.33
10552613	Klk1b4	0.01061	1.33
10343096		0.03865	1.32
10546432	Adamts9	0.04924	1.32
10340166		0.01494	1.32
10338780		0.03724	1.32
10471569		0.01776	1.32

10388284	Olfr389	0.04039	1.32
10607600		0.00800	1.32
10480477	Pax8	0.00259	1.32
10338501		0.04697	1.32
10556573	1110006G14Rik	0.00146	1.32
10464169	1700010L13Rik	0.02225	1.32
10453732	Gm4833	0.04591	1.32
10536363	Tac1	0.00654	1.32
10415013		0.01883	1.31
10430572		0.01626	1.31
10340706		0.00513	1.31
10343216		0.01788	1.31
10447688	4930506C21Rik	0.04823	1.31
10472418	Scn9a	0.04054	1.31
10343765		0.01387	1.31
10368050	Ect2l	0.00227	1.31
10507131	Tal1	0.00066	1.31
10339822		0.03977	1.31
10523903		0.03480	1.31
10343871		0.02852	1.31
10563935		0.03448	1.31
10564045		0.03448	1.31
10564047		0.03448	1.31
10367050	Rdh18	0.00717	1.31
10360398	Ifi202b	0.01953	1.31
10355191	Crygd	0.03009	1.31
10564011	Snord115	0.04429	1.31
10563941		0.01227	1.31
10368175	Pde7b	0.03381	1.31
10607792	Glra2	0.00149	1.30
10503232		0.00780	1.30
10538123	Gimap9	0.00214	1.30
10375838	Col23a1	0.01694	1.30
10438425	Olfr167	0.02131	1.30
10564019		0.02156	1.30
10341053		0.01871	1.30
10344452		0.03920	1.30
10531259	Gm10426	0.01399	1.30
10567380	Umod	0.00771	1.30
10340960		0.01779	1.30
10338723		0.04521	1.30
10563949		0.00638	1.30
10341563		0.04678	1.30
10587000	Dyx1c1	0.03262	1.30

10596135		0.01277	1.30
10342389		0.02049	1.30
10340205		0.04734	-1.30
10342878		0.02929	-1.30
10338964		0.04808	-1.30
10344411		0.04787	-1.30
10338977		0.02389	-1.30
10496324	Slc39a8	0.00444	-1.31
10455092	Pcdhb12	0.00904	-1.31
10342652		0.04461	-1.31
10339127		0.00360	-1.31
10472050	Tnfaip6	0.04986	-1.31
10342580		0.04622	-1.32
10338171		0.04293	-1.32
10490923	Car2	0.04102	-1.32
10342889		0.04238	-1.32
10344207		0.02510	-1.32
10340312		0.04477	-1.32
10343006		0.02581	-1.32
10570957	Sfrp1	0.04515	-1.32
10400302		0.03750	-1.33
10342840		0.02087	-1.33
10523156	Cxcl2	0.00797	-1.33
10429564	Ly6a	0.03831	-1.33
10342872		0.02086	-1.33
10341638		0.01615	-1.34
10342290		0.01773	-1.34
10339833		0.00013	-1.34
10438567	2310042E22Rik	0.04918	-1.35
10343151		0.03417	-1.35
10342853		0.01472	-1.35
10343164		0.02380	-1.35
10338702		0.01070	-1.36
10338548		0.00965	-1.36
10341621		0.02767	-1.37
10340053		0.02748	-1.37
10338527		0.00929	-1.38
10338942		0.03479	-1.38
10342159		0.01727	-1.38
10339329		0.00482	-1.38
10584524	1700001J11Rik	0.00633	-1.38
10340741		0.03005	-1.39
10342815		0.00926	-1.39
10340002		0.01977	-1.40

10438091	2610318N02Rik	0.04067	-1.41
10344032		0.04545	-1.41
10344539		0.03847	-1.41
10342370		0.03721	-1.41
10338490		0.04275	-1.41
10599680	3830403N18Rik	0.00106	-1.41
10342242		0.04895	-1.42
10473636	Olfr1262	0.01561	-1.42
10339752		0.03869	-1.43
10430679		0.01835	-1.43
10340961		0.04626	-1.43
10367744	LOC629446	0.02226	-1.44
10584496	Olfr960	0.04404	-1.44
10338096		0.04763	-1.45
10338769		0.03071	-1.45
10342217		0.04422	-1.45
10339173		0.01800	-1.46
10436050	Dppa4	0.04943	-1.46
10338896		0.00101	-1.46
10379996		0.03218	-1.47
10341559		0.00005	-1.47
10341865		0.04975	-1.47
10342181		0.02448	-1.49
10338268		0.00865	-1.49
10349634		0.00742	-1.49
10340813		0.00293	-1.50
10591853	Tbx20	0.01127	-1.51
10338700		0.01642	-1.51
10342817		0.03512	-1.51
10343593		0.02034	-1.52
10340703		0.01613	-1.52
10340037		0.00326	-1.53
10339099		0.04763	-1.53
10341543		0.02814	-1.53
10338439		0.04478	-1.54
10342033		0.02664	-1.55
10341850		0.00675	-1.55
10343680		0.04012	-1.58
10338160		0.00726	-1.58
10344149		0.03542	-1.58
10338846		0.00326	-1.59
10339193		0.03765	-1.59
10342657		0.02383	-1.59
10339380		0.01167	-1.60

10343321		0.00416	-1.60
10339074		0.03643	-1.60
10344041		0.02589	-1.61
10342874		0.03068	-1.61
10343694		0.00657	-1.61
10338329		0.04629	-1.61
10344372		0.02505	-1.62
10342729		0.01342	-1.64
10343779		0.03391	-1.64
10338820		0.00758	-1.65
10341959		0.02907	-1.65
10339650		0.00655	-1.65
10344200		0.02040	-1.65
10343966		0.04114	-1.66
10344150		0.04214	-1.71
10342575		0.02938	-1.75
10341177		0.00251	-1.76
10339684		0.02096	-1.80
10340179		0.03975	-1.82
10339050		0.00179	-1.82
10339761		0.03695	-1.86
10338807		0.01939	-1.89
10342299		0.00396	-1.99
10341917		0.00566	-2.06
10339242		0.03477	-2.47
10343923		0.01121	-2.66

Appendix Table 2. Genome-wide gene expression analysis of proteoglycan biglycan-treated biglycan null myotubes.

Biglycan null myoblasts were grown into confluence and differentiated for four days. The myotubes were treated with proteoglycan biglycan for 8 hours. RNA was harvested from the cultures and reverse transcribed into cDNA, which was then hybridized to Affymetrix array chips. The results of the microarray analysis are summarized in Table 2. Fold changes greater than 1.3 are shown in the table. The positive values indicate the fold change in upregulation of the listed transcript by

proteoglycan biglycan whereas the negative values indicate the fold change in downregulation of the listed transcript. As in the case of non-glycanated biglycan, proteoglycan biglycan did not induce a strong transcriptional response in biglycan null myotubes under these conditions. Among the regulated annotated transcripts, there are three common responses between non-glycanated and proteoglycan treated cultures: T-box transcription factor TBX20 (Tbx20), Carbonic Anhydrase 2 (Car2) and kallikrein 1-related pepidase b4 (Klk1b4). Tbx20 and Car2 transcripts were downregulated by proteoglycan and non-glycanated forms of biglycan, whereas Klk1b4 was upregulated by both forms. Several other transcripts were uniquely regulated only by proteoglycan or non-glycanated form of biglycan, indicating that the two forms of biglycan can initiate different signaling events.

Appendix Table 3

Probeset ID	p-value	Fold-Change
hsa-miR-640_st	0.0079	5.47
cfa-miR-382_st	0.0119	5.32
cfa-miR-421_st	0.0324	4.56
rno-miR-301a_st	0.0133	3.75
ppy-miR-196_st	0.0430	3.74
mmu-miR-450b-3p_st	0.0105	3.65
cfa-miR-15a_st	0.0055	3.14
mml-miR-196a_st	0.0210	2.96
hsa-miR-1300_st	0.0379	2.76
xtr-miR-199b_st	0.0002	2.61
mdo-miR-212_st	0.0213	2.61
cfa-miR-26b_st	0.0253	2.56
mml-miR-502-5p_st	0.0109	2.55
mmu-miR-26b_st	0.0201	2.52
dre-miR-30a_st	0.0063	2.41
cfa-miR-29c_st	0.0306	2.36
hsa-miR-330-5p_st	0.0076	2.32

bta-miR-148b_st	0.0128	2.31
mmu-miR-193_st	0.0181	2.30
mmu-miR-466i_st	0.0279	2.18
dme-miR-34_st	0.0090	2.18
mmu-miR-183_st	0.0070	2.17
xtr-miR-30e_st	0.0414	2.14
ssc-miR-224_st	0.0078	2.13
rno-miR-146b_st	0.0386	2.12
xtr-miR-10a_st	0.0235	2.11
xtr-miR-15c_st	0.0075	2.10
hsa-miR-539_st	0.0134	2.09
cfa-miR-196b_st	0.0103	2.09
mdv2-miR-M17_st	0.0145	2.06
rno-miR-124_st	0.0302	2.04
ppt-miR419_st	0.0263	2.01
rno-miR-126_st	0.0209	2.00
xtr-miR-148a_st	0.0079	2.00
mml-miR-153_st	0.0246	-2.02
hsa-miR-548b-3p_st	0.0393	-2.03
osa-miR408_st	0.0436	-2.05
mml-miR-877_st	0.0112	-2.05
fru-miR-210_st	0.0006	-2.05
cfa-miR-138a_st	0.0003	-2.06
mmu-miR-673-3p_st	0.0071	-2.10
mml-miR-423-5p_st	0.0089	-2.14
hsa-miR-423-5p_st	0.0261	-2.16
mmu-miR-423-5p_st	0.0051	-2.17
hsa-miR-486-3p_st	0.0156	-2.18
rno-miR-23a-star_st	0.0022	-2.18
mmu-miR-483_st	0.0179	-2.18
hsa-miR-23a-star_st	0.0376	-2.20
osa-miR166c_st	0.0172	-2.23
hsa-miR-27a-star_st	0.0090	-2.29
rno-miR-330-star_st	0.0014	-2.30
hsa-miR-25-star_st	0.0041	-2.36
gga-miR-456_st	0.0027	-2.40
cin-let-7e_st	0.0242	-2.41
ath-miR395b_st	0.0061	-2.41
mml-miR-615-5p_st	0.0251	-2.54
mmu-miR-491_st	0.0192	-2.56
hsa-miR-1260_st	0.0086	-2.66
mmu-miR-330-star_st	0.0106	-2.74
rno-miR-27a-star_st	0.0015	-2.80
mml-miR-548a_st	0.0190	-2.80

Appendix Table 3. Genome-wide microRNA expression analysis of non-glycanated biglycan-treated (8h) biglycan null myotubes.

Biglycan null myoblasts were grown into confluence and differentiated for four days. The myotubes were treated with non-glycanated biglycan for 8 hours. RNA was immediately harvested with miRNeasy purification columns (QIAGEN) and labeled with FlashTag™ Biotin HSR RNA Labeling Kit (Genisphere). Samples were run in Affymetrix miRNA arrays. And the results are summarized in Table 2. A number of microRNAs were up- and downregulated in biglycan null myotubes by biglycan treatment. A positive value indicates the fold change for an upregulated microRNA , whereas a negative value indicates the fold change for a downregulated microRNA.

Appendix Tables 4-7

Further analysis of the microarray study described in Chapter 2. Transcripts that are downregulated by BMP4 in myoblast and myotube cultures of wild type and MuSK null cells are listed in Tables 4-7. The negative values indicate the fold change in downregulation of the listed transcript by BMP4.

Appendix Table 4

Gene Symbol	p-value(N vs. B)	Fold-Change
6330406I15Rik	0.0000214	-4.15
Duxbl	0.0000541	-3.72
Duxbl	0.0000541	-3.72
Duxbl	0.0000639	-3.61
Lrig1	0.0000560	-3.40
Bnc2	0.0005148	-3.34
Mest	0.0000348	-3.31
Adamts5	0.0000029	-3.20
Chst15	0.0000001	-3.16
Sox8	0.0000390	-3.12
Mrgprf	0.0006931	-3.07
Slc40a1	0.0000694	-2.89
Cdkn1c	0.0002003	-2.84
Tgm2	0.0000382	-2.79
E2f2	0.0005093	-2.79
Vipr2	0.0000877	-2.77
Rgs16	0.0000216	-2.64
Lypd6	0.0002860	-2.64
Bdkrb1	0.0006553	-2.63
Sema6a	0.0003070	-2.62
Tm6sf1	0.0001879	-2.60
Lrch1	0.0000196	-2.60
Dtx4	0.0001109	-2.56
Daam2	0.0000656	-2.55
Ramp2	0.0000431	-2.50
Enpp1	0.0000532	-2.48
1810041L15Rik	0.0003347	-2.47
Fgfr4	0.0001609	-2.44
	0.0001612	-2.41
Enpp3	0.0002659	-2.41
2610301F02Rik	0.0000533	-2.36
Arhgap28	0.0003329	-2.36
Gm7325	0.0002460	-2.35
Pdlim2	0.0001043	-2.34
Rgma	0.0000702	-2.33
Tmem184a	0.0000144	-2.32
Cpa4	0.0007659	-2.31
2610301F02Rik	0.0000483	-2.29
Pde2a	0.0000306	-2.27
Ccbe1	0.0007084	-2.24

Prkag3	0.0003616	-2.23
Ccdc88c	0.0000119	-2.22
2610301F02Rik	0.0010167	-2.21
Cdh15	0.0000005	-2.20
Lrrc32	0.0000532	-2.20
Mamstr	0.0009100	-2.19
Ctnnal1	0.0000288	-2.19
Pip4k2a	0.0001842	-2.17
Zfp238	0.0000058	-2.17
Ralgps2	0.0003000	-2.14
Coro2b	0.0003650	-2.12
Filip1	0.0001155	-2.12
Cdc42ep2	0.0001646	-2.09
Rbm24	0.0000501	-2.07
Gprc5c	0.0001175	-2.06
Ampd3	0.0000043	-2.06
Sema7a	0.0009474	-2.05
Klhl31	0.0000093	-2.02
Pnmal2	0.0005892	-2.01
Frmpd1	0.0004263	-2.00
Aif1l	0.0003115	-1.99
Fam83b	0.0001286	-1.98
Spg21	0.0000623	-1.98
Fam122b	0.0004044	-1.96
Sema5a	0.0000214	-1.95
C330016O10Rik	0.0000032	-1.95
Hdac11	0.0000696	-1.93
Klhl31	0.0000181	-1.92
Ndrg1	0.0000246	-1.92
Fam49a	0.0009917	-1.92
Ston2	0.0002517	-1.91
Ccdc23	0.0002880	-1.90
Il17d	0.0006934	-1.90
Kbtbd5	0.0000863	-1.90
Agap1	0.0002084	-1.89
Tspan15	0.0008423	-1.89
Fam65b	0.0001679	-1.88
Klhl30	0.0004261	-1.88
Egln3	0.0009972	-1.86
Chrnd	0.0000037	-1.86
Rgmb	0.0010311	-1.86
Spry1	0.0003263	-1.86
Dmrt2	0.0001814	-1.85
Frmd4b	0.0009842	-1.84

9930013L23Rik	0.0003634	-1.84
Chd7	0.0001923	-1.84
Gprc5c	0.0004738	-1.82
Itga3	0.0010084	-1.82
Notch3	0.0001628	-1.82
Heyl	0.0000305	-1.82
Traf4	0.0000342	-1.82
Clcn5	0.0004309	-1.81
AI464131	0.0009525	-1.81
Maf	0.0002017	-1.80
Chd7	0.0005106	-1.79
Mbnl3	0.0002275	-1.78
Best1	0.0002190	-1.77
Iffo1	0.0000004	-1.77
Gal3st2	0.0004868	-1.77
Gal3st2	0.0006560	-1.77
Pacs2	0.0000134	-1.76
Morc4	0.0002557	-1.76
Chd7	0.0001987	-1.76
Svil	0.0000311	-1.76
Smtnl2	0.0000119	-1.74
Fcgr4	0.0000166	-1.74
Gfra1	0.0001197	-1.74
Zeb1	0.0002503	-1.74
Cap2	0.0000325	-1.74
Plxna1	0.0002050	-1.73
Chd7	0.0002448	-1.73
Fam53b	0.0006727	-1.73
Bicd2	0.0000716	-1.72
Phf17	0.0005239	-1.72
Chd7	0.0000289	-1.71
Olfml2a	0.0000293	-1.71
Ehd4	0.0004606	-1.71
Chd7	0.0006552	-1.71
Nup210	0.0004276	-1.70
Cdk5r1	0.0003189	-1.70
Rassf4	0.0005223	-1.70
Dapk2	0.0003511	-1.70
Chrng	0.0000015	-1.70
Sema3c	0.0000007	-1.70
Sema3e	0.0000277	-1.69
Gdpd1	0.0000414	-1.69
Lrrc30	0.0006275	-1.69
Popdc2	0.0004407	-1.69

Asb2	0.0000257	-1.69
Xrcc5	0.0000456	-1.68
Trim55	0.0009039	-1.68
Kif24	0.0000592	-1.68
Dclre1c	0.0006324	-1.68
Cpa1	0.0000918	-1.67
Arhgap24	0.0006311	-1.67
Arhgap29	0.0000061	-1.67
Rps6ka2	0.0000011	-1.66
Ankrd2	0.0000785	-1.66
Lmnb2	0.0004493	-1.66
Dock11	0.0000073	-1.66
2310015B20Rik	0.0004175	-1.65
Syne1	0.0000040	-1.65
Fbxo10	0.0000281	-1.65
Mfsd2	0.0005685	-1.62
Erbb3	0.0000709	-1.61
Arhgap18	0.0007159	-1.61
Plxdc1	0.0004110	-1.60
Chd7	0.0006499	-1.60
Smad3	0.0000005	-1.60
	0.0002819	-1.60
Slc22a23	0.0003138	-1.60
Mybph	0.0000782	-1.59
Slc9a3r1	0.0006011	-1.59
Fzd9	0.0006109	-1.59
Chd7	0.0009537	-1.58
Spsb1	0.0007464	-1.57
Kitl	0.0007540	-1.57
Casz1	0.0004358	-1.57
Rasl11b	0.0006053	-1.57
Cd200	0.0003042	-1.56
Bid	0.0004567	-1.56
Tpcn1	0.0001069	-1.56
Ccdc134	0.0000213	-1.56
Gpt2	0.0005790	-1.56
1190002N15Rik	0.0003878	-1.56
Slc12a2	0.0007791	-1.55
Dok3	0.0004473	-1.55
Cd82	0.0000093	-1.54
Chd7	0.0001008	-1.54
Ablim1	0.0010537	-1.54
Dusp3	0.0001850	-1.54
Cyfip2	0.0003695	-1.54

Ptprd	0.0001094	-1.53
Il1r1	0.0001670	-1.53
Purb	0.0008843	-1.53
Arhgap22	0.0007595	-1.53
Syne1	0.0000148	-1.53
Amigo1	0.0008859	-1.53
Stard13	0.0000430	-1.53
Btbd17	0.0001645	-1.53
Ankrd23	0.0001154	-1.53
Scn4a	0.0003361	-1.53
Sdpr	0.0005746	-1.52
Fam171a2	0.0000310	-1.52
D14Ertd449e	0.0005901	-1.52
Chd7	0.0001726	-1.52
Ugcg	0.0005628	-1.52
Slc9a9	0.0000562	-1.52
Wisp1	0.0009822	-1.51
2210020M01Rik	0.0006756	-1.51
Ets2	0.0001837	-1.51
D14Ertd449e	0.0006609	-1.51
D14Ertd449e	0.0004112	-1.51
Epb4.1l5	0.0003958	-1.51
Tanc2	0.0007363	-1.51
Chd7	0.0010659	-1.51
Dync1i1	0.0001684	-1.50
Notch1	0.0005415	-1.50
C78339	0.0004487	-1.50
Pxdn	0.0003548	-1.49
Chd7	0.0006375	-1.49
Gm10336	0.0008154	-1.49
Lama5	0.0001344	-1.49
4-Sep	0.0000913	-1.48
D15Wsu169e	0.0003490	-1.48
Fam20a	0.0006558	-1.48
Myom2	0.0007167	-1.48
Olfml2b	0.0007103	-1.47
Adamts7	0.0004595	-1.47
Tmem62	0.0005440	-1.47
Hfe2	0.0001716	-1.47
Fchsd2	0.0002648	-1.47
Met	0.0010149	-1.46
Afap1l2	0.0006751	-1.46
Ppfia4	0.0007139	-1.46
Cpa5	0.0000342	-1.46

Tjp1	0.0003720	-1.46
Tns1	0.0001648	-1.46
Dll1	0.0000406	-1.46
Pygm	0.0001745	-1.46
Txnip	0.0003089	-1.45
Efhd2	0.0005053	-1.45
Plau	0.0006234	-1.45
Mtss1	0.0000074	-1.45
Itga7	0.0009093	-1.45
Atp2a1	0.0000915	-1.45
Baiap2l1	0.0004460	-1.45
Stk17b	0.0000621	-1.44
Reep2	0.0001658	-1.44
	0.0009833	-1.44
Cnot6l	0.0000034	-1.44
Lta4h	0.0000616	-1.43
Skp2	0.0001334	-1.43
Actn3	0.0007608	-1.43
Tubb2b	0.0002943	-1.43
Ddx51	0.0001568	-1.43
Mef2a	0.0004708	-1.42
	0.0002089	-1.42
Dbndd1	0.0005277	-1.42
Atp13a5	0.0007721	-1.42
Bcam	0.0005741	-1.42
Amigo2	0.0010740	-1.42
Ppbp	0.0009399	-1.42
Sorbs3	0.0001509	-1.41
Pnpla2	0.0002227	-1.41
BC018507	0.0000682	-1.41
Bin1	0.0000008	-1.41
Purb	0.0002797	-1.41
Cd97	0.0001901	-1.40
Klhdc6	0.0009893	-1.40
Zfp608	0.0002994	-1.40
Ezh1	0.0001291	-1.40
Exosc9	0.0000082	-1.39
Il34	0.0006272	-1.39
Amotl1	0.0003035	-1.39
Krt80	0.0006019	-1.39
B4galt4	0.0004063	-1.39
Lmf1	0.0000247	-1.38
Lhfpl2	0.0008023	-1.38
Akr1b8	0.0005933	-1.38

Chrnb1	0.0001167	-1.38
Lrba	0.0000498	-1.38
St3gal5	0.0007294	-1.37
	0.0009068	-1.37
Ctsc	0.0004288	-1.37
Wnt9a	0.0004058	-1.37
Stk25	0.0005884	-1.37
Lpin3	0.0002048	-1.37
Gramd4	0.0000025	-1.37
Tmem20	0.0002588	-1.37
Top1	0.0002888	-1.36
Lamb1-1	0.0007479	-1.36
Spats2l	0.0001604	-1.36
Dbn1	0.0000668	-1.36
Ttyh2	0.0000039	-1.35
Fam110b	0.0001362	-1.35
Atp7a	0.0001619	-1.35
Gca	0.0009740	-1.34
Arhgap10	0.0001320	-1.34
Dtna	0.0008527	-1.34
Cdk2	0.0005810	-1.33
Itgb1bp2	0.0008065	-1.33
Edil3	0.0009066	-1.33
Tubb6	0.0001897	-1.33
Tcea3	0.0000086	-1.33
Ckm	0.0001867	-1.33
Fam13c	0.0000498	-1.33
Unc93b1	0.0001296	-1.33
Rnd2	0.0001313	-1.32
Cugbp2	0.0002356	-1.32
Foxo4	0.0002154	-1.32
Apod	0.0007457	-1.32
Sh2b1	0.0004921	-1.32
Mboat2	0.0008968	-1.31
Kif13b	0.0009384	-1.31
Acsl1	0.0004434	-1.31
Zfp322a	0.0003003	-1.31
Lrrc1	0.0002445	-1.31
Exoc7	0.0000656	-1.31
Dhx32	0.0009763	-1.30
Fbxo16	0.0009223	-1.30
D17H6S56E-5	0.0002998	-1.30
Gabrb2	0.0008291	-1.30
RP23-100C5.8	0.0000397	-1.30

Prpf39	0.0006212	-1.30
Hmgn3	0.0008245	-1.30
Nfatc2	0.0009864	-1.29
Psat1	0.0008636	-1.29
Herc1	0.0003193	-1.29
Pja1	0.0004191	-1.29
Slc29a1	0.0005735	-1.29
Afap1	0.0000391	-1.29
Ddhd1	0.0005818	-1.29
Spg20	0.0003120	-1.28
Gpc4	0.0000631	-1.28
Elmod2	0.0003579	-1.28
Unc84a	0.0008693	-1.28
D930014E17Rik	0.0010117	-1.28
Tmem109	0.0002907	-1.28
Ick	0.0000467	-1.28
Hspa12a	0.0010554	-1.28
Ivns1abp	0.0007133	-1.28
Sox6	0.0006008	-1.27
Lsp1	0.0005521	-1.27
Mfsd7a	0.0004216	-1.26
Olfm1	0.0010299	-1.26
Fam117a	0.0009305	-1.26
Col5a3	0.0007260	-1.25
Pak1	0.0005636	-1.25
Gm12888	0.0003339	-1.25
Macf1	0.0000413	-1.25
Ddr2	0.0002458	-1.25
Bcat2	0.0000990	-1.25
Il17rd	0.0008439	-1.25
Sh3d19	0.0007272	-1.25
Ormdl2	0.0007964	-1.25
Fdft1	0.0008487	-1.25
Il17rc	0.0002456	-1.25
Akr1b3	0.0002085	-1.24
Akr1b3	0.0001740	-1.24
Fbxo40	0.0006168	-1.24
Matn2	0.0008516	-1.24
Nat11	0.0006252	-1.24
Akr1b3	0.0003444	-1.23
Iqcb1	0.0000167	-1.23
Tsga14	0.0008146	-1.23
Zfp345	0.0010402	-1.23
Zfp521	0.0000536	-1.23

Col4a1	0.0000539	-1.23
	0.0007426	-1.22
Fads3	0.0004095	-1.22
Ank2	0.0001693	-1.22
E230016K23Rik	0.0010596	-1.22
Ppm1l	0.0007170	-1.22
Serinc2	0.0004424	-1.21
Tmpo	0.0001389	-1.21
Kat2b	0.0000499	-1.21
Ephb3	0.0006023	-1.21
Atp10a	0.0008674	-1.20
Rsad2	0.0009606	-1.20
Suhw4	0.0006522	-1.20
Jag2	0.0002328	-1.20
	0.0002156	-1.20
Tnnt2	0.0001028	-1.20
Tns3	0.0010653	-1.20
Myof	0.0000245	-1.19
Zfp367	0.0001623	-1.19
Fam53a	0.0001783	-1.18
A530098C11Rik	0.0000096	-1.18
Pcx	0.0002013	-1.18
Plat	0.0000242	-1.17
Hdac9	0.0006160	-1.17
AI987944	0.0010865	-1.17
Brp16	0.0007445	-1.17
Usp31	0.0006690	-1.17
Entpd4	0.0006852	-1.17
Reep4	0.0003595	-1.17
	0.0009543	-1.16
Plcl2	0.0008897	-1.16
Myod1	0.0000826	-1.16
Mtap1b	0.0010154	-1.16
Mt2	0.0001084	-1.16
Parp3	0.0004961	-1.15
Nbeal2	0.0007471	-1.15
Adam8	0.0000579	-1.15
Evl	0.0006758	-1.14
Msto1	0.0010184	-1.14
	0.0010175	-1.14
Mvd	0.0008178	-1.13
Numa1	0.0007722	-1.13
Dtl	0.0000093	-1.12
Fam54b	0.0007400	-1.12

Psmd11	0.0007981	-1.12
Arhgap17	0.0002459	-1.11
Xrcc1	0.0005915	-1.11
Phldb3	0.0009385	-1.11
Dmxl1	0.0001392	-1.10
Thoc2	0.0003223	-1.10
Wdr1	0.0003185	-1.10
Cenpq	0.0002256	-1.09
Clcn2	0.0006650	-1.09
Lamc1	0.0000498	-1.09

Appendix Table 4. Transcripts downregulated by BMP4-treatment in wild type myoblasts.

Appendix Table 5

Gene Symbol	p-value(N vs. B)	Fold-Change
Adcyap1r1	0.0000028	-5.20
Cpa1	0.0001414	-4.35
Chrnd	0.0000029	-3.77
Stc1	0.0002201	-3.66
Ndst4	0.0003585	-3.64
	0.0002743	-3.53
Hpgd	0.0000091	-3.35
	0.0006717	-3.34
2610301F02Rik	0.0002716	-3.10
Fam83b	0.0000565	-2.86
Igfbp5	0.0001906	-2.84
2610301F02Rik	0.0000096	-2.83
2610301F02Rik	0.0000103	-2.81
2610301F02Rik	0.0001942	-2.78
Dtx4	0.0000933	-2.75
Tm6sf1	0.0000383	-2.63
Enpp1	0.0000332	-2.58
Cdh15	0.0000219	-2.55
Sprr1a	0.0002499	-2.48
Chrng	0.0000380	-2.48

Ramp2	0.0001086	-2.48
Slc40a1	0.0000193	-2.46
Fgfr4	0.0000137	-2.46
Lypd6	0.0007059	-2.42
Tmem184a	0.0002739	-2.42
Arhgap28	0.0002005	-2.37
Rbm24	0.0000004	-2.34
Chst15	0.0000597	-2.29
	0.0004783	-2.27
Hfe2	0.0005804	-2.26
Ttc9	0.0000015	-2.25
Slc24a3	0.0001676	-2.25
Chd7	0.0000302	-2.20
Lrig1	0.0000044	-2.20
Ctnnal1	0.0001247	-2.19
Tsga14	0.0001482	-2.17
Cap2	0.0000057	-2.17
Chd7	0.0000239	-2.17
Unc13c	0.0000814	-2.16
Coro2b	0.0004026	-2.15
Car2	0.0000008	-2.14
Chd7	0.0005032	-2.11
Vipr2	0.0001241	-2.10
Ccdc88c	0.0002697	-2.10
Chd7	0.0001239	-2.08
Chd7	0.0000151	-2.07
Chd7	0.0001643	-2.04
Agap1	0.0003860	-2.03
Chd7	0.0004892	-2.03
Chd7	0.0004570	-2.02
Cpa4	0.0001468	-2.01
Chd7	0.0002146	-2.00
Gm7325	0.0000931	-1.99
Hivep2	0.0001623	-1.99
Klhl31	0.0001572	-1.99
Adamts5	0.0000140	-1.98
Chd7	0.0001457	-1.98
Chd7	0.0005202	-1.98
Zfp238	0.0000044	-1.98
Popdc3	0.0000782	-1.97
Dll1	0.0000821	-1.95
Notch3	0.0000128	-1.94
Chd7	0.0004652	-1.94
Fbxo32	0.0001011	-1.93

Tdrkh	0.0006300	-1.93
Clcn5	0.0001442	-1.91
Slc9a9	0.0001118	-1.91
Klhl31	0.0001764	-1.89
Chd7	0.0001120	-1.88
Klhdc10	0.0000899	-1.88
Arhgap22	0.0001903	-1.87
Dcn	0.0006473	-1.86
Lrp4	0.0000161	-1.85
Aif1l	0.0002770	-1.84
Pip4k2a	0.0001586	-1.84
Fmo1	0.0001751	-1.83
Jup	0.0001243	-1.83
Rgs16	0.0002544	-1.83
Xrcc5	0.0001207	-1.82
Chd7	0.0005404	-1.82
Stk10	0.0000990	-1.81
Sntb1	0.0001387	-1.81
Bicd2	0.0000025	-1.78
Itga3	0.0001786	-1.77
Unc13c	0.0000694	-1.76
Nptx1	0.0000105	-1.76
Met	0.0001061	-1.76
Sdpr	0.0000687	-1.75
Scx	0.0004083	-1.75
Fam69a	0.0005059	-1.74
Best3	0.0005315	-1.73
P2rx5	0.0000197	-1.72
Shb	0.0005567	-1.72
Slc9a7	0.0005183	-1.71
Myo1e	0.0000003	-1.71
Cd200	0.0000925	-1.71
Chd7	0.0000277	-1.70
Mest	0.0000073	-1.70
Cldn15	0.0005397	-1.70
Zcchc24	0.0002039	-1.68
Kbtbd10	0.0001782	-1.67
	0.0004466	-1.66
Hs6st1	0.0000628	-1.66
Gdpd1	0.0003281	-1.65
Lhfpl2	0.0000146	-1.65
Gem	0.0000656	-1.65
Cd97	0.0003106	-1.65
Gfra1	0.0000231	-1.65

	0.0000572	-1.65
Galntl4	0.0002151	-1.65
AW551984	0.0003040	-1.64
Mycl1	0.0002966	-1.63
Stard13	0.0000628	-1.62
Gpt2	0.0000802	-1.62
Lrch1	0.0000667	-1.61
Actn3	0.0005938	-1.61
Rgmb	0.0002414	-1.61
	0.0002790	-1.61
Syt13	0.0000198	-1.60
Fam122b	0.0001533	-1.60
Chd7	0.0002917	-1.60
Dtna	0.0000980	-1.60
Pion	0.0000019	-1.60
Gas2	0.0006283	-1.60
Cd82	0.0002126	-1.60
	0.0004899	-1.59
Ndrg1	0.0000563	-1.59
Chrnb1	0.0000251	-1.58
Traf4	0.0002500	-1.58
Gadd45a	0.0000380	-1.58
Ifih1	0.0001069	-1.57
Tjp1	0.0003129	-1.57
Txnip	0.0000137	-1.57
1190002N15Rik	0.0000147	-1.57
Adamts4	0.0007051	-1.56
Plk2	0.0006916	-1.55
Bicd1	0.0001450	-1.55
Apcdd1	0.0000411	-1.55
Klf5	0.0004701	-1.55
Fhl2	0.0000263	-1.53
Sema3d	0.0000804	-1.53
9930013L23Rik	0.0002632	-1.53
Pcbd1	0.0004990	-1.53
Trim55	0.0006800	-1.52
Akr1c14	0.0006291	-1.52
Itgb6	0.0000148	-1.52
Pdgfa	0.0003712	-1.52
Dusp3	0.0003170	-1.51
Synj2	0.0000838	-1.51
Myod1	0.0001626	-1.51
Ankrd35	0.0004248	-1.50
Tpcn1	0.0002357	-1.49

Iqsec1	0.0005769	-1.48
Antxr2	0.0000413	-1.48
Dock9	0.0003769	-1.47
Tmem109	0.0002984	-1.47
Skp2	0.0001525	-1.47
Ralgps2	0.0000971	-1.46
Krt80	0.0001474	-1.46
Mtss1	0.0004086	-1.46
Cdh1	0.0001488	-1.45
Ano5	0.0005794	-1.45
Eda2r	0.0000150	-1.44
Syne1	0.0000071	-1.44
Tubb2b	0.0002275	-1.44
Dmpk	0.0001492	-1.44
Slc29a1	0.0003806	-1.43
Pik3c2b	0.0002730	-1.43
C130092O11Rik	0.0000652	-1.43
Chd7	0.0002514	-1.43
Ugcg	0.0000811	-1.43
Olfm1	0.0003338	-1.42
Lphn2	0.0004620	-1.42
Lpin3	0.0005826	-1.42
Pacs2	0.0006733	-1.41
Itga7	0.0001328	-1.41
Sort1	0.0000292	-1.41
Pdgfc	0.0000736	-1.41
Glrb	0.0001839	-1.41
Rerg	0.0004835	-1.41
Cyld	0.0003028	-1.40
Inpp4b	0.0000321	-1.40
Svil	0.0004115	-1.40
Baiap2	0.0005305	-1.40
Bves	0.0000880	-1.39
Ptpla	0.0002489	-1.39
Stam	0.0000360	-1.38
C78339	0.0001219	-1.38
Wisp1	0.0003277	-1.38
Lphn2	0.0006636	-1.37
Acadl	0.0005546	-1.37
Tubb2b	0.0001265	-1.37
Best1	0.0003734	-1.37
Tbx18	0.0003119	-1.36
Hs6st2	0.0006049	-1.36
Syne1	0.0000651	-1.35

Ube2e3	0.0006259	-1.35
Mt2	0.0004739	-1.35
Lphn2	0.0000189	-1.35
Fam178a	0.0005696	-1.34
Ephb6	0.0001508	-1.34
Pitx2	0.0001463	-1.34
Cnot6l	0.0003393	-1.34
Ypel1	0.0003653	-1.33
Gpc1	0.0006417	-1.33
Ivns1abp	0.0003064	-1.33
Ezh1	0.0002966	-1.32
Calcoco1	0.0000480	-1.32
Asb5	0.0003891	-1.32
Lamb1-1	0.0004490	-1.31
St6gal1	0.0000148	-1.31
Maob	0.0005573	-1.31
Sh2b1	0.0004378	-1.31
Akr1b3	0.0006544	-1.30
Syngr2	0.0001531	-1.30
Lphn2	0.0000670	-1.30
Arhgef2	0.0001105	-1.30
Rnf128	0.0001125	-1.30
Akr1b3	0.0000255	-1.30
Akr1b3	0.0002428	-1.30
Ahnak2	0.0000128	-1.29
Fbxo10	0.0001086	-1.29
Prrg4	0.0006853	-1.29
Stard10	0.0005295	-1.29
Ick	0.0002723	-1.28
Stk25	0.0000398	-1.28
	0.0002023	-1.28
4930455F23Rik	0.0003160	-1.27
Map3k9	0.0001815	-1.27
Pacsin2	0.0001521	-1.27
Vwa5a	0.0000203	-1.27
Lmf1	0.0003618	-1.27
Akr1b3	0.0001573	-1.26
Rhbdf1	0.0002887	-1.26
Serinc2	0.0003209	-1.26
Abca2	0.0004818	-1.26
Xrn2	0.0003918	-1.25
Klhl7	0.0002300	-1.25
Parp9	0.0003623	-1.25
Il17rd	0.0003754	-1.25

Tpm2	0.0005828	-1.25
Ccdc134	0.0002501	-1.23
	0.0001714	-1.23
Ext1	0.0006306	-1.23
Vasp	0.0002122	-1.23
Tmem209	0.0005555	-1.23
Stom	0.0001346	-1.23
Klhl24	0.0004269	-1.22
Igf2r	0.0003164	-1.22
Gal3st2	0.0002920	-1.22
Fads3	0.0002755	-1.21
BC031353	0.0001315	-1.20
Zc3h12c	0.0002538	-1.20
Rab11fip5	0.0006123	-1.19
Entpd4	0.0004000	-1.19
	0.0006959	-1.19
Ctnna1	0.0001451	-1.17
Dcaf5	0.0005100	-1.17
Mtap6	0.0006455	-1.17
Colec12	0.0000988	-1.17
Eif4e2	0.0002206	-1.17
Dst	0.0001110	-1.17
Zfp36l2	0.0001325	-1.17
Ggta1	0.0001781	-1.16
Nbr1	0.0005050	-1.15
Olfr820	0.0003139	-1.15
Slc38a9	0.0007032	-1.14
Frmd4a	0.0006123	-1.14
Cnnm3	0.0001414	-1.14
Sh3d19	0.0003417	-1.14
1700025G04Rik	0.0004922	-1.13
Lmln	0.0001396	-1.13
Pikfyve	0.0001838	-1.12
Car3	0.0004176	-1.11
Sec24d	0.0006966	-1.11
Lclat1	0.0002311	-1.10
Rprd1b	0.0003377	-1.10
Zfyve1	0.0005029	-1.10
Tspan6	0.0004392	-1.10
Ptpn21	0.0004059	-1.10
Klk13	0.0003505	-1.10
Zbtb45	0.0006870	-1.09
Ndufs8	0.0004926	-1.09
Apol7b	0.0000998	-1.08

Ube2l3	0.0001781	-1.07
	0.0003404	-1.06
Eif4ebp1	0.0003727	-1.06
Hist1h3f	0.0004130	-1.04

Appendix Table 5. Transcripts downregulated by BMP4-treatment in MuSK null myoblasts.

Appendix Table 6

Gene Symbol	p-value(N vs. B)	Fold-Change
Fgf9	0.0000046	-3.75
	0.0002845	-2.94
E2f2	0.0000097	-2.90
Lrrc26	0.0005241	-2.89
Mest	0.0006330	-2.85
Duxbl	0.0000890	-2.63
Duxbl	0.0000890	-2.63
Duxbl	0.0001782	-2.53
Nptx1	0.0001370	-2.52
Heg1	0.0000703	-2.45
4921525H12Rik	0.0001037	-2.42
Gpr146	0.0000551	-2.36
Egr3	0.0005306	-2.21
Rhobtb2	0.0000866	-2.20
Rgma	0.0000433	-2.20
	0.0000941	-2.19
Mxd1	0.0006945	-2.19
Abra	0.0000652	-2.16
Cdkl5	0.0001211	-2.12
Lrch1	0.0000298	-2.11
Gm10387	0.0002122	-2.11
Lrig1	0.0004189	-2.09
Fam53b	0.0000145	-2.01
Grit	0.0000201	-2.00
Kcnk5	0.0000238	-2.00
Chst15	0.0000297	-1.96
Daam2	0.0000014	-1.95
Sema7a	0.0003653	-1.95

Klk1b8	0.0003336	-1.94
Fam49a	0.0004006	-1.94
Lrrc1	0.0002910	-1.94
2610301F02Rik	0.0000383	-1.93
Il1r1	0.0005947	-1.91
Erbb3	0.0000517	-1.90
Ppargc1a	0.0000485	-1.88
Sdpr	0.0000502	-1.87
Plekha7	0.0007074	-1.86
2610301F02Rik	0.0005047	-1.84
Mc4r	0.0001750	-1.84
Rgmb	0.0000535	-1.80
Pstpip2	0.0001208	-1.78
Mospd1	0.0003195	-1.78
Slc7a8	0.0002770	-1.77
Grtp1	0.0000262	-1.77
Arhgap28	0.0000184	-1.73
Asb2	0.0006515	-1.72
Ralgps1	0.0002598	-1.72
Tbx15	0.0000274	-1.72
Man1c1	0.0000360	-1.70
	0.0004747	-1.68
Filip1	0.0000149	-1.68
Tspan14	0.0006709	-1.68
Osr1	0.0003587	-1.68
Gpt2	0.0002045	-1.68
Bnc2	0.0000572	-1.68
2610301F02Rik	0.0004670	-1.68
Arhgap18	0.0000334	-1.67
2210020M01Rik	0.0000845	-1.67
Gm10009	0.0003104	-1.66
Unc13c	0.0005220	-1.65
Wnt10a	0.0005906	-1.65
Mamstr	0.0002788	-1.65
Mef2d	0.0001481	-1.64
Fam65b	0.0002804	-1.63
Pdlim2	0.0005653	-1.63
2610301F02Rik	0.0005299	-1.61
Sema4c	0.0007481	-1.61
Heyl	0.0004110	-1.61
Pdgfb	0.0004514	-1.61
Rrad	0.0002232	-1.60
Lmo7	0.0005250	-1.60
Atp13a5	0.0001174	-1.58

Sox8	0.0000677	-1.58
Mrgprf	0.0000883	-1.58
Adamts5	0.0006270	-1.58
Tnfaip3	0.0000975	-1.57
Klhl31	0.0000407	-1.57
Slc9a9	0.0002163	-1.56
Cbfa2t3	0.0001574	-1.56
Il33	0.0006369	-1.56
Casz1	0.0000916	-1.55
Thpo	0.0000921	-1.54
Prkag3	0.0000558	-1.54
Unc93b1	0.0005276	-1.54
Rnf122	0.0003810	-1.53
Fn3k	0.0001507	-1.53
	0.0003518	-1.53
Hjurp	0.0005089	-1.52
Dhcr7	0.0003801	-1.52
Reep1	0.0000054	-1.51
Tfrc	0.0004259	-1.51
Sema6a	0.0000158	-1.51
Snx30	0.0004785	-1.50
Stard13	0.0007689	-1.50
Pnmal2	0.0000757	-1.50
Doc2b	0.0000910	-1.50
Colq	0.0004442	-1.49
Slc16a2	0.0000138	-1.48
Igfbp3	0.0000305	-1.48
Gtdc1	0.0000988	-1.48
Fgfbp1	0.0001426	-1.48
Plau	0.0002335	-1.47
D15Wsu169e	0.0004967	-1.47
Ablim1	0.0000332	-1.47
Ctnnal1	0.0003709	-1.47
Klhl31	0.0000655	-1.47
Gramd1b	0.0002090	-1.47
Uts2r	0.0000370	-1.47
Kbtbd5	0.0000458	-1.46
Ankrd23	0.0006935	-1.46
Slc12a2	0.0007107	-1.46
Mylk	0.0005990	-1.46
	0.0003135	-1.44
Plscr2	0.0005201	-1.44
Gramd4	0.0003804	-1.43
Raf1	0.0000879	-1.43

Gprc5c	0.0000216	-1.43
Sh2d4b	0.0006165	-1.43
	0.0007315	-1.43
Shroom3	0.0001793	-1.42
Gm672	0.0006405	-1.42
Nup210	0.0006938	-1.42
Cpeb2	0.0002830	-1.41
Trpv3	0.0003333	-1.41
Gprc5c	0.0000064	-1.40
Thbd	0.0001630	-1.40
Zfp30	0.0004737	-1.40
Slc24a6	0.0003028	-1.40
AI464131	0.0000975	-1.40
Daam1	0.0005181	-1.40
Zcchc24	0.0002423	-1.39
Traf4	0.0001968	-1.39
Ccdc23	0.0001919	-1.39
Rassf7	0.0006846	-1.39
Dgkz	0.0001531	-1.39
Cd34	0.0004649	-1.38
C1galt1c1	0.0004925	-1.38
Gulp1	0.0000729	-1.38
Pbx3	0.0001241	-1.38
Myo1b	0.0000043	-1.37
Fam13c	0.0002301	-1.36
Lphn3	0.0002646	-1.36
Ch25h	0.0001386	-1.36
Mef2d	0.0000574	-1.36
Rbm38	0.0001233	-1.36
Dlgap4	0.0001454	-1.35
Cd82	0.0000621	-1.35
ORF63	0.0007558	-1.35
Ptar1	0.0001132	-1.35
Lonrf3	0.0002546	-1.35
Phka2	0.0001652	-1.35
Trim7	0.0005729	-1.35
Mpp3	0.0005133	-1.34
Oas2	0.0001851	-1.34
Pcdh1	0.0001339	-1.34
Zfp57	0.0000663	-1.34
2410042D21Rik	0.0001619	-1.34
5031414D18Rik	0.0000142	-1.34
Rapgef1	0.0002170	-1.34
Fbxo10	0.0003976	-1.33

Lrrc8d	0.0000454	-1.33
Cyp3a41a	0.0005199	-1.33
Clcn5	0.0001996	-1.33
Adm	0.0005395	-1.32
Prkaa2	0.0003121	-1.32
Ddit4l	0.0002212	-1.32
Eml4	0.0003962	-1.32
Mid1	0.0004414	-1.32
Ube2d1	0.0000259	-1.31
	0.0002508	-1.31
Ppap2a	0.0001298	-1.31
Nfib	0.0000220	-1.31
Dgkd	0.0000890	-1.31
Srgap3	0.0002540	-1.30
Brwd1	0.0004427	-1.30
Cdc42ep4	0.0005583	-1.30
Tet1	0.0002087	-1.30
Ppfia4	0.0002337	-1.30
Arrdc1	0.0002436	-1.30
E860004J03Rik	0.0002803	-1.30
Enox1	0.0002534	-1.29
Tmem38b	0.0005888	-1.28
Ddc	0.0004587	-1.28
9-Sep	0.0003336	-1.28
Hn1	0.0002692	-1.28
Gdpd1	0.0006157	-1.27
Sike1	0.0002917	-1.27
St3gal5	0.0000808	-1.27
Pttg1ip	0.0000887	-1.27
	0.0000986	-1.27
Clasp1	0.0002760	-1.26
Agl	0.0007200	-1.26
Irak2	0.0001103	-1.26
Frmd4b	0.0007005	-1.26
Rps6kb1	0.0001071	-1.26
Hsf4	0.0003845	-1.26
Zfp275	0.0003678	-1.25
Svil	0.0006959	-1.25
Hells	0.0002387	-1.25
Zeb1	0.0003729	-1.25
Tpcn1	0.0007305	-1.25
Bmyc	0.0002198	-1.25
Lpgat1	0.0005078	-1.24
Baiap2l1	0.0007333	-1.24

9030420J04Rik	0.0005035	-1.24
Pcgf3	0.0001061	-1.24
	0.0005791	-1.23
Btbd3	0.0007076	-1.22
Cep68	0.0000037	-1.22
Tmem177	0.0004917	-1.22
Gpsm2	0.0003806	-1.22
Ssbp3	0.0003278	-1.22
Mtap1a	0.0005478	-1.22
Wisp1	0.0002093	-1.21
Cmbl	0.0007405	-1.21
Klk10	0.0001836	-1.21
Rad51	0.0004764	-1.20
Tubb6	0.0000712	-1.20
	0.0002425	-1.20
Itgb1bp2	0.0003095	-1.20
Ahnak	0.0004622	-1.19
Lmtk2	0.0006029	-1.19
Foxj3	0.0005675	-1.19
Flnc	0.0003287	-1.19
Mapk8ip1	0.0000038	-1.19
Smpdl3b	0.0002784	-1.19
Nfkb1	0.0005372	-1.19
Cugbp2	0.0004842	-1.18
Arhgap10	0.0003785	-1.18
Tubb2a	0.0002721	-1.18
Exosc9	0.0005084	-1.18
	0.0001729	-1.18
Cd97	0.0002628	-1.17
Sgsm2	0.0005912	-1.17
Ep400	0.0007493	-1.17
Myof	0.0002287	-1.16
Ttc3	0.0000294	-1.16
Casq2	0.0006576	-1.15
Tmem41a	0.0005291	-1.15
Gpr137b	0.0004426	-1.15
Crybg3	0.0001346	-1.14
Enpp1	0.0005973	-1.14
Mttp	0.0003324	-1.13
Crkrs	0.0007116	-1.12
Akap6	0.0004537	-1.12
Gm2467	0.0002294	-1.12
Crebbp	0.0005433	-1.12
Dyrk1a	0.0007284	-1.12

1810055G02Rik	0.0005265	-1.11
2210404J11Rik	0.0005196	-1.11
Fam96b	0.0006195	-1.11
Ddx17	0.0006333	-1.10
Nudt4	0.0005114	-1.10
Lman2	0.0000868	-1.09
Akr1b3	0.0002253	-1.08
	0.0002355	-1.07
Dedd	0.0003254	-1.07
BC033915	0.0004698	-1.06
Lamp1	0.0005543	-1.03

Appendix Table 6. Transcripts downregulated by BMP4-treatment in wild-type myotubes.

Appendix Table 7

Gene Symbol	p-value(N vs. B)	Fold-Change
Lum	0.0007719	-3.52
Lrrc26	0.0000069	-3.16
Mfsd7c	0.0000287	-3.11
Ddit4l	0.0000138	-3.10
Sema7a	0.0011194	-3.02
Nptx1	0.0000099	-2.94
Rassf2	0.0000064	-2.72
Slc2a6	0.0002215	-2.71
Scn7a	0.0009098	-2.67
Grtp1	0.0005902	-2.65
Mc4r	0.0000356	-2.64
Runx1t1	0.0000058	-2.62
Rgs2	0.0002402	-2.60
Gm7325	0.0001291	-2.58
Osr2	0.0005416	-2.54
Trp63	0.0000324	-2.53
Duxbl	0.0000222	-2.52
Duxbl	0.0000222	-2.52
1600029D21Rik	0.0000589	-2.49
4921525H12Rik	0.0000671	-2.49
Sobp	0.0001756	-2.46
F3	0.0000516	-2.42

Neu2	0.0002460	-2.42
Duxbl	0.0000145	-2.34
Frmd4b	0.0000167	-2.32
4732465J04Rik	0.0000264	-2.25
Lrig1	0.0000646	-2.24
Gm10001	0.0001652	-2.24
Pdgfb	0.0001275	-2.23
Crabp2	0.0008856	-2.22
Sdpr	0.0002267	-2.22
1810041L15Rik	0.0005212	-2.19
Mamstr	0.0001331	-2.19
Dtx4	0.0000095	-2.16
Maf	0.0000305	-2.12
Il33	0.0000304	-2.11
Tnik	0.0003297	-2.10
Arhgap18	0.0001599	-2.10
Sertad4	0.0001156	-2.07
Fzd9	0.0000667	-2.07
Chst15	0.0000103	-2.06
C330016O10Rik	0.0009277	-2.05
Itga3	0.0012101	-2.04
Slco3a1	0.0000379	-2.01
Fam53b	0.0005303	-2.01
Filip1	0.0000899	-2.01
	0.0011301	-2.00
Sema5a	0.0000178	-1.98
Gulp1	0.0005562	-1.97
6330406I15Rik	0.0003047	-1.97
Mest	0.0000121	-1.97
Camk1g	0.0006890	-1.96
Lmcd1	0.0002407	-1.96
Nceh1	0.0003507	-1.95
I830127L07Rik	0.0000515	-1.94
Acsl1	0.0000000	-1.94
Fmo1	0.0001929	-1.94
Lgals12	0.0008628	-1.93
	0.0009695	-1.93
Trim7	0.0002339	-1.93
Slc7a8	0.0003327	-1.92
Lrrc30	0.0007290	-1.92
Arhgap28	0.0000094	-1.91
Sema6a	0.0000789	-1.90
Mfsd7a	0.0004824	-1.90
Tnfrsf19	0.0000284	-1.90

Asb15	0.0000336	-1.88
Igsf10	0.0007079	-1.87
Cd24a	0.0000509	-1.86
Tet1	0.0004377	-1.86
Tnfaip3	0.0001109	-1.86
Kif24	0.0011197	-1.86
Scn4a	0.0001671	-1.85
Zcchc5	0.0000302	-1.85
Igsf10	0.0001964	-1.83
Rnf122	0.0001437	-1.83
Prkag3	0.0000307	-1.82
Tnfaip8	0.0000404	-1.82
Igsf10	0.0002984	-1.81
Olfml2a	0.0000650	-1.81
Atp1b2	0.0001944	-1.81
Chodl	0.0011311	-1.80
Igfbp3	0.0000361	-1.80
Fam65b	0.0005582	-1.80
Tecrl	0.0000171	-1.79
Slc5a6	0.0010341	-1.79
Bnc2	0.0000067	-1.79
Mtss1	0.0000033	-1.79
Steap3	0.0000003	-1.79
Rgmb	0.0000049	-1.79
Klhl3	0.0001000	-1.79
Rasgrp3	0.0010547	-1.79
Zcchc24	0.0006526	-1.78
Gpr146	0.0008811	-1.77
Fn3k	0.0001053	-1.77
Casz1	0.0003177	-1.76
Mpp3	0.0000129	-1.76
Rgs16	0.0001789	-1.75
Syt13	0.0010344	-1.74
Fam135b	0.0012472	-1.74
Rhobtb2	0.0000652	-1.74
Glul	0.0000047	-1.73
Aspa	0.0006975	-1.73
Tet1	0.0000379	-1.72
Atp6v1c2	0.0003134	-1.72
Il15	0.0001238	-1.71
Klhl31	0.0000149	-1.71
Sox6	0.0001232	-1.70
Trim16	0.0004831	-1.70
Fam13c	0.0001673	-1.70

Tbx15	0.0001356	-1.69
Mrgprf	0.0006433	-1.69
Mafa	0.0001022	-1.69
Slc9a9	0.0005388	-1.68
Flrt1	0.0001026	-1.68
5033413D22Rik	0.0000230	-1.68
Mospd1	0.0003675	-1.67
Klk10	0.0010079	-1.66
Erbb3	0.0000755	-1.66
Adamts16	0.0005347	-1.65
Tmem184a	0.0001427	-1.65
Atp2b3	0.0001302	-1.65
Coro2b	0.0000817	-1.64
Lphn3	0.0010652	-1.64
Fsd1l	0.0002759	-1.64
Tspan14	0.0002283	-1.64
D14Ertd449e	0.0002371	-1.64
Gtdc1	0.0010531	-1.64
Tet1	0.0000212	-1.64
Pnkd	0.0001507	-1.63
Lpar1	0.0004387	-1.63
D14Ertd449e	0.0004424	-1.63
Heg1	0.0007083	-1.63
Slc2a5	0.0003320	-1.63
Lrrc15	0.0010595	-1.63
Lama4	0.0000434	-1.63
Dgkd	0.0000035	-1.63
D14Ertd449e	0.0003057	-1.62
Glul	0.0002872	-1.62
Cpne2	0.0000992	-1.62
Galnt5	0.0001757	-1.62
Ralgps1	0.0004341	-1.62
Reep1	0.0002645	-1.62
Kifc3	0.0008480	-1.62
Popdc2	0.0000025	-1.62
Sorcs2	0.0002661	-1.61
2810432L12Rik	0.0006078	-1.61
Daam1	0.0000718	-1.61
Heg1	0.0003233	-1.61
2610301F02Rik	0.0002838	-1.61
Fam135b	0.0002523	-1.60
Antxr2	0.0004733	-1.60
Cgnl1	0.0002057	-1.60
Myh4	0.0005041	-1.60

Ccdc88c	0.0002300	-1.60
Dbp	0.0003715	-1.59
Pnmal2	0.0000124	-1.58
Dhcr7	0.0007005	-1.58
5730419I09Rik	0.0003080	-1.58
Lamb1-1	0.0004967	-1.58
Ctnnal1	0.0005493	-1.58
Lrch1	0.0003398	-1.58
Ccbe1	0.0007573	-1.58
Gas2	0.0001945	-1.58
D0H4S114	0.0003344	-1.58
Ednra	0.0001915	-1.58
Fras1	0.0005443	-1.58
Klhl31	0.0000303	-1.57
5033414K04Rik	0.0000965	-1.57
Pde2a	0.0009307	-1.57
Slc24a3	0.0002559	-1.57
Spire2	0.0012376	-1.57
Ralgps2	0.0007975	-1.56
Ssx2ip	0.0000207	-1.56
Jam3	0.0001360	-1.56
Sox8	0.0000811	-1.56
Stx11	0.0002393	-1.55
Gpr68	0.0012135	-1.55
St3gal4	0.0010419	-1.55
Anpep	0.0008426	-1.55
Rilpl1	0.0009444	-1.54
Cd72	0.0006599	-1.54
Gpt2	0.0002384	-1.54
Camk2a	0.0000476	-1.54
Spg21	0.0008725	-1.54
Klhl30	0.0005874	-1.54
Map2k6	0.0007294	-1.53
Sema4c	0.0006704	-1.53
Myoz3	0.0000697	-1.53
Nup210	0.0001144	-1.52
Gpd1l	0.0003795	-1.52
Frem1	0.0011749	-1.52
Ccl2	0.0010132	-1.52
Cdc42ep2	0.0010561	-1.52
Inpp4a	0.0003303	-1.51
Slc41a1	0.0004059	-1.51
Pdlim2	0.0001386	-1.51
Sema3e	0.0001987	-1.51

Gpr126	0.0000224	-1.51
Zfp503	0.0003160	-1.50
Slco5a1	0.0002747	-1.50
Tcea3	0.0001091	-1.50
Rgma	0.0005848	-1.50
Gan	0.0003136	-1.49
Rnf150	0.0003691	-1.49
C1qtnf1	0.0005087	-1.49
Glis2	0.0005919	-1.49
Ttyh2	0.0010319	-1.49
Gprc5c	0.0009785	-1.49
Zdhhc14	0.0000648	-1.48
D830046C22Rik	0.0007857	-1.48
Mcf2l	0.0002461	-1.48
Garnl4	0.0000157	-1.48
4833442J19Rik	0.0005980	-1.48
6530418L21Rik	0.0011071	-1.47
Fsd2	0.0004613	-1.47
Pdp1	0.0005220	-1.47
Wfs1	0.0005797	-1.47
	0.0000663	-1.47
Atp7a	0.0009846	-1.46
Gfra1	0.0009387	-1.46
Acsl6	0.0006204	-1.46
Synpo2	0.0001918	-1.46
Rbm47	0.0007276	-1.46
Schip1	0.0000378	-1.46
Rev3l	0.0007159	-1.45
Afap1l1	0.0002174	-1.45
Gpr155	0.0009251	-1.45
Sepp1	0.0002459	-1.44
Cldn15	0.0011745	-1.44
Pfkfb4	0.0003285	-1.43
Gprc5c	0.0009910	-1.43
Ip6k3	0.0006022	-1.43
Gatm	0.0000508	-1.43
Gm10035	0.0003891	-1.42
Adamts5	0.0004502	-1.42
Sort1	0.0000860	-1.42
Ddah1	0.0000785	-1.41
Atp2b4	0.0005385	-1.41
Cnr1	0.0001792	-1.41
	0.0001502	-1.41
Itga11	0.0004874	-1.41

Matn2	0.0001063	-1.41
Cabc1	0.0000122	-1.41
Slc25a26	0.0000946	-1.40
Hdac11	0.0005091	-1.40
Necab1	0.0008027	-1.40
Plk2	0.0003242	-1.40
Cd200	0.0000151	-1.40
Tnk2	0.0006440	-1.39
Abr	0.0000219	-1.39
Pip4k2a	0.0002004	-1.39
Gm672	0.0006084	-1.38
Arhgef3	0.0008949	-1.38
Rassf7	0.0001721	-1.38
Oasl2	0.0010275	-1.38
Plscr4	0.0010023	-1.38
Klhl8	0.0011902	-1.38
Ebf3	0.0003617	-1.38
Antxr1	0.0002091	-1.38
Cdkn2c	0.0003739	-1.37
Itga9	0.0005712	-1.37
Srgap3	0.0010084	-1.37
1110003O08Rik	0.0009932	-1.37
Dcn	0.0004499	-1.37
	0.0002832	-1.37
Klhl5	0.0009788	-1.36
Mef2d	0.0002491	-1.36
Rdh5	0.0010769	-1.36
Arhgef6	0.0000996	-1.36
Spg20	0.0005115	-1.35
4930523C07Rik	0.0000658	-1.35
Iffo1	0.0001819	-1.35
Igf1	0.0012483	-1.35
Fhad1	0.0003061	-1.35
Robo1	0.0008355	-1.34
	0.0000033	-1.34
2210011C24Rik	0.0005836	-1.34
Smad3	0.0007121	-1.34
9-Sep	0.0010350	-1.34
Gpsm2	0.0003465	-1.34
Cnot6l	0.0001278	-1.34
Golm1	0.0000001	-1.34
Gpc4	0.0000629	-1.34
Tmem62	0.0000380	-1.33
Prmt2	0.0012170	-1.33

Mfhas1	0.0005969	-1.32
Nfia	0.0001630	-1.32
Ube2e2	0.0008489	-1.32
Hspa12a	0.0008942	-1.32
Clec2d	0.0005843	-1.32
Morc4	0.0007879	-1.32
1700116B05Rik	0.0001667	-1.32
Arhgap22	0.0005609	-1.32
Cadm1	0.0010777	-1.31
Gpr56	0.0009049	-1.31
Pbx3	0.0000377	-1.31
Lgals9	0.0000945	-1.31
Ccdc8	0.0001870	-1.31
Zfp367	0.0007592	-1.31
Plagl1	0.0000215	-1.31
6-Sep	0.0001069	-1.31
Nes	0.0003728	-1.31
Svil	0.0000221	-1.30
Pxdn	0.0002950	-1.30
Pitpnc1	0.0003048	-1.30
Clasp1	0.0009174	-1.30
Macc1	0.0009132	-1.30
Myo18a	0.0003121	-1.29
Rsph1	0.0012212	-1.29
Rin2	0.0010779	-1.29
Tmem177	0.0005345	-1.29
Fnbp1	0.0000288	-1.29
Cntln	0.0003720	-1.29
Rptor	0.0002238	-1.29
	0.0004727	-1.29
5730559C18Rik	0.0006805	-1.29
Pipox	0.0008969	-1.29
Sfxn5	0.0000959	-1.28
Ptgds	0.0011799	-1.28
Ypel3	0.0002675	-1.28
	0.0001266	-1.28
Parp3	0.0011653	-1.28
Zfp422	0.0003814	-1.28
Nfib	0.0006320	-1.28
Il22	0.0004058	-1.28
Adamts14	0.0011272	-1.27
	0.0006693	-1.27
Mef2d	0.0000398	-1.27
Gm16492	0.0007891	-1.27

	0.0002167	-1.27
Cnn2	0.0003997	-1.26
Sgsm2	0.0012080	-1.26
	0.0000010	-1.26
Klf5	0.0007842	-1.26
Btrc	0.0006194	-1.26
Slc9a3r1	0.0002137	-1.26
Il20rb	0.0011864	-1.26
Hrh3	0.0004856	-1.26
Arsb	0.0003754	-1.26
Dysf	0.0001191	-1.25
AI464131	0.0000589	-1.25
Klhdc10	0.0011130	-1.25
Bicd2	0.0005959	-1.25
4933426M11Rik	0.0002758	-1.24
Sulf2	0.0006144	-1.24
Pmaip1	0.0000253	-1.24
Chst10	0.0003443	-1.24
Ehbp1	0.0010043	-1.24
	0.0009202	-1.24
Acpp	0.0004499	-1.24
Ppap2a	0.0008828	-1.24
Sox9	0.0007794	-1.24
Pabpc1l	0.0009369	-1.24
Zfp473	0.0009668	-1.23
Lrrfip1	0.0010260	-1.23
Stard13	0.0006472	-1.23
Tmpo	0.0004364	-1.23
Sync	0.0002768	-1.23
Gamt	0.0000392	-1.23
Ttll1	0.0004726	-1.23
Brd3	0.0010180	-1.22
Ly6e	0.0010958	-1.22
Cdk5r1	0.0001534	-1.22
Tmem182	0.0010704	-1.22
Hddc3	0.0004282	-1.22
Ccpg1	0.0007982	-1.22
Trak1	0.0005620	-1.22
Pcbd1	0.0002601	-1.22
Hoxa7	0.0005522	-1.22
1700025G04Rik	0.0000430	-1.21
Ube2d1	0.0003390	-1.21
Tspan9	0.0002975	-1.21
Trim55	0.0006725	-1.21

Akap1	0.0005634	-1.21
Prune	0.0007284	-1.20
Cdkn1c	0.0002044	-1.20
Osgin2	0.0001631	-1.20
Ccdc111	0.0003039	-1.20
Tspan13	0.0006857	-1.20
Tbx18	0.0004987	-1.20
Ssbp3	0.0000117	-1.20
St6gal1	0.0008657	-1.20
Dlgap4	0.0009546	-1.20
Myh1	0.0005541	-1.19
Copg2	0.0000081	-1.19
Traf3ip2	0.0010664	-1.19
Rasgrp2	0.0004989	-1.19
Cds2	0.0003658	-1.19
Crat	0.0010853	-1.19
Samd4	0.0003362	-1.19
Nedd9	0.0000466	-1.18
Myom2	0.0002899	-1.18
Enthd1	0.0007770	-1.18
Mgam	0.0011734	-1.18
Dock8	0.0010771	-1.18
Lmo7	0.0006554	-1.18
Ubap2	0.0002069	-1.18
Igfbp5	0.0001033	-1.18
Parp10	0.0012029	-1.18
Gm10570	0.0004120	-1.18
Gys1	0.0008782	-1.17
Ahnak	0.0001294	-1.17
Pira2	0.0001695	-1.17
Cplx1	0.0005145	-1.17
Scarb2	0.0005859	-1.17
Nr4a1	0.0003467	-1.17
Sh2d3c	0.0002684	-1.17
Hmcn1	0.0000792	-1.17
Pygm	0.0009729	-1.17
Vdr	0.0010799	-1.16
Olfr419	0.0009757	-1.16
Ankrd23	0.0001329	-1.16
	0.0008378	-1.16
Mup4	0.0010978	-1.16
Entpd4	0.0001356	-1.16
Acap2	0.0007870	-1.16
Fbln1	0.0000918	-1.16

Psme1	0.0003794	-1.15
Mtus1	0.0009074	-1.15
Rnaset2a	0.0000983	-1.15
Scrn1	0.0002679	-1.15
Lmod3	0.0003488	-1.15
Hsd17b4	0.0002664	-1.15
Chi3l1	0.0007822	-1.15
Rnaset2a	0.0002168	-1.15
Ablim2	0.0009087	-1.14
Cmya5	0.0005178	-1.14
Myh8	0.0009070	-1.14
Fcer2a	0.0001455	-1.13
Chd7	0.0010807	-1.13
Pgm5	0.0005868	-1.12
Ano6	0.0000693	-1.12
Isca1	0.0006159	-1.11
Prkar1a	0.0002074	-1.11
C1galt1c1	0.0012239	-1.11
	0.0009858	-1.10
Srl	0.0005447	-1.10
Gpr125	0.0000306	-1.10
	0.0000057	-1.09
1700047I17Rik1	0.0008674	-1.09
1700047I17Rik1	0.0008674	-1.09
Kbtbd10	0.0007341	-1.09
Nnt	0.0002018	-1.08
	0.0010791	-1.08
Ddit4	0.0009305	-1.02
Rpl32	0.0012127	-1.02

Appendix Table 7. Transcripts downregulated by BMP4-treatment in MuSK null myotubes.